

**T-plastin, a cytoskeletal protein with  
important function in axonal growth,  
acts as a modifier of spinal muscular atrophy**

Inaugural-Dissertation  
zur  
Erlangung des Doktorgrades  
der Mathematisch-Naturwissenschaftlichen Fakultät  
der Universität zu Köln

vorgelegt von  
Gabriela-Elena Oprea,  
geborene Bordeianu  
aus Bukarest

2007

Doctoral Thesis "**Identification of T-plastin as Gene Modifier in SMA Discordant Families**" was performed primarily at the **Institute of Human Genetics, University of Bonn** from september 2002 to march 2004 and at the **Institute of Human Genetics, University of Cologne** from march 2004 to 2007. The microarray analysis was performed at the **Institute of Genetics and Centre for Molecular Medicine Cologne**, and the genome scan analysis as well as all pyrosequences, were performed at the **Cologne Centre for Genomics (CCG)**. The confocal imaging was performed at the **Institute for Biochemistry I, University of Cologne** and at the **Centre for Molecular Medicine University of Cologne (CMMC)**.

Berichterstatter/in      Prof. Dr. rer.nat. Brunhilde Wirth  
                                 Prof. Dr. rer. nat. Diethard Tautz

Tag der letzten mündlichen Prüfung: 5 Juni 2007

*For my dear husband, Costy.*

## ACKNOWLEDGEMENTS

There are lots of people I would like to thank for a huge variety of reasons.

Firstly, I would like to thank my Supervisor, Prof. Dr. Brunhilde Wirth for giving me the opportunity to work in her group and for her encouragement all through my doctoral studies. I could not have imagined having a better advisor and mentor for my PhD.

Thank-you to my examiners, Prof. Dr. Diethard Tautz and Prof. Dr. Helmut Klein.

I heartily thank Prof. Dr. Peter Nürnberg and Gudrun Nürnberg for the wonderful collaboration and help on the genome-wide scan analysis; to Prof. Dr. J. L. Schultze and Dr. Svenia Debey with the excellent help on microarray analysis and data interpretation.

I would like to deeply thank to all past and present members of the “SMA group”, especially to Sandra Kröber for her brilliant technical assistance, Frank Schönen for his kind help whenever asked, Heidrun Raschke for introducing me into the cell culture “world” and for her friendship, Markus Riessland for helpful and stimulating discussions and comments on the draft, Maike Warnstedt for critical reading the draft and for the huge help with German language whenever needed, to Irmgard Hölker for her friendship, good advice and encouragement, specially in hard moments.

I especially thank to Mohammad Reza Tolliat for his excellent assistance with pyrosequencing.

I am grateful to Dr. Francisco Rivero-Crespo for his advice in immunofluorescent experiments and for his kind help in handling the confocal microscope.

I would like to say a big “thank-you” to Dr. Ramirez Alfredo for his help in establishing the setup for measuring axons length and whenever a question concerning fluorescence microscopy asked.

I especially thank Nina Dalibor and Oddette Mukabayire-Kramer for their friendship, good advice and encouragement.

I also warmly thank to all Romanian friends for their great support, encouragements, help, for wonderful holidays and for reminding me how active and full of surprises Romanian people are. I’ve missed you a lot, gays.

The heartiest gratitude goes to my family for wonderful support and encouragements.

On a different note, I would like to thank the coffee producers for keeping me thinking and for making me feel okay about drinking so much coffee.

Finally, I owe my warmest thanks to my “male team” at home, my husband Costy, for his encouragement, throughout the whole course of my work, for his help to keep my foot always firmly on the ground. I will always love you.

Thank you, and Be Well and Happy!

---

## TABLE OF CONTENTS

### TABLE OF CONTENTS

### LIST OF ABBREVIATIONS

<b>1. INTRODUCTION.....</b>	<b>1</b>
<b>1.1. Clinical and pathological features of spinal muscular atrophy.....</b>	<b>2</b>
<b>1.2. Survival motor neuron (SMN) gene.....</b>	<b>3</b>
<b>1.3. Gene conversion, deletion and <i>de novo</i> mutations.....</b>	<b>6</b>
<b>1.4. Survival motor neuron transcripts.....</b>	<b>7</b>
<b>1.5. The SMN protein and its functions.....</b>	<b>10</b>
1.5.1. SMN complex.....	13
1.5.2. Motor neuron specific functions of the SMN protein.....	19
1.5.3. Regulation of the SMN protein during development and cellular differentiation.....	25
<b>1.6. Animal models of SMA.....</b>	<b>26</b>
<b>1.7. Therapeutic prospects of SMA.....</b>	<b>27</b>
<b>1.8. SMA discordant families.....</b>	<b>30</b>
<b>2. AIMS.....</b>	<b>35</b>
<b>3. SUBJECTS AND MATERIALS.....</b>	<b>36</b>
<b>3.1. Patients samples.....</b>	<b>36</b>
<b>3.2. Biological samples.....</b>	<b>37</b>
<b>3.3. Equipment.....</b>	<b>37</b>
<b>3.4. Chemicals.....</b>	<b>39</b>
<b>3.5. Kits.....</b>	<b>39</b>
<b>3.6. Reagents, enzymes and additional supplies for cell culture procedures...40</b>	
<b>3.7. Primary antibodies.....</b>	<b>41</b>
<b>3.8. Secondary antibodies.....</b>	<b>41</b>
<b>3.9. Solutions and media.....</b>	<b>41</b>
3.9.1. Frequently used buffers and solutions.....	41

---

3.9.2. Media for eukaryotic and tissue culture procedures.....	46
3.9.3. Media for prokaryotic cells.....	47
<b>3.10. Software and databases.....</b>	<b>47</b>
<b>3.11. Primers and siRNAs.....</b>	<b>48</b>
<b>4. METHODS.....</b>	<b>57</b>
<b>4.1. Prokaryotic cells.....</b>	<b>57</b>
4.1.1. Bacteriology.....	57
4.1.2. Transformation of bacteria by heat-shock.....	57
<b>4.2. Eukaryotic cells.....</b>	<b>58</b>
4.2.1. Cell culture.....	58
4.2.1.1. EBV transformation of peripheral blood lymphocytes.....	58
4.2.1.2. EBV-transformed lymphoblastoid cell culture.....	58
4.2.1.3. Human fibroblasts cell culture.....	59
4.2.1.4. HEK293 cell culture.....	59
4.2.1.5. PC12 cell culture.....	59
4.2.1.6. PC12 differentiation: treatment of PC12 cells with NGF.....	60
4.2.1.7. Cell harvesting and freezing.....	60
4.2.1.8. Cell thawing and recovering.....	60
<b>4.3. DNA techniques.....</b>	<b>61</b>
4.3.1. Plasmid preparation (Mini prep) using Quantum Prep® Plasmid MiniPrep Kit ( <i>Bio-Rad</i> ).....	61
4.3.2. DNA isolation from fresh blood.....	61
4.3.3. DNA isolation from cell culture.....	62
4.3.4. DNA electrophoresis.....	62
4.3.4.1. Agarose gel.....	62
4.3.4.2. Sequencing gel.....	62
4.3.5. Construction of gene constructs and DNA cloning.....	63
4.3.6. Sequencing.....	64
4.3.6.1. Big-Dye sequencing.....	64
4.3.6.2. Clean-up of dye-terminator sequencing reactions.....	64
4.3.6.3. Pyrosequencing.....	65
4.3.7. DNA modification: bisulfite treatment.....	66
4.3.8. DNA amplification.....	67

---

4.3.8.1. Polymerase chain reaction (PCR).....	67
4.3.8.2. Reverse-transcription PCR (RT-PCR).....	68
4.3.8.3. Multiplex PCR.....	68
4.3.8.4. Nested PCR.....	68
4.3.8.5. PCR of bisulfite treated DNA.....	69
4.3.8.6. PCR for genotyping.....	70
4.3.9. PCR products purification.....	70
4.3.10. DNA quantification by spectrophotometry.....	70
4.3.11. DNA extraction from agarose gels.....	71
4.3.12. DNA-protein interaction.....	71
4.3.12.1. <sup>32</sup> P labelling of oligonucleotide probe.....	71
4.3.12.2. <i>In vivo</i> footprinting.....	72
4.3.12.2.1. Genomic DNA isolation.....	72
4.3.12.2.2. Piperidine cleavage.....	73
4.3.12.2.3. Ligation-mediated PCR (LM-PCR).....	73
<b>4.4. RNA techniques.....</b>	<b>75</b>
4.4.1. RNA isolation.....	75
4.4.1.1. RNA isolation from fresh blood.....	75
4.4.1.2. TRIzol method for RNA isolation from cell culture.....	75
<b>4.5. Autoradiography.....</b>	<b>76</b>
<b>4.6. Protein biochemistry.....</b>	<b>76</b>
4.6.1. Protein isolation, expression and purification.....	76
4.6.1.1. Bacterial overexpression: expression and purification of SMN-GST fusion protein.....	76
4.6.1.2. Expression of T-plastin protein in the TNT <sup>®</sup> T7 Quick Coupled Transcription/Translation Reaction ( <i>Promega</i> ).....	77
4.6.1.3. Protein isolation from fresh blood.....	78
4.6.1.4. Protein isolation from cell culture using RIPA buffer (fibroblasts, EBV-transformed lymphoblastoid cell lines, HEK293 cells, PC12 cells).....	78
4.6.1.5. Protein isolation from cell culture using IP buffer (HEK293 cells, PC12 cells).....	78
4.6.2. Protein quantification by spectrophotometry (Bradford assay).....	78
4.6.3. Generation of polyclonal antibody against T-plastin.....	79
4.6.4. Protein analysis.....	79
4.6.4.1. SDS-PAGE electrophoresis.....	79
4.6.4.2. Antibodies.....	80

---

4.6.4.3. Protein transfer.....	81
4.6.4.4. Western blot.....	82
4.6.5. Protein-protein interaction.....	82
4.6.5.1. Co-immunoprecipitation.....	82
4.6.5.2. Magne GST™ Pull-Down assay.....	82
<b>4.7. Cell transfection.....</b>	<b>83</b>
4.7.1. Transient transfection of T-plastin-V5-tagged plasmid in HEK293 and PC12 cells.....	83
4.7.2. Transient transfection of T-plastin siRNA oligos into PC12 cells.....	84
4.7.3. Co-transfection of T-plastin-V5-tagged plasmid DNA and SMN siRNA oligos into PC12 cells.....	84
<b>4.8. Cell imaging.....</b>	<b>85</b>
4.8.1. Immunocytochemistry (ICC).....	85
4.8.2. Confocal scanning fluorescence microscopy.....	86
4.8.3. Non-confocal fluorescence microscopy.....	86
4.8.4. Measurement of neurite outgrowth.....	86
<b>4.9. Microarray analysis.....</b>	<b>86</b>
4.9.1. RNA Cleanup with RNeasy MinElute Cleanup Kit ( <i>Qiagen</i> ).....	87
4.9.2. Quantification and analysis of purity of RNA.....	87
4.9.3. Synthesis of double stranded cDNA from total RNA.....	88
4.9.3.1. First strand cDNA synthesis.....	88
4.9.3.2. Second strand cDNA synthesis.....	88
4.9.3.3. Clean-up of double stranded cDNA with Sample Cleanup Module ( <i>Affymetrix</i> ).....	88
4.9.4. Synthesis and purification of biotin labelled cRNA.....	89
4.9.4.1. Synthesis of biotin labelled cRNA.....	89
4.9.4.2. cRNA cleanup with Sample Cleanup Module ( <i>Affymetrix</i> ).....	89
4.9.4.3. Quantifying the cRNA (IVT: <i>in vitro</i> transcription-product).....	90
4.9.4.4. Checking unfragmented samples on gel electrophoresis.....	90
4.9.5. Fragmenting cRNA for target preparation.....	90
4.9.6. Target hybridization.....	90
4.9.7. Microarrays.....	91
4.9.8. Fluidic station set up and experimental procedure.....	91
4.9.8.1. Preparing fluid station.....	92
4.9.8.2. SAPE staining solution.....	92
4.9.8.3. Antibody solution mix.....	92

---

4.9.8.4. Scanning the microarray.....	93
4.9.9. Array profile.....	93
4.9.9.1. Instrument / software requirements.....	93
4.9.9.2. Critical specification for HG-U133A 2.0 array.....	93
4.9.10. Probe array image inspection.....	94
4.9.11. Average background and noise values.....	94
4.9.12. B2 oligo performance.....	94
4.9.13. Poly-A controls: dap, lys, phe, thr, trp.....	94
4.9.14. Hybridization controls: bioB, bioC, bioD and cre.....	95
4.9.15. Internal controls genes.....	95
4.9.16. Percent genes present.....	95
4.9.17. Scaling and normalization factors.....	95
4.9.18. Single array analysis.....	95
4.9.18.1. Detection algorithm.....	96
4.9.18.2. Detection <i>p</i> -value.....	96
4.9.18.3. Detection call.....	96
4.9.18.4. Signal algorithm.....	96
4.9.19. Comparison analysis (experiment vs. baseline arrays).....	97
4.9.19.1. Change algorithm.....	97
4.9.19.2. Change <i>p</i> -value.....	98
4.9.19.3. Change call.....	98
4.9.19.4. Signal Log Ratio algorithm.....	98
4.9.19.5. The logic of logs.....	98
4.9.19.6. Basic data interpretation.....	99
4.9.19.7. Interpretation of metrics.....	99
4.9.20. Online informatics resource.....	100
4.9.21. Data analysis and software.....	100
<b>4.10. Genome scan analysis.....</b>	<b>100</b>
4.10.1. Arrays.....	100
4.10.2. Statistical analysis.....	101
4.10.2.1. Non-parametric linkage analysis using MERLIN software.....	101
4.10.2.2. Parametric linkage analysis .....	101
<b>4.11. Additional statistical methods.....</b>	<b>102</b>

<b>5. RESULTS.....</b>	<b>103</b>
<b>5.1. Search for SMA modifying factor(s) by candidate gene approach.....</b>	<b>103</b>
5.1.1. Selection of candidate genes.....	103
5.1.2. Selection of <i>ZNF265</i> gene.....	103
5.1.3. Molecular analysis of <i>ZNF265</i> gene in SMA discordant families.....	104
5.1.4. Selection of <i>hnRNP-R</i> gene.....	105
5.1.5. Molecular analysis of <i>hnRNP-R</i> at DNA and RNA level.....	163
5.1.6. Selection of <i>HDAC6</i> gene.....	173
5.1.7. Testing of DNA polymorphism in <i>HDAC6</i> gene.....	108
<b>5.2. Search for SMA modifying genes by differential expression     using Affymetrix microarray technology.....</b>	<b>108</b>
5.2.1. The microarray screen for EBV-transformed lymphoblastoid cell RNAs revealed up- and down-regulated genes in asymptomatic vs. symptomatic sibs in SMA discordant families.....	109
5.2.2. Gene selection.....	111
5.2.3. Confirmation of microarray data by semi-quantitative RT-PCR .....	113
5.2.4. Validation of microarray-based results in another four SMA discordant families .....	114
5.2.5. Description of NR113 candidate.....	115
5.2.6. Description of T-plastin candidate.....	116
<b>5.3. T-plastin, a potential gene modifier in SMA discordant families.....</b>	<b>121</b>
5.3.1. <i>T-plastin</i> and <i>SMN</i> transcripts are expressed at high level in spinal cord and muscles .....	121
5.3.2. Characterization of T-plastin antibody .....	123
5.3.3. <i>T-plastin</i> is expressed in both EBV-transformed lymphoblastoid cells and fresh blood belonging to unaffected sibs <i>SMN1</i> -deleted.....	124
5.3.4. <i>T-plastin</i> is expressed in 6.5 % in the control population .....	125
5.3.5. Validation of the significant difference of <i>T-plastin</i> expression between unaffected and affected sibs at protein level.....	127
5.3.6. Functional analysis of T-plastin protein.....	127
5.3.6.1. SMN and T-plastin associate together <i>in vivo</i> , but do not interact directly.....	127
5.3.6.2. Endogenous SMN co-localizes with V5-tagged T-plastin in the perinuclear area of HEK293 cells.....	130
5.3.6.3. T-plastin and SMN levels increase under NGF stimulation in PC12 cells.....	131
5.3.6.4. The affinity of T-plastin for SMN increases during neurite outgrowth.....	133
5.3.6.5. Endogenous T-plastin and SMN co-localize along neurites and at the	

---

growth cone level in PC12 cells-derived neurons.....	134
5.3.6.6. T-plastin-depleted PC12 cells exhibit a significant reduction in neurite length.....	137
5.3.6.7. T-plastin overexpression in PC12 cells leads to an increase in size of the neurites.....	138
5.3.6.8. T-plastin overexpression is able to rescue partially the neurite length in <i>SMN</i> -depleted PC12 cells.....	142
5.3.6.9. Molecular analysis of <i>T-plastin</i> coding region, promoter, 3'UTR and intron 1.....	144
5.3.7. Expression analysis of <i>T-plastin</i> gene.....	144
5.3.7.1. <i>T-plastin</i> CpG island: quantitative evaluation of methylation levels using pyrosequencing.....	145
5.3.7.2. <i>In vivo</i> footprinting of <i>T-plastin</i> enhancer in EBV-transformed lymphoblastoid cells of SMA discordant families.....	147
5.3.7.3. Haplotype analysis of the <i>T-plastin</i> genomic region revealed a <i>trans</i> -acting mechanism to regulate its expression.....	149
<b>5.4. Search for modifying genes by genome-wide scan analysis.....</b>	<b>153</b>
5.4.1. Power simulation of the genome scan analysis.....	153
5.4.2. Non-parametric linkage data interpretation.....	154
5.4.3. Parametric linkage data interpretation.....	155
5.4.4. Gene organization into categories according to their molecular function.....	156
<b>6. DISCUSSION.....</b>	<b>158</b>
<b>6.1. <i>ZNF265</i>, <i>hnRNP-R</i> and <i>HDAC6</i> are not responsible for         the phenotypic variability of the SMA discordant sibs.....</b>	<b>158</b>
<b>6.2. T-plastin, a novel candidate gene detected by expression         Profiling analysis.....</b>	<b>156</b>
<b>6.3. T-plastin is expressed in all unaffected sibs that carry <i>SMN1</i>         deletion/mutation and in 6.5 % of the control population.....</b>	<b>162</b>
<b>6.4. <i>T-plastin</i> is activated by a <i>trans</i>-acting factor.....</b>	<b>163</b>
<b>6.5. T-plastin might play an important role during NMJ formation.....</b>	<b>164</b>
<b>6.6. T-plastin and <i>SMN</i> form a novel axon-specific complex.....</b>	<b>164</b>
<b>6.7. T-plastin is involved in neurite-like extension formation in         differentiated PC12 cells.....</b>	<b>167</b>
<b>6.8. Genome-wide scan in SMA discordant families revealed         the evidence for new susceptibility loci.....</b>	<b>168</b>

---

6.9. Future directions.....	171
7. SUMMARY.....	173
8. ZUSAMMENFASSUNG.....	175
9. PUBLICATIONS, LECTURES AND POSTER CONTRIBUTIONS.....	177
9.1. ORIGINAL PUBLICATIONS	
9.2. PRINTED LECTURE CONTRIBUTIONS	
9.3. PRINTED POSTER CONTRIBUTIONS	
10. REFERENCES.....	178

## APPENDIX

### Figures:

- I. F1 Pedigrees of the SMA discordant families
- II. F2 pcDNA 3.1\_ *T-plastin*\_V5 vector map
- III. F3 Human *T-plastin* transcript
- IV. F4 *T-plastin* genomic region
- V. F5 *T-plastin* promoter-1<sup>st</sup> exon-1<sup>st</sup> intron (1 kb) region after bisulfite treatment
- VI. F6 *T-plastin* expression analysis by RT-PCR in 79 SMA patients
- VII. F7 Simulation of the genome scan analysis under the assumption of recessive mode of inheritance
- VIII. F8 Simulation of the genome scan analysis under the assumption of dominant mode of inheritance
- IX. F9 Methylation status of *T-plastin* CpG sites in SMA discordant families
- X. F10 Methylation status of *T-plastin* CpG sites in two control groups
- XI. F11 Haplotype blocks within *T-plastin* genomic region
- XII. F12 Motor axons defects in *smn* morphants are rescued by overexpression of human *T-plastin* RNA

**Tables:**

- I. T1 Classical SMA patients checked for *T-plastin* expression
- II. T2 Phenotypic and genotypic description of SMA discordant families used for genome-wide scan
- III. \*T3 Up-regulated transcripts detected by microarray analysis in SMA discordant families
- IV. \*T4 Down-regulated transcripts detected by microarray analysis in SMA discordant families
- V. \*T5 Up-regulated transcripts detected by microarray analysis in classical SMA patients
- VI. \*T6 Down-regulated transcripts detected by microarray analysis in classical SMA patients
- VII. \*T7 Susceptibility regions detected by the genome-wide scan analysis in SMA discordant families
- VIII. \*T8 Raw data for each chromosomal region detected by the genome-wide scan analysis
- IX. \*T9 Raw data for methylation analysis of *T-plastin* CpG island in two control populations
- X. \*T10 Raw data for methylation analysis of *T-plastin* CpG island in SMA discordant families
- XI. \*T11 Raw data for *T-plastin* haplotype blocks analysis

**ERKLÄRUNG****CURRICULUM VITAE**

\*: The tables are contained in the attached CD-ROM.

**LIST OF ABBREVIATION**

aa	amino acid
A	adenine
ABPs	ammonium persulphate
APS	actin binding proteins
bp	base pair
BSA	bovine serum albumin
C	cytosine
cDNA	complementary DNA
cM	centimorgan
cm	centimeter
CNS	central nervous system
DEPC	diethylpyrocarbonate
D-MEM	Dulbecco's modified Eagle medium
DMS	dimethyl sulphate
DMSO	dimethylsulfoxide
DNA	deoxyribonucleic acid
DTT	dithiotreitol
EBV	Epstein-Barr virus
EDTA	ethylenediaminetetraacetic acid
e.g.	exempli gratia
EMG	electromyography
ER	endoplasmic reticulum
ESE	exonic splicing enhancer
ESS	exonic splicing silencer
et al.	et alii
FBS	fetal bovine serum
FCS	fetal calf serum
FL	full length
FITC	fluorescein isothiocyanate
FDA	Food and Drug Administration
For	forward
FVC	forced vital capacity
G	guanine
g	acceleration due to gravity
GSH	glutathione
GST	glutathione-S-transferase

---

h	hour
HAT	histone acetyltransferase
HDAC	histone deacetylase
HMT	histone methyltransferase
HPRT	hypoxanthine phosphoribosyltransferase
ICC	immunocytochemistry
i.e.	id est
IP	immunoprecipitation
IPTG	isopropyl 1-thio- $\beta$ -D-galactoside
ISS	intronic splicing silencer
kb	kilobases
kDa	kilodalton
l	liter
LD	linkage disequilibrium
LMPCR	ligation-mediated PCR
M	molar
m	milli-
Mb	megabases
MBPs	methyl CpG binding proteins
min	minute
ml	millilitre
mm	millimeter
mM	millimolar
mRNA	messenger RNA
NGF	nerve growth factor
ng	nanogram
nm	nanometer
NMJs	neuromuscular junctions
Nmol	nanomol
NPL	non-parametric linkage
nt	nucleotide
OMIM	Online Mendelian Inheritance in Man
PAGE	polyacrylamide gel electrophoresis
PBS	phosphate-buffered saline
PCR	polymerase chain reaction
PFA	paraformaldehyde
pH	power of hydrogen
pmol	picomol

---

PPi	pyrophosphate
Rev	reverse
RNA	ribonucleic acid
RNAi	RNA interference
rpm	revolutions per min
RT	reverse transcription
SAHA	suberoylanilide hydroxamid acid
SD	standard deviation
SDS	sodium dodecyl sulphate
sDMA	symmetrically dimethylated arginine
SGs	stress granules
siRNA	small interfering RNA
SMA	autosomal recessive spinal muscular atrophy
SMARD	SMA with respiratory distress
SMN	survival motor neuron
SMN $\Delta$ 7	survival motor neuron protein lacking exon 7
snoRNP	small nucleolar ribonucleoproteins
snRNPs	small nuclear ribonucleoprotein
ss	splice site
T	thymine
TEMED	N,N,N',N'-tetramethylethylenediamine
UTR	untranslated region
VPA	valproic acid
versus	vs.
$\mu$	micro-
$\mu$ g	microgram
$\mu$ l	microliter
$\mu$ M	micromolar
$\mu$ m	micrometer
#	number

## 1. INTRODUCTION

Spinal muscular atrophy (SMA) is an autosomal recessive neurodegenerative disease characterized by loss of lower motor neurons in the anterior horn of the spinal cord, accompanied by progressive wasting of associated muscles, and ultimately, paralysis. It is estimated to be the second most common autosomal recessive disease with an overall incidence of around 1 in 10,000 live births and a carrier frequency that may be as high as 1 in 35 (Cusin et al. 2003; Feldkotter et al. 2002). SMA exists in a broad spectrum ranking from very severe infantile to very mild chronic forms of the disease, and is conventionally classified into four groups (type I-IV) on the basis of age of onset and achieved motor milestones (Munsat and Davies 1992). The mutational mechanism behind SMA, in around 94 % of typical cases, is lack of *SMN1* gene due to either *SMN1* deletion or *SMN1* to *SMN2* conversion. Furthermore, around 35 different small intragenic mutations have been reported (Ogino and Wilson 2004; Sun et al. 2005; Wirth 2000). *SMN1* is located on chromosome 5q13 in a highly complex genetic region containing a variety of pseudogenes and repetitive elements due to an inverted duplication of approximately 500 kilobases. *SMN* is present in two versions, *SMN1* (telomeric) and *SMN2* (centromeric) which differ by only one nucleotide in the coding region. A transition of a cytosine to a thymine in *SMN2* exon 7 alters the splicing pattern, creating a truncated transcript (*SMN $\Delta$ 7*) which encodes a non-functional protein lacking the last 16 residues at the C-terminal end. The truncated *SMN2* isoform is less stable and has a reduced self-oligomerization activity (Lorson et al. 1998; Pellizzoni et al. 1998). As a consequence, the *SMN2* gene produces reduced amounts of full-length SMN that cannot fully compensate the absence of *SMN1*, leading to specific degeneration of motor neurons in the spinal cord (Coover et al. 1997; Lefebvre et al. 1997).

There are numerous other forms of spinal muscular atrophy which share certain characteristics with proximal SMA, however, they are genetically distinct and often affect different subsets of neurons and muscles. They include autosomal dominant forms of the disease (Sambuughin et al. 1998; van der Vleuten et al. 1998), X-linked forms (Kobayashi et al. 1995; La Spada et al. 1991), recessive forms that affect the distal muscles (Viollet et al. 2002), and a severe form of SMA with respiratory distress (SMARD) (Grohmann et al. 2001).

In contrast to proximal SMA, spinal muscular atrophy with respiratory distress (SMARD) type I has been linked to chromosome 11q13-q21 (Grohmann et al. 1999) with mutations in *IGHMPP2* gene (Grohmann et al. 2001). In SMARD1 distal muscles and upper limbs are more affected than in SMA, and the major symptom is paralysis of the diaphragm (Grohmann et al. 1999). Spinal and bulbar muscular atrophy, also called Kennedy's disease, is a rare, adult-onset form of motor neuron disease that is less common than proximal type I, II and III SMA. This X-linked form of spinal and bulbar muscular atrophy has a different genotype and is associated with CAG repeat mutations (La Spada et al. 1991).

Interestingly, in rare cases homozygous absence of the *SMN1* gene in unaffected siblings of patients with SMA can be observed (Brahe et al. 1995; Cobben et al. 1995; Hahnen et al. 1995). The presence of phenotypic discordance in SMA families is rare, mainly female-specific and can be found in some 10 % of

families with type III SMA and 1.2 % of families with type II SMA (Wirth 2002). The finding that homozygous deletion of *SMN1* and identical *SMN2* copy number present discordant phenotypes strongly implies that additional factors, except for *SMN1* and *SMN2*, are influencing the SMA phenotypes.

### 1.1. Clinical and pathological features of spinal muscular atrophy

SMA was first described in the 1890s by Guido Werdnig of the University of Vienna and Johann Hoffman of Heidelberg University. Beginning with Byers and Banker (Byers and Banker 1961) the classification of SMA according to severity was used to facilitate prognostication. The relationship between age of onset and severity was supported by Dubowitz's observation (Dubowitz 1964): age of onset is the only means of predicting outcome at the time of diagnosis. Based on the work of an international collaboration (Munsat 1995; Munsat and Davies 1992) most pediatric neurologists now use the following nomenclature:

- I. Patients with type I SMA (Werdnig-Hoffman disease) for the symptoms before age 6 months is characterized by severe generalized muscle hypotonia. Patients never achieve the ability to sit, and death usually occurs from respiratory insufficiency within the first two years without respiratory support.
- II. Patients with type II SMA (intermediate) have onset after 6 months of age and before 18 months of age. They achieve the ability to sit unsupported but never stand or walk unaided. Prognosis in this group is largely dependent of the degree of respiratory involvement.
- III. Patients with type III SMA (Kugelberg-Welander disease) usually have their first symptoms between 18 months of age and early childhood. They are able to stand and walk independently at some point during their disease course but often become wheelchair bound during youth or adulthood. Life expectancy is not usually reduced in this group.
- IV. Patients with type IV SMA have onset in late childhood or adulthood (as late as the fifth or sixth decades).

The clinical symptoms in all four groups of SMA include:

- hypotonia;
- symmetrical muscle weakness and atrophy (predominantly of proximal muscle of the shoulder and pelvic girdle);
- tremor of fingers and hands;
- fasciculation of the tongue muscles;
- hyporeflexia and, at a later stage, contractures of some muscle groups. The diaphragm and extraocular muscles remain unaffected until late stages of the disease and there is little or no impairment of sensory system (Hausmanowa-Petrusewicz et al. 2000; Zalewska and Hausmanowa-Petrusewicz 2000).

The symptoms are due to the selective degeneration of alpha motor neurons in the spinal cord and cranial

motor nuclei, leading to the progressive muscle weakness, atrophy and paralysis. Patients with SMA tend to have the greatest rate of loss of muscle power at disease onset (Crawford 2004). This may manifest as a period during which there is clear loss of strength or there may be only the absence of normal motor milestone gains with early growth and development. After this early phase, the rate of loss of muscle strength may slow or stabilize for many years in surviving patients. A recent study indicates that the rate of motor neuron loss may mirror this clinical disease course (Swoboda et al. 2005).

## 1.2. Survival motor neuron (*SMN*) gene

Identifying the genes involved in SMA was complicated by the highly complex and unstable nature of the genome region where they are localized and by phenotypes that range in severity from the very severe (type I) to intermediate (type II) and to very mild (type III and IV) (Pearn 1980).

Linkage of autosomal recessive SMA to chromosome 5q11.2-q13.3 was reported in 1990 (Brzustowicz et al. 1990; Melki et al. 1990). One feature of the DNA region containing the SMA gene is that it contains numerous repeated genes and markers. Moreover, the genetic marker loci and genes have very similar copies of each other. This critical region is prone to *de novo* genomic rearrangements including unequal crossing-over, intrachromosomal rearrangements and gene conversions (Melki et al. 1994b; Wirth et al. 1997a). This region was shown to contain a complex genomic structure with an inverted and duplicated DNA segment of about 500 kb (Lefebvre et al. 1995). Each 500 kb segment, which can be present in 0 to 4 copies per chromosome contains 5 genes:

1. the survival of motor neuron gene (*SMN*);
2. the *BIRC1* (baculoviral IAP repeat-containing 1) gene, also known as *NAIP* (neuronal apoptosis inhibitory protein);
3. the *SERF1* (small EDRK-rich factor 1) gene, also known as *H4F5*;
4. the *GTF2H2* (general transcription factor II H) gene or *p44*;
5. the *OCN* (occludin) gene.

The polymorphic region is proximally flanked by the unique gene *RAD17* and distally by *TFNR* gene (Kelter et al. 2000) (Fig. 1).

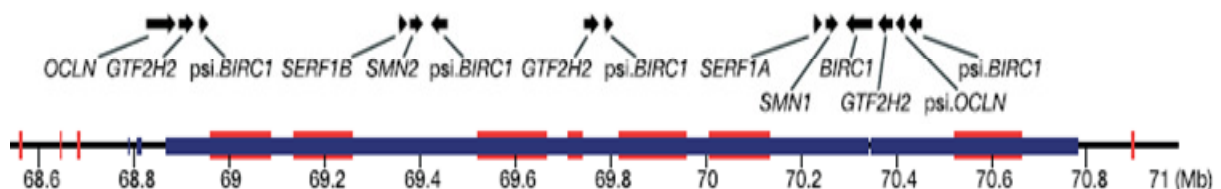


**Fig. 1** Diagram of the “SMA region” showing the duplication pattern along the scale (in Mb) and the gene content of the region. Interchromosomal (red) and intrachromosomal duplications (blue) are indicated (Schmutz et al. 2004).

Deletions in the SMA region were first implicated by marker studies. Three groups first reported deletions in the SMA region in 1995 (Lefebvre et al. 1995; Roy et al. 1995; Thompson et al. 1995). The deletions disrupted two genes: the neuronal inhibitory protein (*NAIP*) and the survival motor neuron (*SMN*) gene. Both genes had duplicated copies and did not exist as single copies. In the case of *NAIP*, there was one functional copy of the gene (Roy et al. 1995); for *SMN* there were two virtually identical genes at the 5q locus, which were originally called telomeric *SMN* and centromeric *SMN* but have been renamed *SMN1* and *SMN2*, respectively (Lefebvre et al. 1995).

The functional *NAIP* gene was deleted in 50% of type I SMA patients, but carriers also had deletion of *NAIP* (Cobben et al. 1995; DiDonato et al. 1997b; Hahnen et al. 1995; Roy et al. 1995; Velasco et al. 1996). In contrast, *SMN1* was absent in 95% to 98% of SMA cases (Cobben et al. 1995; DiDonato et al. 1997a; Hahnen et al. 1995; Lefebvre et al. 1995; Matthijs et al. 1996; Rodrigues et al. 1995; Velasco et al. 1996). The identification of small mutations within the *SMN1* gene in about 3.4% of SMA patients clearly indicated that *SMN1* was the SMA gene (Lefebvre et al. 1995; Parsons et al. 1998; Velasco et al. 1996; Wirth et al. 1999). Thus, the loss or mutation of the *SMN1* gene with the retention of the *SMN2* gene gives rise to SMA (all SMA patients reported to date have at least one *SMN2* gene present). Interestingly, the loss of the *SMN2* gene occurs in 5% of the normal population with no phenotypic effect (Lefebvre et al. 1995; McAndrew et al. 1997). Over 94% of proximal SMA patients harbour deletions or loss-of-function mutations in the telomeric copy of the *SMN* gene (*SMN1*) but retain at least one copy of the centromeric form (*SMN2*) (Lefebvre et al. 1995; Wirth 2000).

The SMA region in the mouse maps to chromosome 13 and contains a single copy of *Smn* (DiDonato et al. 1997a; Endrizzi et al. 1999; Scharf et al. 1996). Thus, the 500 kb inverted duplication that gave rise to two *SMN* genes arose after the divergence of human and mouse lineages. Rat *Smn* is also single-copy gene (Battaglia et al. 1997; La Bella et al. 1998); the common diagnostic feature of both orthologs is that neither undergoes alternative splicing (Battaglia et al. 1997; Bergin et al. 1997; DiDonato et al. 1997a; La Bella et al. 1998; Viollet et al. 1997). In humans, as much as 5 %-10 % of the human genome is duplicated at least once (Mazzarella and Schlessinger 1998). In some instances, these events are directly responsible for inherited disorders, as in the case for 6 % of mutations causing X-linked Duchenne and Becker muscular dystrophy (Hu et al. 1990). On the other hand, most DNA duplications are non-pathogenic; however, once present, they provide a source of material for inter- and intra-chromosomal exchange. Rearrangements involving both low and high copy repeats are responsible for a growing number of disease pathologies (Deininger and Batzer 1999; Kazazian 1998; Mazzarella and Schlessinger 1998). Sequence comparisons between *SMN1* and *SMN2* genes could shed some light upon potential cis-elements involved in *SMN* gene diversification. Twenty three sequence elements were identified within the distal portion of the *SMN* gene (from intron 6 onward) that distinguish *SMN1* from *SMN2* (Rochette et al. 2001); five of these were originally reported by Lefebvre and co-workers in 1995 (Lefebvre et al. 1995). The five nucleotide differences are one in exon 7 (840C-to-T, codon 280, nt. position 27141), exon 8 (nt. position 27869), and intron 6 (nt. position 27092) and another two in intron 7 (nt. position 27289 and 27404), respectively (Fig. 2).

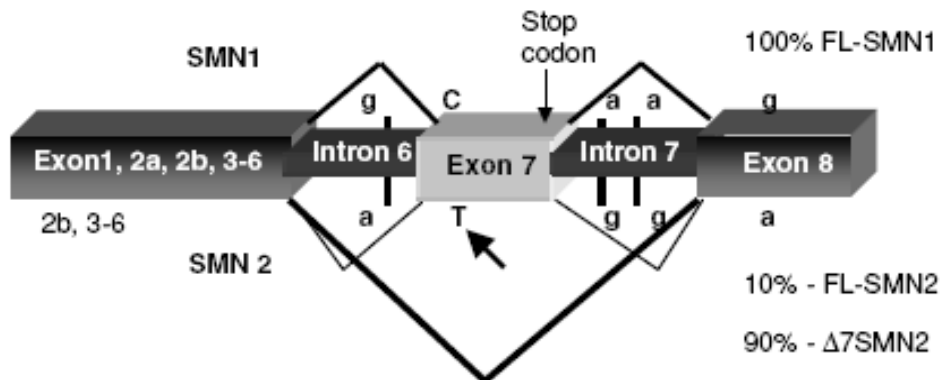


**Fig. 2 Genomic structure, nucleotide, and splicing differences between *SMN1* and *SMN2*.** The *SMN* gene copies can be distinguished by 5 nucleotide exchanges, of which only the C-to-T transition in exon 7 is localized within the coding region. This nucleotide exchange in exon 7 is a translationally silent mutation. Therefore, full-length *SMN1* and full-length *SMN2* mRNA encode identical proteins. However, the C-to-T transition disrupts an exonic splicing enhancer resulting in alternative splicing of *SMN2* pre-mRNA and skipping of exon 7. *SMN2 $\Delta$ 7* transcripts encode a truncated and unstable protein (Wirth et al. 2006a).

*SMN* gene duplication occurred after the divergence of rodents and primates about 75-110 million years ago but prior to the separation of human and chimpanzee lineages more than 5-7 million years ago (Bergstrom et al. 1998; Gagneux et al. 1999; Horai et al. 1995). This duplication does not appear to have an obvious phenotypic effect, and the presence of two *SMN* genes may have provided a selective advantage; whereas ablation of the single ancestral *SMN* gene in the mouse causes embryonic lethality (Schrank et al. 1997), the presence of *SMN2* provides partial compensation in human as demonstrated by the finding that human fetuses with SMA develop much further and much longer than *Smn*-deficient mice (Crawford and Pardo 1996). As many as 20 %-50 % of duplicated genes are preserved but are subjected to loss-of-function mutations that led to gene diversification (Lynch and Conery 2000). The C-to-T mutation in exon 7 of the *SMN2* gene probably represents one such loss-of-function mutation, precluding *SMN2* from completely complementing the loss of *SMN1* (Rochette et al. 2001).

Some 3.4 % of patients with SMA are compound heterozygotes with a deletion of *SMN1* on one chromosome and an intragenic *SMN1* mutation on the other chromosome (Wirth et al. 1999). About 35 subtle mutations have been identified so far, many of these being missense mutations shown to disturb the proper function of the SMN1 protein (Buhler et al. 1999; Lorson and Androphy 1998; Sun et al. 2005). About 4 % of patients showing a clear SMA phenotype undistinguishable from proximal SMA fail to show any mutation within the *SMN1* gene pointing towards genetic heterogeneity (Wirth et al. 1999).

### 1.3. Gene conversion, deletion and *de novo* mutation

Homozygous absence of either *SMN1* in patients with SMA or of *SMN2* in controls can be the result of two different mechanisms: deletion or gene conversion (Burghes 1997; Wirth et al. 1997a; Wirth et al. 1997b). Approximately 50 % of type I SMA patients have a single copy of *SMN2* on each chromosome, so that the *SMN1* gene is deleted and *SMN2* copy number is unaffected (DiDonato et al. 1994; Lefebvre et al. 1995; Melki et al. 1994a; Wirth et al. 1995b). The genotype of one *SMN2* copy on each chromosome, together with the loss of *NAIP*, occurs only on type I SMA chromosomes and implies a large deletion (Burlet et al. 1996; DiDonato et al. 1994; Lefebvre et al. 1995; Melki et al. 1994b; Rodrigues et al. 1996; Wirth et al. 1995a). In type II and type III SMA although patients lack *SMN1*, they most often have one chromosome with one copy of *SMN2* and have the other chromosome with two copies of *SMN2* (Fig. 3) (DiDonato et al. 1994; Wirth et al. 1995a). In type II and III SMA, the *SMN1* gene is missing, but the *NAIP* gene is present, as are the markers that lie in the 5' end of the *SMN1* gene.

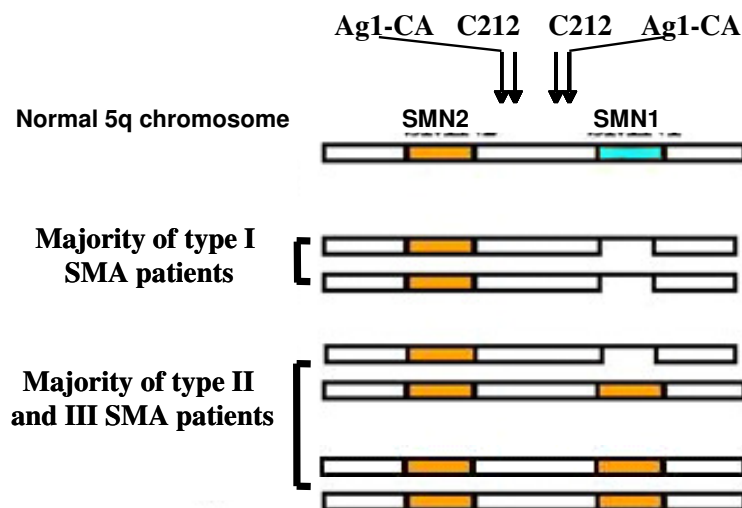


**Fig. 3** Schematic representation of the most frequently observed SMA chromosomes in acute SMA (type I) and mild SMA (type II/III). While type I SMA chromosomes usually carry true *SMN1* deletions on both 5q13 homologs, type II and III SMA chromosomes carry either on one or on both 5q13-homologs an increased *SMN2* copy number caused by gene conversion of *SMN1* into *SMN2* (Wirth 2000).

Because the *SMN1* gene is not detected but the markers reveal that the locus is still present, another mechanism besides deletion of *SMN1* must be operating; the most likely mechanism is conversion of *SMN1* to *SMN2*. Because the *SMN1* gene is absent in all SMA types, the increase in *SMN2* copy number indicates that a large number of type II and III SMA chromosomes contain a converted allele, rather than a deleted allele. In conversion of *SMN1* to *SMN2*, there is gain of copy number of *SMN2*, which will alter the

distribution of *SMN2* alleles; deletion of *SMN1* will not alter the distribution of *SMN2* alleles. Chimeric genes have been identified as SMA alleles and can arise by one of two mechanisms:

1. a deletion that removes the material between the *SMN1* and *SMN2* gene and fuses the 5' end of the *SMN2* gene to the 3' end of the *SMN1* gene or,
2. a conversion event that effects exon 7, but not exon 8 of the *SMN1* gene (Hahnen and Wirth 1996).

The chimeric genes formed by deletion and joining of the *SMN2* to *SMN1* are severe-SMA alleles. Hahnen et al. (1996) showed that chimeric *SMN* genes can occur in type I SMA chromosomes such that there is one chimeric gene on one chromosome 5 (evidence is based on marker studies). Gene conversion leads to an increase of copy number of either *SMN1* or *SMN2*, with simultaneous decrease of the *SMN* counterparts. When *SMN1* is converted into *SMN2*, the chromosomes carry two *SMN2* copies and no *SMN1*. When *SMN2* is converted into *SMN1* the chromosomes carry two *SMN1* copies and no *SMN2*. In the first case an "SMA chromosome" with an increased number of *SMN2* is generated, in the second case a "normal chromosome" with two *SMN1* genes on one chromosome will arise. Additionally, a high percentage of unequal crossing-over, causing either deletions or duplications can be observed in the region that arise as a consequence of the polymorphic character of the 500 kb repeated units. These mechanisms are also responsible for about 2 % of de novo mutations observed among patients with SMA.

#### 1.4. Survival motor neuron transcripts

Almost every protein-coding gene in humans is interspersed by non-coding sequences, known as introns. Splicing is the post-transcriptional process in which these introns are excised from precursor mRNA molecules (pre-mRNA) and the coding exons are ligated (Horiuchi and Aigaki 2006).

The *SMN* gene is ubiquitously expressed. *SMN1* produces mainly full-length transcripts that contain all nine exons (1, 2a, 2b, 3-8) whereas *SMN2* produces mainly alternatively spliced transcripts that lack exon 7 and carry only a small amount (~10%) of full-length (FL) transcripts (Burglen et al. 1996; Helmken et al. 2003; Lefebvre et al. 1995). FL-*SMN* transcripts derived from both *SMN* copies encode an identical FL-*SMN* protein composed of 294 amino acids, with a stop codon located in exon 7. In comparison, the *SMN2* $\Delta$ 7 transcripts encode a truncated *SMN* protein of 282 amino acids, with a C-terminus that differs from the FL-*SMN* protein by the last 4 amino acids. The truncated protein is unstable and shows a reduced oligomerization capacity which has been shown to be essential for the proper *SMN* function (Burglen et al. 1996; Lefebvre et al. 1995; Lorson and Androphy 1998; Lorson et al. 1999; Lorson et al. 1998). Additionally, both *SMN* genes produce very low amounts of alternatively spliced transcripts lacking either exon 3, exon 5 or both (Gennarelli et al. 1995). Skipping of these exons produces in frame proteins lacking the respective encoded domains. Especially the loss of exon 3 is of particular interest, since the corresponding region contains a so called Tudor domain that is essential for the interaction of *SMN* with Sm proteins. Absence or missense mutations within the Tudor domain either abolish or reduce the ability of *SMN* to interact with Sm proteins (Buhler et al. 1999; Mohaghegh et al. 1999; Sun et al. 2005).

*SMN* exon 7 spans 54 nucleotides and harbours a stop codon at nt position 49 to 51. The last position of exon 7 is an adenosine residue, which places exon 7 into the minor group of internal exons lacking a 3'-end G residue (Burge et al. 1999). Exon 7 is characterized by a weak 3'ss due to a suboptimal polypyrimidine tract (Lim and Hertel 2001). Correct splicing of exon 7 depends on various *cis*-acting elements (enhancers and silencers) localized within exon 7 as well as within the introns 6 and 7 (Cartegni and Krainer 2002; Hofmann et al. 2000; Hofmann and Wirth 2002; Kashima and Manley 2003; Lorson and Androphy 2000; Lorson et al. 1999; Miyaso et al. 2003; Young et al. 2002b). They are recognized by various splicing factors, SR and SR-like proteins as well as hnRNPs (Cartegni and Krainer 2002; Helmken et al. 2003; Hofmann et al. 2000; Hofmann and Wirth 2002; Young et al. 2002b). Most of the elements seem to be highly conserved and are also involved in pre-mRNA splicing of the murine *Smn* gene (DiDonato et al. 2001). There is no tissue specificity observed concerning the ratio of FL-*SMN* vs. *SMN* $\Delta$ 7 in a certain individual as demonstrated by quantitative RT-PCR (Helmken et al. 2003; Lorson et al. 1999). In 1999, Lorson and colleagues demonstrated that C-to-T transition in exon 7 is sufficient to cause skipping of this exon of the *SMN2* gene. They constructed wildtype *SMN1* and *SMN2* minigenes (exon 6 to exon 8) as well as hybrid minigenes in which the five nucleotide differences were exchanged one by one either on the *SMN1* background with *SMN2* specific nucleotides or vice-versa, followed by *in vivo* splicing and analysis of *SMN* transcripts (Lorson et al. 1999). They demonstrated that an exonic splicing enhancer (ESE) is disrupted by the C-to-T exchange within the *SMN2* gene, thus being responsible for the alternative splicing (Lorson and Androphy 2000; Lorson et al. 1999). Later, Cartegni and Krainer stated that the C-to-T exchange lies within a conserved heptamer motif, an ESE, CAGACAA, which is directly recognized by the SR-rich splicing-factor SF2/ASF in *SMN1*, but not in *SMN2* derived transcripts. UV-crosslinking experiments showed specific interaction of SF2/ASF with exon 7 *SMN1* but not with *SMN2*, thus promoting exon 7 inclusion (Cartegni and Krainer 2002). In contrast to these findings, the group of Manley demonstrated that the C-to-T exchange in *SMN2* creates a new exonic splicing silencer rather than disrupting an ESE, which finally functions as a binding site for the repressor protein hnRNP-A1. It has been shown that the reduction of hnRNP-A1 in HeLa cells by RNA interference promotes exon 7 inclusion in *SMN2*. Using *in vitro* UV-cross linking, hnRNP-A1 was found to bind exon 7 of *SMN2* but not of *SMN1* (Kashima and Manley 2003). A controversial debate is still ongoing and further experiments have to prove which of the hypotheses is correct. Meanwhile, Singh and colleagues showed that the 5' end of exon 7 contains an extended inhibitory context composed of several overlapping sequence motifs. Together, they regulate a larger sequence than the hnRNP-A1 *binding* site (Singh et al. 2004a, b).

In addition to the 5' end ESE and/or ESS, another ESE is found in the center of exon 7 that binds the SR-like splicing factor Htra2- $\beta$ 1 (Hofmann et al. 2000). Htra2- $\beta$ 1 is the ortholog of *D. melanogaster* transformer-2 (*Tra 2*), a gene essential for sex differentiation which is regulated by alternative splicing (Baker 1989). It is likely to be an important developmental regulator of alternative splicing that acts by binding to purine-rich elements in or near exons (Tacke et al. 1998). Tra2- $\beta$ 1 binds and enhances the incorporation of a novel testis-specific alternative exon of the homeodomain-interacting protein kinase *HipK3* (*HipK3-T*) and promotes exclusion of another exon in the *HipK3* gene, the ubiquitous alternative (U) exon (Venables et

al. 2005). A similar situation was recently reported, whereby Tra2- $\beta$ 1 promotes inclusion of exon 10 and exclusion of exon 2 of the important neural protein Tau (Wang et al. 2005).

The gene for Htra2- $\beta$  has been mapped to chromosome 3q26.2-q27, contains 10 exons, and the coding region spans 21 kb (Nayler et al. 1998). RT-PCR and analysis of *Htra2- $\beta$*  cDNA indicated that at least four different *Htra2- $\beta$*  isoforms are generated by alternative splicing: *Htra2- $\beta$ 1* (exons 1, 3-10), *Htra2- $\beta$ 2* (exons 1-2), *Htra2- $\beta$ 3* (exons 1,4-10), and *Htra2- $\beta$ 4*, which is generated by over reading the polyadenylation signal in exon 2a using the 5' splice site of exon 2b (Nayler et al. 1998). Two of these isoforms, *Htra2- $\beta$ 3* and *Htra2- $\beta$ 4*, appear to be tissue-specific and developmentally regulated, whereas *Htra2- $\beta$ 1* and *Htra2- $\beta$ 2* are ubiquitously expressed bearing high levels in brain and testis (Nayler et al. 1998). Protein-RNA binding experiments showed a strong interaction of Htra2- $\beta$ 1 with the GA-rich region localized in the center of exon 7 of *SMN1* and *SMN2* producing correctly spliced transcripts (Hofmann et al. 2000; Hofmann and Wirth 2002). In addition, the splicing factor SRp30 (an SR-rich splicing factor) as well as hnRNP-G and RPM (belonging to the group of hnRNPs) directly bind Htra2- $\beta$ 1 and further enhance the inclusion of exon 7 (Hofmann and Wirth 2002; Young et al. 2002b) (Fig. 4).

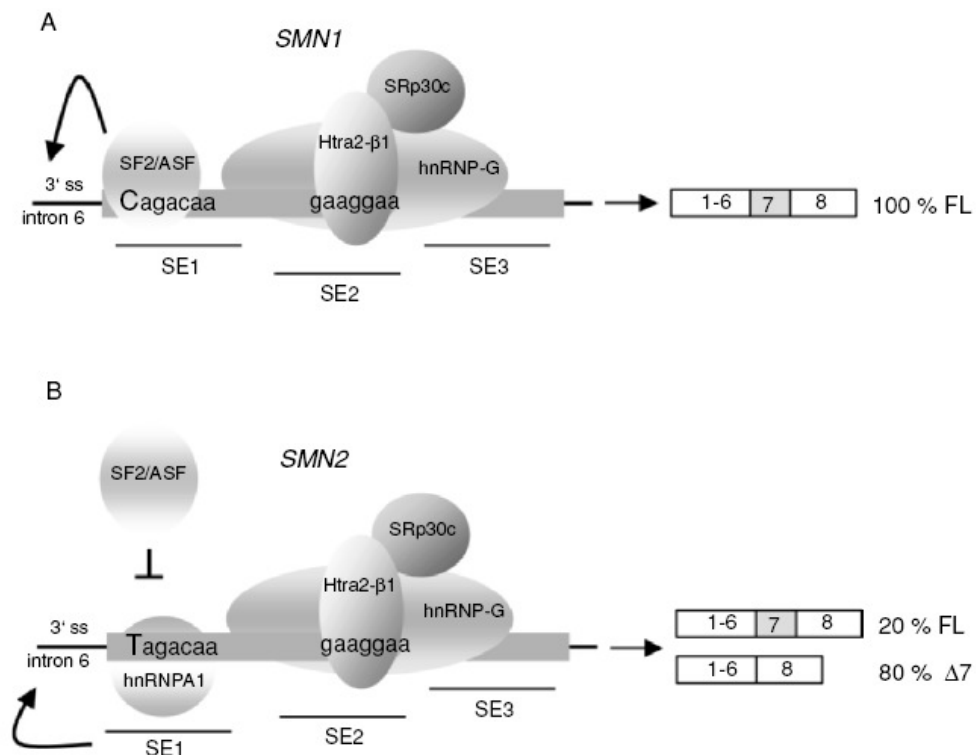


**Fig. 4 Splicing regulation of *SMN* exon 7. (A) *SMN1* exon 7 contains a heptamer sequence (SE1) at the 5' end that is recognized by the SR-protein SF2/ASF. (B) In *SMN2*, the C-to-T transition disrupts the critical heptamer sequence within SE1, and the splicing factor SF2/ ASF cannot bind anymore to exon 7, which results in skipping of this exon. Furthermore, the C-to-T transition in *SMN2* exon 7 promotes an inhibitory effect of hnRNP-A1 and thus facilitates the exclusion of exon 7 (Wirth et al. 2006b).**

Both *SMN1* and *SMN2* contain an ESE in the central part of exon 7 (SE2) that is recognized by Htra2- $\beta$ 1 and its interacting partners hnRNP-G and SRp30c. Overexpression of the SE2-dependent splicing factors restores FL-*SMN2* transcript to about 80 %. At the 3' end of exon 7, another exonic splicing enhancer (SE3) has been identified. Furthermore, intron 7 contains an ISS (ISS-N1) that exerts its function on the positive acting exonic and intronic elements (curved arrows in Fig. 4). The *trans*-acting splicing factors that bind the intronic splicing elements or SE3 are not yet identified (Wirth et al. 2006a).

The abundant heterogeneous nuclear ribonucleoproteins (hnRNPs) that coat nascent transcripts often inhibit splicing, and the effect of Tra2- $\beta$ 1 on the splicing of *tau* and *SMN* is antagonized by hnRNP-A1 and hnRNP G (Andreadis 2005; Hofmann et al. 2000; Hofmann and Wirth 2002; Kashima and Manley 2003; Nasim et al. 2003; Venables et al. 2000). This network of splicing factor binding to the central ESE in exon 7 is the most likely responsible for the 10-15 % FL-mRNA generated by *SMN2*. Overexpression of these splicing factors either separate or in combination restores the splicing capacity of *SMN2* minigenes up to 80 % and substantially increases endogenous SMN protein levels (Brichta et al. 2003; Hofmann et al. 2000; Hofmann and Wirth 2002). A potential therapy of SMA based on the modulation of the *SMN2* splicing pattern that increases FL-SMN levels has been hypothesized (Hofmann et al. 2000).

Exon 7 skipping in *SMN2* is furthermore facilitated by two intronic splicing silencer localized in intron 6 from -112 to -68 bp (element 1) and intron 7 from +59 to +72 (element 2) (Miyajima et al. 2002; Miyaso et al. 2003). However, mutations or deletions within these regions do not affect the correct splicing of wild type *SMN1* pre-mRNA. A 33 kD protein has been shown to interact with element 1 of *SMN2* but not of *SMN1*. Element 2 possesses a characteristic stem-loop structure, in which the correct matching of the nucleotides within the stem is essential. In these works, other genes with a complete matching of the nucleotides within the stem-loop have been identified, although the experimental proof for the role in the regulation of splicing still has to be given (Miyajima et al. 2002; Miyaso et al. 2003).

## 1.5. The SMN protein and its functions

SMN is a ubiquitously expressed protein with a molecular weight of 38kDa. It has been highly conserved through evolution. In humans, SMN is a protein found in the cytoplasm and the nucleus of cells, where it is present throughout the nucleoplasm and is highly enriched within discrete bodies called gems (for "Gemini" of Cajal bodies) (Liu and Dreyfuss 1996).

SMN protein is encoded by eight exons generating a multidomain polypeptide. It contains the central Tudor domain (encoded by exon 3) flanked by a N-terminal lysine (K)-rich sequence (encoded by exon 2) and in the C-terminal regions, by a proline (P)-rich region (encoded by exons 4 and 5), a tyrosine-glycine (YG)-box (encoded by exon 6) and the exon 7 encoded domains. Missense mutations have been identified in several of these regions, suggesting that each of these domains may be functionally important. The Tudor domain, named because of its structural homology to repeats of the *Drosophila tudor* protein, is conserved among different RNA-binding proteins (Ponting 1997; Selenko et al. 2001) and

**Table 1** The SMN protein is present as part of a large macromolecular complex containing a number of common core components and a set of transiently or substoichiometrically interacting partners.

SMN complex component	Direct/Indirect SMN interaction	Function	Reference
<b>Core components</b>			
Gemin1 (SMN)	+		(Liu et al. 1997; Lorson et al. 1998)
Gemin2 (SIP 1)	+	snRNP biogenesis and pre-mRNA splicing	(Liu et al. 1997)
Gemin3 (DP103)	+	snRNP biogenesis and pre-mRNA splicing	(Campbell et al. 2000; Charroux et al. 1999)
Gemin4 (GIP1)	-	snRNP biogenesis and pre-mRNA splicing	(Charroux et al. 2000; Meister et al. 2000)
Gemin5 (p175)	+	snRNP biogenesis and pre-mRNA splicing s	(Gubitz et al. 2002)
Gemin6	-	snRNP biogenesis and pre-mRNA splicing	(Pellizzoni et al. 2001b)
Gemin7	+	snRNP biogenesis and pre-mRNA splicing	(Baccon et al. 2002)
Gemin8	-	snRNP biogenesis and pre-mRNA splicing	(Carissimi et al. 2006)
unrip	-	snRNP biogenesis and pre-mRNA splicing	(Grimmler et al. 2005; Meister et al. 2001b)
<b>Substrates and substoichiometric components</b>			
Sm proteins	+	snRNP biogenesis and pre-mRNA splicing	(Friesen and Dreyfuss 2000; Liu et al. 1997)
LSm4	+	snRNP biogenesis and pre-mRNA splicing	(Brahms et al. 2001; Friesen and Dreyfuss 2000)
Fibrillarin	+	Assembly of snoRNPs	(Jones et al. 2001; Pellizzoni et al. 2001a)
GAR1	+	Assembly of snoRNPs	(Pellizzoni et al. 2001a)
Coilin	+	Recruitment of SMN to Cajal bodies	(Hebert et al. 2001)
U1-A, U2-A'	unknown	snRNP biogenesis	(Liu et al. 1997)
Profilin	+	Control of actin dynamics	(Giesemann et al. 1999)
ZPR1 (zinc-finger protein 1)	+	Caspase activation and apoptosis; snRNP assembly/maturation	(Gangwani et al. 2001)
OSF (Osteoclast-stimulating factor)	+	Regulation of osteoclast formation and activity	(Kurihara et al. 2001)
Nucleolin and B23	-	Cell growth and proliferation control, programmed cell death, cell surface signal transduction, and differentiation and maintenance of neural tissues	(Lefebvre et al. 2002)

RNA helicase A	+	Transcription	(Pellizzoni et al. 2001c)
RNA polymerase II	-	Transcription	(Pellizzoni et al. 2001c)
hnRNP Q and R	+	RNA transport along the axons	(Mourelatos et al. 2001; Rossoll et al. 2002)
hsc70 (heat shock protein 70)	unknown	Post-translational protein transport	(Meister et al. 2001b)
snurportin and importin $\beta$	- and +	Transport of snRNPs to nucleus	(Narayanan et al. 2002)
galectin 1 and 3	-	snRNP biogenesis and pre-mRNA splicing	(Park et al. 2001)
p53	+	Apoptosis	(Young et al. 2002a)
ISG20	unknown	Degradation of single-stranded RNA	(Espert et al. 2006)
FGF-2 (fibroblast growth factor 2)	+	Neurotrophic factor for motor neurons	(Claus et al. 2004)
mSin3A	unknown	Transcriptional regulation	(Zou et al. 2004)
EWS (Ewing Sarcoma)	+	Transcriptional regulation	(Young et al. 2003)
Bcl-2	+	Anti-apoptosis	(Iwahashi et al. 1997)
FUSE binding protein	+	Regulator of transcription and mRNA stability	(Rothe et al. 2006; Williams et al. 2000)
TIA-1 and TIAR	unknown	RNA metabolism, translation regulation, assemblers of stress granules	(Hua and Zhou 2004b)
Rpp20	+	RNA metabolism, component of stress granules	(Hua and Zhou 2004a)
PPP4 (Protein phosphatase 4)	-	Ubiquitous protein phosphatase that dephosphorylates serine and threonine residues	(Carnegie et al. 2003)
TGS1 (trimethylguanosine synthase 1)	+	snRNA cap hypermethylase	(Mouaikel et al. 2003)
<b>Viral proteins</b>			
Papilloma virus E2	+	Nuclear transcription activation	(Strasswimmer et al. 1999)
Epstein-Barr virus nuclear antigen 2a	+	Transcriptial regulators	(Voss et al. 2001)
Epstein-Barr virus nuclear antigen 6 (or 3c)	-	Transcriptial regulators	(Krauer et al. 2004)
Minute virus NS1 and NS2	unknown	Viral replication and a potent transcriptional activator.	(Young et al. 2002c, d)

mediates SMN interaction with arginine-glycine (RG) motifs in several proteins (Gubitz et al. 2004; Meister and Fischer 2002) including the Cajal body marker coilin and the Sm core proteins, after their symmetrically dimethylated mediates arginine (sDMA) isoforms (Boisvert et al. 2002; Friesen et al. 2001b; Hebert et al. 2002; Meister and Fischer 2002). The K-rich sequence is embedded in the interspecies

conserved RNA-binding domain (Bertrand et al. 1999; Lorson et al. 1998). The P-rich domain associates with the actin-binding protein profilin (Giesemann et al. 1999). The YG-box domain is implicated in self-association *in vitro* (Lorson and Androphy 1998) and a putative cytoplasmic retention signal is encoded by exon 7 (Zhang et al. 2003). The central Tudor domain cooperates with the YG-box and the K-rich sequence for the accumulation of SMN in Cajal bodies. One explanation for the role of the YG-box in Cajal bodies localization is that self-oligomerization might enhance SMN accumulation in Cajal bodies by promoting binding to Cajal bodies components, such as snRNPs (Fischer et al. 1997; Liu et al. 1997; Pellizzoni et al. 2001a; Wang and Dreyfuss 2001b). The K-rich sequence encoded by the exon 2b is required for the nucleolar accumulation of truncated SMN proteins (Renvoise et al. 2006). All directly and indirectly interacting SMN partners known so far are listed in table 1 (Wirth et al. 2006b).

Gems have similarities in size and number to Cajal (coiled) bodies and are often associated with them (Liu and Dreyfuss 1996). Cajal bodies were first described in 1903 and are known to contain high levels of factors involved in the transcription and processing of many types of nuclear RNAs, including small nuclear ribonucleoproteins (snRNPs), nucleolar ribonucleoproteins (snoRNPs), and the three eukaryotic RNA polymerases (Gall 2003a, b; Ogg and Lamond 2002). However, since Cajal bodies are deficient in DNA, nascent pre-mRNA, and non-snRNP essential for splicing factors, they are probably not active sites for transcription or splicing (Ogg and Lamond 2002). Instead, they most likely are locals where the assembly and/or modification of the nuclear transcription and RNA processing machinery take place (Gall 2003a, b). Double-label immunofluorescence microscopy using antibodies against SMN as a marker of gems, and p80-coilin as a marker for Cajal bodies (Andrade et al. 1991), revealed that gems and Cajal bodies mostly co-localize in some cell lines and adult tissues but are separated in fetal tissues and several types of cultured cells (Paushkin et al. 2002). This indicates that gems and Cajal bodies are distinct nuclear structures that have a dynamic functional relationship. The interaction between gems and Cajal bodies may be mediated, at least in part, by the capacity of SMN and coilin to bind each other (Hebert et al. 2001). Gems are also separated from interchromatin granule clusters (or speckles), which are DNA – free nuclear domains composed of densely packed ribonucleoprotein particles enriched in mature snRNPs and protein splicing factors (Almond et al. 2003). Newly assembled spliceosomal mRNPs re-entering the nucleus associate with SMN (Narayanan et al. 2004) and transiently move into Cajal bodies (Jady et al. 2003; Sleeman et al. 2001). The role of Cajal bodies in snRNP maturation steps (Jady et al. 2003; Nesic et al. 2004) and in regeneration of snRNPs after splicing has been described (Pellizzoni et al. 1998; Schaffert et al. 2004; Stanek and Neugebauer 2004). It has been shown that cells transfected with SMA mutants showed severe reduction of snRNPs in Cajal bodies (Renvoise et al. 2006).

### 1.5.1. SMN complex

When isolated from cultivated cells, a large proportion of cellular SMN is present as part of a multisubunit macromolecular entity. SMN protein oligomerizes and forms a stable complex called the SMN complex, with a group of proteins named the Gemins. These include Gemin 2 (formerly SIP1) (Liu et al. 1997),

Gemin 3/ DP103 (a DEAD-box RNA helicase) (Campbell et al. 2000; Charroux et al. 1999), Gemin 4 (Charroux et al. 2000; Meister et al. 2000), Gemin 5/ p175 (a WD repeat protein) (Gubitz et al. 2002), Gemin 6 (Pellizzoni et al. 2001b), Gemin 7 (Baccon et al. 2002) and Gemin 8 (Carissimi et al. 2006). This complex is large and sediments in sucrose gradients as hetero-disperse particles of 30-70 S (Paushkin et al. 2002). The Gemins co-localize with SMN in gems and are also present throughout the cytoplasm and, albeit at lower levels, in the nucleoplasm (Baccon et al. 2002; Charroux et al. 1999; Charroux et al. 2000; Gubitz et al. 2002; Liu et al. 1997; Pellizzoni et al. 2002a).

Gemin 4 is the only SMN complex component that also localizes to the nucleolus (Charroux et al. 2000; Paushkin et al. 2002). Based on their stable association with SMN, the Gemins can be considered as integral components of the SMN complex and are readily isolated by coimmunoprecipitation using anti-SMN antibodies or antibodies to the Gemins, even under stringent high salt conditions (750 mM NaCl) (Paushkin et al. 2002). The function of the multi-unit SMN-complex relies on the ordered interplay of the nine components SMN, Gemin 2-8 and unrip. Recent studies have revealed a framework of the SMN-complex with SMN, Gemin 7 and Gemin 8 as its backbone (Otter et al. 2006) (Fig. 5).

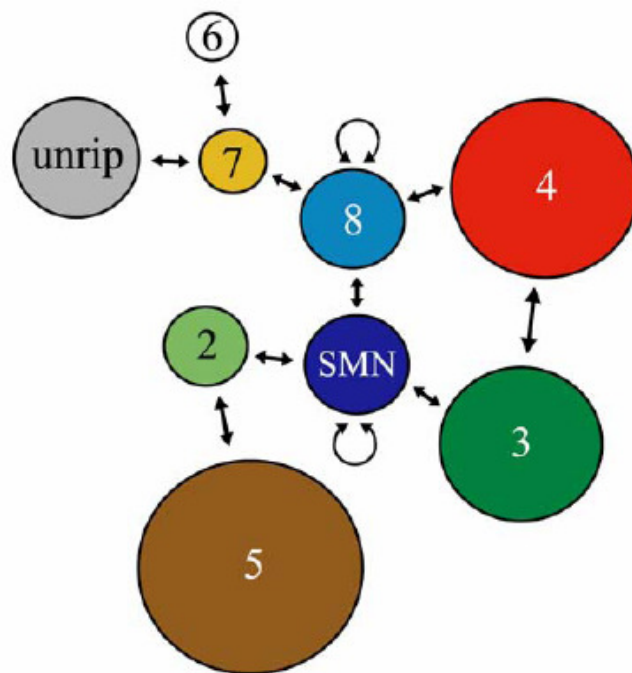


**Fig. 5 Schematic representation of all interactions within the SMN-complex. SMN, Gemin 7 and Gemin 8 provide a binding platform for the other components of the complex. SMN binds Gemin 2, Gemin 3 and Gemin 8. Gemin 8 interacts in turn with Gemin 4 and Gemin 7. Gemin 7 recruits unrip and Gemin 6 via direct interaction (Otter et al. 2006).**

These three proteins provide a binding platform for the other components of the complex via multiple interactions: SMN binds to Gemin 2 (Baccon et al. 2002), Gemin 3 (Campbell et al. 2000; Charroux et al. 1999) and Gemin 8. Gemin 8, in turn, interacts with Gemin 4 and 7. Finally, Gemin 7 recruits unrip and Gemin 6 via direct interaction (Baccon et al. 2002; Carissimi et al. 2006; Grimmeler et al. 2005). The peripheral protein Gemin 5 can be dissociated upon treatment with high salt (Otter et al. 2006). This finding suggests its incorporation into the complex via weak interaction mediated by Gemin 2 and possibly Gemin 4.

Conflicting data regarding the function of Gemin 5 have been recently reported (Battle et al. 2006; Feng et al. 2005; Shpargel and Matera 2005). In two reports RNAi was used to show that Gemin 2 is dispensable for the assembly reaction (Feng et al. 2005; Shpargel and Matera 2005). In contrast, evidence for an essential role of Gemin 5 in the formation of U snRNPs has been provided in another recent report (Battle et al. 2006).

Gemin 2 was formerly referred to an SIP-1 (SMN interacting protein 1) and binds to a distinct site at the N-terminus (aa 13-14) of SMN. Although Gemin 2 and SMN are closely interacting proteins, part of the same complex, the same pathway and exhibit the same cellular location in gems and cytoplasm, it has been shown that SIP1 is neither responsible for 5q-unlinked SMA nor for the phenotypic variability observed in SMA families (Helmken et al. 2000). The SMN protein likely plays a central role in the structural organization of the SMN complex as it is the essential to bring together the different subunits. The presence of multiple subunits and the seemingly modular organization of the SMN complex due to SMN's ability to oligomerize, which is impaired in *SMN* mutants of SMA patients (Lorson et al. 1998; Pellizzoni et al. 1999), support the current view of the SMN complex as a dynamic macromolecular machine capable of multiple tasks.

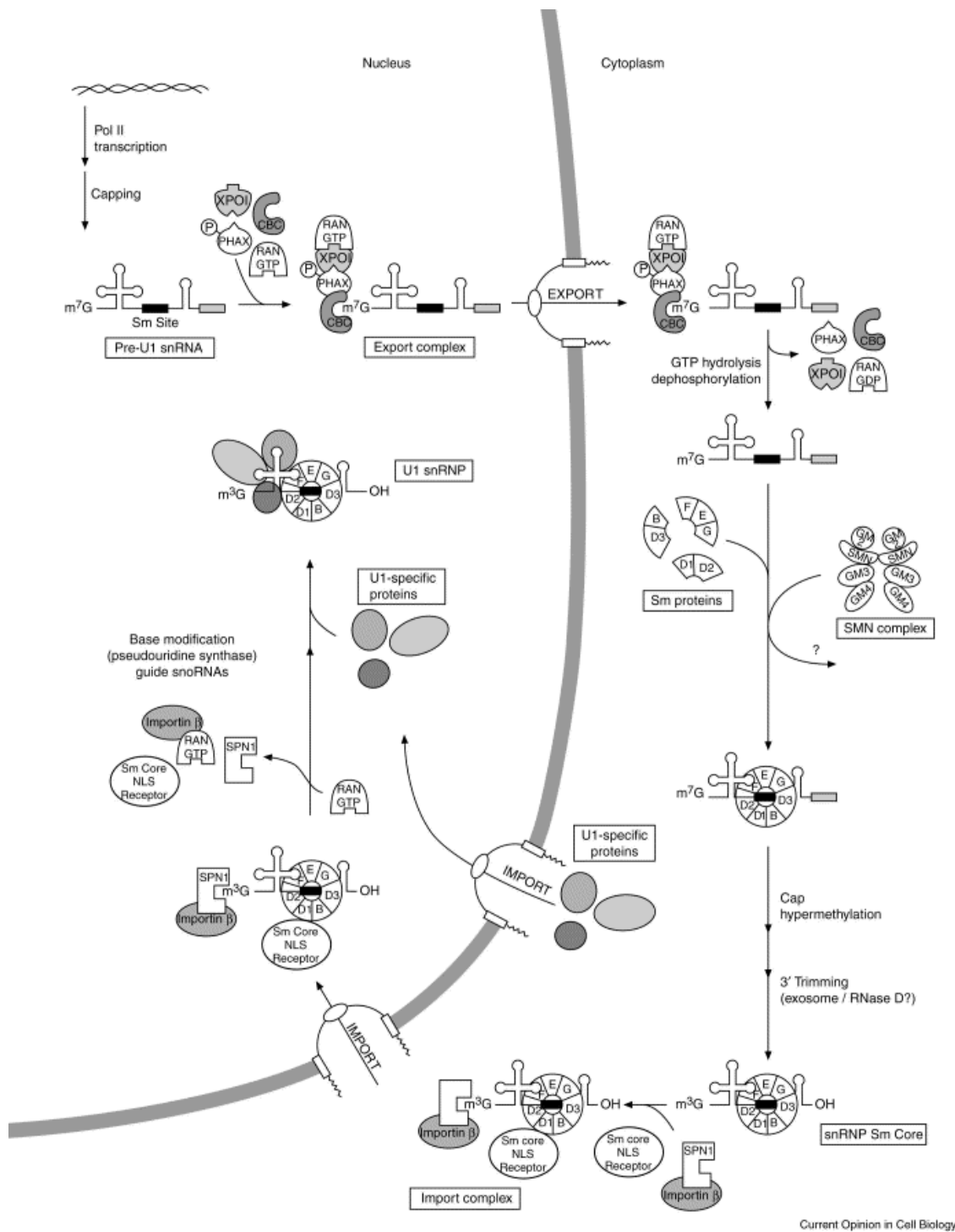
The SMN complex interacts with several proteins, some of which can be considered SMN complex substrates. Among these substrates are the Sm proteins and Sm-like (Lsm) proteins of the snRNPs, which are essential components of the splicing machinery. Intriguingly, each component of the SMN complex has the capacity to bind to a subset of the Sm/Lsm proteins (Baccon et al. 2002; Charroux et al. 1999; Charroux et al. 2000; Gubitz et al. 2002; Liu et al. 1997; Pellizzoni et al. 2002b). Additional SMN complex substrates are the snoRNP proteins, fibrillarin and GAR1, as well as hnRNP U, Q and R, RNA helicase A, coilin, nucleolin, and Epstein–Barr virus nuclear antigen 2 (Barth et al. 2003; Hebert et al. 2001; Jones et al. 2001; Lefebvre et al. 2002; Mourelatos et al. 2001; Pellizzoni et al. 2001a; Rossoll et al. 2002). Recently, it was also reported that protein phosphatase 4 (PPP4), a ubiquitous essential protein serine/threonine phosphatase, is associated with the SMN complex via binding to Gemin4 and/or Gemin3, and overexpression of catalytic (PPP4c) and regulatory (R2) domains of PPP4 was found to modify the temporal localization of newly formed snRNPs in HeLa cells (Carnegie et al. 2003). However, whether and how this phosphatase protein affects the functions of Gemin 3, Gemin 4 and/or the SMN complex awaits further clarification. Gemin 3 and 4 have also been shown to be components of a 15S microRNP complex that contains eIF2C2, a member of the Argonaute protein family, and numerous miRNAs (Dostie et al. 2003; Mourelatos et al. 2002). These findings raised the interesting possibility that *SMN* deletions or loss-

of-function mutations in SMA patients may also affect the activity of miRNPs by, for example, affecting the balance of the shared complex components Gemin 3 and 4 between SMN complexes and miRNPs (Dostie et al. 2003). Finally, the list of proteins reported to interact with SMN also includes several proteins that neither contain RG-rich motifs nor interact with RNPs, such as profilin, the FUSE binding protein, ZRP1, p53, and the NS1 protein of min virus of mice (Young et al. 2002a; Young et al. 2002c). Recent studies have demonstrated that the zinc finger protein ZRP1 is part of a cytoplasmic snRNP complex that contains SMN, Sm proteins, U snRNA, snuportin 1 and importin  $\beta$  (Narayanan et al. 2002). The binding partner of ZRP1 in the SMN complex has not been yet identified, but it has been established that ZRP1 does not bind directly to SMN (Gangwani et al. 2001). ZRP1 co-localizes with SMN in the nucleus where both proteins accumulate in gems and Cajal bodies. It is likely that the binding of ZRP1 to SMN complexes is significant because mutations that are associated with SMA disease disrupt the association of ZRP1 with SMN complexes (Gangwani et al. 2001). Furthermore, it is established that SMA patients express low levels of ZRP1 (Helmken et al. 2003). *Zpr1* gene silencing and *Zpr1* gene disruption in mouse development has demonstrated that ZRP1 is an essential protein (Gangwani et al. 2005). ZRP1 deficiency causes defects in both the cytoplasmic and nuclear population of spliceosomal snRNPs. Specifically cytoplasmic snRNPs are not detected in *Zpr1*<sup>-/-</sup> embryos. Furthermore, ZRP1 deficiency markedly disrupts the subnuclear structures (gems and Cajal bodies) where final maturation of snRNP complexes is observed (Gangwani 2006).

Most of the SMN complex substrates identified so far are constituents of various RNP complexes and contain sequence domains enriched in arginine and glycine residues. These RG-rich domains were shown to mediate the binding to the SMN complex (Barth et al. 2003; Brahms et al. 2001; Friesen et al. 2001a; Pellizzoni et al. 2001a; Pellizzoni et al. 2001c) and this motif among these binding partners may explain how the SMN complex can recognize such a multitude of different substrates. Moreover, modification of specific arginine residues within these RG-rich domains by symmetrical dimethylation greatly enhances the affinity of several of these substrates to SMN (Barth et al. 2003; Brahms et al. 2001; Friesen et al. 2001a).

It is of note that most SMN complex substrates characterized so far are components of various RNP complexes that are involved in diverse aspects of RNA processing. Studies in *Xenopus laevis* oocytes and mammalian cells have shown that SMN is involved in several aspects of cellular RNA metabolism including: snRNP assembly, pre-mRNA splicing, transcription and biogenesis of small nucleolar RNPs (sno RNPs) (Buhler et al. 1999; Fischer et al. 1997; Jones et al. 2001; Meister et al. 2001a; Meister et al. 2002; Meister and Fischer 2002; Pellizzoni et al. 2001a; Pellizzoni et al. 2001c; Pellizzoni et al. 1998; Pellizzoni et al. 2002b; Yong et al. 2002). It therefore became apparent that the SMN complex might take part in many aspects of cellular RNA metabolism. Indeed, a well-characterized function of the SMN complex is its role in the assembly of the spliceosomal snRNPs (Yong et al. 2004).

The spliceosome is the macromolecular entity that promotes and controls the splicing reaction. Within the assembled spliceosome, intron excision occurs in two chemical steps: first 5'ss cleavage and lariat formation, then 3'ss cleavage and exon ligation. Following exon ligation, complete spliceosome



Current Opinion in Cell Biology

**Fig. 6** The U snRNP biogenesis pathway. A cartoon model of the U1 snRNP maturation is shown. Subsequent to transcription and capping, the pre-U1 snRNA becomes complexed with several factors. In the following step the Sm proteins interact with the U snRNA's Sm site. This step is facilitated by the SMN complex. Subsequent to cap hypermethylation and 3' trimming, the snRNP Sm core is imported into the nucleus. Import is mediated by snurportin 1, which binds to the snRNA's m<sup>3</sup>G cap (Will and Luhrmann 2001).

disassembly would then free up its components for *de novo* synthesis of other spliceosomes. The functional subunits of the spliceosome are uridine-rich small nuclear ribonucleoproteins particles (U snRNP), which are composed of one (U1, U2, U5) or two (U4/U6) uridine-rich RNAs and characteristic sets of proteins (Will and Luhrmann 2001). Spliceosomes and their U snRNP subunits are formed in a highly ordered process. Seven so-called Sm proteins, which are common to all spliceosomal U snRNPs, are assembled on the U snRNA to form the core structure of these particles (Kambach et al. 1999a; Kambach et al. 1999b). These “Sm core domains” of U snRNPs additionally receive a distinct set of proteins, which confer specific activities to each snRNP (Will and Luhrmann 2001). During the past decade, it became evident that the assembly of U snRNP core structures requires assistance by the SMN protein *in vivo*. Using cell extracts and affinity purified components, it was shown that the SMN complex is essential and sufficient to mediate the ATP-dependent assembly of the seven-membered ring of the common Sm proteins around a highly conserved sequence motif of less than 10 nucleotides, called the Sm site, present in most snRNAs (Fig. 6).

The best-characterized function of the SMN complex is the assembly of the heptameric core of Sm proteins on spliceosomal snRNAs (Meister et al. 2002; Yong et al. 2004). After transcription, the Sn class of snRNAs (U1, U2, U4 and U5) are exported to the cytoplasm where they are assembled with the seven Sm proteins (SmB/B'), SmD1 to SmD3, SmE, SmF and SmG to form the Sm core. Newly translated Sm proteins bind first to pICln and the PRMT5 complex, which carries out the symmetrical dimethylation of specific arginine residues of a subset of Sm proteins, and then to the SMN complex (Friesen et al. 2001a; Friesen et al. 2001b; Friesen et al. 2002; Meister et al. 2001a; Meister et al. 2001b). This post-translational modification is carried out by a 20S arginine methyltransferase complex, the methylosome that contains the methyltransferase JBP1/ PRMT5, pICln, and MEP50 (a WD repeat protein) (Friesen et al. 2001a; Friesen et al. 2002; Meister et al. 2001a). The SMN protein complex is required for the specific assembly of Sm core complexes in U snRNAs. This is mediated by SMN interaction with the U snRNA (Yong et al. 2004) and with the Arg/Gly-rich COOH tails of SmB, SmD1 and SmD3 (Friesen and Dreyfuss 2000). High-affinity interactions with SMN require these Sm proteins to be modified to contain symmetrical dimethyl-arginine (Brahms et al. 2001; Friesen et al. 2001a). SMN plays a second role in the maturation of snRNPs following the assembly of snRNAs with Sm proteins. The Sm core undergoes hypermethylation to form the 2', 2', 7'-trimethyl-guanosine (TMG)5'-cap that is required for the recruitment of import receptors necessary for the translocation of snRNPs into the nucleus (Will and Luhrmann 2001).

Trimethylguanosine synthase 1 (TSG1), the enzyme that is responsible for the formation of the TMG 5'-cap, interacts with SMN (Mouaikel et al. 2003). The hypermethylated 5'-cap of U snRNA recruits snuportin 1 to the snRNP complex (Huber et al. 1998) and snuportin 1 is able to bind both SMN (Narayanan et al. 2002) and importin  $\beta$  (Huber et al. 1998) to facilitate nuclear import of mature snRNP complexes. Moreover, the SMN complex was found to function as a specificity factor for this assembly process by ensuring that Sm cores are only formed on the correct RNA molecules (Pellizzoni et al. 2002b). The ability of the SMN complex to facilitate and safeguard accurate snRNP assembly is based on its capacity to bind both Sm proteins and also snRNAs. Indeed, the SMN complex binds directly with high affinity and in

sequence-specific manner to several snRNAs (Yong et al. 2004; Yong et al. 2002). These observations suggest that the SMN complex brings the protein and RNA components together for snRNP assembly, thus serving as a genuine assemblyosome for Sm cores on snRNAs. Clearly, in the intricate microenvironment of the cell, a stringent specificity of snRNP assembly is of pivotal importance since haphazard binding of Sm proteins to nontarget RNAs would interfere with the functions of these RNAs. Thus, the SMN complex is not only an essential mediator of snRNP assembly but also provides stringent control over this process. Aside from its roles in snRNP assembly, the SMN complex most likely functions in the formation of other RNPs. For example, based on its direct interactions with fibrillarin and GAR1, two protein constituents of box C/D and box H/ACA snoRNPs, respectively, the SMN complex may play a role in the biogenesis of snoRNPs, which are involved in the post-transcriptional processing and modification of ribosomal RNAs (Jones et al. 2001; Pellizzoni et al. 2001a). Furthermore, a dominant negative mutant of SMN, SMN $\Delta$ N27, inhibits pre-mRNA splicing *in vitro* (Pellizzoni et al. 1998). Transient expression of this mutant in HeLa cells leads to a dramatic reorganization of snRNPs, RNA polymerase II (Pol II) transcription and processing machinery in the nucleus, probably by impairing the regeneration of functionally active snRNPs or other components of the spliceosome and the components of the Pol II transcription complex (Pellizzoni et al. 2001a; Pellizzoni et al. 1998). The involvement of the SMN complex in the biogenesis of the Pol II transcription factories may be mediated by its ability to interact with RNA helicase A, which binds Pol II and functions in transcription (Nakajima et al. 1997; Pellizzoni et al. 2001c). Recent reports have also suggested specific roles for SMN in the motor neuron. Studies in zebrafish using SMN-specific antisense morpholinos to knock down the SMN protein level throughout the entire embryo revealed motor axon-specific pathfinding defects (McWhorter et al. 2003). Furthermore, primary motor neurons isolated from a transgenic SMA mouse model were reported to exhibit reduced axon growth in culture when compared to motor neurons isolated from wild-type mice (Rossoll et al. 2003). The same study also showed that overexpression of SMN and hnRNP R in differentiating PC12 cells promotes neurite outgrowth and modulates the localization of  $\beta$ -actin mRNA in neurites, thus raising the possibility that SMN is involved in the transport of specific mRNA molecules in motor axons (Rossoll et al. 2003). However, whether the clinical symptoms of SMA are caused by deficiencies in functions of SMN that are specific to the motor neuron or common to all cells but at higher demand in this cell type must still be resolved.

### 1.5.2. Motor neuron specific functions of the SMN protein

The SMN protein is ubiquitously expressed in all cells, but the reason why a lack of SMN full-length protein specifically affects motor neurons remains unknown. The promoters of *SMN1* and *SMN2* were found to be virtually identical (Boda et al. 2004; Monani et al. 1999). Monani et al. identified an approximately 200 base pair element within the two promoters that results in high gene expression specifically in motor neurons (Monani et al. 1999). In 2004, Boda et al. transfected embryonic neurons and fibroblasts cells with a construct containing 4.6 kb of the *SMN* promoter and found that reporter gene

expression was specifically higher in neurons vs. fibroblast cells. These studies suggest that the *SMN* promoter is most active in motor neurons (Boda et al. 2004).

This issue of why reduced levels of a housekeeping protein like SMN may eventually lead to motor neuron degeneration in SMA remains to be solved.

- I. While the cause of motor neuron specific death in SMA patients is unknown, there are studies that suggest that the loss of motor neurons may not necessarily be the result of problems in assembly of U snRNPs and the resulting effect on mRNA splicing (Jablonka et al. 2004). A link between a defect of snRNP biogenesis and SMA is suggested by the impaired interaction with Sm proteins of SMN mutants of SMA patients and by the reduced snRNP assembly activity of extracts from SMA fibroblasts (Buhler et al. 1999; Pellizzoni et al. 1999; Wan et al. 2005). However, it is not known whether or how deficiencies in a function required by all cells may lead to the preferential degeneration of motor neurons in the spinal cord. One possibility is that motor neurons have a greater requirement for SMN function in snRNP assembly compared with other cell types. The first evidence that SMN function in snRNP assembly may not be uniformly required in all cells has been shown by (Gabanella et al. 2005). The levels of SMN activity observed in snRNP assembly were different among tissues and were most prominent in the developing CNS, due to the presence of a larger pool of SMN complexes competent for snRNP assembly in extracts from neuronal tissues. This observation may have important implications on the pathophysiological consequence of SMN deficiency in SMA patients. Jablonka et al. found that the majority of SMN protein that is unbound to Gemin 2 is localized in the axons and dendrites of motor neurons. Here, the SMN protein does not appear to be part of the same complex in the cell body that is involved in the assembly of U snRNPs (Jablonka et al. 2001). For the first time was demonstrated that SMN co-localizes with Gemin 2 and Gemin 3 in granules that distribute to neuronal processes and growth cones of primary hippocampal and motor neurons, and ES cell-derived motor neurons (Zhang et al. 2006). The observation for the lack of spliceosomal Sm proteins in processes suggests an additional function for SMN complexes that are localized to neuronal processes (Zhang et al. 2006).
- II. Recently, growing evidence has pointed out that the association between SMN and the cytoskeleton in axons and the axonal transport of SMN may be of relevance in the pathogenesis of SMA. The results of a study by Pagliardini et al. in 2000 suggest that SMN protein may be involved in axonal and dendritic transport of specific mRNAs (Pagliardini et al. 2000). It has been demonstrated that SMN protein accumulates in the axons and growth cones of neuron-like cells *in vivo* (Fan and Simard 2002) and anterior horn cells *in vivo* (Tizzano et al. 1998). These observations have been bolstered by experiments identifying the presence of SMN-containing granules within the neurites of chick cortical neurons and rat spinal motor neurons that associate with microtubules and exhibit bidirectional movement between the cell body and the growth cone (Zhang et al. 2003). These particles are RNP particles and suggest a specific role for the SMN protein in neuronal cells and, perhaps, an even more specific one in motor neurons. The same group observed that the SMN $\Delta$ 7 protein appears to be confined to the nucleus and may not translocate down axons. Neurons with a majority of SMN $\Delta$ 7 protein were found to have neurites that were 25 % shorter than neurons with FL-SMN. These results point to a

motor neuron specific function of SMN in SMA (Zhang et al. 2003). It is now fairly well-established that SMN can bind RNA (Bertrand et al. 1999; Lorson and Androphy 1998) and ribonucleoprotein particles (Jones et al. 2001; Liu and Dreyfuss 1996; Mourelatos et al. 2001). In addition to being a constituent of snRNPs, SMN may well be a constituent of a different RNP complex that in motor axons is capable of transporting specific RNAs to the growth cone in response to local cues during development. Data indicating a specific interaction between SMN and  $\beta$ -actin mRNA mediated by the protein hnRNP-R level support this idea (Rossoll et al. 2003). Reduced growth cone size,  $\beta$ -actin levels, and shorter neurites in primary motor neurons from SMA mice add further weight to this line of thought. In yet another report, FL-SMN appears to interact with two novel binding proteins, hnRNP-R and hnRNP-Q. These two proteins, like the Gemins, will not interact with the truncated SMN protein isoforms (Mourelatos et al. 2001; Rossoll et al. 2002). hnRNP-Q appears necessary for efficient pre-mRNA splicing *in vivo* (Mourelatos et al. 2001). Interestingly, hnRNP-R is specifically co-localized with SMN in motor axons and growth cones (Rossoll et al. 2002). The potential involvement of SMN protein in axonal processes, such as the translocation of  $\beta$ -actin mRNA (Rossoll et al. 2003) and/or the stability of  $\beta$ -actin mRNA (Jablonka et al. 2004), is perhaps a strong indication as to why the defect in the SMN1 gene may specifically lead to the loss of motor neurons and SMA. A 54 nucleotide sequence within 3' UTR of  $\beta$ -actin mRNA, termed the zipcode, is both necessary and sufficient for  $\beta$ -actin mRNA localization (Kislauskis et al. 1994). The mRNA binding protein, zipcode binding protein (ZBP1) binds directly to the  $\beta$ -actin zipcode (Ross et al. 1997) and this interaction is required for mRNA localization (Farina et al. 2003). ZBP1 has a nuclear localization and export sequences, and its shuttling between the nucleus and the cytoplasm allows for the export of an mRNP localization complex (Oleynikov and Singer 2003). In fibroblasts, the  $\beta$ -actin mRNP complex with ZBP1 is localized predominantly along actin filaments (Oleynikov and Singer 2003). In neurons, ZBP1 and  $\beta$ -actin mRNA are also co-localized in granules that are transported predominantly along microtubules, which allows for longer distance trajectories (Tiruchinapalli et al. 2003). Since, hnRNP-R was shown to associate with  $\beta$ -actin mRNA and enhances its localization, an SMN-hnRNP-R complex might contribute to  $\beta$ -actin mRNA localization. An exciting study showed that knock-down of SMN in zebrafish resulted in axon-specific pathfinding defects, that were partially rescued by full-length human SMN, but not by SMN $\Delta$ 7 (McWhorter et al. 2003). These studies suggest an inefficiency of SMN associated RNPs in motor neuron axons in SMA. As motor neurons have unusually long axons, their localized mRNPs could be more vulnerable to low levels of SMN. The presence of SMN in axons and dendrites of nerve cells, at a long distance from the nucleus, indicates some additional role for this protein, with profound implications for the characteristic loss of motor neurons in spinal muscular atrophy. In 2005, Sharma et al. found that SMN has some role in the transport of mRNPs in neuronal processes. The "axonal" SMN was found to be a part of a complex that is similar to that involved in nuclear splicing, except that it lacks the Sm core proteins of the nuclear snRNPs and is not associated with coilin p80, the marker protein of nuclear Cajal bodies. In addition, SMN may link the transport of mRNA and actin cytoskeleton via its interaction with profilin IIa (Sharma et al. 2005). Profilin can sequester actin monomers or promote polymerization by de-sequestering of

actin from the thymosin/  $\beta$ -actin pool and by adding these monomers to the free barbed ends of microfilaments (Pantaloni and Carlier 1993). Profilin also interacts with phosphatidylinositol 4,5-biphosphate (Lassing and Lindberg 1985) and with proline-rich sequences in Ena/VASP proteins (Gertler et al. 1996; Lambrechts et al. 2000b), N-WASP (Rohatgi et al. 1999) and diaphanous-related formin (Braun et al. 2002; Lambrechts et al. 2000b; Obermann et al. 2005; Watanabe et al. 1997). Five profilin isoforms have been identified in mammals, profilin I, IIa, IIb, III and IV, of which IIa and IIb arise from alternative splicing (Braun et al. 2002; Lambrechts et al. 2000b; Obermann et al. 2005). Profilin I is expressed ubiquitously, while profilin IIa is the major isoform in neuronal tissues both during development and in adult life (Lambrechts et al. 2000a). Profilin is also found in gems and Cajal bodies in the nucleus where it co-localizes with SMN, p-80 coilin and the Sm core proteins (Giesemann et al. 1999). The specific interaction with profilin IIa and the failure of profilin IIa to interact with pathogenic SMN mutants open a new view on the role of SMN in SMA pathogenesis. As a regulator of actin dynamics, profilin IIa is involved in correct neurite outgrowth (Da Silva et al. 2003). Knockdown of both profilin I and II inhibited neurite outgrowth (Sharma et al. 2005), possibly impairing actin dynamics by reducing the availability of profilin-G-actin complexes for microfilament growth. Co-localization of profilins with SMN in nuclear gems/Cajal bodies (Giesemann et al. 1999) and recent interest in the role of nuclear actin in intranuclear transport (Percipalle et al. 2001) raise the possibility of active transport of SMN complexes within the nucleus. Unrip (unr-interacting protein) is a novel member of the GH-WD repeat protein family and was identified as a component of SMN complexes purified from HeLa cells (Meister et al. 2001b). Although unrip itself has no intrinsic RNA binding properties, it has been shown to interact directly with unr, which is a member of the cold shock family of single stranded RNA-binding proteins (Hunt et al. 1999). Involvement with many aspects of RNA metabolism, and not splicing alone, is an emerging theme in studies of SMN and its associated proteins. By high-resolution fluorescence and quantitative imaging methods, it was possible to detect the presence and cotransport of an SMN-Gemin complex in neuronal processes and ES cell-derived motor neurons (Zhang et al. 2006). In contrast, spliceosomal Sm proteins were confined to the nucleus and perinuclear cytoplasm. The data suggested the presence of SMN and Gemin containing particles that do not co-localize (Zhang et al. 2006). These results suggest the presence of diverse types of SMN complexes that have functions in neurons, other than its well characterized role to assemble snRNPs in all cells.

- III. The idea of proteins involved not just in mRNA localization but also in regulating translation in neurites is not new. Both, FMRP, the defective protein in Fragile X mental retardation syndrome, and the cytoplasmic poly A element binding protein, have been implicated in these roles (Bassell and Kelic 2004). SMN may have a similar role in motor neurons, thus explaining the specific defect characteristic of the disease phenotype.
- IV. The involvement of SMN in RNA metabolism continues to be investigated in order to further understand the molecular biology of the disease. A 2004 study by Anderson et al. found that the RNA binding protein BRUNOL3 is up-regulated in the heterozygous SMA (i.e., *Smn +/-*) mice and human primary cell cultures (Anderson et al. 2004). This up-regulation correlated with more severe SMA phenotypes. SMN

and BRUNOL3 are both expressed at similar stages of development and BRUNOL3 has a specific neuromuscular expression pattern. Two members of the hnRNP protein family were described as binding partners of SMN. hnRNP-R and hnRNP-Q interacted with wild type *Smn*, but not with mutated *Smn* isoforms (Rossoll et al. 2002). Both hnRNP-R and hnRNP-Q specifically bind mRNAs and are involved in mRNA processing including editing, in mRNA transport and finally act as regulators which modify binding to ribosomes and RNA translation (Mourelatos et al. 2001; Pellizzoni et al. 1999). Such functions appear highly important for neurons with long processes, in particular motor neurons in which specific mRNAs have to be transported over long distances.

- V. The first evidence that SMN interacts with the transcription corepressor mSin3A revealed that a subset of SMN protein may be involved in the repression of genes critical to motor neuron survival. mSin3A-interacting domain is encoded by exon 6 of *SMN* (Zou et al. 2004). In mammalian cells, mSin3 is expressed as the highly related mSin3A and mSin3B proteins (Ayer et al. 1995). mSin3 associates with histone deacetylases (HDACs), methyl transferases and other factors to regulate the accessibility to chromatin (Sif et al. 2001; Wysocka et al. 2003; Yang et al. 2003; Zhang and Dufau 2002).
- VI. Motor neuron loss in SMN-deficient cells appears to be due to apoptosis (Fidzianska 2002; Fidzianska and Rafalowska 2002; Soler-Botija et al. 2002). SMN might have a direct role in the apoptotic process; SMN protein has been shown to associate *in vitro* and *in vivo* with p53, a tumor suppressor protein that regulates neuronal death by apoptosis (Young et al. 2002a). The tumor suppressor protein p53 is a multifunctional factor involved in cell cycle control (Sherr 2000; Sherr and Weber 2000), DNA repair (Huang et al. 1996), transcription activation (Fritsche et al. 1993; Hupp et al. 1992), and apoptosis (Vousden 2000; Vousden and Woude 2000). p53 can induce apoptosis through several pathways, including mechanisms that are dependent or independent of p53-mediated transcriptional activity (Bates and Vousden 1999; Vousden 2000). SMN interacts directly with p53 and the region encoded by *SMN* exon 2 mediates the SMN-p53 association (Young et al. 2002a). The degree of inhibition correlates with the effects of each mutation on SMN dimerization and SMA disease severity. Following endogenous p53 activation, SMN and p53 accumulates in Cajal bodies. In contrast, in SMA patients-derived fibroblasts with very low SMN protein level, p53 is localized within the nucleolus and not in Cajal bodies (Young et al. 2002a). The interaction between p53 and SMN suggests that the two proteins have an associated function. SMN can function as an anti-apoptotic factor in neuronal cells and has been reported to functionally interact with the anti-apoptotic factor Bcl-2 in a tissue culture model (Iwahashi et al. 1997; Kerr et al. 2000). An anti-apoptotic function of SMN may be significant, with regards to disease, because surviving motor neurons from SMA patients display signs of apoptosis, such as chromatolysis and swelling (Broccolini et al. 1999; Simic et al. 2000). Mutations in *SMN* in SMA patients destroy its anti-apoptotic synergy with Bcl-2, suggesting that it is this defect that underlies the pathogenesis of SMA (Iwahashi et al. 1997). The loss of function of both SMN and NAIP proteins is probably responsible for neuronal-cell death in SMA, suggesting that anti-apoptotic proteins may regulate neuronal survival. By using the SV vector system, Kerr et al. showed that full-length SMN

inhibits virus-induced neuronal apoptosis, whereas the SMN mutants derived from SMA patients (Y272C and SMN $\Delta$ 7) enhance neuronal apoptosis (Kerr et al. 2000).

- VII. It has been demonstrated that SMN interacts with various proteins, including Papilloma virus E2, a nuclear regulator of viral gene expression (Strasswimmer et al. 1999), minute virus of mice NS1 which performs a critical function in viral gene expression and genome replication (Young et al. 2002c, d), and Epstein-Barr virus nuclear antigen 6, a transcriptional regulator which also plays a role in the EBV-induced immortalization of primary B-lymphocytes *in vitro* (Krauer et al. 2004). The association with SMN is assumed to be required to maintain the function of these viral proteins. This function links SMN to gene expression regulation that may be impaired in motor neurons belonging to SMA patients.
- VIII. SMN protein facilitates also the assembly of stress granules (Hua and Zhou 2004b). Cytoplasmic RNA granules in germ cells (polar and germinal granules), somatic cells (stress granules and processing bodies), and neurons (neuronal granules) have emerged as important players in the post-transcriptional regulation of gene expression. RNA granules contain various ribosomal subunits, translation factors, decay enzymes, helicases, scaffold proteins, and RNA-binding proteins, and they control the localization, stability, and translation of their RNA cargo (Anderson and Kedersha 2006). So-called heat stress granules (SGs) contain mRNA encoding most cellular proteins but exclude mRNAs encoding heat shock proteins (Nover et al. 1989). These cytoplasmic microdomains form when translation is initiated under conditions in which the concentration of the active eukaryotic translation initiation factor 2 (eIF2)-guanosine triphosphate (GTP)-transfer RNA for methionine (tRNA<sup>Met</sup>) ternary complex is reduced (Anderson and Kedersha 2002). In response to stress, eukaryotic cells reprogram mRNA metabolism to repair stress-induced damage and adapt to changed conditions. During this process, the translation of mRNA encoding “housekeeping” proteins is aborted, whereas the translation of mRNAs encoding molecular chaperones and enzymes involved in damage repair is enhanced. Selective recruitment of specific mRNA transcripts into SGs is thought to regulate their stability and translation (Anderson and Kedersha 2002). Stalled 48S preinitiation complexes are the core constituents of SGs, which include small but not large ribosomal subunits as well as the early translation initiation factors eIF2, eIF3, eIF4E and eIF4G (Kimball et al. 2003). In addition, SGs contain PABP1 (Kedersha et al. 1999), the p54/Rck helicase (Wilczynska et al. 2005), the 5'-3' exonuclease XRN1 (Kedersha et al. 2005), and many RNA-binding proteins that regulate mRNA structure and function, including HuR (Gallouzi et al. 2000), Staufen (Thomas et al. 2005), Smaug (Baez and Boccaccio 2005), TTP (Stoecklin et al. 2004), Fragile X mental retardation protein (Mazroui et al. 2002), G3BP (Tourriere et al. 2003), CPEB (Wilczynska et al. 2005) and SMN (Hua and Zhou 2004b). SGs also contain putative scaffold proteins such as Fas-activated serine/threonine phosphoprotein (Kedersha et al. 2005). FRAP analysis revealed that many SG-associated RNA-binding proteins (e.g. TIA1, TIAR, TTP, G3BP and PABP) rapidly shuttle in and out of SGs despite the large size (several micrometers) and apparent solidity of these cytoplasmic domains (Kedersha et al. 2000; Kedersha et al. 2005). Given that these proteins also regulate mRNA translation and decay, their rapid flux through SGs supports the notion that SGs are triage centers that shorten, remodel and export specific mRNA transcripts for reinitiation, decay or storage. The assembly of

translationally inactive initiation complexes lacking eIF2 allows the RNA-binding protein TIA-1 or TIAR (or both) to redirect untranslated mRNAs from polyribosomes to stress granules. By regulating the equilibrium between polysomes and stress granules, TIA-1 and TIAR may influence the frequency with which individual transcripts are sorted for translation or triage in both stressed and unstressed cells. Endogenous cytoplasmic SMN co-localizes with TIA-1/R and G3BP in SGs, implicating a novel function for SMN (Hua and Zhou 2004b). Detailed analysis suggested that to form large and smooth granules, the Tudor domain as well as exon 6 and exon 7 are indispensable. Defects of SGs formation in SMA fibroblasts, which express lower levels of SMN protein, support the notion that SMN plays a role in SG formation.

### 1.5.3. Regulation of SMN protein during development and cellular differentiation

SMN is highly expressed during embryogenesis, but levels decline rapidly after birth. In SMA transgenic mice, the length of the dendrites is significantly reduced whereas the number of motor neurons is not significantly affected as compared to controls (Jablonka et al. 2000). Conditional neuronal knock-out mice (*SMN $\Delta$ 7*) lack axonal sprouting (Cifuentes-Diaz et al. 2002). Consistent with these findings, knock-down of the *Smn* protein by antisense morpholinos in zebrafish-embryos revealed a significant axonal dysmorphology. These fail to reach motor neuron endplates due to early branching and truncation, which suggests an important role of SMN in the pathfinding of axons (McWhorter et al. 2003).

In 2006, Giavazzi et al. clearly demonstrated the early presence of SMN in the developing CNS. By investigation of the expression and regional localization of the SMN protein during prenatal and postnatal development in the germinative neuroepithelium, spinal cord, brainstem, cerebellum and cerebral cortex from human samples, Giavazzi et al. found that at the earliest examined embryonic age (6 weeks, 3 days) all cells within the spinal cord were immunoreactive for SMN. This expression pattern of SMN was also evident in the ventricular and subventricular zones of the developing neocortex at the gestational age of 14 weeks (Giavazzi et al. 2006). The presence of SMN in the nuclei of all cells during early development is consistent with the housekeeping functions so far proposed for SMN, such as the role in spliceosomal assembly and pre-mRNA maturation, which has been suggested as the basic cellular mechanisms leading to SMA (Pellizzoni et al. 1998). The SMN expression became clearly evident in axons at later development stages. At 22 weeks gestation, axons from motor neurons leaving the spinal cord and entering the neural roots and axons in the descending corticospinal tract at the level of bulbar pyramids were intensely SMN- immunoreactive (Giavazzi et al. 2006). The axonal expression of SMN was still clearly evident at early postnatal days, like in the bulbar neuropil at birth, and tended later to decrease as demonstrated by the reduction and disappearance of SMN staining in the pyramidal tract. This suggests a novel role for SMN that becomes predominant in neurons at a certain phase of their development.

## 1.6. Animal models of SMA

Animal models of SMA are vitally important in continuing to understand why the disease is caused by a loss of the SMN protein. Mice have only one *Smn* gene, as opposed to the human genome which contains two, *SMN1* and *SMN2*. As it is probably the case in humans, complete knock-out of the *Smn* gene in mice is embryonically lethal (Schrank et al. 1997). Nematode, fly and mouse models with no functional SMN protein have a uniformly early embryonic lethal phenotype.

A heterozygous knock-out mouse model (*Smn*<sup>+/-</sup>) leads to motor neuron degeneration between birth and six months of age, and this model resembles one aspect of human type III SMA (Jablonka et al. 2000). Other mouse models of SMA have been generated by introducing the human *SMN2* transgene into the mice that homozygously lack *Smn* (*Smn*<sup>-/-</sup>); this mimics the genetics of the human disease (Hsieh-Li et al. 2000; Monani et al. 2000). A mutant *SMN A2G* transgene, when expressed in the presence of *SMN2* in a *Smn*<sup>-/-</sup> mouse, created a mild SMA mouse (clinically and pathologically similar to type III); the mutation in the *SMN2* transgene appeared to cause a delay in the onset of motor neuron loss (Monani et al. 2003). Homozygous *SMN* knock-out mice with 8 copies of human *SMN2* are phenotypically normal, which clearly suggests that sufficient full-length SMN from *SMN2* can completely ameliorate the disease phenotype and makes *SMN2* the most obvious target to modulate in therapeutic strategies (Monani et al. 2000).

The Cre/loxP recombination system of bacteriophage P1 is another approach used to create mouse models of SMA. This system was used to selectively knock-out *Smn* exon 7 from either neurons or skeletal muscle and to circumvent embryonic death that resulted from a lack of *Smn* gene. Mice with neuron-specific *Smn* exon 7 deletion displayed severe and progressive motor defects, resulting in death at a mean age of 25 days. After death, morphological analysis was performed and muscle denervation was evident in several skeletal muscles (Frugier et al. 2000). In a 2004 study of neuron specificity, specific regions of the CNS were examined in the course of SMA progression in the Cre/loxP model. Axonal degeneration of the phrenic and facial motor nerves and cell body loss of motor neurons in the spinal cord was observed beginning at 20 days of age (Ferri et al. 2004).

Cre/loxP recombinase directed deletion of *Smn* exon 7 in skeletal muscles led to progressive muscular dystrophy with muscle paralysis beginning approximately 3 weeks after birth. From 15 days of age, the *Smn* transcript lacking exon 7 was predominantly transcribed and death occurred at a mean age of 33 days. This mouse study indicates that the defect in the *Smn* gene affects skeletal muscle, and the effects in the skeletal muscle may contribute to the motor problems in patients with SMA (Cifuentes-Diaz et al. 2001).

Animal models in fruit fly (*Drosophila melanogaster*) and zebrafish (*Danio rerio*) have also been generated, and they are expected to be particularly useful in understanding the pathology and physiology of SMN deficits. The recently isolated *Drosophila Smn* mutant suggests that neuromuscular junction defects are a characteristic of the disease phenotype (Chan et al. 2003). The motor neuron development in zebrafish is well understood, and defects in axon-specific pathfinding were discovered in zebrafish that had reduced levels of SMN in the embryo (McWhorter et al. 2003).

A mammalian cell culture model of SMA was created using RNA interference-based elimination of the murine *Smn* mRNA in P19 teratocarcinoma cells. This could be another useful model for understanding the pathophysiology of the disease (Trulzsch et al. 2004).

### 1.7. Therapeutic prospects of SMA

Currently, there is no cure or treatment to repair the nerve damage, but support care including physiotherapy and respiratory drainage are very important. The prognosis for individuals with SMA varies depending on the type of SMA and the degree of respiratory function. Development of a therapy for spinal muscular atrophy is an exceptional challenge for the scientific community. Meanwhile, SMA seems to become one of the first inherited diseases in humans which may be cured by transcriptional activation and correction of the splicing of a copy gene. Disclosure of the molecular cause of SMA and the molecular basis of the alternative splicing of *SMN2* exon 7 gives the opportunity to develop therapeutic strategies that modulate transcription, splicing and translation regulation of *SMN2*. Various therapeutic strategies have been considered so far:

1. Elevation of the endogenous FL-SMN protein level encoded by *SMN2*
  - transcriptional *SMN2* activation via the gene promoter
  - restoration of the correct splicing of *SMN2* pre-mRNA
  - taking advantage of the pathway being responsible for the translation regulation of *SMN2* in some unaffected individuals carrying homozygous *SMN1* mutations
2. Compensation of the lack of sufficient SMN protein by
  - stem cell therapy
  - gene therapy
3. Improvement of motor neuron viability through alternative pathways

Since each SMA patient lacking *SMN1* carries one to four or sometimes even more *SMN2* gene copies (Brahe 2000; Burghes 1997; Feldkotter et al. 2002), researchers world-wide eagerly started to search for substances that increase *SMN2*-derived SMN protein levels in order to identify candidate drugs for SMA therapy. Several compounds were described to increase SMN protein levels in fibroblasts and/or lymphoblastoid cell lines derived from SMA patients, including the histone deacetylase (HDAC) inhibitors: sodium butyrate (Chang et al. 2001), valproic acid (Brichta et al. 2003; Sumner et al. 2003), phenylbutyrate (Andreassi et al. 2004), SAHA and M344 (Hahnen et al. 2006; Riessland et al. 2006), as well as interferon (Baron et al. 2000), hydroxyurea, a cell cycle inhibitor (Chang et al. 2002), aclarubicin, an anthacycline antibiotic (Andreassi et al. 2001), sodium vanadate, a phosphatase inhibitor (Zhang et al. 2001), and indoprofen, a nonsteroidal anti-inflammatory drug (Lunn et al. 2004). HDAC inhibitors are acting on both, transcriptional activation and/or splicing correction of *SMN2* pre-mRNA, indoprofen and interferon are activating the transcription of *SMN2* only, whereas aclarubicin and sodium vanadate are only facilitating the correct splicing of exon 7 of *SMN2* pre-mRNA. While most of these substances are not

suitable for SMA therapy due to unfavourable toxicity profiles, some HDAC inhibitors are already FDA (Food and Drug Administration) approved drugs and used in the therapy of various diseases.

One of the most exciting findings in SMA research was the identification of HDAC inhibitors as a group of drugs that increase the SMN protein levels *in vitro* and *in vivo* by activating the transcription and/or correcting the splicing of *SMN2*. Activation and repression of gene transcription largely depends on chromatin structure. Chromatin consists of DNA, histones and non-histone proteins. Approximately two superhelical turns of DNA containing 146 base pairs are wrapped around an octamer of core histones H4, H3, H2A and H2B forming the basic unit named nucleosome (Luger et al. 1997). Nucleosomes are repeating units building up the chromatin and showing a dynamic structure that can be condensed or relaxed depending on the balance of post-transcriptional histone modifications. Post-transcriptional modifications occurring at the N-terminal tails of histones are subject to acetylation, methylation and phosphorylation. The enzymes responsible for the acetylation are histone acetyltransferases (HATs) that add acetyl groups to N-terminal lysines of H3 and H4 histones. Thus the chromatin structure becomes more relaxed and transcription factor complexes have better access to promoter regions in order to activate gene transcription. In contrast, histone deacetylases (HDACs) remove acetyl groups, the chromatin structure becomes more compact and gene transcription is repressed. Histone modifications are reversible (Marks et al. 2004; Zhang and Reinberg 2001). In humans, there are three classes of HDAC enzymes. Class I includes HDAC 1, 2, 3, and 8; these are small molecules of 22-25 kDa localized exclusively in the nucleus. Class II includes HDAC 4, 5, 6, 7, 9, and 10, these are larger molecules of 120-135 kDa shuttling between nucleus and cytoplasm in response to certain cellular signals. Class III HDACs are most likely not acting on histones, but rather on transcription factors such as p53 or p21 (Marks et al. 2004).

The first HDAC inhibitor shown to increase SMN levels in EBV-transformed lymphoblastoid cell lines was sodium butyrate (NaBu). Furthermore, *SMN* transgenic mice treated with NaBu survived double as long as compared to untreated mice (Chang et al. 2001). Sodium butyrate is characterized by a very short terminal half-life of only a few minutes in human serum and is therefore inadequate for SMA therapy.

Phenylbutyrate, a sodium butyrate derivative, has a longer half-life in human serum (2-4 h) than sodium butyrate and in patients with urea cycle disorders it appears to be well tolerated (Maestri et al. 1996). In fibroblast cell cultures from type I, II or III SMA patients, *SMN2*-mRNA full-length transcript levels were increased in a transcription assay after treatment with phenylbutyrate. This drug was also effective in elevating the amount of SMN protein and the number of gems (Andreassi et al. 2004). Preliminary findings in a clinical trial suggest that the phenylbutyrate treatment in type II SMA patients improved motor functions on the Hammersmith functional scale (Mercuri et al. 2006). Leukocytes from type II or III SMA patients had an increase in *SMN2* full-length mRNA following oral administration of phenylbutyrate (Brahe et al. 2005). The promising results of these recent studies indicate that further investigation of phenylbutyrate is warranted and necessary.

VPA (valproic acid) mainly inhibits HDAC2. Besides of reversible binding to the catalytic center, it also facilitates its effect on HDAC2 through increased ubiquitination of HDAC2 followed by elevated

proteasomal degradation (Kramer et al. 2003). VPA is characterized by a much more suitable half-life of about 8-10 h in human serum and significantly increases SMN protein levels in cultured fibroblast cell lines. Treatment of cultured fibroblasts with 0.5  $\mu$ M to 500  $\mu$ M VPA increased the *SMN2* mRNA and protein level about 2-4 fold depending on the *SMN2* copy number. An exceptionally interesting finding was that VPA not only activates the transcription of the *SMN* gene but also restores the correct splicing of *SMN2* transcripts most likely through Htra2- $\beta$ 1, which showed similarly increased values of about 2-4 folds in VPA treated cells (Brichta et al. 2003). These findings suggest a double mechanism of action on *SMN2* in humans. Additionally, VPA activates the transcription of *SMN* in neuroectodermal tissue such as organotypic hippocampal brain slices from rat and humans (obtained from epilepsy surgery) as well as rat motor neurons (Brichta et al. 2003; Hahnen et al. 2006). The effect of VPA (1-10 mM) on *SMN* expression in cultured fibroblasts derived from SMA patients has been confirmed by Sumner and colleagues (Sumner et al. 2003).

Among the second generation HDAC inhibitors, M344 and SAHA evolved as potent candidate drugs by increasing *SMN2* protein levels already at low micromolar doses in human organotypic hippocampal brain slices as well as in rat motor neurons (Hahnen et al. 2006; Riessland et al. 2006).

High-throughput screening led to the detection of aclarubicin, a drug that modifies the splicing pattern of *SMN2*. Aclarubicin treated fibroblast cell cultures derived from type I SMA patients had higher levels of exon 7 containing transcript. In fact, the amount of SMN protein and gems was reported to be at normal level after the treatment. Unfortunately, aclarubicin is highly toxic and not likely to be useful in the clinic (Andreassi et al. 2001).

A recent study by Chang et al. provides possible evidence that the SMN protein is degraded by the ubiquitin-proteasome pathway. Since there appears to be a correlation between the amount of full-length SMN protein and the severity of the disease, proteasome inhibitors are a potential new treatment target (Chang et al. 2004).

Neuroprotective targets include glutamate excitotoxicity. As studied in models of ALS, anti-glutamate agents such as gabapentin and riluzole have been shown to have a mild neuroprotective effect. In one of the earliest randomized double blind trials, gabapentin was tested in patients with type II or III SMA; no benefit was observed in patients as assessed by muscle strength or forced vital capacity (FVC) (Miller et al. 2001). Another study with gabapentin found that after 12 months, patients with type II or III SMA who were tested with the drug demonstrated a significant improvement in leg and arm muscle strength. There were not, however, any improvements in FVC or timed functional tests (Merlini et al. 2003). Riluzole, a glutamate inhibitor, was tested in mice and humans with SMA. Riluzole treatment in SMA mice had a neuroprotective effect on the progress of the terminal axon degeneration in neurons (Haddad et al. 2003). A riluzole study in SMA patients by Russman et al. found that the drug appears to be safe (Russman et al. 2003). To the 10 participants in this limited study were given riluzole orally for nine months, and there were no beneficial effects reported (Russman et al. 2003). A clinical trial of riluzole in patients with type I SMA is currently underway. Other neuroprotective drugs, such as anti-apoptotic agents, free radical

scavengers, and trophic factors, are also being investigated as therapies to SMA remain to be established.

Albuterol, a beta-adrenergic agonist, has been shown to increase muscle strength in healthy volunteers (Caruso et al. 1995). It is also being studied for the treatment of Duchenne Muscular Dystrophy. Kinali et al. gave albuterol orally to children with type II and III SMA for six months (Kinali et al. 2002). The study reported a statistically significant increase in clinical outcome measurements of muscle strength, FVC and lean body mass and no serious side effects. There were, however, several participants that had an increase in joint contractures during the course of the study (Kinali et al. 2002).

The non-steroidal anti-inflammatory drug (NSAID) and cyclooxygenase (COX) inhibitor indoprofen was found by high-throughput screening to up-regulate production of endogenous SMN protein and to increase the number of nuclear gems. Pregnant mice treated with indoprofen had more embryos with the SMA phenotype (mice that homozygously lacked *Smn* and had one copy of the human *SMN2* transgene). Therefore, indoprofen increased the viability of SMA mice in this mouse model. The drug did not appear to alter the splicing pattern of the genes, which offers an exciting possibility of combination with drugs that modify mRNA splicing. The authors speculate that indoprofen acts co-translationally (Lunn et al. 2004).

Studies investigating gene therapy and stem cell replacement therapy are currently underway. Most recently, gene therapy using a lentivirus vector successfully delivered *SMN1* to various muscles in a mouse model of SMA, which restored SMN protein to motor neurons via retrograde transport (Azzouz et al. 2004).

Independently, two research groups showed that small synthetic molecules are able to restore the correct splicing of exon 7 leading to significantly elevated levels of FL-*SMN2* transcripts (Cartegni and Krainer 2003; Skordis et al. 2003). Cartegni and Krainer developed so called antisense peptide nucleic acids (PNAs) which are peptide chimeric molecules. The PNAs have a natural peptide-like backbone and standard nucleobases that form highly specific and stable complexes with the target RNA. At the C-terminus, the PNA is bound to a peptide composed of 10 RS repeats. These molecules are nuclease resistant, form stable PNA-RNA complexes and can cross the cell membrane (Cartegni and Krainer 2003). Skordis and colleagues designed tailed oligoribonucleotides that were complementary to *SMN2* exon 7 and contained additional noncomplementary sequences (tails) that were predicted to mimic ESE sequences (GAA repeats, known to efficiently recruit Htra2- $\beta$ 1) (Skordis et al. 2003). Although these molecules act very efficiently in experiments *in vitro*, it is not yet known if a systemic administration is successful and, most importantly, if they will pass the blood-brain barrier.

## 1.8. SMA discordant families

Genotype modification is a phenomenon in which one or several genes determine the rate of development of a character, whereas the fact of the presence or absence of the character is determined by another gene. Genes which change the function of the main gene are called modifiers. The existence of gene modifiers is a widely spread phenomenon. Apparently, each gene in an organism interacts with others and

therefore acts as their modifier (Davies et al. 2005).

Understanding the genetic factors underlying common disorders is a difficult task because each gene and environmental factors can contribute a small risk. In this regard, there exists a land between Mendelian and multifactorial disorders. This land is inhabited by genes, such as modifier genes and redundant genes that have many effects on the phenotype. Understanding the mode of action of these genes will help in determining how susceptibility genes may interact to give rise to a multifactorial phenotype (Davies et al. 2005).

In most SMA families, there is a high degree of similarity between the clinical picture of affected siblings (Rudnik-Schöneborn et al. 1994). Nevertheless, there are quite a few reports in which large phenotypic variability has been described among siblings with identical 5q13 homologs (Brahe et al. 1995; Cobben et al. 1995; Hahnen et al. 1995; Wang et al. 1996). Of the 5q13-linked SMA patients, 94.4 % show homozygous absence of *SMN1* exon 7 and 8 or exon 7 only, whereas 3.6 % present a compound heterozygosity with a subtle mutation on one chromosome and a deletion/gene conversion on the other chromosome (Wirth 2000). In most families affected by SMA, siblings with the same genotype share similar phenotypes including age of onset and motor abilities. In the phenotypically SMA discordant families, all siblings carrying identical homozygous *SMN1* mutations also have identical *SMN2* copy numbers and identical 5q13 haplotypes, ruling out *SMN2* or a gene in the SMA region as a potential modifier. The severity of SMA is strongly influenced by *SMN2*, the highly homologous copy of *SMN1*. The more *SMN2* copies a patient has, the milder is the SMA phenotype (Burghes 1997; Campbell et al. 1997; McAndrew et al. 1997; Wirth et al. 1999). Using real-time PCR, quantitative analysis of *SMN2* copy number was carried out in 375 patients with type I, II or III SMA. 80 % of patients with type I SMA were found to have 1 or 2 copies of *SMN2*, 82 % of type II patients had 3 copies and 96 % of patients with type III SMA carried 3 or 4 copies of the gene (Feldkotter et al. 2002). Increasing the production of full-length SMN protein from *SMN2* transcripts is one of the main targets of research in SMA as increased full-length SMN protein levels would be expected to result in clinical improvement.

The fact that siblings with identical 5q13-homologous absence of *SMN1* can show variable phenotypes suggests that SMA is also modified by other factors which function either on transcriptional level, to produce more full-length transcripts, or on translational level, to increase the amount of SMN2 protein. Along with that, an increased level of full-length SMN transcript and protein in unaffected *SMN1*-deleted siblings is observed in comparison with their affected siblings. The intrafamilial variability is especially interesting since the milder affected sibs or the unaffected *SMN1*-deleted sibs are in most cases females (Brahe et al. 1995; Cobben et al. 1995; Hahnen et al. 1995; Wang et al. 1996; Wirth et al. 1999). It cannot be completely excluded that the healthy *SMN*-deleted sibs will develop SMA later in their lives. However, the clinical picture and age of onset of SMA in sibs is often rather concordant, and a variation in age of onset of >15 years between sibs (as seen) is extremely rare (Rudnik-Schöneborn et al. 1994).

A candidate gene approach including analysis of SMN and SMN-interacting proteins was performed in 13 phenotypically SMA discordant families (Helmken et al. 2003). The RNA levels of full-length and  $\Delta 7SMN$  determined from EBV-transformed cell lines were identical, except for one single case. By analyzing the

SMN protein expression in 7 SMA discordant families with affected and asymptomatic siblings, the asymptomatic individuals revealed significantly higher levels as compared to their affected siblings in lymphoblastoid cell lines (Fig. 7 A) but not in primary fibroblast lines (Fig. 7 B). These data indicate that an SMA modifier directly acts on the translation regulation or stability of SMN. Additionally, eight SMN interacting proteins (Gemin 2, Gemin 3, RNA helicase A, ZPR1, profilin 2, hnRNP-Q; FUSE binding protein and p80 coilin), as well as 2 proteins (Htra2- $\beta$ 1 and hnRNP-G) involved in the splicing regulation of *SMN* exon 7 were investigated in all 7 SMA discordant families. Corresponding genes were analyzed on DNA level by sequencing the complete region and on RNA level by semi-quantitative RT-PCR. Neither of the families presented differences among the siblings. However, similar to SMN, all SMN interacting proteins that were analyzed by quantitative Western blot (Gemin 2, Gemin 3, hnRNP-Q, ZPR1) revealed a significant increase in their expression levels in asymptomatic individuals (Fig. 7 A).

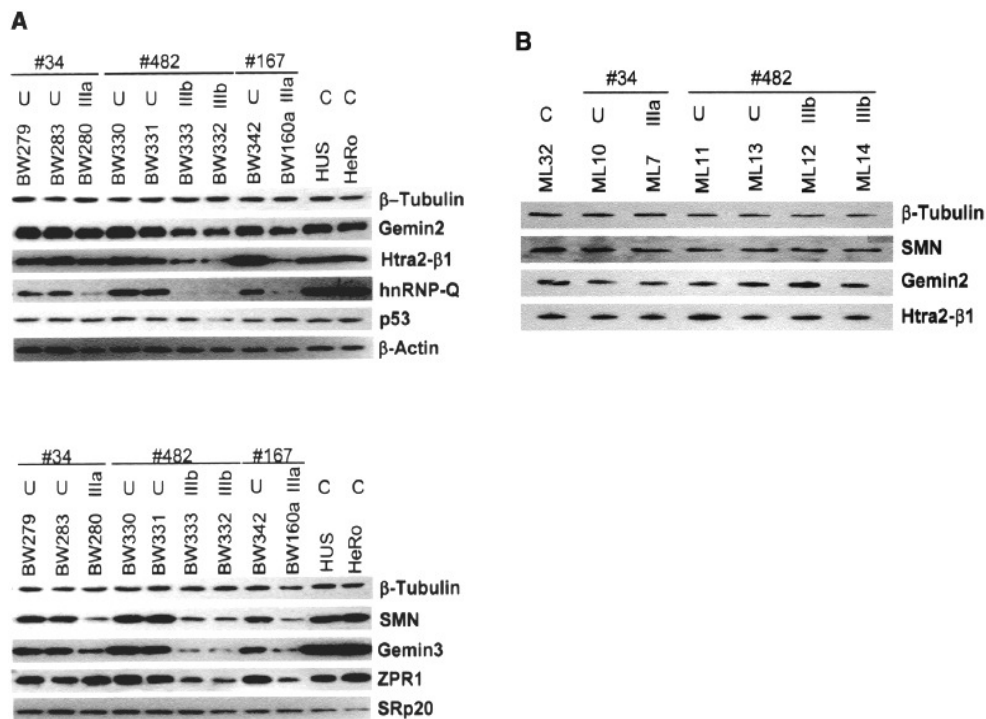


**Fig. 7** Semi-quantitative analysis of SMN-interacting proteins in cell lines derived from discordant families and control individuals in two independent Western blots. (A) In lymphoblastoid cell lines the expression level of SMN and of proteins interacting with SMN, as well as of Htra2- $\beta$ 1, differs noticeably between homozygously deleted unaffected individuals and their affected siblings. The expression level of p53 as well as SRp20 was the same in affected and unaffected individuals. Analysis with antibodies against  $\beta$ -tubulin and  $\beta$ -actin verified that equal amounts of total protein lysates were loaded. *U* unaffected sib, *C* control individual. (B) Western blot analysis of protein content in primary fibroblast cultures. Protein levels of SMN, Gemin 2, and Htra2- $\beta$ 1 are not down-regulated in affected individuals (type IIIa and IIIb SMA) compared with unaffected siblings (Helmken et al. 2003).

Therefore, it has been suggested that the intrafamilial phenotype variability is not based on any of the genes examined so far (Helmken et al. 2003; Helmken et al. 2000; Helmken and Wirth 2000). Htra2- $\beta$ 1 was found to be up-regulated similarly. However, Htra2- $\beta$ 1 failed to present any difference on DNA and RNA level in discordant families (Helmken and Wirth 2000). Nevertheless, this SR-like splicing factor reverts the *SMN2* exon 7 splicing pattern when overexpressed (Hofmann et al. 2000). Therefore, the expression level of Htra2- $\beta$ 1 in SMA discordant families it has been tested.

Strikingly, the Htra2- $\beta$ 1 protein level was decreased depending on the SMN level and phenotype. A reduced amount of the remaining SMN protein correlates with a decrease of Htra2- $\beta$ 1 independent of the modifying pathway, since it applies to discordant and non-discordant families. Another essential splicing factor, SRp20, was not affected by an alteration of the SMN protein level. However, since SMN does not interact with Htra2- $\beta$ 1, an indirect mechanism of regulation is most likely responsible for the correlation of the expression level between SMN and Htra2- $\beta$ 1 (Helmken et al. 2003).

Interestingly, only for one discordant family a significant difference in the ratio of FL-*SMN* vs. *SMN* $\Delta$ 7 was observed, while the total amount was the same. In all other families the ratio FL-*SMN* vs. *SMN* $\Delta$ 7, as well as total amount of *SMN* transcripts, was identical among affected and unaffected siblings. But nevertheless, affected siblings bear reduced levels of SMN protein, whereas unaffected siblings have as much SMN protein as control individuals (Helmken et al. 2003).

Given the fact that no sequence or transcription differences among intrafamilial siblings were found, it has been postulated that the SMA phenotype is modified by a factor that directly influences the SMN protein complex (Helmken et al. 2003). Moreover, this modulating effect is tissue-specific, because only in protein samples derived from lymphoblastoid cell lines, but not from primary fibroblast, a difference was observed. One can only speculate that the differential expression caused by the modifying gene also occurs in spinal cord. Nevertheless, there is no way to approach this issue at the moment, since no SMA discordant mice are known so far. Previous studies of alternatively spliced *SMN2* transcripts, protein level or number of gems from fibroblasts or lymphoblastoid cell lines also failed to show any significant difference between type III SMA patients and controls (Coovert et al. 1997; Gavrillov et al. 1998; Lefebvre et al. 1997), a situation similar to the most of our phenotypic SMA discordant families.

From the conclusion that modulation of SMN expression in discordant siblings seems to happen at the translational level, it has been assumed that SMN-interacting proteins, such as Gemin 2, Gemin 3, ZPR1 and hnRNP-Q may act as potential modifying factors. Interestingly, in both SMA discordant families and type I-III SMA patients, as response to reduced SMN protein levels, a down-regulation of SMN-interacting proteins in gems (Gemin 2, Gemin 3, ZPR1), as well as hnRNP-Q, which links SMN to splicing has been observed (Mourelatos et al. 2001; Rossoll et al. 2002). This indicates that the SMN protein level regulates the expression of its interacting partners analysed, except for p53. For Gemin 2, a tight co-regulation with SMN has been determined in SMA patients and heterozygous mice (Jablonka et al. 2001; Wang and Dreyfuss 2001b). hnRNP-Q protein was suggested to have a probable function in RNA transport along axons and thus a significant decrease may contribute to the degeneration of alpha-motor neurons (Rossoll et al. 2002).

---

However, highly interesting was the finding that the required amount of SMN and of the SMN-interacting proteins in the SMA discordant families were exceedingly different compared with the type I-III SMA patients. Thus type III SMA patients of discordant families reveal SMN levels similar to those of type I patients of non-discordant families. This is most likely the result of the modifying gene(s) acting in phenotypically discordant families. Furthermore, since the elevated SMN protein levels in the discordant families clearly correlate with the phenotype (reduced amounts in patients vs. high amount in unaffected siblings) the effect cannot be due the EBV transformation, but due to an intrinsic mechanism, obviously the modifying gene.

By direct sequencing or DHPLC analysis of Gemin 2, Gemin 3, RNA helicase A, ZPR1, hnRNP-Q, p80coilin, FUSE binding protein and hnRNP-G, the existence of any mutation, polymorphism or transcription variance among discordant siblings was excluded. This demonstrated that these genes are highly unlikely to act as SMA modifying factor(s) (Helmken et al. 2003; Helmken et al. 2000; Helmken and Wirth 2000). The discovery of the modifying factor that prevents these individuals from developing SMA might be of therapeutic relevance. It remains speculative whether or not the molecular mechanism that prevents these individuals from developing SMA is regulated by a gender-specific factor (Helmken and Wirth 2000).

## 2. AIMS

The molecular basis of spinal muscular atrophy (SMA) is the loss of the survival of motoneuron (*SMN1*) gene function, while the severity of the disease is mainly influenced by the copy number of *SMN2* genes, a nearly identical copy of *SMN1*. In most SMA families unaffected siblings share similar phenotypes including age of onset and motor abilities. However, in rare cases significant phenotypical discrepancies were found among the siblings carrying identical mutations of *SMN1* and identical number of *SMN2* copies, suggesting the influence of a SMA modifying gene. In very mildly affected or asymptomatic siblings, high SMN protein levels are expressed by *SMN2* genes, protecting these persons from developing SMA.

The main objective of this work was to find the natural factor(s) that is/are able to protect some individuals from developing SMA despite the fact that they carry the same homozygous *SMN1* mutations. Several complementary strategies were used to maximize the chance to identify SMA modifying gene(s):

1. The initial part of the project was focused on a candidate gene approach to search for mutations/polymorphisms or expression differences on DNA or RNA level of three putative modifying genes (*ZNF265*, *hnRNP-R* and *HDAC6*) in SMA discordant families. The selection of these candidates was made on the presumption that proteins that associate with the SMN protein and/or are involved in the same pathway might act as potential modifiers. Both *ZNF265* and *hnRNP-R* associate with SMN and are involved in RNA metabolism. *HDAC6* and SMN are both involved in gene repression pathways.
2. In a second step, a search for differentially expressed genes in phenotypically SMA discordant families using Affymetrix microarray was performed. RNA targets were isolated from EBV-transformed lymphoblastoid cells belonging to one SMA discordant family where a tissue-specific action of the modifier gene already has been shown. This profiling gene expression analysis was approached in the hope to identify up- and down-regulated transcripts that might rescue the SMA phenotype.
3. The third part of the work was concentrated on a genome-wide scan analysis of world-wide collected SMA families to further identify potential modifying genes by linkage and association studies.

Combined analysis of all these three approaches should allow the identification of candidate genes, genes that were planned to be further characterized at molecular and protein level, as well as to investigate how they might modulate the disease severity and might have a regulatory effect on the SMN protein expression and function.

In its main part, the dissertation work deals with the analysis and characterization of T-plastin, the most important SMA modifying candidate gene, identified by the differential gene expression analysis.

### 3. PATIENTS SAMPLES AND MATERIALS

#### 3.1. Patients samples

All patients fulfilled the diagnostic criteria for proximal muscular atrophy defined by the International SMA Consortium (Munsat and Davies 1992) and Zerres and Rudnik-Schöneborn (Zerres and Rudnik-Schöneborn 1995). According to Zerres and Rudnik-Schöneborn (1995), type III SMA patients with an age of onset before three years are classified as type IIIa and those with an age of onset after three years as type IIIb. Informed consent was obtained from all individuals. A phenotypic and genotypic description of the SMA discordant families is given in table 2 and the pedigrees are shown in Fig. F1 in appendix. Gene symbols used in this thesis follow the recommendation of the HUGO Gene Nomenclature Committee (Povey et al. 2001).

**Table 2 Phenotypic and genotypic description of five families with siblings showing identical 5q13-homologs and homozygous deletions of *SMN1*, but variable phenotypes.**

Fam. No.	EBV-transformed cell line	Primary fibroblast cell line	DNA No.	Sex	Phenotype	Genotype	SMN2 copies
34	BW279	-	153	F	unaffected	$\Delta 7SMN1/\Delta 7SMN1$	3
	BW283	ML10	155	F	unaffected	$\Delta 7SMN1/\Delta 7SMN1$	3
	BW280	ML7	157	F	SMA IIIa	$\Delta 7SMN1/\Delta 7SMN1$	3
482	BW330	ML13	2023	F	unaffected	$\Delta 7SMN1/\Delta 7SMN1$	3
	BW331	ML11	2024	F	unaffected	$\Delta 7SMN1/\Delta 7SMN1$	3
	BW333	ML14	2026	M	SMA IIIb	$\Delta 7SMN1/\Delta 7SMN1$	3
	BW332	ML12	2027	M	SMA IIIb	$\Delta 7SMN1/\Delta 7SMN1$	3
167	BW342	-	678	F	unaffected	$\Delta 7SMN1/\Delta 7SMN1$	3
	BW160a	-	677	F	SMA IIIa	$\Delta 7SMN1/\Delta 7SMN1$	3
800	LN422	-	4175	F	unaffected	$\Delta 7SMN1/\Delta 7SMN1$	3
	LN421	-	3956	M	SMA IIIb	$\Delta 7SMN1/\Delta 7SMN1$	3
646	BW413	-	3026	F	unaffected	$\Delta 7SMN1/\Delta 7SMN1$	3
	BW412	-	3025	M	SMA IIIb	$\Delta 7SMN1/\Delta 7SMN1$	3
185	T36/97	-	783	F	unaffected	$\Delta 7SMN1/\Delta 7SMN1$	2
	BW282	-	785	M	SMA II	$\Delta 7SMN1/\Delta 7SMN1$	2

Seventy eight SMA patients and 46 control individuals were accessible for *T-plastin* expression studies. From all SMA patients, lymphoblastoid cell lines were at hand for RNA and DNA analysis, while from control individuals only the RNA and DNA isolated from fresh blood were available. The short characterization of the SMA patients is listed in table T1 in appendix.

For genome scan analysis genomic DNA samples from 42 SMA discordant families were collected world wide as follows: 6 families from Spain, 4 families from France, 6 families from Italy, 2 families from

Netherlands, 7 families from USA, 5 families from Poland and 12 families from Germany. In all SMA discordant families at least two siblings with different phenotypes (affected vs. asymptomatic or different types of SMA) were available. In 38 families the parents were available. A detailed view of the families is shown in table T2 in appendix.

### 3.2. Biological samples

RNA isolated from brain, spinal cord and muscle belonging to one SMA fetus was used in expression analyses. The RNA was isolated from these tissues by the TRIzol method. RNA from the same tissues but from adult, control individuals were purchased from *ClonTech* as follows:

- Human brain RNA, Cat.#. 636530
- Human skeletal muscle RNA, Cat.#. 636534
- Human spinal cord RNA, Cat.#. 636554

### 3.3. Equipment

Centrifuges:

Allegra X22-R, *Beckman Coulter*

5415 D, *Eppendorf*

5415 R, *Eppendorf*

Heating block: HTMR-133, *HLC*

Spectrophotometer:

BioPhotometer, *Eppendorf*

Cuvettes: UV-Vette, *Eppendorf*

Thermocycler:

GeneAmp 9600, *Perkin Elmer*

GeneAmp 9700, *Applied Biosystems*

Polyacrylamide gel electrophoresis chamber:

Model S2, *Biometra*

Agarose gel electrophoresis chamber:

SGE-020-02, *CBS Scientific*

pH meter: pH Level 1, *inoLab*

SDS gel electrophoresis chamber:

Mini-Protean 3 Cell, *Biorad*

Tissue culture hood:

Hera Safe, *Heraeus*

## Microscopes:

Leica DMIL, *Leica*

Leica TCS-SP, *Leica*

Axioplan 2 imaging microscop, *Zeiss*

## Power supplies

PowerPac 1000, *Biorad*

PowerPac HC, *Biorad*

High Voltage Power Pac P30, *Biometra*

## Shaker:

3015, *GFL*

VS.R23, *Grant BOEKEL*

## Imaging systems:

Chemidoc XRS, *Biorad*

Gel Doc 2000, *Biorad*

## Sequencer:

ABI 3730, *Applied Biosystems*

## Pyrosequencers:

PSQ™96MA, *Biotage*

PSQ™HS 96 (A), *Biotage*

## Western Blot transfer chamber:

Mini Trans-Blot Cell, *Biorad*

Autoradiography cassette, *Agfa*Developer machine: CURIX 60, *Agfa*

## Imaging system:

ChemiDoc XRS, *Biorad*

## Incubator:

Hera Cell 150, *Heraeus*

Neubauer counting chamber, *Optik-Labor*MagneSphere® Technology Magnetic Separation Sand, *Promega*

## Equipment required for microarray analysis:

Agilent® Gene Array Scanner, *Affymetrix*

GeneChip® Fluidic Station 400, *Affymetrix*

Hybridization Oven 640, *Affymetrix*

## Equipment required for genome scan:

GeneChip® Scanner 3000, *Affymetrix*

## Arrays:

GeneChip® Human Genome HG-U133A 2.0 Array, *Affymetrix*

GeneChip® Mapping 10K Array, *Affymetrix*

Gel dryer:

Mididry D62, *Biometra*

Membrane pump:

Type MP26, *Biometra*

Concentrator 5301, *Eppendorf*

### 3.4. Chemicals

Whenever possible, only chemicals with the purity grade “pro analysis” were used for the experiments described in this work. All standard chemicals and organic solvents were purchased from the following companies: *Roche Molecular Biochemicals*, Mannheim; *Invitrogen*, Niederlande, BV, Leek (Netherlands); *Merk*, Darmstadt; *MWG*, Ebersberg; *Amersham*, Freiburg; *Promega*, Mannheim; *Sigma Chemie*, Taufkirchen; *Serva*, Heidelberg; *Stratagene*, La Jolla (USA); *Applichem*, Darmstadt; *Roth*, Karlsruhe. For RNA isolation and analysis, only chemicals free of RNases have been used.

### 3.5. Kits

Big Dye® Terminator v1.1 Cycle Sequencing Kit, *Applied Biosystem*

Bioarray High Yield RNA TranscripLabeling Kit (ENZO), *Affymetrix*

CpGenome DNA Modification Kit, *MP Biomedicals*

Custom Superscript ds-cDNA synthesis Kit, *Invitrogen*

DyeEx™ 2.0 Spin Kit, *Qiagen*

GeneChip® Eukaryotik Hybridization Control Kit, *Affymetrix*

GeneChip IVT Labeling Kit, *Affymetrix*

MagneGST™ Pull-Down system, *Promega*

PAXgene Blood RNA Kit, *Qiagen*

pcDNA 3.1/V5-His-TOPO® Kit, *Invitrogen*

Pyro Gold Reagent, PSQ HS 96A, *Biotage*

Pyro Gold Reagent, PSQ 96 MA, PyroMak™ ID, *Biotage*

Pyro Gold SQA Reagents, PSQ 96 MA, PyroMak™ ID, *Biotage*

Qiaex II Gel Extraction Kit, *Qiagen*

QIAquick PCR Purification Kit, *Qiagen*

Quantum Prep® Plasmid MiniPrep Kit, *Bio-Rad*

RNeasy MinElute Cleanup Kit, *Qiagen*

RNeasy Mini Kit, *Qiagen*

SuperScript First-Strand Synthesis System for RT-PCR Kit, *Invitrogen*

SuperSignal West Pico Chemiluminiscent Substrate Kit, *Pierce*

Top10 One Shot Kit, *Invitrogen*

TnT T7 QuickCoupled Reticulocyte Lysate, *Promega*

Zenon<sup>®</sup> AlexaFluor<sup>®</sup> 488 Mouse IgG<sub>1</sub> Labeling Kit, *Invitrogen*

Zenon<sup>®</sup> AlexaFluor<sup>®</sup> 568 Mouse IgG<sub>1</sub> Labeling Kit, *Invitrogen*

Zenon<sup>®</sup> AlexaFluor<sup>®</sup> 488 Mouse IgG<sub>2a</sub> Labeling Kit, *Invitrogen*

Zenon<sup>®</sup> AlexaFluor<sup>®</sup> 568 Mouse IgG<sub>2a</sub> Labeling Kit, *Invitrogen*

Zenon<sup>®</sup> AlexaFluor<sup>®</sup> 568 Mouse IgG<sub>1</sub> Labeling Kit, *Invitrogen*

Zenon<sup>®</sup> AlexaFluor<sup>®</sup> 568 phalloidin, *Invitrogen*

Zenon<sup>®</sup> AlexaFluor<sup>®</sup> 488 Rabbit IgG Labeling Kit, *Invitrogen*

Zenon<sup>®</sup> AlexaFluor<sup>®</sup> 568 Rabbit IgG Labeling Kit, *Invitrogen*

### 3.6. Reagents, enzymes and additional supplies for cell culture procedures

#### Reagents

Oligo d(T) primers, # SP230, *Operon*

Blue Slik, # 42500.01, *Serva*

Ready-to-Go PCR beads, # 279559-01, *Amersham*

100 bp DNA Ladder, # 15628-050, *Invitrogen*

1 kb DNA Ladder, # 15615-016, *Invitrogen*

Precision Plus Protein All Blue Standards, # 161-0373, *Bio-Rad*

Dimethylsulfate, # D5279-05, *Sigma*

$\gamma$ -<sup>32</sup>P-ATP, # PB10168-250, *Amersham*

Piperidine, # 104094, *Sigma*

DAPI, # H-1200, *Vector Laboratories Inc*

Protein G Sepharose 4 Fast Flow, # 17-0618-01, *GE Healthcare*

Sephadex G-50 spin columns, # 17-0045-02, *GE Healthcare*

#### Enzymes

RQ1 RNase-Free DNase, # M6101, *Promega*

Taq DNA Polymerase Recombinant, cat. # 10342020, *Invitrogen*

Ribonuclease H, # 18021014, *Invitrogen*

T4 DNA Ligase 100 U, # M1801, *Promega*

T4 Polynucleotide Kinase 500 U, # E70031Y *Amersham*

Vent DNA polymerase 200 U, # M0254S, *NEB*

## Additional materials for cell culture procedures

SuperFect Transfection Reagent, # 301305, *Qiagen*  
DharmaFECT™ 1 Transfection Reagent, T-2001-03, *Dharmacon*  
DharmaFECT™ 4 Transfection Reagent, T-2004-03, *Dharmacon*  
Nerve growth factor 2.5S, # 13257019, *Invitrogen*  
EBV supernatant  
DMSO, # D2650, *Sigma*  
Cyclosporin A, # 30024, *Sigma*  
OPTIMEM® I, # 31985, *Invitrogen*  
Tissue culture dish, 60 mm, Collagen Type I coated, # 628950, *Greiner Bio-One GmbH*  
6 well multiwell plate, Collagen Type I coated, # 657950, *Greiner Bio-One GmbH*  
Collagen I, 22 mm Round No.1 German Glass Coverslips, # 354089, *BD Bioscience*  
Disposable Filter Unit 0.45 µm FP30/0.45 CA-S, # 10462100, *Whatman*  
Disposable Filter Unit 0.2 µm FP30/0.2 CA-S, # 10462200, *Whatman*

### 3.7. Primary antibodies

α-SMN, monoclonal IgG1, # S55920, *BD Transduction Laboratories*  
α-T-plastin, polyclonal IgG1, *Eurogentec*  
α-β-tubulin, monoclonal IgG1, # T4026, *Sigma*  
α-β-actin, monoclonal IgG2a, *Sigma*  
α-V5, monoclonal IgG2a, # R96025, *Invitrogen*

### 3.8. Secondary antibodies

Horseradish peroxidase conjugated goat anti-mouse IgG, # 115-035-000, *Dianova*  
Horseradish peroxidase conjugated goat anti-rabbit IgG, # 31460, *Pierce*

### 3.9. Solutions and Media

#### 3.9.1. Frequently used buffers and solutions

<u>Ammonium Persulfate (APS) solution (10%):</u>	For 10 ml
APS	1.0 g
Deionized H <sub>2</sub> O	to a final volume of 10 ml

---

	store at -20°C
<u>Blocking solution (6%):</u>	For 100 ml
Nonfat dry milk	6 g
TBS Tween buffer	To a final volume of 100 ml
<u>Bradford solution:</u>	For 1l
Coomassie Brilliant Blue G250	100 mg
H <sub>3</sub> PO <sub>4</sub> (85%)	100 ml
Ethanol (95%)	50 ml
Deionized H <sub>2</sub> O	To a final volume of 1 l
	Store at 4°C
<u>Cell lysis solution:</u>	For 100 ml
0.2 M NaCl	4 ml of 5 M stock
0.1 mM TrisCl (pH 8.0)	10 ml of 1 M stock
5 mM EDTA	1 ml of 0.5 M stock
0.2 % SDS	2 ml of 10% stock
Proteinase K	add fresh 10 µl of 100 µg/µl stock per 0.5 ml
<u>Diethylpyrocarbonate (DEPC) treated H<sub>2</sub>O:</u>	For 1 l
DEPC	1 ml
Deionized H <sub>2</sub> O	To a final volume of 1 l
	Mix overnight and autoclave
<u>DNA loading buffer (10x):</u>	For 50 ml
100 mM EDTA (pH 7.7)	10 ml 0.5 M EDTA (pH 7.7)
1% SDS	2.5 ml 20% SDS
50% Glycerol	28.7 ml 87% Glycerol
0.1% Bromphenol Blue	0.05 g
Deionized H <sub>2</sub> O	To a final volume of 50 ml
<u>dNTP mix:</u>	For 1 ml
dNTP (100 mM)	12.5mM of each dNTP (total volume: 50 µl)
Deionized H <sub>2</sub> O	To a final volume of 1000 µl
<u>Electrophoresis buffer (10X):</u>	For 1 l
Tris-Base	30.29 g

---

Glycine	144.12 g
SDS	10.0 g
Deionized H <sub>2</sub> O	To a final volume of 1 l
<u>Ethidium bromide solution (1%):</u>	For 100 ml
Ethidium bromide	1.0 g
Deionized H <sub>2</sub> O	to a final volume of 100 ml store in the dark at 4°C
<u>IP buffer:</u>	for 500 ml
150 mM NaCl	4.383 g
50 mM Tris-HCl pH 7.5	25 mL of 1M Tris-HCl (pH 7.5)
5 mM EDTA	25 ml of 100 mM EDTA (pH 8.0)
0.5% NP40	25 ml of 10% v/v NP40
1% Triton x 100	50 ml of 10% v/v Triton x 1000
<u>100 mM IPTG stock solution:</u>	For 20 ml
IPTG (Isopropyl-β-D-Thiogalactosid), Sigma	500 mg
Deionized H <sub>2</sub> O	20 ml Store at -20°C
<u>Laemmli buffer for SDS PAGE (2x):</u>	for 100 ml
Tris-Base	0.757 g
Glycerol	20 ml
Bromphenol Blue	10 mg
SDS	6 g
(prior to use: β-Mercaptoethanol)	10 ml
Deionized H <sub>2</sub> O	To a final volume of 90 ml without β- Mercaptoethanol and store at room temperature
<u>Lysis buffer (pH 7.4):</u>	For 500 ml
155 mM NH <sub>4</sub> Cl	77.5 ml 1M NH <sub>4</sub> Cl
10 mM KHCO <sub>3</sub>	5 ml 1 M KHCO <sub>3</sub>
0.1 mM EDTA	100 μl 0.5 M EDTA
Deionized H <sub>2</sub> O	400 ml Adjust pH to 7.4 with HCl
Deionized H <sub>2</sub> O	To a final volume of 500 ml Store at 4°C

10x One-Por-All (OPA) buffer, Amersham

<u>PCR buffer (10x):</u>	For 500 ml
500 mM KCl	250 mM 1 M KCl
100 mM Tris-HCl (pH 8.3)	50 ml 1 M Tris (pH 8.3)
15 mM MgCl <sub>2</sub>	7.5 ml 1 M MgCl <sub>2</sub>
0.1% gelatine	0.5 g
Deionized H <sub>2</sub> O	To a final volume of 500 ml
	Sterile filtration

<u>Phosphate buffered saline (PBS) (10x):</u>	For 1 l
120 mM NaCl	80.0 g
2.7 mM KCl	2.0 g
5 mM Na <sub>2</sub> HPO <sub>4</sub>	14.4 g
5 mM Na <sub>2</sub> HPO <sub>4</sub> (pH 7.3)	2.4 g
Deionized H <sub>2</sub> O	To a volume of 800 ml
	Adjust pH to 7.4
Deionized H <sub>2</sub> O	To a final volume of 1 l and autoclave

<u>Ponceau solution:</u>	For 100 ml
50.5% Ponceau s	0.5 g
1% Acetic acid glacial	1 ml
Deionized H <sub>2</sub> O	To a final volume of 100 ml

<u>2x Quick Ligation buffer:</u>	For 25 ml
132 mM Tris-Cl	3.3 ml of 1 M stock
20 mM MgCl <sub>2</sub>	0.5 ml of 1 M stock
2 mM DTT	50 µl of 1 M stock
2 mM ATP	Add fresh 100 µl of 500 mM stock
15% PEG	3.75 ml
	Adjust the pH to 7.6

<u>RIPA buffer:</u>	For 50 ml
150 mM NaCl	1.5 ml 5 M NaCl
1% IGEPAL	5 ml 10% IGEPAL
0.5% Doc (Deoxycholic acid)	2.5 ml 10% DOC
0.1% SDS (Sodium Dodecyl sulfate)	0.5 ml 10 % SDS
50 mM Tris (pH 8.6)	2.5 ml 1 M Tris (pH 8.6)

---

Deionized H <sub>2</sub> O	To a final volume of 50 ml
<u>RT mix:</u>	For 1000 µl
5x buffer (supplied with reverse transcriptase)	400 µl
DTT (100 mM)	200 µl
dNTP (100 mM)	25 µl each dNTP
DEPC treated deionized H <sub>2</sub> O	300 µl
<u>Sodium Dodecyl Sulfate (SDS) solution 10%:</u>	For 100 ml
SDS	10.0 g
Deionized H <sub>2</sub> O	To a final volume of 100 ml
<u>TBE buffer (5x):</u>	For 1 l
445 mM Tris base	54 g
445 mM Borate	27.5
10 mM EDTA	20 ml 0.5 M EDTA (pH 8.0)
Deionized H <sub>2</sub> O	To a final volume of 1000 ml
<u>TBS Tween buffer:</u>	For 5 l
20 mM Tris	12.1 g
137 mM NaCl	40.0 g
0.5% Tween 20	25 ml
Deionized H <sub>2</sub> O	To a final volume of 5 l
	Adjust to pH 7.56
<u>TE<sup>-4</sup> buffer:</u>	For 100 ml
Tris (1M, pH 8.0)	1 ml
EDTA (0.5 M, pH 8.0)	20 µl
Deionized H <sub>2</sub> O	To a final volume of 100 ml
<u>Transfer buffer:</u>	For 5 l
Tris- Base	12.1 g
Glycine	56.3 g
Methanol	1000 ml
Deionized H <sub>2</sub> O	To a final volume of 5 l

<u>Tris-HCl (1 M pH 6.8):</u>	For 400 ml
Tris-HCl	60.0 g
Deionized H <sub>2</sub> O	To a final volume of 400 ml Adjust pH to 6.8

<u>Tris-HCl (1.5 M, pH 8.8):</u>	For 400 ml
Tris-HCl	90.5
Deionized H <sub>2</sub> O	To a final volume of 400 ml Adjust pH to 8.8

### 3.9.2. Media for eukaryotic cell and tissue culture procedures

<u>Medium for human fibroblasts:</u>	For 556.4 ml
DMEM with 4500 mg/l Glucose, L-Glutamine, Pyruvate (#4196-029, <i>Invitrogen</i> )	500.0 ml
Fetal calf serum ( <i>Biochrom</i> )	50.0 ml
Penicillin-Streptomycin ( <i>Invitrogen</i> )	5.0 ml
Amphotericin B ( <i>PromoCell</i> )	1.4 ml of a stock with the concentration 250 µg/ml

<u>Medium for human EBV-transformed lymphoblastoid cells:</u>	For 631.4 ml
RPMI 1640 Medium without L-Glutamine (#31870-025, <i>Invitrogen</i> )	500.0 ml
Fetal calf serum ( <i>Biochrom</i> )	120.0 ml
Penicillin-Streptomycin ( <i>Invitrogen</i> )	5.0 ml
Amphotericin B ( <i>PromoCell</i> )	1.4 ml of a stock with the concentration 250 µg/ml
L-Glutamine	5.0 ml of a stock with the concentration 200 mM

<u>Medium for HEK293 cells:</u>	For 556.4 ml
DMEM w/Glutamax-I (#61965-026, <i>Invitrogen</i> )	500.0 ml
Fetal calf serum ( <i>Biochrom</i> )	50.0 ml
Penicillin-Streptomycin ( <i>Invitrogen</i> )	5.0 ml
Amphotericin B ( <i>PromoCell</i> )	1.4 ml of a stock with the concentration 250 µg/ml

<u>Medium for undifferentiated PC12 cells:</u>	For 555.0 ml
DMEM with 4500 mg/l Glucose, L-Glutamine, Pyruvate (#4196-029, <i>Invitrogen</i> )	500.0 ml

---

Fetal bovine serum ( <i>Invitrogen</i> )	25.0 ml
Horse serum ( <i>Invitrogen</i> )	50.0 ml
<u>Medium for differentiated PC12 cells:</u>	For 525.0 ml
DMEM with 4500 mg/l Glucose, L-Glutamine, Pyruvate (#4196-029, <i>Invitrogen</i> )	500.0 ml
Fetal bovine serum ( <i>Invitrogen</i> )	25.0 ml

### 3.9.3. Media for prokaryotic cells

<u>LB medium:</u>	For 500 ml
NaCl	5 g
Yeast Extract, <i>Applichem</i>	2.5 g
Bacto-Trypton, <i>Applichem</i>	5 g
MgSO <sub>4</sub>	1.2 g
Deionized H <sub>2</sub> O	Up to 500 ml
	Adjust pH to 6.7-7.0

<u>LB-agar for agar plates:</u>	For 500 ml
Bacto Agar, <i>Applichem</i>	7.5 g
LB medium	Up to 500 ml

SOC medium, *Invitrogen*

### 3.10. Software and databases:

Microsoft® Office Professional Edition 2003, *Microsoft Corporation* (word processing, data analysis)

Adobe Photoshop 8.0.1., *Adobe systems Inc.* (image editing)

EndNote 9, *Thomson ResearchSoft* (organization of the references)

SigmaPlot 9.0, *Systat Software, Inc* (creation of graphs)

OneDScan, *Scananalytik* (densitometric analysis of agarose gels and western blots)

Quantity One 4.5.1., *Biorad* (scanning and densitometric analysis of the gels and western blots)

FinchTV Version 1.3.1., *Geospiza Inc.* (analysis of sequencing results)

BioEdit 7.0.4.1., *Tom Hall* (DNA sequence alignment and analysis)

Pyro Q-CpG software, *Biotage* (analysis of the pyrograms)

PSQ-Assy Design, *Biotage* (design of pyrosequencing primers)

NCBI [www.ncbi.nlm.nih.gov](http://www.ncbi.nlm.nih.gov)

HUSAR <http://genius.embnet.dkfz-heidelberg.de>

Pfam [www.sanger.ac.uk/Pfam](http://www.sanger.ac.uk/Pfam)

ENSEMBL [www.ensembl.org](http://www.ensembl.org)

GDB <http://www.gdb.org>

UCSC Genome Browser [www.genome.ucsc.edu/cgi-bin/hgGateway](http://www.genome.ucsc.edu/cgi-bin/hgGateway)

Medline [www.ncbi.nlm.nih.gov/PubMed](http://www.ncbi.nlm.nih.gov/PubMed)

OMIM [www.ncbi.nlm.nih.gov/entrez/query.fcgi?db=OMIM](http://www.ncbi.nlm.nih.gov/entrez/query.fcgi?db=OMIM)

iHOP [www.ihop-net.org/UniPub/iHOP](http://www.ihop-net.org/UniPub/iHOP)

NetAffx [www.netaffx.com](http://www.netaffx.com)

Gene Ontology [www.geneontology.org](http://www.geneontology.org)

### 3.11. Primers and siRNAs

All primers were purchased from the companies *MWG* or *Metabion* and used for PCR, semi-quantitative RT-PCR, sequencing, pyrosequencing and genotyping. Primers were delivered in lyophilized form and subsequently diluted in HPLC water to achieve primer stock solutions with a concentration of 100 pmol/μl. Stock solutions were stored in aliquots at -20°C and served for the preparation of working solutions with the concentration of 10 pmol/μl.

For the candidate gene approach three SMN-interacting proteins (*ZNF265*, MIM: 604347; *HDAC6*, MIM: 300272; *hnRNP-R*, MIM: 607201) were chosen to be screened for mutations or nucleotide variants. All 11 exons of *ZNF265* gene were sequenced on genomic level in five SMA discordant families using primers listed in table 3.

**Table 3 Oligonucleotides used to sequence the complete coding region of *ZNF265* gene.**

Locus	#	Primer name	Sequence 5'→3'	T <sub>m</sub> (°C)	Amplicon size (bp)
-34	1905	ZNFEX1F	ATAGCTGCGGGTGGCTGT	58	454
+488	1854	ZNFEX1R	AAAGCTTCCACTAACAAACTC		
+2205	1855	ZNFEX2-3F	TTCCAGATATGTAGTGAGGAC	57	385
+2590	1856	ZNFEX2-3R	CCAGATCTATTATTTTGAAG		
+3914	1857	ZNFEX4F	TCTGCTTAAATGGTTCAGTCC	57	384
+4298	1858	ZNFEX4R	CACTTACTGTGGCTCTACTCG		
+8361	1859	ZNFEX5F	TTTTTTGTTGTCTGGAGATTTG	56	367
+8728	1860	ZNFEX5R	AATTTCAAATGCTTGTGTCAGC		
+8612	1961	ZNFEX6F	AGTGCAATTTGAGTCTTCAGC	57	357
+8969	1982	ZNFEX6R	TATTTTCACCAAGTGTCTGAGG		

+9914	1963	ZNFEX7F	AGGTGCTCAGTCCACCTAACTG	58	497
+10411	1864	ZNFEX7R	TTTAGTCAAAGCATGAGGC		
+11565	1865	ZNFEX8F	TTCAGTGTTTCATATCACAAAGC	57	240
+11805	1866	ZNFEX8R	AATAAGGGGAAAAAAGCAG		
+13900	1867	ZNFEX9-10F	TGATCCAGAAGTCTTCTGTTG	56	434
+14334	1868	ZNFEX9-10R	GTAGAAAGTCGGAACACAAGA		
+15144	1869	ZNFEX11F	TTGCTTTCTTACCACTTCTGC	56	174
+13318	1870	ZNFEX11R	CTGGGTAAAGTAGTGGTGTCC		

Bp: base pair; F: forward orientation; R: reverse orientation; Tm: annealing temperature; #: the internal laboratory number of the respective primer.

In case of *HDAC6* two SNPs were selected for association studies in our SMA discordant families: rs1467379 located in exon 21 (T/C) and rs1127346 (C/T) located in exon 24. Both nucleotide variants cause an amino acid exchange at protein level: rs146379 a leucine to proline exchange, and rs1127346 a threonine to isoleucine exchange, respectively. The genotyping of both SNPs was performed at genomic level by sequencing using primers shown in table 4.

For *hnRNP-R* two primers were designed to amplify the transcript on cDNA level for expression analysis and two SNPs located in the intronic region were selected for association studies in five SMA discordant families: rs2842604 (A/C; located in intron 6) and rs911927 (C/G; located in intron 10). The primers used for *hnRNP-R* gene analysis are represented in table 5.

The primers listed in table 6 were used for semi-quantitative PCR of candidate genes found to be up-regulated in microarray analysis (*T-plastin*, MIM: 300131; *NR113*, MIM: 603881, *TNFSF14*, MIM: 604520; *Septin 2*, MIM: 601506; *Plod 2*, MIM: 601865, *CD24*, MIM: 600074) and for *SMN* transcripts (*SMN*, MIM: 600354). The target transcripts were co-amplified in multiplex PCR reactions with internal control genes described in section 4.3.8.3.

**Table 4 Primers used for rs146379 and rs1127346 genotyping.**

Locus	#	Primer name	Sequence 5'→3'	Tm (°C)	Amplicon size (bp)
+15237	2653	Hdac6 ex20-21_for	CTGCCACTCAGCACTAAATG	58	586
+15823	2654	Hdac6 ex20-21_rev	TTCATATCATCAGCCACATG		
+20443	2655	Hdac6 ex24-25_for	ACAGGGGAGCCACTCTG	58	755
+21198	2656	Hdac6 ex24-25_rev	TAAGCTGAAGACCCCATCTCC		

Bp: base pair; ex: exon; for: forward orientation; rev: reverse orientation; Tm: annealing temperature; #: the internal laboratory number of the respective primer.

**Table 5 Primers used for *hnRNP-R* expression and genotyping.**

Locus	#	Primer name	Sequence 5'→3'	Tm (°C)	Amplicon size (bp)
5' UTR	2023	hnRNP-R-ex123_for	GATACCATCGGACAGGATTTC	58	474
Exon 4	2037	hnRNP-R-ex123_for	TCCAGTGGTCACATCAAGTG		
+16550	2004	SNP2842604_for	ATTTGAAGCAGCATTGTTAATG	57	310
+16860	2005	SNP2842604_rev	GATTTTGGTATAATGAGGGGG		
+25039	2006	SNP911927_for	CCATGCCTGGCCTATCTCAC	57	367
+25406	2007	SNP911927_rev	CCCAACTAAGTTTCCTTCAGT		

Bp: base pair; ex: exon; for: forward orientation; rev: reverse orientation; Tm: annealing temperature; #: the internal laboratory number of the respective primer.

**Table 6 Oligonucleotides used for semi-quantitative PCRs.**

Locus	#	Primer name	Sequence 5'→3'	Tm (°C)	Amplicon size (bp)
Ex 1	575	SMN_for	ATCCGCGGGTTTGCTATG	57	290
Ex 2	1927	SMN_rev	GTTGTAAGGAAGCTGCAGTAT		
Ex 6	2335	Septin2_for	GTTGAAATTGAAGAGCGAGG	57	570
Ex 10	2336	Septin2_for	AGTCATTGTGCTCTGGGTTT		
Ex 4	2331	Plastin 3T_for	TGATATTGCCAAGACCTTCC	58*	980
Ex 11	2332	Plastin 3T_rev	AGGATTGACACCAAGAGAGTTC		
Ex 1	2345	CD24_for	TACCCACGCAGATTTATTCC	58*	495
Ex 1	2346	CD24_rev	TGTCCATATTTCTCAAGCCAC		
Ex 3	2351	TNSF14_for	GAGCGAAGGTCTCACGAGGTCA	58	418
Ex 3	2352	TNSF14_rev	CCAGGCGTTCATCCAGCACA		
Ex 4	2353	Plod2_for	AAAGGCAAACCACAAAGTGG	58*	337
Ex 7	2354	Plod2_rev	ATTCTTAGCTCTGGCTTTGCC		
Ex 2	2349	NR1I3_for	CTACCACTTTAATGCGCTGACT	57	584
Ex 6	2330	NR1I3_rev	GTCTTTGGAGACAGAAAGTGG		
Ex 2	2343	NR1I3_for	AATGCGCTGACTTGTGAGG	57	319
Ex 4	2344	NR1I3_rev	ACAAACTGTTCAAACATGGTGC		

Bp: base pair; Ex: exon; for: forward orientation; rev: reverse orientation; Tm: annealing temperature; \*: 5% of DMSO solution was added to the PCR reaction; #: the internal laboratory number of the respective primer

The primers listed in table 7 were used for sequencing of the complete coding region of the *T-plastin* gene (from exon 1 to exon 16), of the 3'UTR region as well as the two regulatory elements of the gene (the promoter region and the first part of the intron 1). *T-plastin* sequence (AF117295) was numbered with nucleotide 1 representing the first transcription site. The primer locations are shown in Fig. F4 in appendix section.

**Table 7 Primers used to sequence both the *T-plastin* coding region and the regulatory elements.**

Locus	#	Primer name	Sequence 5'→3'	T <sub>m</sub> (°C)	Amplicon size (bp)
-17	2520	P3Tgenex1_for	GAGGGAGCGCTGGCTTTAG	61	339
+249	2521	P3Tgenex1_rev	ACCTCCCTCTCCCCAAC		
+48786	2477	P3Tgen_Ex_2for	TACTTTGGCCCTTCCTTAAAC	56	539
+49374	2478	P3Tgen_Ex_2rev	CTCGACCAAAAAAAAAAAAAAAG		
+60921	2479	P3Tgen_Ex_3for	TTCAAACAACCTTTATGTTCCCC	55	454
+61375	2480	P3Tgen_Ex_3rev	CATTTAGTGGGCAGGATGAC		
+67875	2481	P3Tgen_Ex_4for	AACTCAAGCCCAGTTTTTTTG	53	356
+68248	2482	P3Tgen_Ex_4rev	AATGTTTTTCTAGACCCCGTC		
+68527	2483	P3Tgen_Ex_5for	AAGTGTCTGGGTTTCCACAC	57	363
+68890	2484	P3Tgen_Ex_5rev	TTGAGGTGAACCTGTCAAGC		
+72705	2485	P3Tgen_Ex_6for	TGAAAGAGATGTTATAGTAAGC	53	287
+72992	2486	P3Tgen_Ex_6rev	GATTGGGAGCCTACAGAGTG		
+73627	2487	P3Tgen_Ex_7for	GTGAAGGGAGAAAGTAGACTGC	60	276
+73903	2488	P3Tgen_Ex_7rev	ATCACCTCCATTAAGTGAGAGC		
+75577	2489	P3Tgen_Ex_8for	TCAAAAGACTGAATGAACCTTGG	55	328
+75905	2490	P3Tgen_Ex_8rev	GACAACAAGGCTTGGTGATAC		
+79130	2491	P3Tgen_Ex_9for	AAAAATCCAATGCAAATAGCC	52	303
+79433	2492	P3Tgen_Ex_9rev	AATGCTTAAAATTGCCAACTCT		
+82052	2493	P3Tgen_Ex_10for	ACCCAGACTATGACAGTGGG	59	345
+82397	2494	P3Tgen_Ex_10rev	TGTA AAAATCATTGTGCCTATG		
+83706	2495	P3Tgen_Ex_11for	GAAGAATGCTTGAAACTCG	55	277
+83973	2496	P3Tgen_Ex_11rev	CCATTCATGACATTCGTA ACTG		
+84836	2497	P3Tgen_Ex_12for	TTTAAGGAAAGTCAAGTCCCAG	57	263
+85099	2498	P3Tgen_Ex_12rev	GCTCAGCGTCAAGAGTTTTAG		
+85171	2522	P3Tgen_Ex_13for	CGTATGCAGATTAACAAATGG	57	364
+85535	2500	P3Tgen_Ex_13rev	GCATCTCCCACTTAACATCC		
+86302	2501	P3Tgen_Ex_14for	AAGCATCTTTCTGATGTTTGC	54	302
+86604	2502	P3Tgen_Ex_14rev	AGCCCAACACTAATTCTCACTC		
+86626	2523	P3Tgenex15_for	TTCACTGGGCTTTGTTTTTG	59	251
+86877	2524	P3Tgenex15_rev	GCGTTCTTTTCATACTATTAGC		
+88221	2525	P3Tgenex16_for	ATTTTCATCCTGATTTTGTTTCC	57	281
+88502	2526	P3Tgenex16_rev	TGAAAAGTCCTTTGAATGGC		
+88365	2657	plst3_3utr_reg1_for	GCAGGGGAATGAAGAGAGTG	61	308
+88753	2658	plst3_3utr_reg1_rev	ATCCCATCATCTAAGCAAGTCC		
+88690	2659	plst3_3utr_reg2_for	TGCTCTGTTATCTTTTCGCC	56	428
+89118	2660	plst3_3utr_reg2_rev	GGGTATGAGAGGGAAGATGC		
+89087	2661	plst3_3utr_reg3_for	ACCTTAAATTTGCATCTTCCC	56	315
+89402	2662	plst3_3utr_reg3_rev	AACAGCTTGACAAAGCAAGAG		
+803 <sup>†</sup>	2780	intron1_reg1_p3t_rev	TCCTACTAGCCCAGAGATGTTT	60	820
+697	2781	intron1_reg2_p3t_for	CTTCCCTCCCTTGTCTTAG		
+1518	2782	intron1_reg2_p3t_rev	ACTGCATCTCGAGGATCAAG	57	821
+1426	2783	intron1_reg3_p3t_for	AAAGTAAAACCATTGAGGGG		
+2238	2784	intron1_reg3_p3t_rev	TGGGAAAGTTGTTTCAGTGTC	56	812
+2159	2785	intron1_reg4_p3t_for	TTGATACATCGAGTTGGTTGG		
+2949	2786	intron1_reg4_p3t_rev	TTTGGGCTCATTAGATCATACC	57	790
-3219	2572	P3T_Pm_3_for	TGGCAGGTGCCTATAATACC	57*	558
-2661	2573	P3T_Pm_561_rev	TCTCACAGACCTTGTGAATCAG		
-2680	2574	P3T_Pm_545_for	TCACAAGGTCTGTGAGAATCC	57*	472
-2204	2575	P3T_Pm_1017_rev	TTCTGTTTAAACAAGCTCCAC		

-2225	2576	P3T_Pm_998_for	TGGAGCTTGTTAAACAGGAATC	56*	406
-1818	2577	P3T_Pm_1404_rev	TCAAAAAAGCTTACATTGGTCC		
-1850	2578	P3T_Pm_1372_for	CTACCCTACTCGGACCAATG	59*	478
-1358	2579	P3T_Pm_1850_rev	TTTTCTACTGGTTCAGGTTTGG		
-1372	2580	P3T_Pm_1836_for	TGAACCAGTAGAAAATCTCCCA	56*	443
-929	2581	P3T_Pm_2279_rev	AGAAAAAGTCTAAGCCCTTTCC		
-951	2582	P3T_Pm_2257_for	AGGAAAGGGCTTAGACTTTTTTC	56*	623
-328	2583	P3T_Pm_2880_rev	TTGGGAACAAGAATTTGAATG		
-349	2584	P3T_Pm_2859_for	GCATTCAAATTTCTTGTCC	53*	396
+47	2585	P3T_Pm_3255_rev	CTCAGACAACCTTCTGCACCTC		

Bp: base pair; Ex: exon; for: forward orientation; P3T or plst3: Plastin 3 (T isoform); Pm: promoter; reg: region; rev: reverse orientation; Tm: annealing temperature; \*: 5% of DMSO solution was added to the PCR reaction; #: the internal laboratory number of the respective primer; †: the forward primer used to sequence the first region of the T-plastin 3'UTR region was primer # 2525.

The primers listed in tables 8 and 9 were used for *T-plastin* CpG island analysis by pyrosequencing. The CpG island was divided in 7 regions (named from CpG1 to CpG7) and two primer pairs for each region were designed for nested PCR amplification. In the first round primers shown in table 8 were used and in the second round of PCR amplification the internal primers listed in table 9 were used. For each region in the second PCR round designed primers with or without biotin label depending on the orientation of the sequencing primer were used in pyrosequencing (see table 10). The primers listed in tables 8 and 9, as well as all CpGs within the *T-plastin* genomic region are shown in Fig. F5 in appendix section.

**Table 8 Primers sequences for the first round of nested PCR amplification of *T-plastin* CpG island.**

Start Position	#	Name	Sequence 5'→3'	Tm (°C)	Am. (size) (bp)	Q
-291	2820	CpG1_1stbis_P3T_for	AGTTAGGTATGTTGCATTT	48	364	+
+84	2821	CpG1_1stbis_P3T_rev	CAAAATCCTAAATCTAACC			
-31	2767	CpG2_1stbis_P3T_for	GGTTGGTAGGAGGGGAGGG	57	291	-
+261	2823	CpG2_1stbis_P3T_rev	AAAACCTCCAACCTAAAATTTCTC			
+66	2824	CpG3_1stbis_P3T_for	GGTTAGATTTAGGATTTTG	48	346	+
+412	2825	CpG3_1stbis_P3T_rev	AACCCAAAACCTAACAACAA			
+240	2826	CpG4_1stbis_P3T_for	GAGAAATTTTAGTTGGAGTTTT	52	382	+
+622	2772	CpG4_1stbis_P3T_rev	ACTTAAACCAACCAATCACC			
+537	2915	CpG5_1stbis_P3T_for	GATTTAGGAAATTT	42	276	-
+813	2916	CpG5_1stbis_P3T_rev	AAAAAATACTATCCTACT			
+740	2917	CpG6_1stbis_P3T_for	AGTTTTTTTATGAGTAAGTA	45	269	+
+1009	2918	CpG6_1stbis_P3T_rev	ATAAACACAAACAAATACAA			
+796	3119	CpG7_1stbis_P3T_for	AGTAGGATAGTATTTTTTT	43	493	-
+1289	3120	CpG7_1stbis_P3T_rev	ACCTTCTACAAAAATTC			

1stbis: first round of bisulfite treated DNA; bp: base pair; CpG: CpG region; for: forward orientation P3T: Plastin 3 (T isoform); rev: reverse orientation; Q: Q-solution; Tm: annealing temperature; #: the internal laboratory number of the respective primer.

**Table 9 Oligonucleotide sequences for the second round of nested PCR amplification of *T-plastin* CpG island.**

Start position	#	Name	Sequence 5'→3'	Tm (°C)	Am. Size (bp)	Q
-256	2899	Bio- CpG1_2ndbis_P3T_for	Biotin- TAAGTAGGAAGGGGAGATTTAG	56.5	291	+
+46	2766	CpG1_2ndbis_P3T_rev	CACTCAAACAACCTTCTACACCT			
-256	2765	CpG1_2ndtbis_P3T_for	TAAGTAGGAAGGGGAGATTTAG	56.5	291	+
+46	2900	Bio- CpG1_2ndbis_P3T_rev	Biotin- CACTCAAACAACCTTCTACACCT			
+25	2967	Bio- CpG2_2ndbis_P3T_for	Biotin- AGGTGTAGAAGTTGTTTGAGTG	60	212	+
+237	2768	CpG2_2ndbis_P3T_rev	ACCTCCCTCTCCCCCAACC			
+25	2822	CpG2_2ndbis_P3T_for	AGGTGTAGAAGTTGTTTGAGTG	60	212	+
+237	2901	Bio- CpG2_2ndbis_P3T_rev	Biotin- ACCTCCCTCTCCCCCAACC			
+146	2902	Bio- CpG3_2ndbis_P3T_for	Biotin-TGGGTAGGAGTGGGTTT	51	223	-
+369	2770	CpG3_2ndbis_P3T_rev	ACCACTTAATACAATAAAATAC			
+146	2769	CpG3_2ndbis_P3T_for	TGGGTAGGAGTGGGTTT	51	223	-
+369	2968	Bio- CpG3_2ndbis_P3T_rev	Biotin- ACCACTTAATACAATAAAATAC			
+308	2903	Bio- CpG4_2ndbis_P3T_for	Biotin- GGGAGTTTTTTTTATTAGTATT	52	271	-
+579	2827	CpG4_2ndbis_P3T_rev	AAAAAATAACAACTACTAACTC			
+308	2771	CpG4_2ndbis_P3T_for	GGGAGTTTTTTTTATTAGTATT	52	271	-
+579	2904	Bio- CpG4_2ndbis_P3T_rev	Biotin- AAAAAATAACAACTACTAACTC			
+557	2905	Bio- CpG5_2ndbis_P3T_for	Biotin- GAGTTAGTAGTTTGTATTATTTTT	50	235	-
+792	2906	CpG5_2ndbis_P3T_rev	CCAAAAATATTCTCCTACTAAA			
+557	2773	CpG5_2ndbis_P3T_for	GAGTTAGTAGTTTGTATTATTTTT	50	235	-
+792	2907	Bio- CpG5_2ndbis_P3T_rev	Biotin- CCAAAAATATTCTCCTACTAAA			
+771	2909	Bio- CpG6_2ndbis_P3T_for	Biotin- TTTAGTAGGAGAATATTTTGA	52	195	+
+966	2910	CpG6_2ndbis_P3T_rev	ATAAACTATTACCTCCCTCC			
+771	2908	CpG6_2ndbis_P3T_for	TTTAGTAGGAGAATATTTTGA	52	195	+
+966	2969	Bio- CpG6_2ndbis_P3T_rev	Biotin- ATAAACTATTACCTCCCTCC			
+917	3123	Bio- CpG7_2nd_P3T_for	Biotin- TTTGGAGAGAGAGAGT	40.3	327	-
+1272	3122	CpG7_2nd_P3T_rev	TCAACCTTCTACACCAC			
+917	3121	CpG7_2nd_P3T_for	TTTGGAGAGAGAGAGT	40.3	327	-
+1272	3124	Bio- CpG7_2nd_P3T_rev	Biotin- TCAACCTTCTACACCAC			

2ndbis: second round of bisulfite treated DNA; bio: biotin; bp: base pair; for: forward orientation; CpG: CpG region; P3T: Plastin 3 (T isoform); rev: reverse orientation; Q: Q-solution; Tm: annealing temperature; #: the internal laboratory number of the respective primer.

**Table 10 Sequencing primers used to analyse *T-plastin* CpG island.**

CpG region	#	Primer orientation	Sequence 5'→3'	Examined CpGs
CpG1	2955	For	TTTGGGTGTTTATTTT	-155
	2920	For	AGTTGATGTGATAGG	-111
	2956	Rev	CCACCATTA ACT	-63, -80
	2922	Rev	CCTCCTACCAACCCCC	-37, -45, -49, -52
	2921	Rev	CTCAAACA ACTTCTACA	+23, -10
CpG2	2923	For	TGTAGAAGTTGTTTG	+47, +54, +57, +64
	2924	For	TAAGTGT TTTTGTA	+110, +113, +116, +131, +141
	2957	Rev	CCTACAAAACACTTA	+93, +85
	2925	For	TGGGTAGGAGTGGGTTT	+163, +174
	3108	For	GTTAAGTTTAGTAGG	+196, +200, +203, +208, +215
CpG3	2927	Rev	TCACTCACACCCAT	+288, +282, +278
	2965	For	GGGAGAGGGAGG	+238
	2966	For	AAATGGGTGTGAGT	+306, +329, +332, +340
CpG4	2929	For	AGTTTGGGT TGGAGT	+424, +450, +453, +458, +464
	2960	For	AAGTGGAAAGGGAG	+480, +498
	2930	Rev	TAACAAACTACTAA	+555, +539, +535
CpG5	2961	Rev	TCTCCAAAACCCCAAAT	+623, +600, +595, +591
	2962	Rev	AAACCTCATACCTTCCCT	+669, +657, +651
	2932	Rev	AATACTTACTCATAAA	+733, +729, +727, +724, +718
CpG6	2963	For	AGTAGGATAGTATTTT	+814
	2964	Rev	ACCTCTCTCTCCAAAAT	+913, +902, +893, +890, +885, +881, +879, +877, +873, +867
	3110	Rev	ATAAACTATTACCTCCC	+945, +942
CpG7	3127	For	TTGTAATGAGAGG	+1051, +1057, +1060, +1070, +1083
	3128	For	TTAGTTTTAAAGTTG	+1104, +1107, +1110
	3129	For	TTAGTGTGTTGGT	+1129, +1135, +1139, +1142, +1149, +1154, +1172
	3133	Rev	AACCTCTCATTAC	+1034, +1021
	3134	Rev	CACAAACAATACAA	+983, +972

For: forward orientation; CpG: CpG region; Rev: reverse orientation; #: the internal laboratory number of the respective primer.

The primers used to amplify and to genotype 15 tagging SNPs within the *T-plastin* genomic region are listed in table 11. All primers were designed using PSQ-Assay software.

**Table 11 Primer sequences and genotyping details.**

#	Name	Label	Sequence 5'→3'	Tm (°C)	Am. Size (bp)	Alleles
3148	rs17096100_for	-	GGGGCTGTACTTGGCCTTAAA	71.5	234	A/C
3149	rs17096101_rev	biotin	ATGACGTGTAAGGTCCCAACAAC			
3150	rs17096102_seq	-	CAATAATAAACTGATGAAG			
3151	rs10875528_for	biotin	AGGGAACATGGATAAAGAACAAGA	69	106	G/T
3152	rs10875529_rev	-	CACTGGTGTTTTAAAACGCTGAAT			
3153	rs10875530_seq	-	TGTTAAAAAATATGTATACC			
3154	rs17326695_for	-	TTGGCCTCACATATTCAGAAATC	69	184	C/T
3155	rs17326695_rev	biotin	TTGGAGGCTTCCTATGAAAAAAGT			
3156	rs17326695_seq	-	GGCTAGTGCTGTGGAG			
3157	rs1557770_for	biotin	GTTCCCAACATGCCGTTA	70	234	G/T
3158	rs1557770_rev	-	TGCAGGGAGAGGAGAATGGT			
3159	rs1557770_seq	-	ATCTTGTGGGATTAATAAA			
3160	rs2522179_for	-	CCAGGAAATGATGAAGGCTATTGA	71	238	C/T
3161	rs2522179_rev	biotin	TGAATGCATGGGTTGGCTTAT			
3162	rs2522179_seq	-	AGAGCCAAATTATCATTAAAG			
3163	rs2522180_for	-	GCCCTTTGGCAAGAAAACGA	72	155	A/T
3164	rs2522180_rev	biotin	TGGGGACTTCTGCATACATGAAT			
3165	rs2522180_seq	-	GAGCCACACCCATT			
3166	rs17326716_for	biotin	AGAAGCCAGCGTCTTAAAAGCTAT	69	117	A/T
3167	rs17326716_rev	-	TGCCCTAGTCTAAGATTAACCTCG			
3168	rs17326716_seq	-	GTCTAAGATTAACCTCGTCA			
3169	rs2522188_for	-	GATTGAATGCAGAAGCAGATATGA	68.5	216	C/T
3170	rs2522188_rev	biotin	TCAAAAATTGCGACTACGAAAC			
3171	rs2522188_seq	-	TTCTAGGTTAAACATTAAG			
3175	rs6643869_for	-	GGGTTATTGGAGCAGTGTACGT	69	173	A/G
3176	rs6643869_rev	biotin	TGTGACTGAAGGCTAACTCTACCC			
3177	rs6643869_seq	-	AGGTTTTAGATATATCCAAG			
3178	rs5987946_for	biotin	TGTCATCCTGCCACTAAATGTAC	71	208	C/T
3179	rs5987946_rev	-	CGGGAGAGAGAACACTTCAAAGA			
3180	rs5987946_seq	-	CAGTGCTCTTTTTCTCAAT			
3181	rs5987947_for	biotin	GGCTCACCATAGCAAGTGAAAT	69	240	C/T
3182	rs5987947_rev	-	ATGGCCCTCGATCTTCTGA			

3183	rs5987947_seq	-	ACTTAGTCAATTTGCTTCTT			
3184	rs5987956_for	-	CTAGAAGAGATAGGAAGGGCCTCA	69	68	C/T
3185	rs5987956_rev	biotin	AATGACAGGAGAGAAGCCAAATA			
3186	rs5987956_seq	-	ATAGGAAGGGCCTCA			
3187	rs5987763_for	biotin	AATACAGATTTTGCTGGGTCTGCT	70.5	158	A/G
3188	rs5987763_rev	-	CATTTGGGGGCATAGCATTT			
3189	rs5987763_seq	-	AAGGAATAGTGTACTACAAT			
3190	rs2843611_for	biotin	TGACTGTGGATGAATGAAACATAA	68.5	159	A/G
3191	rs2843611_rev	-	TCGAGTCGCTTAATGTAAAGCC			
3192	rs2843611_seq	-	ACCACTTTTTAATCCTCTC			
3193	rs12390767_for	biotin	TTTTACAAGGTCCCATGAGTTGAG	70	164	C/T
3194	rs12390767_rev	-	AGGGCTAGACAGGAATCAGATCA			
3195	rs12390767_seq	-	ATCAAGTATGTGACATTTCT			

Am: amplicon; Bp: base pair; for: forward orientation; rev: reverse orientation; seq: primer used for sequencing; Tm: annealing temperature; #: the internal laboratory number of the respective primer.

In addition, four small interfering RNAs (siRNAs) have been used for the transfection experiments of rat PC12 cells. They are listed below:

- Rn\_PLS3\_2HPsiRNA, #SI07192366, *Qiagen* (target: rat *T-plastin* transcript)
- Rn\_PLS3\_3HPsiRNA, #SI01962373, *Qiagen* (target: rat *T-plastin* transcript)
- Rn-SMN1\_1HPsiRNA, #SI00265860, *Qiagen* (target : rat *SMN1* transcript)
- AllStar Negative Control siRNA, #1027280, *Qiagen*

All siRNA were pre-designed by the *Qiagen* company based on the rat *T-plastin* or *SMN* transcripts. The siRNAs were delivered in lyophilized form. To obtain a 20  $\mu$ M stock solution, 250  $\mu$ l siRNA Suspension Buffer (*Qiagen*), were added to 5 nmol siRNA. Subsequently, the dilution was incubated at 90°C for 1 min and at 37°C for another 60 min according to the manufacturer's protocol to disrupt higher aggregates. Stocks were stored at -20°C and further diluted with siRNA Suspension Buffer to obtain 1  $\mu$ M working dilutions prior to use.

## 4. METHODS

### 4.1. Prokaryotic cells

#### 4.1.1. Bacteriology

*Escherichia coli* has been engineered to improve culture performance and synthesis of a recombinant protein. Experiments using *E. coli* cells should always be done on fresh cultures, either from a freshly streaked plate or from a glycerol stock. The *E. coli* cultures are routinely cultured at 37°C on Luria-Bertani (LB) agar or in LB broth containing Ampicillin (30 µg/ml). Most strains of bacteria including *E. coli* can be stored for one to two years in glycerol solution at -20°C. At -70°C they can be stored almost for life time. 0.5 ml of glycerol solution was prepared in 2 ml screw-cap vial. 1 ml of an overnight-grown culture was transferred into the vial, thoroughly vortexed and stored at -70°C. To revive a stored strain, some culture was streaked on the LB plate containing appropriate antibiotics for a single colony.

#### 4.1.2. Transformation of bacteria by heat-shock

In bacteria, transformation refers to a genetic change brought about by taking up and expressing DNA and competence refers to the state of being able to take up DNA. Artificial competence is not encoded in the cell's genes. Instead it is induced by laboratory procedures in which cells are passively made permeable to DNA, using conditions that do not normally occur in nature. These procedures are comparatively easy and simple, and are widely used to genetically engineer bacteria. Artificially competent cells of standard bacterial strains may also be purchased frozen, ready to use. Chilling cells in the presence of divalent cations such as Ca<sup>2+</sup> (in CaCl<sub>2</sub>) prepares the cell walls to become permeable to plasmid DNA. Cells are incubated with the DNA and then briefly heat shocked, which causes the DNA to enter the cell. This method works well for circular plasmid DNAs but not for linear molecules such as fragments of chromosomal DNA.

Two µl of the cloning reaction were added into a vial of One Shot<sup>®</sup> TOP10 chemically competent cells *E. coli* (*Invitrogen*), mixed gently and incubated on ice for 25 min. The cells were heat-shocked for 30 sec at 42°C in a water bath and immediately transferred to ice. Two hundred fifty µl of room temperature SOC medium were added, the tubes tightly capped were shaking horizontally at 37°C at 200 rpm for 1 h. Two different volumes from each transformation (50 µl and 100 µl, respectively) were plated on prewarmed selective plates (containing 80 µg ampicillin) and incubated overnight at 37°C. From the each plate 8 colonies were picked and resuspended in 10 µl of ddH<sub>2</sub>O. Two µl of resuspended colonies were used to direct analysis by PCR of the positive transformants. A combination of T7 forward primer (T7\_promoter\_for: 5'-TAATACGACTCACTATAGGG-3', *Invitrogen*) and the reverse primer that binds within the insert has been used. The reactions were incubated 10 min at 94°C to lyse the cells and to inactivate nucleases. The PCR products were visualized by agarose gel electrophoresis. Once a correct

clone was identified, the remaining resuspended colony was used to inoculate a liquid culture for DNA extraction and long term storage.

## **4.2. Eukaryotic cells**

### **4.2.1. Cell culture**

#### **4.2.1.1. EBV transformation of peripheral blood lymphocytes**

Epstein Barr Virus (EBV) transformation is a reliable method to immortalize mammalian cells. Transformation of peripheral blood lymphocytes by EBV is a laboratory procedure developed as a combination of a sound scientific operation and state-of-the-art technology involving tissue culture. Immortalization of cells takes 6-8 weeks to generate large amounts of cells that can be indefinitely grown as a continuing source of genetic material, RNA and proteins.

Heparinized blood cells were transferred to 50 ml Falcon tubes, treated with 40 ml of lysis buffer to lyse red blood cells and incubated for 10 min at room temperature. Samples were then centrifuged at 1,500 rpm for 10 min at room temperature. The supernatant was carefully removed and another 40 ml lysis buffer added to the pellets. Samples were centrifuged in the same conditions and the supernatant was completely removed with a pipette and 2 ml of EBV supernatant were added and mixed well. Tubes were incubated for 1 h at 37°C to allow the infection of B lymphocytes by EBV. Three ml of RPMI medium (*Invitrogen*) supplemented with 25 % FCS, 1 % P/S, 1 % L-glutamine and 0.3 % Amphotericin were added to the tubes and the content was then transferred to sterile flasks that contained 10 µl of cyclosporine (10 µg/ml). The cells usually start showing morphological changes after 3 to 4 days when dividing cells can be seen as dumbbell shaped structures under an inverted microscope. Typical morphological changes manifested by an actively growing cell culture comprise cellular clumps which can be seen with a naked eye. Usually it takes six to eight weeks to obtain a fully transformed culture showing typical manifestation of big cellular masses.

#### **4.2.1.2. EBV-transformed lymphoblastoid cell culture**

EBV infects only certain mammalian epithelial cells and B lymphocytes. *In vitro*, EBV immortalizes B-cells by activating a number of cell cycle regulating genes as well as B-cell specific genes (Gussander and Adams 1984; Klamann and Thorley-Lawson 1995). Usually B-cell infections are latent and only strong stimulation can cause the lytic cycle. EBV DNA is replicated as an episomal ring and 10-20 copies per cell are typical (Gussander and Adams 1984). The cell lines from human lymphocytes serve as a permanent source for DNA, RNA and protein isolation and this technique has found widespread use as the principal method of generating a permanent source of DNA for genotyping.

Epstein-Barr virus-transformed lymphoblastoid cells from type I–III SMA patients, discordant siblings and control individuals were transferred into 40 ml flasks using RPMI 1640 Medium (*Invitrogen*). Cells were incubated for 2-4 weeks at 5 % CO<sub>2</sub> and 37 °C.

#### 4.2.1.3. Human fibroblasts cell culture

Interesting opportunities have arisen in the past to carry out biochemical studies on cultures of fibroblasts from biopsies taken from humans. Cell culture provides a powerful tool for studying the role of fibroblasts in various contexts (Witowski and Jorres 2006). Skin material obtained from primary culture of fibroblasts was obtained from surgical specimens that are disposed.

2x10<sup>5</sup> cells of fibroblast cultures derived from SMA patients, discordant siblings and control individuals were transferred into 10 cm dishes using DMEM medium with 4500 mg/L glucose, L-glutamine and pyruvate (*Invitrogen*). Cells were incubated for 2-3 days at 5 % CO<sub>2</sub> and 37 °C.

#### 4.2.1.4. HEK293 cell culture

HEK293 cells were generated by transformation of human embryonic kidney cell cultures (hence HEK) with sheared adenovirus 5 DNA, and were first described in 1977 (Graham et al. 1977). Standard HEK293 cells do not adhere well to tissue culture dishes and this line has been extensively used as an expression tool for recombinant proteins (Thomas and Smart 2005).

2x10<sup>6</sup> HEK293 cells were seeded onto 10x14 cm Petri dishes and cultured at 37°C in 5 % CO<sub>2</sub> in Dulbecco's Modified Eagle Medium (DMEM) containing 4 mM L-glutamate, 4.5 mg/ml glucose and 0.11 mg/ml sodium pyruvate (*Invitrogen*), supplemented with 100 U/ml Penicillin and 100 µg/ml Streptomycin until >90 % confluence.

#### 4.2.1.5. PC12 cell culture

PC12 cells are a secondary cell line that was originally derived from a pheochromocytoma (a tumor of the adrenal gland) that developed in an irradiated rat. Under ordinary culture conditions, they have properties similar to those of immature rat adrenal chromaffin cells (Greene and Tischler 1976). PC12 cells represent a useful model for the analysis of neuronal differentiation (Greene and Tischler 1976).

PC12 cells were plated on the collagen-coated dishes or coverslips (*BD Bioscience*). Undifferentiated adherent PC-12 cells were cultured in DMEM supplemented with 10 % horse serum, 5 % fetal bovine serum, 1:100 dilution of Pen/Strep. Cells were grown at 37°C in 5 % CO<sub>2</sub>.

#### **4.2.1.6. PC12 differentiation: treatment of PC12 cells with NGF**

One important feature of PC12 cells is their ability to respond to nerve growth factor (NGF), and therefore they serve as a model system for primary neuronal cells. NGF-treated PC12 cells cease proliferation, grow long neurites, and show changes in cellular composition associated with neuronal differentiation (Greene and Tischler 1976). When grown in the presence of nerve growth factor (NGF), PC12 cells extend neurites, become electrically excitable, become more responsive to exogenously applied acetylcholine, have increased numbers of calcium channels, and increase the biosynthesis of several neurotransmitters (Greene et al. 1982).

When cells were 50-60 % confluent, the medium was removed, cells washed one time with PBS and differentiated in DMEM with 5 % fetal bovine serum (low-serum conditions) supplemented with 100 ng/ml NGF. Differentiation was complete after 3-4 days.

#### **4.2.1.7. Cell harvesting and freezing**

Cryogenic preservation (storage below  $-100^{\circ}\text{C}$ ) of cell cultures is widely used to maintain backups or reserves of cells without the associated effort and expense of feeding and caring for them. A wide variety of chemicals provide adequate cryoprotection. However, dimethylsulfoxide (DMSO) and glycerol are the most convenient and widely used. DMSO is most often used at a final concentration of 5 to 15 % (v/v).

Prior to freezing cells were maintained in an actively growing state to insure maximum health and a good recovery. The culture medium was changed the previous day.

Adherent cells were harvested by trypsinization and the trypsin was neutralized by adding a double volume of medium and transferred to a centrifuge tube. Cells were centrifuged for 10 min at 1500 RPM and the supernatant was discarded. Cells were resuspended in 1 ml 90 % FCS and 10 % DMSO sterile filtered through a  $0.2\ \mu\text{m}$  filter.

When PC12 cells were 70-90 % confluent, cells were dislodged from the dish, collected by low speed centrifugation, and frozen in DMEM with 15 % FBS and 10 % DMSO.

EBV-transformed lymphoblastoid cells were centrifuged for 10 min at 1500 RPM and the supernatant was discarded. Cells were resuspended in 1 ml 90 % RPMI 1640 medium, 9 % DMSO and 1 % FCS sterile filtered through a  $0.2\ \mu\text{m}$  filter.

Freezing samples were placed in styrofoam container with lid and frozen at  $-80^{\circ}\text{C}$ . Once frozen, cells were stored in a liquid nitrogen tank.

#### **4.2.1.8. Cell thawing and recovery**

Using appropriate safety equipment, the vials were removed from its storage location and transferred to a  $37^{\circ}\text{C}$  water bath to thaw. Rapid thawing (60-90 sec at  $37^{\circ}\text{C}$ ) provides the best recovery for most cell cultures; it reduces or prevents the formation of damaging ice crystals within cells during rehydration. The

content of the vials was then transferred to a 50 ml Falcon tube and cell samples centrifuged 10 min at 2,000 rpm. The supernatant was discarded and cells resuspended in 5 ml of medium, transferred to a suitable flask or culture dish and incubated under normal conditions.

### **4.3. DNA techniques**

#### **4.3.1. Plasmid preparation (Mini prep) using Quantum Prep® Plasmid MiniPrep Kit (*Bio-Rad*)**

The original alkaline lysis method for purifying plasmid DNA from bacterial cultures requires organic reagents to obtain high-quality DNA. This kit uses a proprietary silica matrix to bind DNA. Two ml of an overnight culture were transferred to a microcentrifuge tube and cells were pelleted by centrifugation for 30 sec at top speed. All supernatant was removed by pipetting. The cell pellet was completely resuspended with 200 µl of the Cell Resuspension Solution by vortexing. 250 µl of Cell Lysis Solution were added and mixed by gently inverting the capped tube about 10 times. When cell lysis had occurred, the solution became viscous and slightly clear. 250 µl of Neutralization Solution were added and a visible precipitate formed after inverting the capped tube about 10 times. Cell debris were pelleted for 5 min in a microcentrifuge. While waiting for the centrifugation step, a spin column was inserted into a 2 ml Wash Tube. The supernatant was transferred to a spin Column and 200 µl of thoroughly suspended matrix were added and mixed up and down. Samples were centrifuged for 30 sec at high speed. The filtrate was discarded and the matrix was washed twice with 400 µl of Wash Buffer by centrifugation for 30 sec. After the last wash, samples were centrifuged at top speed for 2 min to remove residual traces of ethanol. The column was placed in a clean 1.5 ml tube and 100 µl of deionized water were added to elute DNA. After a centrifugation step at top speed, the columns were discarded and the eluted DNA stored at -20°C.

#### **4.3.2. DNA isolation from fresh blood**

Human genomic DNA can be isolated from fresh blood either by phenol/chloroform method or by salting out procedure (Miller et al. 1988). The salting out procedure was used to extract DNA from fresh blood. This procedure avoids using phenol and chloroform by using high salt concentrations to remove proteins. It is rapid, safe and inexpensive. Ten ml of blood sample were collected in tubes containing EDTA as anti-coagulant and then transferred to a 50 ml Falcon tube and supplemented with lysis buffer to a final volume of 50 ml. After mixing and incubation on ice for 15 min, samples were centrifuged at 4°C and 2,000 rpm for 15 min. the supernatant was discarded and the remaining leukocytes pellet was suspended in 10 ml of nucleus lysis buffer. After addition of 700 µl 10 % SDS solution and 400 µl Pronase E solution (20 mg/ml), samples were shaken at 37°C in a water bath overnight. On the next day, digested cell lysates were supplemented with 3.2 ml saturated NaCl solution vigorously mixed and centrifuged two times at 4,000 rpm for 10 min. The supernatant was then transferred to a new 50 ml Falcon tube, the protein pellet was

discarded. After precipitating the DNA from the supernatant using isopropanol, the DNA was fished with a glass stick, washed with 70 % ethanol, air dried, and finally diluted in 200 to 500  $\mu\text{l TE}^{-4}$ .

#### **4.3.3. DNA isolation from cell culture**

DNA extraction is a routine procedure to collect DNA for subsequent molecular analysis. There are three basic steps in a DNA extraction: first, the cells are broken by grinding and the membrane lipids are removed by adding a detergent. Second, the cellular and histone proteins are removed by adding a protease, by precipitation with sodium or ammonium acetate, or by using a phenol-chloroform extraction step. Third, the DNA is precipitated in cold ethanol or isopropanol. DNA is insoluble in alcohol and clings together. In this step is also the salt removed.

Genomic DNA was isolated from EBV-transformed lymphoblastoid cell lines from SMA patients, controls and SMA discordant families. Cells were transferred into a 50 ml Falcon tube and centrifuged for 10 min at 2,000 rpm at room temperature. The supernatant was removed and 2.7 ml of cell lysis buffer were added to the cells and incubated overnight at 37°C to extract DNA. After the incubation time 2 vol of isopropanol were added and the tubes were inverted till the DNA became visible. Tubes were centrifuged at +4°C for 20 min at top speed. Carefully the supernatant was discarded, removed and pellets were washed with 70 % ethanol and centrifuged in the same conditions. After removing the supernatant, samples were allowed to dry at room temperature for 20 min and let to dissolve in 100  $\mu\text{l}$  of HPLC water for three days at room temperature.

#### **4.3.4. DNA electrophoresis**

##### **4.3.4.1. Agarose gel**

Gel electrophoresis is a technique used to separate macromolecules (nucleic acids) that differ in size, charge or conformation. When nucleic acid molecules that have a consistent negative charge imparted by their phosphate bone, are placed in an electric field, they migrate toward the anode. Agarose is a polysaccharide extracted from seaweed. It is typically used at concentrations of 0.5 to 3 %. Agarose gels have a large range of separation, but relatively low resolving power. For DNA fragments from about 150 to 800 bp an agarose gel of 2 % concentration was prepared by dissolving the proper amount in TBE buffer. For the fragment larger than 800 bp an 1 % agarose gel was used.

##### **4.3.4.2. Sequencing gel**

The purpose of sequencing is to determine the order of the nucleotides of a DNA fragment. After the sequencing reaction, the mixture of strands, all of different length and all ending with a radioactive label have to be separated. This is done on a acrylamide gel, which is capable of separating DNA molecules on

a gel electrophoresis. Smaller fragments migrate faster, so the DNA molecules are separated according to their size.

The products for *in vivo* footprinting analysis were run on a 20 % sequencing gel. The gel was prepared as follows: 40 g urea were dissolved in 16 ml acrylamide/bisacrylamide (19:1), 8 ml TBE buffer and HPLC water up to 80 ml. The solution was filtrated to remove the urea crystals. Carefully, both plates were cleaned first with ddH<sub>2</sub>O. The front plate was then cleaned three times with 70 % ethanol and the back plate once with 70 % ethanol and then treated with BlueSlick (*Serva*). When the gel was ready to apply, 400 µl APS and 55 µl TEMED were added to the gel. Once polymerized (after 2-3 h) the gel was assembled in the electrophoresis tank and filled with 1x TBE as buffer. Samples were heated at 95°C for 5 min, cooled on ice, spun briefly and loaded. The gel was run at 40 W constant power, until the loading buffer reached the bottom of the gel.

#### 4.3.5. Construction of gene constructs and DNA cloning

Cell cloning requires that the foreign DNA fragments which are introduced into a host cell must be able to replicate. If not, the foreign DNA would soon be diluted out as the host cell undergoes many rounds of cell division. However, foreign DNA fragments will generally lack an origin of replication that will function in the host cell. They require, therefore, to be attached to an independent replicon so that their replication is controlled by the replicon's origin of replication. Plasmids are small circular double-stranded DNA molecules which individually contain very few genes. Their existence is intracellular, being vertically distributed to daughter cells following host cell division, but they can be transferred horizontally to neighboring cells during bacterial conjugation.

The PCR products were cloned in the pcDNA3.1 vector using the pcDNA3.1/V5-His<sup>®</sup> TOPO<sup>®</sup> TA Expression Kit (*Invitrogen*) which provides a highly efficient one-step cloning strategy for the direct insertion of Taq polymerase-amplified PCR products. Because this vector does not contain an ATG initiation codon, the native initiation codon was included to express the desired protein. The PCR products were cloned in frame with the V5 epitope and polyhistidine tag in order to detect and/or purify the tagged protein (a map of the construct is summarized in Fig. F2 in appendix section).

**Table 12 Components for cloning reactions.**

Reagent	Volume
Fresh PCR product	4 µl
Salt solution	1 µl
TOPO <sup>®</sup> vector	1 µl
<b>Total reaction</b>	<b>6 µl</b>

The primers used to clone T-plastin were primers #2454 (T-plastin\_for: 5'-GAGGTGCAGAAGTTGTCTGAG-3') and #2586 (T-plastin\_rev: 5'-CACTCTCTTCATTTCCCTGC-3')

using as template RNA isolated from one primary fibroblast line. The PCR reactions were set in 25  $\mu$ l reaction volume using 2  $\mu$ l cDNA as described in section 4.3.8.1. The PCR products were checked by agarose gel electrophoresis. The TOPO<sup>®</sup> cloning reaction was set as shown in table 12.

The reactions were mixed gently and incubated for 25 min at room temperature. The reactions were placed on ice and proceed to One Shot<sup>®</sup> Chemical Transformation as described in Section 1.1. Two different volumes from each transformation (50  $\mu$ l and 100  $\mu$ l, respectively) were plated on prewarmed selective plates (containing 80  $\mu$ g ampicillin) and incubated overnight at 37°C. From each plate 8 colonies were picked and resuspended in 10  $\mu$ l of ddH<sub>2</sub>O. Two  $\mu$ l of resuspended colonies were used to direct analysis by PCR of the positive transformants. A combination of T7 forward primer (see section 4.1.2) and the reverse primer that binds within the insert has been used. The reactions were incubated 10 min at 94°C to lyse the cells and to inactivate nucleases. The PCR products were visualized by agarose gel electrophoresis. Once a correct clone was identified, the remaining resuspended colony was used to inoculate a liquid culture for DNA extraction and long term storage (GVO# 300: pcDNA 3.1-T-plastin-V5 vector).

#### 4.3.6. Sequencing

##### 4.3.6.1. Big-Dye sequencing

DNA sequencing, first devised in 1975, has become a powerful technique in molecular biology, allowing analysis of genes at the nucleotide level. The ideal working temperature for the polymerase is 60°C (normally it is 72°C), but because it has to incorporate dNTPs which are chemically modified with a fluorescent label, the temperature is lowered. Cycle sequencing was performed with the BigDye<sup>®</sup> Terminator v1.1 Cycle Sequencing Kit according to the manufacturer's instruction (*Applied Biosystem*), using 60 ng of template DNA (PCR product) or 300 ng of plasmid DNA, respectively. To the reaction tubes 1  $\mu$ l Mix, 1  $\mu$ l primer (see table 3 for *ZNF265* gene, table 4 for *HDAC6*, table 5 for *hnRNP-R* and table 7 for *T-plastin* gene), and 3  $\mu$ l of 5 x sequencing buffer were added in a total volume of 12  $\mu$ l. Cycle sequencing included a 5 min initial denaturation at 94°C followed by 26 cycles of 10 sec at 94°C, 5 sec at 50°C and 4 min at 60°C, with a final extension of 7 min at 72°C.

##### 4.3.6.2. Clean-up of dye-terminator sequencing reactions

The purification of the sequencing products was performed using DyeEx<sup>™</sup> 2.0 Spin Kit (*Qiagen*). The DyeEx 2.0 procedure is based on the gel-filtration chromatography, which separates molecules according to their molecular weight. When sequencing reactions are applied onto DyeEx 2.0 spin column, impurities such as dye terminators and salts diffuse into the pores and are retained in the gel-filtration material while DNA fragments, which are too large to enter the pores, are eluted in the flow-through. Spin columns were gently vortexed to resuspend the resin and the cap of columns was removed. The bottom closure of the

spin columns was snapped off and spin columns were placed in a 2 ml collection tube. Columns were centrifuged for 3 min at 3,000 rpm. Carefully the spin columns were transferred to clean centrifuge tubes and the sequencing reactions were applied slowly to the gel bed. The sequencing reaction was pipetted directly onto the center of the gel-bed surface and then centrifuged in the same conditions. Spin columns were removed from the microcentrifuge tubes and the eluted DNA samples were then dried in a vacuum centrifuge.

#### 4.3.6.3. Pyrosequencing

Pyrosequencing is a DNA sequencing technique that is based on the detection of released pyrophosphate (PPi) during DNA synthesis. In a cascade of enzymatic reactions, visible light is generated that is proportional to the number of incorporated nucleotides (Ronaghi 2001). This method presents a DNA-template-primer complex with a dNTP in the presence of exonuclease-deficient Klenow DNA polymerase. The four nucleosides are sequentially added to the reaction mix in a predetermined order. If the nucleotide is complementary to the template base and thus incorporated, PPi is released. PPi is used as substrate, together with adenosine 5'-phosphosulfate (APS), by ATP sulphurylase, which results in the formation of adenosine triphosphate (ATP). Luciferase then converts the ATP to oxyluciferin, AMP and PPi and visible light that is detected by either a luminometer or charge-coupled device. The light produced is proportional to the number of nucleosides added to the extended primer chain, and results in a peak indicating the number and the type of the nucleotide present in the form of a program (Fakhrai-Rad et al. 2002). After generation of the template by PCR the product is purified using streptavidin-coated magnetic beads. Two applications of pyrosequencing were approached: the genotyping of single-nucleotide polymorphisms and methylation analysis. For analysis of SNPs by pyrosequencing, the 3' end of a primer is designed to hybridize one or a few bases before the polymorphic position. For the CpG methylation analysis, the design is flexible, as the distance from the first base to be sequenced can be varied. The primer can usually be positioned in a region free of CpG sites. The approach uses bisulfite treatment and PCR to differentiate methylated cytosines from unmethylated cytosines. Pyrosequencing was carried out using PSQ 96MA System (*Biotage*) according to the manufacturer's protocol, including single strand binding protein (*PyroGold reagent*).

In a 96-well PCR plate containing 25 µl PCR reaction, 70 µl of mix containing 3 µl Streptavidin Sepharose HP beads, 50 µl binding buffer and 17 µl HPLC water were added. The plate was vortexed for 10 min at room temperature to keep the beads dispersed. Then, the Vacuum Prep Tool was slowly lowered into the PCR plate to capture the beads containing the immobilized templates on the filter probes. The Vacuum Prep Tool was moved in 70 % ethanol for 5 sec, then in denaturation solution (10 mM NaOH) for 5 sec and in washing buffer for 5 sec as well. After releasing the vacuum, the beads were released in a PSQ 96 Plate Low, pre-filled with 0.5 µM sequencing primer (see table 10 for methylation analysis and table 11 for haplotype analysis) in 40 µl annealing buffer by moving the Vacuum Prep Tool in small circles rubbing the filter probes against the bottom of the wells. The plate with samples was heated at 85°C for two min and

then let cool at room temperature. The enzyme and substrate, as well as nucleotides, were pipetted according to the volume information given in the PSQ CpG Software or in the PSQ 96 MA SNP software v2.1. All samples were analyzed in the PSQ 96 instrument (*Biotage*).

#### 4.3.6. DNA modification: bisulfite treatment

Methylation of cytosines located 5' to guanosine is known to have a profound effect on the expression of many eukaryotic genes (Bird 1992). In the bisulfite reaction, all unmethylated cytosines are deaminated and sulfonated, converting them to uracils, while 5-methylcytosines remain unaltered.

The bisulfite modification of DNA samples was performed using CpGenome<sup>TM</sup> DNA Modification Kit (*Qbiogene*).

One  $\mu\text{g}$  DNA in 100  $\mu\text{l}$  of water (10 ng/ml) together with 3M NaOH were mixed and incubated 10 min at 50°C on a heat block. 550  $\mu\text{l}$  of freshly prepared DNA Modification Reagent I were added to the samples and incubated at 50°C for 16 h in a heat block. During this incubation time, bases are exposed by denaturing the DNA to its single stranded form using mild heat at an alkaline pH. Reagent I contains a sodium salt of bisulfite ion ( $\text{HSO}_4^-$ ) that causes unmethylated cytosine to be sulfonated and hydrolytically deaminated, yielding a uracil sulfonate intermediate. After 16 h incubation with Reagent I, 5  $\mu\text{l}$  of well-suspended DNA Modification Reagent III were added to the DNA samples together with 750  $\mu\text{l}$  of DNA Modification Reagent II and mixed briefly.

DNA solutions were incubated at room temperature for 10 min. During this incubation time DNA is bound to a micro-particulate carrier (Reagent III) in the presence of another salt (Reagent II). Samples were centrifuged for 10 sec at 5,000 x g to pellet the DNA Reagent III. DNA was desalted by adding 1 ml of 70 % EtOH and centrifuged for 10 sec at 5,000 x g. The supernatant was discarded and this step was repeated for a total of three times. After the supernatant from the third wash has been removed, the tubes were centrifuged at high speed for 2 min and the remaining supernatant removed with a plastic pipette tip. The conversion to uracil was completed by alkaline desulfonation and desalting using 50  $\mu\text{l}$  of the 20 mM NaOH 90 % ethanol solution. The pellet was resuspended by vortexing and incubated at room temperature for 5 min. Pellets were spun for 10 min at 5,000 x g to move all the contents to the tip of tube. Pellets were washed with 1 ml of 90 % ethanol, vortexed and spun again. The supernatant was removed and this step was repeated one additional time.

After the supernatant from the second wash has been removed, samples were centrifuged at high speed for 3 min and all of the remaining supernatant was removed. Pellets were air dried for 20 min at room temperature. The DNA was eluted from the carrier by heating at 60°C for 15 min in TE buffer. Samples were centrifuged at high speed for 3 min and the supernatant transferred to a new tube.

Bisulfite treated DNA samples were stored at -20°C and proceeded to pyrosequencing.

### 4.3.8. DNA amplification

#### 4.3.8.1. Polymerase chain reaction (PCR)

PCR is based on the recognition by a short piece of single stranded DNA (the primer) of a sequence on a larger, single stranded fragment of DNA (template strand). When the primer recognizes the template and anneals to the recognition sequence, the 3'-end of the primer is used by DNA polymerase to synthesize a new DNA strand (elongation). When the temperature is raised, the new DNA strand will denature from the template, and the template is once again open for annealing of a new primer when the temperature is decreased. By adding a second primer which recognizes the template strand complementary to the first template, the elongation can proceed in the direction of the first primer. In the first round of elongation, this, ideally, will double the amount of template strands.

PCR involves preparation of the sample, the master mix and the primers, followed by detection and analysis of the reaction products. The DNA samples used were either genomic DNA, cDNA (obtained after RT-PCR reaction) or plasmid DNA. The PCR reactions were prepared as described in table 13.

**Table 13 Reaction components for PCR.**

Component	Volume/reaction ( $\mu$ l)
<b>Master mix</b>	
Sterile water	variable
1.25 mM dNTP	4
10xPCR Buffer	2.5
25mM MgCl <sub>2</sub>	1
Primer for	1
Primer rev	1
Taq polymerase	0.3
<b>Template</b>	
Genomic DNA, cDNA, plasmid DNA	variable*
<b>Total volume</b>	<b>25</b>

\*: 20 ng genomic DNA, 40 ng cDNA, 40 ng plasmid DNA.

Information about primers (number, sequence, annealing temperatures) are shown in table 3 for *ZNF265*, table 4 for *HDAC6*, table 5 for *hnRNP-R* and table 7 for *T-plastin*.

The cycling conditions were according to the primer annealing temperature, fragment length and the CG content.

The standard PCR conditions were: 10 min at 94°C denaturation, followed by 31 cycles of 30 sec at 94°C, 30 sec at annealing temperature shown in table 4, and 30 sec at 72°C. The final extension step was at 72°C for 10 min. The PCR products were resolved on an 1-2 % agarose gel.

#### 4.3.8.2. Reverse-transcription PCR (RT-PCR)

Reverse-transcription (RT-reaction) is a process in which single-stranded RNA is reversely transcribed into complementary DNA (cDNA) by using a reverse-transcriptase enzyme, primer, dNTPs, RNase inhibitor. RT-reaction is also called first strand cDNA synthesis.

RNA was isolated from EBV-transformed lymphoblastoid cell lines, primary fibroblast, HEK296 cell and PC12 cells, respectively, using TRIzol (*Invitrogen*). First-strand cDNA synthesis was performed using "SuperScript First-Strand Synthesis System for RT-PCR Kit" (*Invitrogen*).

Two µg of RNA were used as template for first-strand synthesis. Together with 1 µl oligo-d(T) primers and 1 µl dNTP, the RNA was denatured at 65°C for 5 min. The RNA samples were then placed on ice and 4 µl of RT-buffer, 4 µl of 25 mM MgCl<sub>2</sub>, 2 µl of 0.1 M DTT and 1 µl of RNase OUT were added. After mixing, the tubes were placed for 2 min at 37°C. Then 0.25 µl SuperScript II were added to the samples and the cDNA synthesis was performed at 37°C for 1 h. The reaction was stopped by 15 min. incubation at 70°C. In order to remove the RNA, 1 µl of RNase H was added and the samples were incubated for 20 min at 37°C.

#### 4.3.8.3. Multiplex PCR

Multiplex polymerase chain reaction is a variant of PCR, in which two or more loci are simultaneously amplified in the same reaction. The multiplex PCR reactions of all target genes using 2 µl cDNA were performed using the primers described in table 3. As internal control the *HPRT* gene using primer #785 and #786 (*HPRT\_for*: 5'-TGTAATGACCAGTCAACAGG-3' and *HPRT\_rev*: 5'-ATTGACTGCTTCTTACTTTCT-3') or the *actin* gene using primer #2473 and #2474 (*actin\_cDNA\_for*: 5'-CAGAAGGATTCTATGTGGG-3' and *actin\_cDNA\_rev*: 5'-TTGAAGGTAGTTTCGTGGATG-3') were co-amplified. In a total volume of 25 µl 10 pmol of each primer of the target transcript and 5 pmol of each primer of the internal control, 200 µM dNTPs, 1U Taq polymerase and 1 µl 50 mM MgCl<sub>2</sub> were added. 5 % DMSO was used in the PCR reactions as indicated with "\*" in table 6. Cycling conditions included a 10 min initial denaturation at 94°C, followed by 22 cycles to ensure quantitative measurements during linear phase of 30 sec at 94°C, 30 sec at the annealing temperature specified in table 5 for *hnRNP-R* and table 6 for *SMN*, *Septin 2*, *T-plastin*, *CD24* and *Plod 2*, 25-45 sec at 72°C and a final extension of 10 min at 72°C. PCR products were resolved on an 0.8-1.5 % agarose gel.

#### 4.3.8.4. Nested PCR

Nested PCR means that two-pairs of PCR primers were used for a single locus. The locus is amplified in a first round by the first primer pair. The second pair of primers (nested primers) binds within the first PCR product and produces a second PCR product that will be shorter than the first one. This strategy has been used to amplify besides all CpG regions for pyrosequencing, *NR1I3* gene (see table 6). Two µl cDNA were

used in 25  $\mu$ l PCR reaction as final volume. To the DNA were added 4  $\mu$ l of 1.25 mM dNTPs mix, 2.5  $\mu$ l of 10xPCR buffer, 1  $\mu$ l of 50 mM  $MgCl_2$  and 10 pmol of each primer #2349 and #2330, 5% DMSO and 1U Taq-polymerase. Cycling conditions for the first round included a 10 min initial denaturation step at 94°C followed by 20 cycles of 30 sec at 94°C, 1 min at 57°C, 45 sec at 72°C and a final extension of 10 min at 72°C. Five  $\mu$ l of PCR product amplified in the first round were used for a second round of amplification using as internal primers 10 pmol of each NR113 primer (#2343 and #2344). The reactions were prepared as described in section 4.3.8.3 and run in the same conditions.

#### 4.3.8.5. PCR of bisulfite treated DNA

The efficacy of bisulfite PCR is generally low; mispriming and non-specific amplification often occurs due to the T richness of the target sequences. Therefore, a good primer design is crucial, since the dimer formations are greatly facilitated by the T and A richness of the sense and antisense oligos, respectively. Moreover, the primers designed for the bisulfite-treated template frequently amplify non-specific PCR products because of the mispriming of the highly redundant genome generated by the treatment. Ideally, 2 sets of primers should be designed to anneal to the DNA. The primers should be 20-21 bp in length and should possess similar dissociation temperatures. The product produced after the second round should be 100-200 bp in size. Internal secondary structure should be avoided. For the second round one primer is biotinylated to the 5'-end. PCR assays were designed to amplify the whole CpG island in the T-plastin promoter region. Primers targeted CpG-free regions to ensure that the PCR product would proportionally represent the methylation characteristics of the source DNA. Pyrosequencing primers were subsequently designed to focus on a series of seven "target" CpG regions, named CpG1 to CpG7 regions. In total, 99 CpG dinucleotides were checked for analysis, and in each assay one or two non-CpG cytosines provided an internal control of the completeness of bisulfite treatment. The nested PCR procedure consisted of amplification of 1  $\mu$ l of the bisulfite treated DNA in a final volume of 25  $\mu$ l with 2.5  $\mu$ l of 10xPCR buffer, 4  $\mu$ l of 1.25 mM dNTPs, 1  $\mu$ l of 50 mM  $MgCl_2$ , 10 pmol of external primers (table 8) and 1U of Taq-polymerase. When necessary 5  $\mu$ l of Q-solution (*Qiagen*) were added as indicated in table 5. The PCR conditions were as follows: an initial denaturation step for 10 min at 94°C followed by 5 min at 80°C and 45 cycles of 30 sec at 94°C, 1 min at the annealing temperature described in table 5 and 30 sec at 72°C. The final extension was performed for 10 min at 72°C. The internal primers used in the second round of the nested PCR are listed in table 9. When a sequencing primer in the forward orientation was desired for the pyrosequencing reaction, then a reverse biotinylated primer was chosen and vice versa. Two  $\mu$ l of the first round PCR reaction were used together with 2.5  $\mu$ l of 10xPCR buffer, 4  $\mu$ l of 1.25 mM dNTPs, 1  $\mu$ l of 50 mM  $MgCl_2$ , 10 pmol of unbiotinylated primer, 0.3 pmol of biotinylated primer and 1U of Taq-polymerase in a total of 25  $\mu$ l PCR reaction. In some cases, the addition of 5  $\mu$ l of Q-solution improved the efficiency of the PCR reaction (tables 8 and 9). The PCR cycling program was optimized as described for the first round using the annealing temperature indicated in table 9. Confirmation of PCR products quality and freedom of contamination was established on a 2 % agarose gel with ethidium bromide staining.

#### 4.3.8.6. PCR for genotyping

PCR was performed on genomic DNA isolated from five SMA discordant families, five SMA patients that showed *T-plastin* expression in RNA samples extracted from EBV-transformed cell lines and two families of healthy volunteers that showed *T-plastin* expression in RNA samples isolated from fresh blood. PCR primers were designed using Primer PSQ Assay Design (*Biotage*). Primer sequences, annealing temperatures and the target SNPs are described in table 8. PCR was carried out using 5 ng genomic DNA together with 2.5 µl of 10xPCR buffer, 4 µl of 1.25 mM dNTPs, 1 µl of 50 mM MgCl<sub>2</sub>, 10 pmol of unbiotinylated primer, 0.3 pmol of biotinylated primer and 1U of Taq polymerase in a total of 25 µl PCR reaction. PCR conditions were 10 min at 94°C followed by 35 cycles of 30 sec at 94°C, 1 min at the annealing temperature described in table 8 and 30 sec at 72°C. The final extension was performed for 10 min at 72°C.

#### 4.3.9. PCR products purification

The PCR products were purified using QIAquick PCR Purification Kit (*Qiagen*). This kit is designed for rapid DNA cleanup of double- or single-stranded PCR products (100 bp -10 kb). Five volumes of buffer PB were added to 1 volume of the PCR sample, mixed and transferred to the QIAquick columns. Samples were centrifuged for 1 min at high speed and the flow-through discarded. The PCR products were washed with 700 µl buffer PE and another centrifugation step under the same conditions performed. To remove residual ethanol from the membrane, an additional centrifugation step for 2 min at top speed was performed. The samples were eluted in 40 µl ddH<sub>2</sub>O that were applied directly to the center of each QIAquick membrane. Columns were centrifuged for 1 min at high speed and the purified PCR products stored at 4°C.

#### 4.3.10. DNA quantification by spectrophotometry

The concentration of DNA sample can be checked by the use of UV spectrophotometry. Both RNA and DNA absorb UV light very efficiently making it possible to detect and quantify either at concentrations as low as 2.5 ng/µl. Based on extinction coefficient, the absorbance at 260 nm in a 1-cm quartz cuvette of a 50 µg/ml solution of double stranded DNA or a 40 µg/ml solution of single stranded RNA is equal to 1. The DNA concentration was calculated as follows:

$$\text{DNA concentration } (\mu\text{g/ml}) = (\text{OD}_{260}) \times (\text{dilution factor}) \times (50 \mu\text{g DNA/ml}) / (1 \text{ OD}_{260} \text{ unit})$$

The ratio of the absorbance at 260 nm/ absorbance at 280 nm is a measure of the purity of a DNA sample; it should be between 1.65 and 1.85.

#### 4.3.11. DNA extraction from agarose gels

The extraction and purification of some PCR products from agarose gel were performed using the QIAEX II Gel Extraction Kit (*Qiagen*). The PCR products were loaded on a 2 % agarose gel in TBE buffer and after running the DNA bands were excised from the agarose gel with a clean, sharp scalpel. The gel slices were weighed and 3 volumes of Buffer QX1 to 1 volume of gel were added together with 10 µl of QIAEX II. Samples were incubated at 50°C for 10 min to solubilize the agarose and bind the DNA, vortexing every 2 min to keep QIAEX II in suspension. Samples were centrifuged 30 sec and the supernatant carefully removed. Pellets were resuspended in 500 µl Buffer QX1 by vortexing. After 30 sec centrifugation all traces of supernatant were removed. The pellets were washed twice with 500 µl Buffer PE and centrifuged under the same conditions. After these washing steps the pellets were air dried for approximately 30 min. DNA was eluted in 20 µl ddH<sub>2</sub>O and the pellet resuspended by vortexing. After 5 min incubation at room temperature, the pellets were centrifuged 30 sec at high speed and the supernatant carefully transferred into a clean tube and stored at -20°C.

#### 4.3.12. DNA-protein interaction

##### 4.3.12.1. <sup>32</sup>P labelling of oligonucleotide probe

The use of radioactively labelled probes has widespread application, due to the technical requirements in using radioactive labelling reagents such as <sup>32</sup>P or <sup>35</sup>S.

To prepare the <sup>32</sup>P- labeled primer used in LM-PCR reaction (section 4.3.12.2.3) in order to amplify the T-plastin enhancer region, all the reagents were mixed as shown in table 14.

**Table 14 Components used for <sup>32</sup>P labelling of the T-plastin oligonucleotide probe.**

Reagent	Quantity
Oligo DNA (primer #)	10 pmol (2.5 µl)
10x OPA buffer	1.5 µl
γ- <sup>32</sup> P-ATP	5 µl
T4 DNA kinase	1 µl
dH <sub>2</sub> O	2 µl

Samples were incubated at 37°C for 1 h. In the meanwhile the Sepharose G-20 spin columns (*Amersham*) were vortexed well and then placed in 1.5 ml tube and spun at 3,000 rpm for 1 min. The columns were placed in new 1.5 ml tubes and 12 µl of labelled samples were applied to the top-center of the resin. Samples were then centrifuged at 3,000 rpm for 2 min. The labelling mix was prepared by adding 12 µl of end-labelled primer 3' and 13 µl of HPLC water to one PCR bead.

#### 4.3.12.2. *In vivo* footprinting

A variety of methods are available to analyze protein–DNA interactions *in vivo*. One method commonly used to examine the interaction of proteins and DNA is *in vivo* footprinting. DMS *in vivo* footprinting was used to determine the regions that contribute to the differential expression pattern in human tissues in an *in vivo* setting. In principle, the small molecule DMS diffuses rapidly into the nuclei of living cells and methylates guanine residues in the major groove of DNA and, to a lesser extent, adenine residues in the minor groove (Maxam and Gilbert 1980; Mueller and Wold 1989). Dimethyl sulfate alkylates at the N7 position of guanines or N3 position of adenines in double-stranded DNA; the resultant lability of the methylated purines is the basis for the guanine and adenine base-specific cleavage sequencing (Maxam and Gilbert 1980). Transcription factors binding to the DNA inhibit or stimulate guanine methylation, leading to protection or hypermethylation, respectively. Such genomic footprints were visualized by comparing samples of DNA that have been exposed to the methylating agent DMS in the living cell (*in vivo*) with samples treated with this agent.

*In vivo* footprinting was performed on EBV-transformed lymphoblastoid cell lines belonging to five SMA discordant families and controls. *In vivo* footprinting was accomplished by treatment of cells with dimethyl sulfate (DMS). Cells in exponentially growing suspension cultures were counted and harvested by centrifugation at 500 x g. To obtain partial DMS methylation *in vivo*, three individual samples of 10<sup>8</sup> cells each were treated with 1 ml of growth medium containing 1 % DMS for 2 min at 37°C. Exposure to DMS was stopped by the addition of 49 ml of ice-cold PBS followed by immediate low-speed centrifugation (1,500 rpm). Residual DMS was removed by an additional PBS wash. The pelleted cells were resuspended in 3.0 ml of PBS.

##### 4.3.12.2.1. Genomic DNA isolation

The genomic DNA of DMS-treated EBV-transformed lymphoblastoid cell lines were obtained by adding 2.7 ml of the cell lysis solution. Samples were allowed to incubate at 37°C overnight, after which the genomic DNA was phenol-chloroform extracted and ethanol precipitated. Briefly, to the tubes containing DMS-treated DNA an equal volume of phenol-chloroform solution was added. Tubes were inverted several times and centrifuged for 10 min at +4°C at top speed. The top phase (DNA sample) was transferred to a tube containing equal volume of phenol-chloroform and then mixed and centrifuged under the same conditions. The top phase was transferred to a new tube containing equal volume of chloroform, mixed and again centrifuged as above. The top phase was removed to a fresh tube and 1/10 vol of 3 M Sodium Acetate and 3 vol of 100 % ethanol were added to the samples. DNA samples were incubated on ice 10 min and centrifuged for 10 min in cold at top speed. Supernatants were discarded and DNA pellets washed once with 80 % ethanol and centrifuged under the same conditions. The ethanol was then removed and pellets dried for 30 min at room temperature. Pellets were resuspended in 100 µl of HPLC water and let to dissolve overnight at 37°C.

#### 4.3.12.2.2. Piperidine cleavage

Piperidine is a 1-ring heterocyclic compound formed from the polyamine cadaverine in the human intestine. After DMS chemical modification, the polynucleotide chain become susceptible to cleavage by piperidine (Rubin and Schmid 1980). Following *in vivo* DMS treatment, extracted genomic DNA from each cell type was cleaved at all methylated guanines by incubation in 200  $\mu$ l of 1 M piperidine for 30 min at 90°C. The piperidine was removed by lyophilization, and the cleaved DNA pellets were resuspended in 360  $\mu$ l of TE buffer. Residual piperidine was removed by two successive ethanol precipitations. The first entailed addition of 40  $\mu$ l of 3 M sodium acetate followed by 1 ml of 100 % ethanol and incubation for 30 min at -70°C. DNA samples were pelleted by microcentrifugation for 15 min at 4°C and resuspended in 500  $\mu$ l of TE buffer. The DNA pellets were ethanol precipitated a second time by the addition of 170  $\mu$ l of 8 M ammonium acetate and 670  $\mu$ l of isopropanol and incubation for at least 30 min at -70°C. The precipitated samples were pelleted by microcentrifugation as described above, washed with 500  $\mu$ l of 75 % ethanol, and microcentrifuged for 5 min at room temperature. The resulting DNA pellets were resuspended in double-distilled water to a final concentration of 0.4  $\mu$ g/ $\mu$ l.

#### 4.3.12.2.3. Ligation-mediated PCR (LM-PCR)

LM-PCR is based on the principle of detecting the cleavage products of a footprinting reagent (such as dimethyl sulfate followed by piperidine cleavage) in a gene of interest within a genomic DNA sample by primer extension with a gene-specific primer followed by the blunt ligation of an asymmetric linker (designed to ligate in only one orientation) that is not gene-specific.

PCR amplification with a nested, gene-specific PCR primer and a primer corresponding to the sequence of the linker yields detectable levels of the family of cleavage products that can then be resolved by gel electrophoresis and detected by autoradiography after a final nested primer extension with an end-labeled primer (Mueller and Wold 1989).

The general strategy of LM-PCR implies the first strand synthesis using a gene-specific primer (primer 1) that is hybridized to the cleaved DNA substrate. Annealed primer 1 is then extended with a DNA polymerase to create a blunt end at the site of the original cleavage event. To this blunt end a staggered linker (with one blunt end) of defined length and sequence is ligated. After the ligation reaction, the DNA is exponentially amplified using a primer that recognizes the ligated sequence (linker primer) and a gene-specific primer (primer 2). After exponential amplification, the LM-PCR product is visualized by primer extension of a radioactively labelled third gene-specific primer (primer 3).

Two micrograms of DMS-treated and piperidine-cleaved genomic DNA were used for LMPCR. Single-stranded DNA fragments with guanine residues at both termini result from the DMS treatment and piperidine cleavage. To provide appropriate substrates for linker ligation, double-stranded, blunt-ended molecules were generated by primer extension from *T-plastin*-specific enhancer (oligonucleotide 1A). This first-strand primer extension was accomplished by incubation of 2  $\mu$ g of DMS-treated and piperidine-

cleaved DNA with 0.3 pmol of oligonucleotide 1A, 1 × Vent DNA polymerase buffer (*New England Biolabs*), 4 mM MgSO<sub>4</sub>, 0.25 mM of each deoxynucleoside triphosphate, 2.5 µl of 10x Vent polymerase buffer, 2 µl MgSO<sub>4</sub>, 5 % DMSO and 0.5 U of Vent DNA polymerase (*New England Biolabs*) in a total volume of 25 µl. The DNA was denatured at 94°C for 5 min, annealed by incubation at 55°C for 20 min, and extended by a subsequent incubation of 10 min at 72°C. Ligation of the unidirectional linker described by Mueller and Wold (Mueller and Wold 1989), was completed by the addition of 5 µl of 100 pmol of double stranded linker, 10 µl of 2 × Quick ligase buffer, 2 µl of 100 mM ATP and 1 U of T4 DNA ligase to the PCR product. This mixture was incubated at 16°C overnight, after which the DNA was recovered by ethanol precipitation. Briefly, to the ligated products 5 µl of 3M Natrium acetate, 2.5 µl of glycogen and 250 µl 100 % ethanol were added. The content was mixed gently and incubated at -20°C for 1 h. Samples were then centrifuged at 10,000 rpm in cold for 15 min. The ethanol was removed and pellets were washed with 70 % ice-cold ethanol by centrifugation under the same conditions. Precipitated DNA samples were air dried for 30 min at room temperature and resuspended in 22.5 µl HPLC water. The ligated DNA was then mixed with 10 pmol of primer 2 and applied on one PCR bead. The mixture was pipetted until it appeared clear. These samples were placed in a thermocycler, denatured for 10 min at 95°C and cycled 25 times with a profile of 95°C for 1 min, 63°C for 2 min, and 72°C for 1 min, with a final extension of 4 min at 72°C. Following amplification, *T-plastin*-enhancer specific PCR products were labeled by the addition of 5 µl of labeling cocktail and subjected to a first denaturation step for 5 min at 95°C followed by 5 rounds of 95°C for 2 min, 63°C for 2 min, and 72°C for 3 min. The last extension step was performed at 72°C for 5 min. Each reaction mixture was then subjected to phenol-chloroform extraction and ethanol precipitation prior to electrophoresis on a 20 % sequencing polyacrylamide gel. The reactions were visualized by autoradiography with Kodak BioMax MR.

The oligonucleotide sequences of the nested *T-plastin* enhancer primer set used for the analysis of the sense strand by LM-PCR were oligonucleotide Enhancer 1\_for (#3208): 5'-ACCTGACCCTGCAAAATCC-3' (start position -912); oligonucleotide Enhancer 2\_for (#3209): 5'-TCTCTGAGTTGATTTTGGATATACG-3' (start position -880) ; and oligonucleotide Enhancer 3\_for (#3210): 5'-GTTGATTTTGGATATACGATGAACC-3' (start position -874).

Oligonucleotide sequences of the nested primer set used to analyze the minus strand by LM-PCR were oligonucleotide Enhancer 1\_rev (#3211): 5'-CCAGAGAAAATTTGGAGACATG' (start position -694); oligonucleotide Enhancer 2\_rev (#3212): 5'-TACTCTCCCCAGACTGCCATTTC-3' (start position -736); and oligonucleotide Enhancer 3\_rev (#3213): 5'-CCCAGACTGCCATTTCTTCTC-3' (start position -744). The design and location of LM-PCR primers is summarized in Fig. F4 in appendix.

The unidirectional linker oligonucleotide sequences have been described by Mueller and Wold and are as follows: Longer linker, 5'-GCGGTGACCCGGGAGATCTGAATTC-3', and Shorter linker, 5'-GAATTCAGATC-3'.

## 4.4. RNA techniques

### 4.4.1. RNA isolation

#### 4.4.1.1. RNA isolation from fresh blood

Total RNA (from fresh blood) was isolated using PAXgene Blood RNA Kit (*PreAnalytix*) which allows the isolation of total RNA from 2.5 ml human whole blood collected in the PAXgene Blood RNA tube. PAXgene blood RNA tubes were let stand at room temperature as recommended by the manufacturer. Total RNA isolation from blood samples collected in PAXgene tubes was carried out on day three after blood sampling. The PAXgene Blood RNA tubes were centrifuged for 10 min at 4,500 rpm. The supernatant was removed by decanting and 5 ml RNase-free water were added to the pellet. The pellet was resuspended by vortexing and centrifuged for 10 min at 4,500 rpm. The entire supernatant was discarded and the pellet was resuspended in 360  $\mu$ l Buffer BR1 by vortexing. The samples were transferred into 1.5 ml microcentrifuge tubes and 300  $\mu$ l Buffer BR2 and 40  $\mu$ l Proteinase K were added to the samples. After vortexing, the samples were incubated for 10 min at 55°C on a heating block at maximum speed. The samples were centrifuged for 3 min at maximum speed and the supernatant was transferred to a fresh 1.5 ml tube. 350  $\mu$ l 100 % ethanol was added and mixed by vortexing. The samples were transferred to the PAXgene column and centrifuged for 1 min at 10,000 rpm. 700  $\mu$ l Buffer BR3 was added to the column and centrifuged for 1 min at 10,000 rpm. The samples were washed 2 times with 500  $\mu$ l Buffer BR4 each and eluted in 40  $\mu$ l Buffer BR5. The eluate was incubated for 5 min at 65°C in a heating block for denaturation and chilled immediately on ice.

#### 4.4.1.2. TRIzol method for RNA isolation from cell culture

RNA was isolated from EBV-transformed lymphoblastoid cell cultures, human fibroblasts, HEK293 and PC12 cells using TRIzol (*Invitrogen*). Cells were pelleted by centrifugation in a 1.5 ml Eppendorf tube, and all supernatant removed (PBS or culture medium). Cells were resuspended by flicking the tube. Cells were lysated with 1 ml TRIzol per  $1 \times 10^7$  cells by repetitive pipetting carefully, avoiding spillage. The suspension was mixed until all cell debris dissolved, and no clumps were apparent. The mixture was incubated at room temperature for 5 min to complete homogenisation. At this point the samples were frozen at -80°C for one night. 0.2 ml chloroform was added to the samples, gently mixed, and incubated 10 min at room temperature. Samples were centrifuged at 12,000 rpm for 15 min at 4°C. The upper, clear part was transferred into new tubes and 2 vol isopropanol added, mixed well and incubated at room temperature for 10 min. Samples were centrifuged at 12,000 rpm for 10 min at 4°C. The supernatant was removed and pellets were washed with 100  $\mu$ l 75 % ethanol. After an additional centrifugation step under the same conditions (10 min, 12,000 rpm, 4°C) the pellets were air dried for 10 min. Pellets were dissolved

in the proper amount DEPC treated H<sub>2</sub>O. Each RNA sample was diluted in 100 µl H<sub>2</sub>O and absorption measured at 260 nm.

## 4.5. Autoradiography

Autoradiography is a technique using X-ray film to visualize molecules or fragments of molecules that have been radioactively labeled. Autoradiography has many applications in the laboratory. This method was used to visualize the DNA fragments applied on a sequencing gel do detect the protein-DNA interaction (*in vivo* footprinting). When the gel run was finished, the gel was allowed to cool for 15 min at room temperature. The shorter plate was removed carefully without breaking the gel, and the gel was fixed in 10 % methanol/ 10 % acetic acid for 20 min, by placing the gel plate in a tray and carefully pouring on sufficient fix to cover the gel, without the level of the liquid rising over the entire plate. Carefully a piece of pre-wet 3 MM paper in fixing solution was placed onto the gel, then a second 3 MM paper, and the two papers were peeled away with the gel attached. The additional piece of 3 MM paper was discarded and the paper with the gel placed on the gel dryer. The gel was covered with Saran-wrap and dried under vacuum for 30 min, with the heating turned up to maximum, and with dry ice place under the vacuum draining flask. The gel was exposed overnight to BioMax film at -70°C using a BioMax screen.

## 4.6. Protein biochemistry

### 4.6.1. Protein isolation, expression and purification

#### 4.6.1.1. Bacterial overexpression: expression and purification of SMN-GST fusion protein

In general, fusion proteins between a protein with glutathione-S-transferase (GST), are soluble and are easily purified from lysed cells under nondenaturing conditions by absorption with glutathione-agarose beads, followed by elution in the presence of free glutathione. pGEX vectors can be used in bacterial systems to express foreign polypeptides. Each pGEX vector contains an open reading frame encoding GST, followed by unique restriction endonuclease sites for BamH I, Sma I, and Eco RI. After subcloning of the SMN cDNA fragment into the pGEX vector (GVO# 331 pGEX-SMN-GST wt; kindly provided by A. Burghes) in the correct reading frame, the competent *E. coli* cells were transformed and selected on LB ampicillin plates. The transformed colonies were picked after 16 h incubation at 37°C into 4 ml LB/ ampicillin medium. A control culture inoculated with bacteria transformed with the parental pGEX vector was included. The liquid cultures were incubated with vigorous agitation in a 37°C shaking incubator for 16 h. The expression of fusion protein was induced by adding 100 mM IPTG. The incubation time was continued another 7 h. Liquid cultures were transferred to microcentrifuge tubes and centrifugated 1 min at maximum speed at room temperature. The immobilization of GST-fusion proteins was performed onto MagneGST™ Particles using MagneGST™ Pull-Down System (*Promega*). The MagneGST™ Pull-Down

System provides GSH-linked magnetic particles that allow simple immobilization of GST-fusion bait proteins from bacterial lysates. After discarding the supernatants, pellets were resuspended in 200  $\mu$ l of Cell Lysis Reagent by pipetting at room temperature. To reduce viscosity and to increase the purity of GST-fusion protein, 2  $\mu$ l of RQ1 RNase/free DNase were added and cell suspensions incubated at room temperature for 30 min on a rotating platform. During this incubation the MagneGST™ Particles were thoroughly resuspended by inverting the bottle several times to obtain a uniform suspension. Twenty  $\mu$ l of MagneGST™ particles were pipetted into a 1.5 ml tube and tubes were placed in the magnetic stand to allow the MagneGST™ Particles to be captured by the magnet. Carefully the supernatant was removed and discarded. The tubes were removed from the magnetic stand and by adding 250  $\mu$ l of MagneGST™ Binding/ Wash Buffer the particles were resuspended by pipetting. This step was repeated two more times. After the final wash, particles were resuspended in 100  $\mu$ l of MagneGST™ Binding/ Wash Buffer and 200  $\mu$ l of cell lysate containing the GST-fusion protein or the GST control and incubated with constant gentle mixing for 30 min at room temperature on a rotating platform. The tubes were placed in the magnetic stand and the MagneGST™ Particles were allowed to be captured by the magnet. The supernatants were removed and saved for gel analysis. 250  $\mu$ l of MagneGST™ Binding/ Wash Buffer were added to the particles, gently mixed and incubated at room temperature for 5 min while mixing occasionally by tapping. The tubes were placed in the magnetic stand and the supernatant carefully removed and discarded. Another 250  $\mu$ l of MagneGST™ Binding/ Wash Buffer were added to the particles and mixed gently by inverting the tube. The tubes were placed in the magnetic stand and supernatant removed and discarded. The washing step was repeated for a total of three washes. After the last wash, the particles were resuspended in 20  $\mu$ l of MagneGST™ Binding/ Wash Buffer. Five  $\mu$ l of the immobilized GST-fusion or GST control were used for the GST Pull-Down Assay.

#### 4.6.1.2. Expression of the T-plastin protein in the TNT® T7 Quick Coupled Transcription/ Translation Reaction (*Promega*)

The TNT® T7 Quick Master Mix allows the convenient single-tube coupled transcription/ translation of genes cloned downstream from T7 RNA polymerase promoters. TNT® T7 Quick Coupled transcription/ translation reactions are typically performed in a total volume of 50  $\mu$ l, which generally yields sufficient material for two pull-down reactions of 20  $\mu$ l each and for analysis of transcription/ translation efficiency.

**Table 15 TNT® T7 Quick Reaction Using pcDNA 3.1-T-plastin-V5 plasmid DNA.**

Components	Reaction Using Unlabeled Methionine
TNT® T7 Quick Master Mix	40 $\mu$ l
Methionine, 1 mM	1 $\mu$ l
Plasmid DNA template (0.5 $\mu$ g/ $\mu$ l)	2 $\mu$ l
Nuclease- Free Water	7 $\mu$ l

All the reagents were removed from -70°C and thawed on ice. The reaction components were assembled as shown in table 15 using as template pcDNA3.1-T-plastin-V5 plasmid. In the negative control reaction, no plasmid DNA was added. The reactions were incubated at 30°C for 90 min and stored at -20°C.

#### **4.6.1.3. Protein isolation from fresh blood**

The proteins from fresh blood were isolated using BD Vacutainer CPT Cell Preparation Tube with Sodium Citrate (*Preanalytical Systems*, Becton Dickinson and Company, Franklin Lakes). The blood was collected into the tube using the standard technique for BD Vacutainer Evacuated Blood Collection Tubes. After collection, the tubes were stored upright at room temperature until centrifugation. Blood samples were centrifuged at room temperature for 15 min at 3,000 rpm. After centrifugation, approximately half of the plasma was aspirated without disturbing the cell layer. The cell layer was collected with a Pasteur pipette and transferred to a 15 ml size canonical centrifuge tube. Up to 15 ml PBS were added and the cells were mixed by inverting the tubes 5 times. The samples were then centrifuged 15 min at 1,600 rpm and the supernatant was discarded. The cells were washed with 10 ml PBS by inverting the tubes 5 times. After 10 min centrifugation at 1,600 rpm the supernatant was removed and the cells were harvested in RIPA buffer.

#### **4.6.1.4. Protein isolation from cell culture using RIPA buffer (fibroblasts, EBV-transformed lymphoblastoid cell lines, HEK293 cells, PC12 cells)**

Fibroblast cells, EBV-transformed lymphoblastoid cell cultures, HEK293 and PC12 cells were harvested in RIPA buffer (150 mM NaCl, 1 % NP40, 0.5 % DOC, 0.1 % SDS, 50 mM Tris, pH 8.0) to prepare protein extracts. The samples were incubated for 15 min at room temperature and centrifuged at +4°C for 30 min at top speed. The supernatants were transferred in new 1.5 ml tubes.

#### **4.6.1.5. Protein isolation from cell culture using IP buffer (HEK293 cells, PC12 cells)**

HEK293 and PC12 cells were harvested in IP-buffer (25 mM HEPES pH 8.0, 150 mM KCl, 2 mM EDTA, 20 mM NaF, 1 mM DTT, 0.5 % NP40) to prepare protein extracts. The samples were incubated for 15 min at room temperature and then centrifuged at +4°C for 30 min at top speed.

#### **4.6.2. Protein quantification by spectrophotometry (Bradford assay)**

In contrast to nucleic acids, proteins have a UV absorption maximum of 280 nm, mostly due to the tryptophan residues. The Bradford assay is a rapid and accurate method commonly used to determine the total protein concentration of a sample. The assay is based on the observation that the absorbance maximum for an acidic solution of Coomassie Brilliant Blue G-250 shifts from 465 nm to 595 nm when

binding to protein occurs. Both hydrophobic and ionic interactions stabilize the anionic form of the dye, causing a visible color change. Within the linear range of the assay (~5-25 mg/mL), the more protein present, the more Coomassie binds. Bradford solution was used as blank and the samples were diluted 1:500 in Bradford solution. After 10 min at room temperature the protein concentration was read using a spectrophotometer.

#### **4.6.3. Generation of polyclonal antibody against T-plastin**

Rabbit polyclonal antibody against human T-plastin was produced by immunization of two rabbits at the Eurogentec Company with a synthetic polypeptide (H<sub>2</sub>N-MATTQISKDELDELKC-CONH<sub>2</sub>). The antibody recognizes 16 aa localized at the N-terminus of the T-plastin protein. The standard program for rabbit antibody was an 87 day program. Peptide antibody production is initiated by the judicious selection of a peptide sequence from the antigen's amino acid sequence, and is followed by the synthesis of the peptide and conjugation to a carrier protein. The peptide conjugate is then used for the immunization in place of the natural antigen. In the host animal, antibodies will be raised against the peptide sequence. The 2-month 2-rabbit program offers the rapid production of protein polyclonal antibodies. The program includes four immunizations, pre-immune test sample, small bleed and final bleed. The antibody is purified to eliminate other proteins by affinity purification that is the most common technique. The specificity of T-plastin antibody was determined by Western blot using either T-plastin protein transcribed in TnT system or proteins isolated from human fibroblasts, HEK293 cells, PC12 cells and EBV-transformed lymphoblastoid cell cultures. Three different dilutions were checked: 1:1,000; 1: 2,500 and 1: 5,000. The optimal conditions were found to be the blot incubation with a 1:5,000 anti-T-plastin antibody dilution.

#### **4.6.4. Protein analysis**

##### **4.6.4.1. SDS-PAGE electrophoresis**

Electrophoresis is a technique used to separate and sometimes purify macromolecules -especially proteins and nucleic acid- that differ in size, charge or conformation. Proteins can have either a net positive or a net negative charge, and migrate according to their charge. SDS-polyacrylamide gel electrophoresis (SDS-PAGE) separates proteins according to their molecular weights. Polyacrylamide is a crosslinked polymer of acrylamide. The length of the polymer chain is dictated by the concentration of acrylamide used, which is typically between 3.5 % and 20 %. Because oxygen inhibits the polymerization process, they must be poured between glass plates. The first step was to prepare the gel cassette sandwich. Before setting up the casting stand assembly, the casting stand, casting frames and glass plates were cleaned and dried. The casting frame was placed upright with pressure clamps in the open position and facing toward on a flat surface. A short plate was placed on the top of spacer plate and the two glass plates were placed into the casting frame. The gel cassette assembly was placed then on the

gray casting stand gasket. Both running gel solution and stacking gel solution were prepared as described in table 16.

**Table 16 Discontinuous 12% polyacrylamide gel preparation.**

Running gel solution		Stacking gel solution	
Component	Volume (ml)	Component	Volume (ml)
Acrylamide/ bisacrylamide mix	10.8	Acrylamide/ bisacrylamide mix	2
1.5M Tris/HCl pH= 8.8	7.5	1M Tris/HCl pH= 6.8	5.6
Distilled water	1.4	Distilled water	1.25
10% SDS	0.2	10 % SDS	0.1
10% APS	0.1	10 % APS	0.05
TEMED	0.1	TEMED	0.05

The running gel was poured smoothly to prevent it from mixing with air and some 100 % ethanol was layered on the top of the gel to avoid polymerization inhibition. The gel was allowed to polymerize for 30 min, when the ethanol was removed and discarded. The stacking gel solution was poured until the top of the short plate was reached. The desired comb was inserted between the spacers and the stacking gel was allowed to polymerize for 30 min. Then, the comb was gently removed and the walls were rinsed thoroughly with distilled water.

The gel cassette was removed from the casting stand and placed into the slots at the bottom of each side of the electrode assembly and lowered into the mini tank. The inner chamber was filled with 125 ml of running buffer until the level reaches halfway between the tops of the taller and shorter glass plates of the gel cassette. 200 ml of running buffer were added to the lower buffer chamber. The electrical leads were inserted into a suitable power supply and 100 volt constant were used for electrophoresis. When electrophoresis was complete, the gel was removed by gently separating the two plates of the gel cassette. The gel was removed by floating it off the glass plate by inverting the gel and plate under transfer solution.

#### 4.6.4.2. Antibodies

Antibodies used in these experiments were as follows:

- Mouse monoclonal anti- $\beta$ -tubulin (*Sigma*);
- Mouse monoclonal anti-SMN (*BD, Transduction Laboratories*);
- Mouse monoclonal anti- $\beta$ -actin (*Sigma*);
- Mouse monoclonal anti-V5 (*Invitrogen*);
- Rabbit polyclonal anti-T-plastin (*Eurogentec*);
- Phalloidin conjugated with AlexaFluor 568 (*Invitrogen*);
- Horseradish peroxidase conjugated goat anti-mouse IgG (*Dianova*);

- Horseradish peroxidase conjugated goat anti-rabbit IgG (*Pierce*)

**Table 17 Recommended dilutions for Western blot and immunocytochemistry analysis.**

Antibody (anti-)	Western blot	Immunocytochemistry
<b>Primary antibodies</b>		
SMN	1: 5,000	1: 500
T-plastin	1: 5,000	1: 500
$\beta$ -tubulin	1: 2,000	n.u.
$\beta$ -actin	1: 10,000	n.u.
Phalloidin	n.u.	1: 200
V5	1: 5,000	1: 500
<b>Secondary antibodies</b>		
Mouse IgG	1: 2,500	n.u.
Rabbit IgG	1: 10,000	n.u.

n.u.: not used

#### 4.6.4.3. Protein Transfer

This procedure is the middle step of the 3-step process of Western immunoblotting. The first step was SDS-PAGE to resolve a mixture of proteins by size. The second step detailed in this protocol, is the transfer of resolved proteins from the gel to a membrane support (i.e., nitrocellulose) via electroelution. The product of this second step is referred to as the blot. The protein transfer buffer was chilled (+4°C) and the nitrocellulose membrane was cut to the dimensions of the gel. The nitrocellulose membrane was soaked in transfer buffer until needed. Two fiber pads and two filter papers were slowly submerged into a container that sufficiently allowed the fiber pads and filter papers to be immersed in transfer buffer until completely wet. The pads were pressed down while they were submerged to remove air bubbles trapped inside pads. The colored gel holder cassette was placed on the assembly tray. The presoaked fiber pad and filter paper were placed on the top of the black side of the cassette and air bubbles were removed with a roller. The gel was placed carefully on the filter paper avoiding air bubbles formation. The pre-cut nitrocellulose membrane was placed over the front side of the gel. A wet filter paper and fiber pad were placed on the top of the membrane and by rolling, any air bubbles were removed. The white side of the gel holder cassette was lowered and the handle was locked into the close position. The locked gel holder cassette was moved from the assembly tray into the groove of the blotter tank, aligning the white side of the cassette with the red electrode. A stir bar was added to the transfer tank and placed on the stir plate. A frozen ice pack was placed into the transfer tank in the compartment behind the black electrode. The tank was filled with transfer buffer to the level marked on the tank. The electroelution was performed at constant voltage of 30 volt overnight.

#### 4.6.4.4. Western blot

Western blot analysis can detect one protein in a mixture of any number of proteins. This method is dependent on the use of high-quality antibody directed against a desired protein. All the following incubations and washes were conducted at +4°C with gentle shaking using an oscillating platform shaker. Volumes are specified for 8.7 x 13.3 cm Bio-Rad gel blots. Blots were incubated for 2 h in 50 ml 6 % Milk-TBS-Tween. The membranes were transferred to a tray containing the primary antibody diluted in 10 ml of 2 % blocking buffer and incubated for 2 h. Blots were washed three times, for 10 min each, with 0.1 % TBS-Tween. The secondary antibody diluted according to table 17 into 2 % blocking buffer was added and incubated for 1 h. Membranes were washed for five times, for 5 min each, with 0.1 % TBS-Tween. Immunostaining of the membranes and detection of the signal with Chemiluminescent reagent (*Pierce*) was carried out according to standard protocols.

#### 4.6.5. Protein-protein interaction

##### 4.6.5.1. Co-immunoprecipitation

Immunoprecipitation is a technique in which an antigen is isolated by binding to a specific antibody attached to a sedimentable matrix. Antibodies can be bound noncovalently to immunoabsorbents such as protein A- or protein G-agarose, or can be coupled covalently to a solid-phase matrix. HEK293 and PC12 cells were harvested in IP-buffer. Fifty µl of protein-G-sepharose resin slurry (50 % slurry in lysis buffer) per 1 ml of cell lysate were used to pre-clear the lysate for 1 h at +4°C. Samples were centrifuged for 1 min at 2,000 rpm and the supernatant transferred to a sterile microcentrifuge tube on ice. Equivalent amounts of pre-cleared cellular extracts were incubated with 4 µl of polyclonal anti-T-plastin antibody bound to protein-G-sepharose and rocked for 4 h at +4°C. Samples were centrifuged for 1 min at 2,000 rpm at +4°C, the supernatant removed and bound fractions were washed in 400 µl IP- buffer four times. After the last wash, 20 µl of SDS-PAGE sample buffer were added to the resin. Samples were heated at 95°C for 2 min, centrifuged for 1 min at 2,000 rpm, resolved by 12 % SDS-PAGE and transferred to nitrocellulose and detected with monoclonal anti-SMN or anti-β-actin antibody using chemiluminescence (*Pierce*).

##### 4.6.5.2. Magne GST™ Pull-Down assay

GST pull-down uses a GST-fusion protein (bait) bound to glutathione (GSH)-coupled particles to affinity purify any proteins (prey) that interacts with the bait. Bait and prey proteins can be obtained from multiple sources including cell lysates, purified proteins, expression systems and *in vitro* transcription/translation systems. The prey protein, T-plastin, was expressed in the transcription/ translation reaction (from *Promega*); the *E. coli* expressed GST-fusion (bait) protein (SMN-GST) was immobilized on the the Magne

GST<sup>TM</sup> Particles. To each 5 µl aliquot of particles carrying GST-fusion protein or GST control 20 µl of the TNT® T7 Quick coupled transcription/ translation reaction were added. The MagneGST<sup>TM</sup> Binding/ Wash Buffer was added to a final volume of 200 µl for each pull-down reaction. Samples were incubated for 1 h at room temperature on a rotating platform with gentle mixing. At the end of this incubation period, samples were briefly vortexed to remove non-specific adherent proteins and reduce background. Tubes were placed in a magnetic stand and supernatant (C4) carefully removed and saved for analysis. 400 µl of MagneGST<sup>TM</sup> Binding/ Wash Buffer were added and mixed gently by inverting the tube. Samples were incubated for 5 min at room temperature while mixing occasionally by tapping the tube. Tubes were placed in a magnetic stand and supernatants were removed and discarded. Another 400 µl of MagneGST<sup>TM</sup> Binding/ Wash Buffer were added and the samples were mixed by tapping the tubes. After placing the tubes in a magnetic stand and discarding the supernatant, the wash step was repeated for a total of five washes. After the last wash, 20 µl of 1x SDS loading buffer were added and samples were eluted by incubation for 5 min at room temperature with mixing. The tubes were placed in the magnetic stand and the eluate was removed for analysis. For Western blot analysis, 50 % of undiluted eluted sample (after boiling) was loaded onto the 12 % SDS-PAGE gel.

#### 4.7. Cell transfection

Transfection -delivery of foreign molecules such as DNA into eukaryotic cells- has become a powerful tool for the study and control of gene expression, e.g. for biochemical characterization, mutational analyses, or investigation of the effects of regulatory elements or cell growth behaviour. When cells are transiently transfected, the DNA is introduced into the nucleus of the cell, but does not integrate into the chromosome (Tang et al. 1996). This means that many copies of the gene of interest are present, leading to high levels of the expressed protein. Transcription of the transfected gene can be analyzed within 24-96 h after introduction of the DNA depending on the construct used. Optimization of cell culture technique is necessary to ensure that cells are healthy and in optimal conditions for transfection.

##### 4.7.1. Transient transfection of T-plastin-V5-tagged plasmid in HEK293 and PC12 cells

HEK293 cells were grown in DMEM medium supplemented with 10 % FCS. Conventional PC12 cells were cultured in DMEM supplemented with 5 % FBS and 10 % horse serum. For all transfection experiments,  $2 \times 10^4$  cells/ml were plated on 60 mm culture dishes the day before transfection. PC12 cells and HEK293 were transfected with either pcDNA3.1-T-plastin\_V5 plasmid or empty vector. For PC12 cells transfections only collagen-coated coverslips and 60 mm culture dishes were used in order to increase the adherent capacity of the cells. On the day of transfection, 5 µg of plasmid DNA was diluted with cell growth medium containing no serum, proteins or antibiotics to a total volume of 150 µl. The solution was mixed for a few sec and spun down to remove drops from the top of the tube. 30 µl SuperFect Transfection Reagent (*Qiagen*) were added to the DNA solution and samples were incubated 10 min at

room temperature to allow transfection-complex formation. While complex formation took place, the growth medium was aspirated from the culture dish and cells washed once with PBS. One ml cell growth medium (containing serum and antibiotics) was added to the reaction tube containing the transfection complexes. After pipetting up and down twice, the transfection complexes were transferred immediately to the cells in the 60 mm dishes. Cells were incubated with the transfection complexes for 3 h under their normal growth conditions. When the incubation time was out, the medium containing the remaining complexes was removed from the cells by gentle aspiration, and cells were washed once with 4 ml PBS. Fresh cell growth medium (containing serum and antibiotics) was added and cells were grown under their normal growth conditions over night. To obtain maximal levels of gene expression in PC12 cells, a second round of transfection under the same conditions was performed after 24 h and cells were assessed for expression of the transfected gene after 48 and 72 h, respectively.

#### **4.7.2. Transient transfection of T-plastin siRNA oligos into PC12 cells**

Cells were diluted in antibiotic-free medium (DMEM, low serum conditions) to a concentration of  $5 \times 10^4$  cells/ml. 200  $\mu$ l of cells were plated into each 24-well collagen-coated plate and incubated overnight at 37°C with 5 % CO<sub>2</sub>. Twenty five  $\mu$ l of 1  $\mu$ M siRNA solution were diluted with 25  $\mu$ l OPTIMEM medium and 1  $\mu$ l of transfection reagent (DharmaFECT 1 or 4) in 49  $\mu$ l OPTIMEM medium in separate tubes. The tubes were incubated for 5 min at room temperature. The content of the two tubes was combined, mixed by pipetting up and down and incubated for 20 min at room temperature. At the end of the incubation time 400  $\mu$ l of DMEM medium were added to the transfection mix. In the meanwhile, the culture medium was removed from the wells and 400  $\mu$ l of transfection mix added. Cells were incubated at 37°C in 5 % CO<sub>2</sub> for 24 h. After 24 h, another transfection under the same conditions was performed. Cells were incubated additionally for 48-72 h. For ICC experiments, the transfection was performed on collagen-coated coverslips under the same conditions.

#### **4.7.3. Co-transfection of T-plastin-V5-tagged plasmid DNA and SMN siRNA oligos into PC12 cells**

One day before transfection,  $5 \times 10^6$  PC12 cells were plated in medium without antibiotics on collagen-coated coverslips in 60 mm collagen-coated Petri dishes. Two  $\mu$ g of plasmid DNA (pcDNA3.1-T-plastin-V5 or empty vector) together with 100 pmol SMN siRNA or control siRNA were co-transfected using Lipofectamine 2000 Transfection Reagent (*Invitrogen*) after 20 min incubation at room temperature. Before use, 10  $\mu$ l of Lipofectamine 2000 were diluted in 490  $\mu$ l OPTIMEM medium without serum and incubated for 5 min at room temperature. Cells were incubated with the transfection complexes overnight under their normal conditions. For a high efficiency of transfection, 24 h after the first transfection, a second transfection was performed under the same conditions.

## 4.8. Cell imaging

### 4.8.1. Immunocytochemistry (ICC)

ICC is a technique used to assess the presence of a specific protein or antigen in cells (cultured cells, cell suspension) by use of a specific antibody, which binds to it, thereby allowing visualization and examination under a microscope.

1. Adherent cell culture slide preparation. The adherent cells were grown on coverslips in 60 mm Petri dishes at 37°C, 5 % CO<sub>2</sub>. When they reached 40-60 % confluence, cells were thoroughly washed 3 times with PBS for 2 min each wash step.
2. Fixation. To ensure free access to the antibody to its antigen, the cells must be fixed and permeabilized. Organic solvents such as alcohols and acetone remove lipids and dehydrate the cells, while precipitating the proteins on the cellular architecture. Crosslinking reagents (such as paraformaldehyde) form intermolecular bridges, normally through free amino groups, thus creating a network of linked antigens. Crosslinkers preserve cell structure better than organic solvents, but may reduce the antigenicity of some cell components, and require the addition of a permeabilization step, to allow the access of the antibody to the specimen. Three appropriate fixation methods were chosen according to the relevant application:
  - i. Acetone fixation. Cells were fixed in -20°C acetone for 5 min
  - ii. Methanol-Acetone mix fixation. Cells were fixed in 1:1 methanol and acetone mixture at -20°C for 10 min
  - iii. Paraformaldehyde-Acetone fixation. Cells were fixed in 4 % PFA at 37°C for 15 min and then permeabilized with cooled acetone for 5 min at -20°C.
3. Antibody Staining. The next step of cell staining involves incubation of cell preparations with the antibody. Unbound antibody is removed by washing and the bound antibody was detected directly. The primary antibody was directly labelled using Zenon labelling technology that utilizes a fluorophore-labelled Fab fragment directed against the Fc portion of an intact IgG primary antibody in order to form a labelling complex. The antibody was labelled with a Zenon IgG labelling reagent to obtain 3:1 molar ratio of Fab to antibody target. One µg of antibody in 20 µl PBS was mixed with 5 µl of the Zenon IgG labelling reagent and incubated 5 min at room temperature. Five µl of the Zenon blocking reagent were added to the reaction mixture. The solution was incubated 5 min at room temperature. After that the antibody solution was applied to samples and incubated for 1 h at room temperature protected from light. When staining was complete, the cell samples were washed three times with PBS. A second fixation was performed and when fixation was completed, the cell samples were washed again three times with PBS. The cell samples were counterstained with DAPI.
4. In the next step, cells were examined under the non- or confocal microscope

#### 4.8.2. Confocal scanning fluorescence microscopy

Confocal laser scanning microscopy (CLSM or LSCM) is a valuable tool for obtaining high resolution images and 3-D reconstructions. The key feature of confocal microscopy is its ability to produce blur-free images of thick specimens at various depths. Images are taken point-by-point and reconstructed with a computer, rather than projected through an eyepiece. The principle for this special kind of microscopy was developed by Marvin Minsky in 1953, but it took another thirty years and the development of lasers for confocal microscopy to become a standard technique toward the end of the 1980s.

Confocal images were taken with an inverted Leica TCS-SP laser-scanning microscope with a 63xHCX PL APO NA 1.32 or 100x HCX PL APO 1.40 oil immersion objectives. Fluorochromes Alexa 488, FITC and Alexa 568 were excited with the 488 nm Argon laser and the 543 nm Helium Neon laser, respectively. Emission fluorescence was collected in red (> 543 nm) and green (488 nm) channels simultaneously. Images were collected and processed using AdobePhotoshop Software.

#### 4.8.3. Non-confocal fluorescence microscopy

A fluorescence microscope is a light microscope used to study properties of organic or inorganic substances using the phenomena of fluorescence and phosphorescence instead of, or in addition to, reflection and absorption. In most cases, a component of interest in the specimen is specifically labelled with a fluorescent molecule called a fluorophore (such as GFP, green fluorescent protein). The cells were observed and analyzed using an Axioplan 2 imaging microscope (Zeiss) equipped with an AxioCam camera.

#### 4.8.4. Measurement of neurite outgrowth

Typically, PC12 cells were plated on collagen-coated coverslips and cultured overnight. NGF (100 ng/ml) was added to the cells in culture medium containing 5 % FBS serum. After stimulation for the indicated times with NGF, cells were washed and fixed with 4 % PFA. For each experiment at least three different coverslips from three independent experiments were used for the measurement. Cells were photographed with an Axioplan imaging microscope at 100 x magnification. A bar of 20  $\mu\text{m}$  was placed and used as standard to determine the length of neurites from each cell. Approximately, a total of 200 cells per coverslip were measured for neurite length.

### 4.9. Microarray

Microarrays are simply ordered sets of DNA molecules of known sequence. Usually rectangular, they can consist of a few hundred to hundreds of thousands of sets. Each individual feature goes on the array at precisely defined location on the substrate. The microarray technology consists of spotting PCR products or long oligonucleotides (50mer-70mer) on glass slides at densities of up to 6,000 spots/cm<sup>2</sup>. These slides

are hybridized using fluorescent targets (cDNAs or genomic DNAs). The fluorescent molecules most commonly used are members of the cyanine family, Cy3 or Cy5. After hybridization, the signals are detected using a fluorescence scanner. The use of two different fluorochromes allows the determination of hybridization signals from two distinct strains in one single experiment. Once the fluorescent intensities have been obtained, the major part of the work is the analysis of the data in order to extract the biological information.

#### 4.9.1. RNA Cleanup with RNeasy MinElute Cleanup Kit (*Qiagen*)

After TRIzol RNA extraction a cleanup using Qiagen RNeasy MinElute Cleanup Kit (*Qiagen*) is performed to obtain better yields of cRNA from the *in vitro* transcription-labeling reaction. A maximum of 45 µg RNA in a maximum volume of 200 µl can be used in the RNA cleanup protocol. This amount corresponds to the binding capacity of the RNeasy MiniElute spin columns. The samples were adjusted to a volume of 100 µl with RNase-free water. 350 µl buffer RLT were added and mixed thoroughly. 250 µl of 96 % ethanol was added to the diluted RNA samples and mixed thoroughly by pipetting. 700 µl of the sample were applied to an RNeasy MinuElute spin column placed in a 2 ml collection tube. Samples were centrifuged for 15 sec at 8,000 x g (> 10,000 rpm). The flow-through and collection tube were discarded. The spin columns were transferred in new 2 ml collection tubes and 500 µl of buffer RPE was added on the column. The column was washed for 15 sec by centrifugation at 8,000 x g. The flow-through was removed and 500 µl of 80 % ethanol was added to the column. To dry the membrane, samples were centrifuged for 2 min at 8,000 x g. The flow-through and collection tubes were discarded. The columns were transferred into new 2 ml collection tubes and centrifuged for 5 min at full speed to avoid carryover of ethanol. It is important to dry the silica membrane since residual ethanol may interfere with downstream reactions e.g. elution of RNA. To elute, the spin columns were transferred to new 1.5 ml collection tube and 14 µl of RNase-free water were added directly onto the center of the silica-gel membrane. Samples were eluted by centrifugation for 1 min at maximum speed.

#### 4.9.2. Quantification and analysis of purity of RNA

The absorbance was checked at 260 and 280 nm for determination of sample concentration and purity. To ensure significance, readings of A<sub>260</sub> should be greater than 0.1. The A<sub>260</sub>/A<sub>280</sub> ratio should be close to 2.0 for pure RNA (ratios between 1.8 and 2.3 are acceptable). For accurate values the absorbance measurements were made in 10 mM TrisCl, pH 7.5. The spectrophotometer was calibrated with the same solution.

$$\text{RNA concentration } (\mu\text{g/ml}) = (\text{OD}_{260}) \times (\text{dilution factor}) \times (40 \mu\text{g RNA/ml}) / (1 \text{ OD}_{260} \text{ unit})$$

The integrity and size distribution of total RNA purified with RNeasy Kit can be checked by agarose gel electrophoresis and ethidium bromide staining. The respective ribosomal bands should appear as sharp

bands on the stained gel. 28S ribosomal RNA bands should be present with an intensity approximately twice that of the 18S RNA band. If the ribosomal bands in a given lane are not sharp, but appear as a smear as smaller sized RNAs, it is likely that the RNA sample suffered major degradation during preparation.

### **4.9.3. Synthesis of double stranded cDNA from total RNA**

#### **4.9.3.1. First strand cDNA synthesis**

The cDNA synthesis was performed using SuperScript II (*Life Technologies*) following the supplier's instructions. The following HPLC purified primer was used:

T7-(dT) 24 primer

5'- GGCCAGTGAATTGTAATACGACTCACTATAGGGAGGCGG(dT)24-3'

The 40 µg RNA samples together with T7-(dT)24 primer (100 pmol/µl) in DEPC-water (for final reaction volume of 20 µl) were incubated at 70° C for 10 min for primer hybridization. After a quick spin the samples were placed on ice. To the reaction tubes 4 µl of 5x first strand cDNA buffer, 2 µl of 0.1 M DTT and 1 µl of 10 mM dNTP mix were added and samples were incubated at 42° C for two min to allow the temperature adjustment. 5 µl of SuperScript II RT (200 U/µl) was added to the tube and incubated at 42° C for 1 h to allow the first strand synthesis.

#### **4.9.3.2. Second strand cDNA synthesis**

Samples were centrifuged briefly to bring down condensation on sides of tube and first strand reaction tubes were placed on ice. To the first strand reaction tubes the second strand final reaction components were added: 91 µl DEPC-H<sub>2</sub>O, 30 µl 5x second strand reaction buffer, 3 µl 10 mM dNTP mix, 1 µl 10 U/*E.coli* DNA ligase, 4 µl of 10 U/*E.coli* DNA polymerase I, 2 U/µl *E.coli* RNase H. Tubes were gently tapped to mix, then briefly spun in a microcentrifuge to remove condensation and incubated at 16° C for 2 h in a cooling waterbath.

After incubation time, 2 µl of 10U T4 DNA polymerase were added and samples were returned to 16° C for 5 min. Then 10 µl 0.5 M EDTA was added and samples were used for clean-up procedure.

#### **4.9.3.3. Clean-up of double stranded cDNA with Sample Cleanup Module (*Affymetrix*)**

600 µl cDNA Binding Buffer were added to the 162 µl final double-stranded cDNA synthesis preparation. The colour of the mixture was checked to be yellow, similar to cDNA Binding Buffer without the cDNA synthesis reaction. 500 µl of the sample were added to the cDNA cleanup spin column sitting in a 2 ml Collection Tube and centrifuged for 1 min at 8,000 x g (> 10,000 rpm). Flow through was discarded. The spin column was reloaded with the remaining mixture and centrifuged as above. The flow-through was

removed as well as the collection tube. The spin column was transferred into a new 2 ml collection tube and 750  $\mu$ l cDNA wash buffer were pipetted onto the spin column followed by a centrifugation step for 1 min at 8,000 x g. The cap of the spin column was opened and centrifuged for 5 min at maximum speed to allow complete drying of the membrane. The flow-through and the collection tube were removed. The spin column was then transferred into a 1.5 ml collection tube and 14  $\mu$ l of cDNA elution buffer were added directly onto the spin column membrane and samples were incubated for 1 min at room temperature and then centrifuged 1 min at maximum speed to elute.

#### **4.9.4. Synthesis and purification of biotin labelled cRNA**

##### **4.9.4.1. Synthesis of biotin labelled cRNA**

The GeneChip IVT Labeling Kit has been used to synthesize the biotin-labelled cRNA for both the one-cycle and two cycle target labelling assay. Following the cDNA cleanup step the concentration of cDNA has been determined for further applications. The needed amount of template cDNA was then transferred to RNase-free microcentrifuge tube and the following reaction components were added in the order indicated in the protocol: RNase free water (to give a final reaction volume of 40  $\mu$ l), 4  $\mu$ l 10x IVT Labeling Buffer, 12  $\mu$ l IVT Labeling NTP Mix, 4  $\mu$ l IVT Labeling Enzyme Mix. Carefully the reagents were mixed and collected at the bottom of the tube by brief (5 sec) microcentrifugation. Samples were incubated at 37°C for 16 h. To prevent condensation that may result from water-bath-style incubators, incubations were performed in a thermal cycler.

##### **4.9.4.2. cRNA cleanup with Sample Cleanup Module (*Affymetrix*)**

To the *in vitro* transcription reaction 60  $\mu$ l of RNase-free water were added and mixed by vortexing for 3 sec. Then 350  $\mu$ l IVT cRNA Binding Buffer were added to the samples and mixed by vortexing for 3 sec. 250  $\mu$ l of 100 % ethanol were added to the lysate and mixed very well by pipetting. The 700  $\mu$ l sample was then transferred to the IVT cRNA cleanup spin column sitting in a 2 ml collection tube and centrifuged for 15 sec at 8,000 x g. The flow-through and collection tube were discarded and the spin column transferred into a new 2 ml collection tube. 500  $\mu$ l IVT cRNA Wash Buffer were added onto the spin column and samples were centrifuged for 15 sec at 8,000 x g. After discarding the flow-through, 500  $\mu$ l 80 % ethanol were pipetted onto the spin column and centrifuged under the same conditions as above. The flow-through was removed and the spin column was centrifuged with the cap opened for 5 min at maximum speed to allow complete drying of the membrane. Both flow-through and collection tubes were then removed. The columns were placed into new 1.5 ml collection tubes and 11  $\mu$ l of RNase-free water were added directly onto the spin column membrane. Samples were the centrifuged for one min at top speed to elute.

#### 4.9.4.3. Quantifying the cRNA (IVT *-in vitro* transcription-product)

In order to determine the cRNA (IVT product) yield the spectrophotometer analysis has been used. For photometric quantification of the purified cRNA 0.5 µl cRNA were diluted in 69.5 µl TE (1:140 dilution). The absorbance was checked at 260 nm and 280 nm to determine sample concentration and purity. For calculation of cRNA when using total RNA as starting material, an adjusted cRNA yield might be calculated to reflect carryover of unlabeled total RNA. Using an estimate of 100 % carryover, the formula below has been used to determine adjusted cRNA yield:

Adjusted cRNA yield=  $RNA_m - (total\ RNA_i)(y)$

$RNA_m$  = amount of cRNA measured after IVT (µg)

Total RNA<sub>i</sub> = starting amount of total RNA (µg)

y = fraction of cDNA reaction used in IVT

The adjusted yield was then used for fragmentation procedure.

#### 4.9.4.4. Checking unfragmented samples on gel electrophoresis

One aliquot (1 µg) of the purified IVT product was saved for analysis by gel electrophoresis. Gel electrophoresis of the IVT product is done to estimate the yield and size distribution of labelled transcripts. Parallel gel runs of unpurified and purified IVT product can help to determine the extent of a loss of sample during the clean-up process. The RNA samples and markers were mixed with loading dye and TE-buffer and heated to 65°C for 5 min before loading on the gel. To visualize the RNA the gel was stained with ethidium bromide.

#### 4.9.5. Fragmenting cRNA for target preparation

The cRNA must be at a minimum concentration of 0.6 µg/µl to start the fragmentation procedure. 2 µl of 5 x Fragmentation Buffer were added for every 8 µl of RNA plus RNase-free water to a final volume of 40 µl. The Fragmentation Buffer has been optimized to break down full length cRNA to 35-200 bases fragments by metal-induced hydrolysis. Samples were incubated at 94°C for 35 min. After incubation time tubes were placed on ice and one aliquot (1 µg) saved for gel analysis. The standard fragmentation procedure should produce a distribution of RNA fragment sizes from approximately 35-200 bases. Fragmented samples were stored at -20°C undiluted until ready to perform the hybridization.

#### 4.9.6. Target hybridization

Probe array was first equilibrated at room temperature before use. It is important to allow the array to normalize to room temperature completely. Meanwhile, the following components were mixed for each sample.

**Table 18 Hybridization cocktail used for HG-U133A arrays.**

Reagent	Standard array	Final component concentration
Fragmented cRNA	15 µg	0.05 µg/µl
Oligonucleotide B2 (3nM)	5 µl	50 pM
20x eukaryotic hybridization controls (bioB, bioC, bioD, cre)	15 µl	1.5, 5, 25 and 100 pM respectively
Hering sperm DNA 10 mg/ml	3 µl	0.1 mg/ml
Acetylated BSA 50 mg/ml	3 µl	0.5 mg/ml
2x hybridization buffer	150 µl	1x
H <sub>2</sub> O	To final of 300 µl	
Final volume	300 µl	

The hybridization cocktail was heated to 99°C for 5 min in a heat block. Meanwhile the array was wet by filling it through one of the septa with 250 µl 1x Hybridization Buffer and incubated at 45°C for 10 min with rotation (60 rpm). When the incubation time for hybridization cocktail was over, it was transferred for 5 min to a 45°C heat block. Then, the hybridization cocktail was centrifuged at maximum speed for 5 min to remove any insoluble material from the hybridization mixture.

The buffer solution from the probe array cartridge was removed and filled with 250 µl of the clarified hybridization cocktail avoiding any insoluble matter in the volume at the bottom of the tube. The probe array was then placed in the rotisserie box in a 45°C oven. Arrays were rotated at 60 rpm and let to hybridize for 16 h.

#### 4.9.7. Microarrays

The GeneChip Human Genome U133A Array (HG-U133A) (*Affymetrix*) has been used which offers comprehensive analysis of genome-wide expression on a single array. HG-U133A is a single array representing 14,500 well-characterized human genes that can be used to explore human biology and disease processes. It comprised more than 22,000 probe sets and 500,000 distinct oligonucleotide features.

#### 4.9.8. Fluidic station set up and experimental procedure

After 16 h of hybridization, the hybridization cocktail was removed from the probe array and set aside in a microcentrifuge tube. The probe array was filled completely with 259 µl of non-stringent wash buffer.

#### 4.9.8.1. Preparing fluid station

First the file location was defined and then the experiment name and information were entered. The intake buffer reservoir A was changed to non-stringent wash buffer and the intake buffer reservoir B to stringent wash buffer. For the water reservoir autoclaved, distilled water was used.

#### 4.9.8.2. SAPE staining solution

Streptavidin phycoerythrin (SAPE) was removed from the refrigerator and the tube tapped to mix it well before preparing the stain solution. The components were mixed as indicated in table 19.

**Table 19 Preparation of the SAPE solution.**

Components	Volume	Final concentration
2x MES Stain Buffer	600 $\mu$ l	1 x
Acetylated BSA 50 mg/ml	48 $\mu$ l	2 mg/ml
SAPE (1 mg/ml)	12 $\mu$ l	1 mg/ml
H <sub>2</sub> O, mol-biol grade	540 $\mu$ l	
Total	1,200 $\mu$ l	

All the components were very well mixed and centrifuged for 5 min at room temperature at maximum speed. The supernatant was removed without carryover of insoluble material at the bottom of the tube and divided into 2 aliquots of 600  $\mu$ l each to be used for stains 1 and 3 respectively.

#### 4.9.8.3. Antibody solution mix

The antibody solution was prepared as indicated in table 20.

**Table 20 Antibody solution mix preparation.**

Components	Volume	Final concentration
2x MES Stain Buffer	300 $\mu$ l	1 x
50 mg/ml acetylated BSA	24 $\mu$ l	2 mg/ml
10 mg/ml Normal Goat IgG	6 $\mu$ l	0.1 mg/ml
0.5 mg/ml biotinylated antibody	3.6 $\mu$ l	3 $\mu$ g/ml
H <sub>2</sub> O, mol-biol grade	226.4 $\mu$ l	
total	600 $\mu$ l	

In the fluidic station dialog box on the workstation, the correct experiment name was selected in the drop-down Experiment list. When the washing/staining program was finished, the probe array window was

checked for large bubbles or air pockets.

#### 4.9.8.4. Scanning the microarray.

Before starting the workstation the laser was switched on. The scanner was warmed up prior to scanning by turning the laser on at least 15 min before use. The experiment to be scanned from the drop-down list was chosen and Run button was clicked and the instruction followed.

#### 4.9.9. Array profile

Sequences used in the design of the HG-U133A array were selected from GeneBank, dbEST and RefSeq. The sequence clusters were created from the UniGene database (Build 133, April 20, 2001). Oligonucleotide probes complementary to each corresponding sequence are synthesized *in situ* on the array. Eleven pairs of oligonucleotide probes are used to measure the level of transcription of each sequence represented on the GeneChip Human Genome U133A 2.0 Array.

##### 4.9.9.1. Instrument/software requirements

The GeneChip Operating Software (GCOS) including the GeneChip Scanner 3000 High-Resolution Scanning Patch has been used.

##### 4.9.9.2. Critical specification for HG-U133A 2.0 Array

The GeneChip<sup>®</sup> Human Genome U133A 2.0 Array is a single array representing 14,500 well-characterized human genes that can be used to explore human biology and disease processes (table 21). Oligonucleotide probes complementary to each corresponding sequence are synthesized *in situ* on the array. Eleven pairs of oligonucleotide probes are used to measure the level of transcription of each sequence represented on the GeneChip Human Genome U133A 2.0 Array (HG-U133A 2.0).

**Table 21 HG-U133A 2.0 Array.**

	HG-U133A 2.0 Array
Number of arrays in set	1
Number of transcripts	18,400
Number of genes	14,500
Number of probe sets	>22,000
Feature size	11 $\mu$ m
Oligonucleotide probe length	25-mer
Probe pairs/sequence	11

Control sequences included	
<ul style="list-style-type: none"> <li>• Hybridization controls</li> <li>• Poly-A controls</li> <li>• Normalization control set</li> <li>• Housekeeping / Control genes</li> </ul>	Bio B, bio C, bio D, cre dap, lys, phe, thr 100 probe stes GAPDH, beta-actin, ISGF3 (STAT1)
Detection sensitivity	1:100,000
(as measured by detection of pre-labelled transcripts derived from human cDNA clones in a complex human background)	

#### 4.9.10. Probe array image inspection

The array was inspected for the presence of image artefacts (i.e. high/ low intensity spots, scratches, high regional or overall background etc.).

#### 4.9.11. Average background and noise values

Although there are no official guidelines regarding background, Affymetrix has found that typical Average Background values range from 20 to 100 for arrays scanned with Gene Array Scanners calibrated to the new PMT setting (10 % of maximum). Arrays being compared should ideally have comparable background values.

#### 4.9.12. B2 Oligo performance

The boundaries of the probe area are easily identified by the hybridization of B2 oligo, which is spiked into each hybridization cocktail. B2 Oligo serves as a positive hybridization control and is used by the software to place a grid over the image. Variation in B2 hybridization intensities across the array is normal and does not indicate variation in hybridization efficiency.

#### 4.9.13. Poly-A controls: dap, lys, phe, thr, trp

Dap, lys, phe, thr and trp are *B. subtilis* genes that have been modified by the addition of poly-A tails, and cloned into pBluescript vectors, which contain both T3 and T7 promoter sequences. Amplifying these poly-A controls with T3 RNA polymerase will yield sense RNAs, which can be spiked into a complex RNA sample, carried through the sample preparation process, and evaluated like internal control genes. Amplifying these genes with T7 RNA polymerase and biotinylated ribonucleotides will yield antisense cRNA, which can be spiked into a hybridization cocktail and evaluated like the 20x Eukaryotic Hybridization Controls (bioB, bioC, bioD and cre).

#### 4.9.14. Hybridization controls: bioB, bioC, bioD and cre

BioB, bioC and bioD represent genes in the biotin synthesis pathway of *E. coli*. Cre is the recombinase gene from P1 bacteriophage. The GeneChip Eukaryotic Hybridization Controls are composed of a mixture of biotin-labelled cRNA transcripts of bioB, bioC, bioD and cre prepared in staggered concentrations (1.5 pM, 5 pM, 25 pM and 100 pM for bioB, bioC, bioD and cre, respectively).

The 20x Eukaryotic Hybridization Controls are spiked into the hybridization cocktail, independent of RNA sample preparation and are thus used to evaluate sample hybridization efficiency to gene expression arrays. BioB is at the level of assay sensitivity (1:100,000 complexity ratio) and should be called "Present" at least 50 % of the time. BioC, bioD and cre should always be called "Present" with increasing signal values, reflecting their relative concentrations.

#### 4.9.15. Internal controls genes

For the majority of the GeneChip expression arrays, *actin* and *GAPDH* are used to assess RNA sample and assay quality. Specifically, the signal values of the 3' probe set to the 5' probe set is generally no more than 3.

#### 4.9.16. Percent genes present

The number of probe sets called "Present" relative to the total number of probe sets on the array is displayed as a percentage in the Expression Report file. Percent Present (% P) values depend on multiple factors including cell/tissue type, biological or environmental stimuli, probe array type and overall quality of RNA. Replicate samples should have similar *p* values.

#### 4.9.17. Scaling and normalization factors

For replicates and comparisons involving a relatively small number of changes, the scaling/ normalization factors (calculated by the global method) should be comparable among arrays. Scaling/normalization factors calculated by the "Selected Probe Sets" method should also be equivalent for arrays being compared.

#### 4.9.18. Single array analysis

Single array analysis was used to build databases of gene expression profiles, facilitate sample classification and transcript clustering, and monitor gross expression characteristics. In addition, the analysis provided the initial data required to perform comparisons between experiment and baseline arrays. The analysis generated a detection *p*-value which was evaluated against user-definable to

determine the detection call. This call indicated whether a transcript was reliably detected (Present) or not detected (Absent). Additionally, a signal value was calculated which assigned a relative measure of abundance to the transcript.

#### **4.9.18.1. Detection algorithm**

The detection algorithm used probe pairs intensities to generate a detection  $p$ -value and assigned a Present, Marginal or Absent call. Each probe pair in a probe set was considered as having a potential vote in determining whether the measured transcript is detected (Present) or not detected (Absent). The vote was described by a value called the determination score (R). The score was calculated for each probe pair and was compared to a predefined threshold Tau. Probe pairs with scores higher than Tau voted for the presence of the transcript. Probe pairs with scores lower than Tau voted for the absence of the transcript. The voting result was summarized as a  $p$ -value. The higher the discrimination scores are above Tau, the smaller the  $p$ -value and the more likely the transcript will be present. The lower the discrimination scores are below Tau, the larger the  $p$ -value and the more likely the transcript will be absent.

#### **4.9.18.2. Detection $p$ -value**

A lower  $p$ -value is a reliable indicator that the result is valid and that probability of the error in the calculation is small.

#### **4.9.18.3. Detection call**

The user-modifiable detection  $p$ -value cut-offs, Alpha 1 ( $\alpha_1$ ) and Alpha 2 ( $\alpha_2$ ) provide boundaries for defining Present, Marginal or Absent calls. At the default settings, determined for probe sets with 16-20 probe pairs (defaults  $\alpha_1 = 0.04$  and  $\alpha_2 = 0.06$ ), any  $p$ -value that falls below  $\alpha_1$  is assigned a Present call, and above  $\alpha_2$  is assigned an Absent call. Marginal calls are given to probe sets which have  $p$ -values between  $\alpha_1$  and  $\alpha_2$ .

#### **4.9.18.4. Signal algorithm**

Signal is a quantitative metric calculated for each probe set, which represents the relative level of expression of a transcript. Similar to the detection algorithm, each probe pair in a probe set is considered as having a potential vote in determining the signal value. The vote, in this case, is defined as an estimate of the real signal due to the hybridization of the target. The mismatch intensity is used to estimate stray signal. The real signal is estimated by taking the log of the perfect match intensity after subtracting the stray signal estimate. The probe pair vote is weighted more strongly if this probe pair signal value is closer to the median value for a probe set. Once the weight of each probe pair is determined, the mean of the

weighted intensity values for a probe set is identified. This mean is corrected back to linear scale and is output as signal.

When the mismatch intensity is lower than the perfect match intensity, then the mismatch is informative and provides an estimate of the stray signal. Rules are employed in the signal algorithm to ensure that negative signal values are not calculated. Negative values do not make physiological sense and make further data processing, such as log transformation, difficult. Mismatch values can be higher than perfect match values for a number of reasons, such as cross hybridization. If the mismatch is higher than the perfect match, the Mismatch provides no additional information about the estimate of stray signal.

#### **4.9.19. Comparison analysis (experiment vs. baseline arrays)**

In a Comparison Analysis, two samples, hybridized to the GeneChip probe arrays of the same type, are compared against each other in order to detect and quantify changes in gene expression. One array is designed as the baseline and the other as an experiment. The analysis compared the different values of each probe pair in the baseline array to its matching probe pair on the experiment array. Two sets of algorithms are used to generate change significance and change quantity metrics for every probe set. A change algorithm generates a change  $p$ -value and an associated change. A second algorithm produces a quantitative estimate of the change in gene expression of Signal Log Ratio.

Before comparing two arrays, scaling and normalization methods must be applied. Scaling and normalization correct for variations between two arrays. Two primary sources of variation in array experiments are biological and technical differences. Biological differences may arise from many sources such as genetic background, growth conditions, time, weight, sex, age and replication. Technical variation can be due to the experimental variables such as quality and quantity of the target hybridized, reagents, stain and handling error. Normalization and scaling techniques can be applied by using data from a selected user-defined group of probe sets, all from all probe sets. When normalization is applied, the intensity of the probe sets (or selected probe sets) from the experiment are normalized to the intensity of the probe sets (or selected probe sets) on the baseline array. When scaling is applied, the intensity of the probe sets (or selected probe sets) from the experimental array and that from the baseline array are scaled to a user-defined target intensity. In general, global scaling in the preferred method is required when comparing two arrays.

##### **4.9.19.1. Change algorithm**

During a comparison analysis, each probe set on the experiment array is compared to its counterpart on the baseline array, and a change  $p$ -value is calculated indicating an increase, decrease, or no change in gene expression.

#### 4.9.19.2. Change $p$ -value

A total of three, one-sided  $p$ -values are computed for each probe set. These are combined to give one final  $p$ -value which is provided in the data analysis output. The  $p$ -value ranges in scale from 0.0 to 1.0 and provides a measure of the likelihood of change and direction. Values close to 0 indicate likelihood for an increase in transcript expression level in the experiment array compared to the baseline, whereas values close to 1.0 indicate likelihood for a decrease in transcript expression level. Values near 0.5 indicate a weak likelihood for change in either direction. Hence, the  $p$ -value scale is used to generate discrete change calls using thresholds.

#### 4.9.19.3. Change call

The final change  $p$ -value described above is categorized by the cutoff values called gamma 1 and gamma 2. These cut-offs provide boundaries for the change calls: Increase (I), Marginal Increase (MI), No Change (NC), Marginal Decrease (MD), or Decrease (D).

#### 4.9.19.4. Signal Log Ratio algorithm

The Signal Log Ratio estimates the magnitude and direction of change of a transcript when two arrays are compared (experiment vs. baseline). It is calculated by comparing each probe pair on the experiment array to the corresponding probe pair on the baseline array. This strategy cancels out differences due to different probe binding coefficients and is therefore more accurate than a single array analysis. The log scale is base 2, making it intuitive to interpret the Signal Log Ratios in terms of multiples of two. Thus, a Signal Log ratio of 1.0 indicates an increase of the transcript level by two fold and -1.0 indicates a decrease by two fold. A Signal Log Ratio of zero would indicate no change.

**Table 22 Terminology comparison (statistical algorithms vs. empirical algorithms).**

Statistical algorithms	Empirical algorithms
Signal	Average difference
Detection	Absolute call
Change	Difference call
Signal Log Ratio	Fold change

#### 4.9.19.5. The logic of logs

Quantitative changes in gene expression are reported as a Signal Log Ratio in the statistical algorithms as opposed to a fold change that was reported in the empirical algorithms. Since  $\log_2$  is used, a Signal Log Ratio of 1 equals a fold change of 2 and a Signal Log Ratio of 2 equals a fold change of 4. Alternatively,

the following formula might be used:

$$\text{Fold Change} = \begin{cases} 2^{\text{Signal Log Ratio}} & \text{Signal Log Ratio} \geq 0 \\ (-1) \times 2^{-\text{Signal Log Ratio}} & \text{Signal Log Ratio} < 0 \end{cases}$$

#### 4.9.19.6. Basic data interpretation

The use of GeneChip gene expression arrays allows interrogation of several thousands of transcripts simultaneously. One of the formidable challenges of this assay is to manage and interpret large data sets. One standardized approach for sorting gene expression data involves the following metrics:

- Detection
- Change
- Signal Log Ratio

Detection is the qualitative measure of presence or absence for a particular transcript. A fundamental criterion for significance is the correlation of the detection calls for a particular transcript between samples. When looking for robust increases, it is important to select for transcripts that are called “Present” in the experimental sample. It has been eliminated the “Absent” to “Absent” changes, which are uninformative.

Change is the qualitative measure of increase or decrease for a particular transcript. When looking for both significant increases and decreases, it is important to eliminate “No Change” calls.

Signal Log Ratio is the quantitative measure of the relative change in the transcript abundance. Robust changes can be consistently identified by selecting transcripts with a fold change of  $> 2$  for increases and  $< 2$  for decreases. This corresponds to a Signal Log Ratio of 1 and -1, respectively.

#### 4.9.19.7. Interpretation of metrics

When sorting through gene expression data in Microarray Suite, some transcripts provided conflicting information. Here are some examples:

1. A transcript is called “Increase” but has a Signal Log Ratio of less than 1.0.
2. A transcript is called “No Change” but has a Signal Log Ratio of greater than 1.0.
3. A transcript is called “Absent” in both experimental and baseline files but is also called “Increase”.

These contradictions arise due to the fact that detection, change and Signal Log Ratio are calculated separately. The benefit of this approach is that transcripts can be assessed using three independent metrics. Thus, in order to determine the most robust changes it is crucial to use all three metrics in conjunction. Basic steps for determining robust increases are:

1. to eliminate probe sets in the experimental sample called “Absent”
2. to select for probe sets called “Increase”
3. to eliminate probe sets with a Signal Log Ratio of below 1.0.

Basic steps for determining robust decreases:

1. to eliminate probe sets in the baseline sample called "Absent".
2. to select for probe sets called "Decrease".
3. to eliminate probe sets with a Signal Log Ratio of above -1.0.

#### 4.9.20. Online Informatics Resource

The NetAffx website ([www.netaffx.com](http://www.netaffx.com)) is a unique resource created by Affymetrix that allows researchers to correlate their GeneChip array results to a catalog of array design and annotation information. These annotations provide structural and functional information, helping to draw biologically relevant conclusions about the experimental results.

#### 4.9.21. Data analysis and software

For data collection, assessment and statistical analyses, the Affymetrix Microarray Analysis Suite Version 5.0 program (MAS5.0) has been used. Quality control assessment included the percentage of probe sets called present, signal-to-background ratio and 3' to 5' ratio in housekeeping controls for IVT procedure validation. For data analysis each array was scaled to an overall intensity of 100 to enable comparison of all hybridization data. Resulting CEL files were further analyzed with DNA-Chip Analyzer (dCHIP 1.2<sup>®</sup>) and R software (Bioconductor project). Changes in the expression profile between the two different experimental groups were determined by comparison analysis which contained the change indicating a qualitative call (increase, decrease, no change) in transcript level differences. Statistical significance was calculated by 2-sample 2-tailed *Student's t* test. Comparisons were considered statistically significant at  $p < 0.05$ .

### 4.10. Genome scan analysis

Genome-wide linkage scans have traditionally employed panels of microsatellite markers spaced at intervals of approximately 10 cM across the genome. However, there is a growing realization that a map of closely spaced single-nucleotide polymorphisms (SNPs) may offer equal or superior power to detect linkage, compared with low-density microsatellite maps.

#### 4.10.1. Arrays

The genome scan was carried out using 10K (10,000 SNPs) Affymetrix chip at the service facility of the Cologne Centre for Genomics ([www.ccg.uni-koeln.de](http://www.ccg.uni-koeln.de)). Each array contained 11,555 biallelic polymorphic sequences randomly distributed throughout the genome, except for the Y chromosome. Each SNP on the array is represented by 40 different 25 bp oligonucleotides, each with slight variations that allow accurate

genotyping. The median physical distance between SNPs is ~ 150 kb and the mean distance between SNPs is 210 kb. The average heterozygosity for these SNPs is 0.37 with an average minor allele frequency of 0.25.

The samples were prepared for the chip hybridization according to the manufacturer's instructions (*Affymetrix Inc.*, Santa Clara, CA, USA), using 250 ng DNA of each proband. For reading the hybridization signals, the GeneChip Scanner 3000 (*Affymetrix Inc.*) was used and the data was analyzed using the GDAS program (version 2.0; *Affymetrix Inc.*). Of the 11,555 SNPs on the GeneChip™ Mapping 10 K Array, 301 SNPs were X-linked and 360 were not physically mapped in NCBI build 34. The SNP annotation files ([www.affymetrix.com](http://www.affymetrix.com)) include the genetic positions of the SNPs related to deCODE, Marshfield and SLIM1 maps.

#### **4.10.2. Statistical analysis**

Linkage analysis is the interference of the position of two or more loci by examining patterns of allele transmission from parent to offspring, or patterns of allele sharing by relatives. Linkage analysis is a statistical test to look if the genetic marker co-segregates with the loci (disease) in the families. The result of the linkage analysis is represented by LOD scores at various recombination fractions with positive (3) scores for linkage and negative (-2) against linkage. LOD scores of 3 shows a significant evidence for linkage, with 5 % chance of error.

##### **4.10.2.1. Non-parametric linkage analysis using MERLIN software**

The general idea of non-parametric linkage (NPL) analysis is that, in the vicinity of a disease locus, sib pairs who are concordant for disease status (i.e. both affected or both unaffected) should show an increase in allele-sharing, and those who are discordant for disease status (i.e. one affected and one unaffected) should show a decrease in allele sharing, from the level of allele-sharing expected of sib pairs. MERLIN is a program for carrying out single and multipoint non-parametric linkage, QTL, and Variance Component analysis (Abecasis et al. 2002). It is very similar in functionality to GENEHUNTER, except it only carries out non-parametric linkage analysis. One of the main advantages of MERLIN is that it was designed with the intention of analysing dense SNP maps (Abecasis et al. 2002). To this end it utilises sparse inheritance trees in the same way as the newer versions of GENEHUNTER (Kruglyak et al. 1996) to, but it also employs several other algorithms which enhance performance. In comparison to GENEHUNTER and ALLEGRO (Gudbjartsson et al. 2000), MERLIN is approximately 30 times faster.

##### **4.10.2.2. Parametric linkage analysis**

Parametric linkage analysis requires mod of inheritance to be specified prior to analysis. Standard LOD score analysis is called parametric because, it requires precise genetic model, detailing disease allele

frequency, marker allele frequency, and penetrance of each genotype (Abreu et al. 1999). The penetrance is defined as the frequency of expression of an allele when in present in the genotype of the organism (for instance if 9/10 of individuals carrying an allele, the trait is said to be 90 % penetrant). As parametric linkage analysis is more powerful when the specified model is close to the true underlying mode of inheritance (Abreu et al. 1999), it has been carried out parametric analyses using one dominant (0.0000, 1.0000, 1.0000) and one recessive (0.0000, 0.0000, 1.0000) inheritance model. For a polygenic trait, evidence for linkage at a given locus may not be detectable assuming genetic homogeneity that is in the complete data set of linked and unlinked families. It has been therefore computed heterogeneity lod scores (HLOD) for varying proportions of linked families ( $\alpha$ ) using Genehunter V2.0. Due to the small size of the individual families investigated each family contributed relatively little linkage information, making it difficult to divide them into distinct categories of linked and unlinked families. We assessed the genome-wide significance level of the linkage results empirically using Allegro V1.0. Multipoint linkage analysis in complex diseases requires the use of fast algorithms that can handle many markers and a large number of moderately sized pedigrees with unknown mode of inheritance.

#### **4.11. Additional statistical methods**

Data are present as means (+/- SD) and analyzed using Student's *t* test with  $p < 0.05$  considerate significant. The *t*-test assessed whether the means of two groups are statistically different from each other.

## 5. RESULTS

### 5.1. Search for SMA modifying factor(s) by candidate gene approach

A combination of linkage mapping and a candidate gene approach has been the most successful method of identifying disease genes to date. The candidate gene approach is useful for quickly determining the association of the genetic variant with a disorder and for identifying genes of modest effect.

The presence of phenotypic discordance in SMA families that are characterized by *SMN1*-deleted sibs with identical *SMN2* copy number but discordant phenotypes (Cobben et al. 1995; Hahnen et al. 1995; Wang et al. 1996; Wirth et al. 1999) strongly implies that additional factors, except for *SMN1* and *SMN2* are influencing the SMA phenotype.

SMN-interacting proteins, such as Gemin 2, Gemin 3, ZPR1, p80 coilin, FUSE binding protein, profilin IIa, RHA, hnRNP-G and hnRNP-Q, were shown to be tight co-regulated with SMN in SMA discordant families (Helmken et al. 2003; Helmken et al. 2000). Molecular analysis of these genes showed no mutation or nucleotide difference, and no differential RNA expression, and failed to be classified as SMA modifying genes. It is known already that many mutations do not result in amino acid changes, however, and therefore do not alter the resulting protein or its function. Furthermore, many mutations occur in non-coding DNA regions and might be associated with an altered phenotype or increased disease risk. Therefore, another three candidate genes (*ZNF265*, *HDAC6* and *hnRNP-R*) were further investigated at DNA and/or RNA level, in hope to identify potential modifying factors that prevent some siblings from developing SMA despite the lack of *SMN1*.

#### 5.1.1. Selection of candidate genes

##### 5.1.1.1. Selection of *ZNF265* gene

Gene transcription and pre-mRNA splicing are dynamic and highly coordinated processes that occur in a spatially organized manner in the nucleus (Singer and Green 1997). Splicing takes place in the spliceosome, a large RNA-protein complex composed of various small nuclear ribonucleoprotein particles (snRNPs), and many other protein factors that include members of the highly conserved serine/arginine rich (SR) protein family. SR proteins, by RNA-protein and protein-protein interactions, coordinate the passage of the spliceosomal complex through the splicing reaction (Caceres et al. 1997; Fu 2004; Manley and Tacke 1996).

ZNF265 (formally named "Zis") is a zinc finger- and RS domain-containing protein (Adams et al. 2000; Karginova et al. 1997) that was first identified, along with rennin, because of its modulated expression in differentiating renal juxtaglomerular cells (Karginova et al. 1997); it is now known to be expressed by most tissues, especially early in development (Adams et al. 2000). ZNF265 co-localizes with SMN in the nucleus, as well as with the authentic SR protein SC35 (at the periphery of the SC35-staining aggregates)

and with the snRNP protein antigen Sm (Adams et al. 2001). ZNF265 also co-localizes with the transcription factors YY1 and p300 (Adams et al. 2001), both of which have been shown to co-localize within active transcriptional compartments and, in the case of p300, with RNA polymerase II (Bannister and Kouzarides 1996; Ogryzko et al. 1996; von Mikecz et al. 2000; Yang et al. 1996). These co-localizations are consistent with a role of ZNF265 in transcription and/or splicing. In this regard, ZNF265 may be co-transcriptionally recruited with RNA polymerase II to pre-mRNA transcripts, as has been reported for other RS domain-containing proteins (Corden and Patturajan 1997). The fact that ZNF265 interacts with U1-70K and U2AF<sup>35</sup> point to its early commitment to the spliceosome, as the latter factors are necessary for the first detectable association between splice sites during formation of the E complex (Michaud and Reed 1993; Wu and Maniatis 1993; Xiao and Manley 1998). Based on the composition of affinity-purified E complex, this association has been proposed to occur through direct or indirect interaction of U1snRNP and U2AF<sup>35</sup> bound to the 5' and 3' splice sites, respectively (Michaud and Reed 1993). One model has suggested that SF2/ASF or SC35 was subsequently able to form a bridge between U1-70K and U2AF<sup>35</sup> (Wu and Maniatis 1993). The finding that ZNF265 interacts more strongly with U1-70K than with U2AF<sup>35</sup>, suggests that earlier binding of ZNF265 to U1-70K, as opposed to U2AF<sup>35</sup>, during recruitment to the spliceosome (Adams et al. 2001).

*In vitro* splicing reactions showed that ZNF265 is immunoprecipitated in a complex that includes spliced mRNA (Adams et al. 2001). This result indicated that ZNF265 binds directly or indirectly to mRNA, but much less to pre-mRNA. This property is shared with other splicing factors, such as SF2/ASF and RNPS1 (Hanamura et al. 1998; Mayeda et al. 1999), both of which synergistically stimulate general splicing. ZNF265 can regulate alternative splicing in a concentration-dependent manner (Adams et al. 2001). Namely, overexpression of ZNF265 resulted in exclusion of exons 2 and 3 from the Tra2-β1 pre-mRNA, which led to an increase in the production of the β3 alternatively spliced isoform (Adams et al. 2001).

In conclusion, ZNF265 co-localizes with the spliceosome, associate with mRNA and essential splicing factors U1-70K and U2AF35, as well as regulates the alternative splicing of Tra2-β1. Therefore, it was obvious to ask whether ZNF265 might influence the variability of the SMA phenotype.

#### 5.1.1.2. Molecular analysis of *ZNF265* gene in SMA discordant families

To answer the question whether *ZNF265* gene can be a modifying factor for SMA phenotype variability, the gene was analyzed in 30 sibs belonging to 12 SMA discordant families (families are marked with "1" in table T2 in appendix). All SMA discordant families displayed identical 5q13 haplotypes and identical *SMN1* mutations on both parental chromosomes but variably phenotypes (unaffected and affected, types II and III or types IIIa and IIIb, respectively). *ZNF265* gene (located on chromosome 1) was searched for DNA sequence variances by sequencing the complete coding region from genomic fragments that encompass each of the 11 exons by using intronic flanking primers (see table 3 from Methods). Neither a mutation nor a polymorphism within the coding region or exon-intron boundaries was identified. It has been concluded therefore that the intrafamilial phenotypic variability in SMA discordant families is not

caused by mutations/polymorphisms within *ZNF265* gene.

### 5.1.1.3. Selection of *hnRNP-R* gene

Heterogeneous nuclear ribonucleoproteins (hnRNPs), which directly bind to nascent RNA polymerase II transcripts, play an important role in both transcript-specific packaging and alternative splicing of pre-mRNAs. Using yeast two-hybrid techniques, Rossoll et al. (2002) identified hnRNPR (Rossoll et al. 2002) and the highly related gry-rbp/hnRNPQ (Mourelatos et al. 2001) as novel SMN interaction partners. hnRNPs are among the most abundant proteins in the eukaryotic nucleus and play important role in processing of precursor mRNA (Dreyfuss et al. 1993; Weighardt et al. 1996). They assemble on nascent RNA polymerase II transcripts to form hnRNP complexes, where they co-localize with small nuclear snRNPs. hnRNP proteins have a modular structure consisting of one or more RNA binding domains and at least another auxiliary domain, which mediates protein-protein interactions but may also contribute to nucleic acid binding (Biamonti and Riva 1994; Dreyfuss et al. 1993; Weighardt et al. 1996).

Among the three types of RNA binding motifs identified in hnRNP proteins, the consensus sequence RNA binding domain (RBD), also named RNA recognition motif (RRM), is the most frequently found motif (Burd and Dreyfuss 1994). hnRNP-R is mainly expressed in motor axons and at much lower degree in sensory axons. Highest expression levels of hnRNP-R during development of the spinal cord can be found during late embryogenesis around E19 (Rossoll et al. 2002). The reduction of hnRNP-R level after birth apparently is due to post-transcriptional and/or post-translational mechanisms as previously observed for Gemin 2 (Jablonka et al. 2001; Wang and Dreyfuss 2001a).

hnRNP-R co-localizes with SMN in the cytoplasm of the motor neurons including the axons. It was also found in the nucleus but not concentrated in gems (Rossoll et al. 2002). Thus it is unlikely that hnRNP-R participates in specific functions of SMN complexes such as pre-mRNA splicing and regeneration of the spliceosomal complexes (Pellizzoni et al. 1999).

hnRNP-R specifically binds mRNAs, being involved in mRNA processing including editing, in mRNA transport and finally acts as a regulator, which modify binding to ribosomes and RNA translation (Blanc et al. 2001; Grosset et al. 2000; Mizutani et al. 2000). Such functions appear highly important for neurons with long processes, in particular motor neurons in which specific mRNAs have to be transported over long distances.

The length of motor axons can exceed the diameter of the cell body by a factor of more than 5,000, thus underlining the relevance of control mechanism for mRNA transport to distant cellular sites such as to growth cones or motor endplates (Gallant 2000; Mohr and Richter 2000). Smn and hnRNP-R are concentrated and co-localize in the distal axon of isolated embryonic motor neurons. At the electron microscopic level, it could be demonstrated that Smn immunoreactivity is associated with microtubules in motor axons during post-natal development (Pagliardini et al. 2000). hnRNP-R interacts with wild type murine Smn but not with truncated or mutant Smn forms identified in SMA (Mourelatos et al. 2001).

Because hnRNP-R and SMN are closely interacting proteins, part of the same cellular protein complex,

the same pathway and exhibit the same cellular location in motor neurons, hnRNP-R was a good candidate as potential modifier in SMA discordant families.

#### 5.1.1.4. Molecular analysis of *hnRNP-R* at DNA and RNA level

In order to test whether hnRNP-R might act as modifying factor in SMA, five SMA discordant families (marked with “2” in table T2 in appendix) were tested for SNPs association with SMA/unaffected phenotype. In contrast to mutations, which occur at low frequencies (less than 1%) in the general population, polymorphisms are common genetic variants, occurring more frequently (Davies et al. 2005). Within genes, the number of SNPs varies widely, from one or two to several hundred. It is likely however, that all SNPs are not equally important, and analysis is often restricted to those in: a) exons, particularly if leading to an amino acid substitution; b) regulatory regions, which may affect binding of transcription factors; c) exon/intron boundaries, which may influence splicing; d) conserved regions, as this usually implies a significant function (Davies et al. 2005). No SNP was found within the *hnRNP-R* gene coding region but two SNPs located in the intronic region were selected for association studies in all five SMA discordant families: rs2842604 (A/C) located in intron 6 and rs911927 (C/G) located in intron 10. The nucleotide variants were checked by sequencing the target region from genomic fragments. Both SNPs were successfully genotyped in the five SMA discordant families comprising 7 unaffected *SMN1*-deleted sibs and 6 affected (type III SMA) *SMN1*-deleted sibs. For all five families the DNA samples from parents were also available. As shown in table 23 no association between a certain allele and SMA phenotype was found.

**Table 23 Genotyped SNPs across the hnRNP-R locus in five SMA discordant families.**

dbSNP number	Position	Allele variant	Unaffected sibs <i>SMN1</i> -deleted			Affected sibs <i>SMN1</i> -deleted		
			A/C	AA	CC	A/C	AA	CC
rs28426064	+16727	A/C	3	3	1	4	1	1
rs911927	+25167	C/G	3	1	3	3	2	1

Additionally, *hnRNP-R* gene was checked at transcription level to verify whether any difference between discordant sibs at RNA level could be observed. In order to prove this hypothesis, quantitative analysis of RT-PCR products using primers that were localized in 5'UTR region and exon 4 amplifying *hnRNP-R* from lymphoblastoid cell lines from 13 sibs of five SMA discordant families was performed. No quantitative difference between *hnRNP-R* transcripts and the total amount of RNA was found. A representative image is shown in Fig. 8 for three SMA discordant families.

Therefore, *hnRNP-R* was excluded to act as potential modifier in SMA discordant families



tubulin (Saji et al. 2005).

Because SMN protein was found to be involved in gene repression (Zou et al. 2004) via interaction with HDAC proteins, *HDAC6* gene (besides, located on chromosome X) was chosen as candidate gene as potential modifier in SMA model.

#### **5.1.1.6. Testing of DNA polymorphisms in *HDAC6* gene**

The human genome contains about 10-30 million SNPs with an average of SNP every 100-300 bases (Montpetit et al. 2006). More than 4 million SNPs have been identified and the information is publicly available. SNPs occur mostly outside the coding regions but SNPs in the coding regions would be interesting as they add to variation in the function of the protein. Therefore, two SNPs located in the coding region of *HDAC6* gene were found interesting since both of them cause an amino acid exchange at protein level. One SNP, rs146379 (T/C; position +15625) located in exon 21 causes a leucine to proline exchange at position 700; rs1127346 (C/T; position +20681) located in exon 24 causes a threonine to isoleucine substitution at position 994. Both SNPs were genotyped in the same five families as above and no informative SNP was found. For rs146379 all individuals (both unaffected and affected) were carrying T allele; for rs1127346 all sibs were carrying the C allele. Both SNPs were not informative and no conclusion could be drawn. Therefore *HDAC6* gene was excluded to function as potential factor able to modify the SMA phenotype. Other molecular mechanisms must be responsible for the intrafamilial phenotypic discrepancies in SMA discordant families, mechanisms hard to be detected by candidate gene approach.

## **5.2. Search for SMA modifying genes by differential expression profiling using Affymetrix microarray technology**

Gene expression profiling has been applied to many aspects of human biology including stress responses of human cells (Belcher et al. 2000; Guillemin et al. 2002; Iyer et al. 1999), identification of signalling cascades (Coller et al. 2000; Diehn et al. 2002; Fambrough et al. 1999; Shaffer et al. 2000), or regulated expression of cell cycle-associated genes (Mirza et al. 2003; Whitfield et al. 2002). For clinical investigation and medicine, gene expression signatures are used to better define biological processes that might be associated with disease, therapy or severe adverse events following therapy (Debey et al. 2004). Examination of gene expression levels can provide insights into the temporal changes that occur in induced cells and into the molecular differences between various cells or tissue samples. Microarrays detect gene expression levels in parallel by measuring the hybridization of mRNA to many thousands of genes immobilized on a glass surface (the "chip") providing a sensitive and high-throughput method well suited to take advantage of the sequence and clones produced in genome sequencing efforts (Keller and Yao 2002).

### 5.2.1. The microarray screen for EBV-transformed lymphoblastoid cell RNAs revealed up- and down-regulated genes in asymptomatic vs. symptomatic sibs in SMA discordant families

To address the clinically relevant difference between symptomatic vs. asymptomatic sibs with *SMN1* deletion, in SMA discordant families, a gene expression profiling of EBV-transformed lymphoblastoid cells from one SMA discordant family and four classical SMA patients was carried out using oligonucleotide arrays. Total RNA isolated from EBV-transformed lymphoblastoid cell cultures from SMA discordant family #482 (that comprises two unaffected sibs- BW 330 and BW 331- and two affected ones- BW 332 and BW 333), two type I (BW 226 and BW 409) and two type III (BW 12 and BW 309) SMA patients (marked with “3” in table T1 in appendix) was used to hybridize HG-U133A Affymetrix chip to detect transcripts differentially expressed in asymptomatic vs. symptomatic sibs. The two types of SMA patients (type I and type III) were used under the assumption that only the transcripts differentially expressed due to the modifier gene and not due to the lack of SMN protein would be detected. In the first step of analysis, the data from unaffected siblings (tables T3 and T4 that are contained in the attached CD-ROM) were compared with the data from affected sibs to obtain pools of transcripts up- and down-regulated in unaffected than affected sibs. Then, these pools of data were compared with the transcripts found to be differentially expressed in the two SMA types used as controls (tables T5 and T6 that are contained in the attached CD-ROM). In this manner, all the transcripts co-regulated by *SMN1* deletion were excluded. The SMA discordant family #482 (for a detailed characterization of this family see Fig. F1 in appendix) in the microarray expression experiment comprises two unaffected females (BW 330 and BW 331, respectively) and two affected males (BW 332 and BW 333). Each healthy female was compared with each affected male so that four combinations were possible (BW 330 vs. BW 332; BW 330 vs. BW 333; BW 331 vs. BW 332; BW 331 vs. BW 333). The unaffected sibs were analyzed as “baseline” in comparison with the affected sibs that were analyzed as “experiment”. All transcripts that were found to be up-regulated in the “baseline” were collected as “increase baseline” and are listed in table T3 that is contained in the attached CD-ROM. All transcripts that were found to be down-regulated in the “baseline” vs. “experiment” were collected as “decrease baseline” and are shown in table T4 that is contained in the attached CD-ROM. In the “increase baseline” analysis 106 transcripts were found to be up-regulated and only 28 (24.5 %) were detected to be differentially expressed in all four combinations (100 %). In the “decreased baseline” 180 transcripts were found to be down-regulated in unaffected sibs and 48 (26.6 %) were differentially expressed in all four combinations (100 %).

A functional classification of the 286 transcripts detected to be regulated in SMA discordant sibs was performed by collecting annotations and keywords from NetAffx website (<http://www.affymetrix.com/analysis/index.affx>). The genes were categorized according to the biological process (Fig. 9 A and D), molecular function (Fig. 9 B and E), or to the cellular component to which they belong (Fig. 9 C and F). The most up-regulated transcripts in unaffected vs. affected SMA discordant sibs were involved in cell-cycle control (10 %), signal transduction and transcription (each 11 %) (Fig. 9 A). The

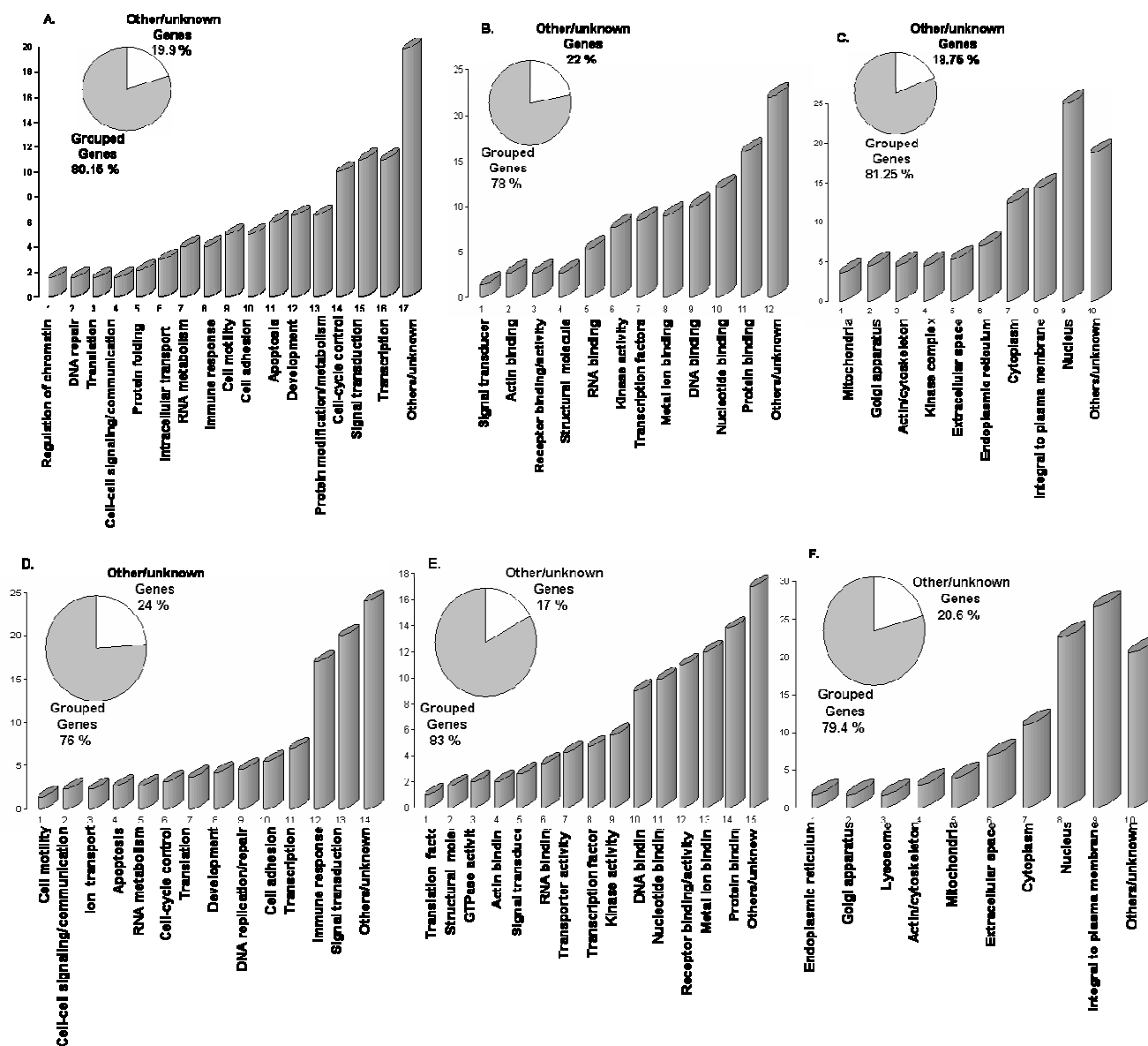


**Fig. 9** Percentage of the transcripts regulated in SMA discordant sibs serving a known molecular function, participating in known biological processes and forming known pathways. Genes were grouped according to their annotations as defined by NetAffx. In the case of very small group sizes or of the hypothetical transcripts a new group was created termed “Other/unknown Genes”. Percent of both up-regulated (A, B and C) and down-regulated (D, E and F) transcripts are categorized according to biological process (A and D), molecular function (B and E) or to cellular compartment (C and F). When a transcript was involved in more than one process/function it was scored for each category. The inserts (*pie charts*) show that the majority of the transcripts were included into summarized categories.

proteins encoded by the respective genes were found to bind either nucleotides (12 %) or/and other proteins (16 %) (Fig. 9 B). The location for these proteins was found to be mostly in the nucleus (25 %) (Fig. 9 C). The most down-regulated genes in unaffected sibs have an important role either in immune response (17 %) or in signal transduction (20 %) (Fig. 9 D). The proteins bind DNA (9 %), nucleotides (9.9 %), receptors (11 %), metal ions (12 %) or other proteins (13.8 %) (Fig. 9 E).

Interestingly, in both data sets (up- or down-regulated transcripts), genes and functions related to nucleus, plasma membrane and the membrane fraction represent about half of all regulated transcripts (39.35 % in the up-regulated transcripts set and 49.37 % in the down-regulated transcripts set, respectively).

It is important to bear in mind that the observed differences in this study was found by analysis of the RNA from lymphocytes rather than motor neurons, the cell type affected in SMA patients. Given the fact that it is impossible to have this biological material, the EBV-transformed lymphoblastoid cell cultures were the best options. In 2003, a study on EBV-transformed lymphoblastoid cell cultures belonging to 15 SMA discordant families showed that the potential modifier acts in a tissue-specific manner (Helmken et al. 2003). The effect of the modifier was detected in lymphocytes but not in primary fibroblasts cells from SMA discordant families. A potential finding of this study concerns a series of transcripts which are highly differentially regulated in SMA modified phenotype, which may play a role in SMA and represent candidates for as yet unidentified disease-protecting gene(s) and, maybe, unknown pathways for SMN.

### 5.2.2. Gene selection

Selection of relevant genes is a common task in most gene expression studies. The detection of the most significantly differentially expressed genes has been a central research focus. It has been analyzed the global expression of transcripts in the lymphoblastoid cells of SMA discordant individuals. Differentially expressed genes potentially involved in the protection to develop SMA are summarized in table 24.

There were considered those RNAs that were more than 3 fold abundant/less abundant in the asymptomatic than symptomatic sibs. Thus, from 28 transcripts found up-regulated in the "baseline experiment" only 6 RNAs were called "Present", "Increase" (see 4.9.19.6 Basic data interpretation) and having a mean of the Signal Log Ratio of  $> 1.5$  (value that corresponds to a 3 fold increase), fulfilling the selection criteria for up-regulated genes. From 48 transcripts found down-regulated in "baseline experiment", 12 transcripts were called "Absent", "Decrease" and having a mean of Signal Log Ration  $< -1.5$  (value that corresponds to a 3 fold decrease). By this study there were also detected various genes whose expressions are affected in a different manner by the lack of *SMN1* gene in SMA discordant sibs (table 24).

Because we assumed that the modifier gene should be up-regulated in unaffected sibs (protecting in this manner the *SMN1*-deleted individuals to develop SMA) the study was focused on the transcripts that have been found to be up-regulated in unaffected (BW 330 and BW 331) compared with their affected sibs (BW 332 and BW 333).

**Table 24 Expression changes in genes potentially involved in the regulation of SMA modified phenotype. The gene candidates presented similar Signal Log Ratios for each comparison made (for a more detailed overview see tables T3 and T4 that are contained in the attached CD-ROM).**

Gene symbol	Gene bank number	Gene name	Mean of Log Ratio	Fold change (Affymetrix)	Change
<b>PLS3</b>	NM_005032	Plastin 3 (T isoform)	5.23	39	Increase
<b>NR113</b>	AV699347	Nuclear receptor subfamily 1, group I, member 3	4.8	29	Increase
<b>CD24</b>	NM_013230	Small cell lung carcinoma cluster 4 antigen	2.2	5	Increase
<b>PLOD 2</b>	NM_000935	Procollagen-lysine, 2-oxoglutarate, 5-deoxygenase (lysine hydroxylase)	1.78	3.5	Increase
<b>TNFSF14</b>	NM_003807	Tumor necrosis factor (ligand) superfamily, member 14	1.6	3	Increase
<b>SEPT 2</b>	AL568374	Septin 2	1.6	3	Increase
<b>IL1R2</b>	U64094	Soluble type II interleukin-1 receptor	-4.6	25.6	Decrease
<b>DPYD</b>	NM_000110	Dihydropyrimidine dehydrogenase	-4.2	19	Decrease
<b>SYNJ2</b>	AF318616	Synaptojanin 2	-3.6	12.8	Decrease
<b>T-Star</b>	NM_006558	Sam68-like phosphotyrosine protein	-3.5	12	Decrease
<b>GPM6A</b>	D49958	Glycoprotein M6A	-3	8	Decrease
<b>GA733</b>	NM_002353	Gastrointestinal tumor-associated antigen GA7331-1 protein	-3	8	Decrease
<b>APP</b>	NM_000484	Amyloid beta (A4) precursor protein	-2.6	6.4	Decrease
<b>D4S234</b>	NM_014392	Neuron specific protein	-2.4	5.6	Decrease
<b>AICDA</b>	AB040431	Activation-induced cytidine deaminase	-2.2	4.8	Decrease
<b>CRE-BPa</b>	NM_004904	cAMP response element-binding protein	-1.5	3	Decrease
<b>CYP7B1</b>	NM_004820	Cytochrome P450, subfamily VIIB polypeptide 1	-2	4	Decrease
<b>UNC13</b>	NM_006377	Unc-13 homolog B ( <i>C.elegans</i> )	-2	4	Decrease

### 5.2.3. Confirmation of microarray data by semi-quantitative RT-PCR

The expression profile of total RNA isolated from EBV-transformed lymphoblastoid cell lines belonging to one SMA discordant family revealed up-regulation of six candidate genes in asymptomatic individuals: *T-plastin* (*PLS3*), *SEPTIN 2*, *CD24*, *NR113*, *PLOD 2* and *TNFSF14*. Validation of microarray-based results was achieved using semi-quantitative PCR analysis. The same batch of RNAs used in microarray analysis isolated from the same SMA discordant family was employed and quantification revealed a good correlation between the fold change obtained in microarray and RT-PCR only for *T-plastin*, *NR113* and *CD24* transcripts (Fig. 10 A). The two techniques demonstrated a generally similar degree of differential expression only in these three cases. This selection step excluded from our study the three candidates (*SEPTIN 2*, *TNFSF14* and *PLOD 2*) that showed by RT-PCR no significant difference between unaffected and affected individuals (Fig. 10 B). By this method only the transcripts found to be up-regulated above 5 fold in the microarray analysis were confirmed.

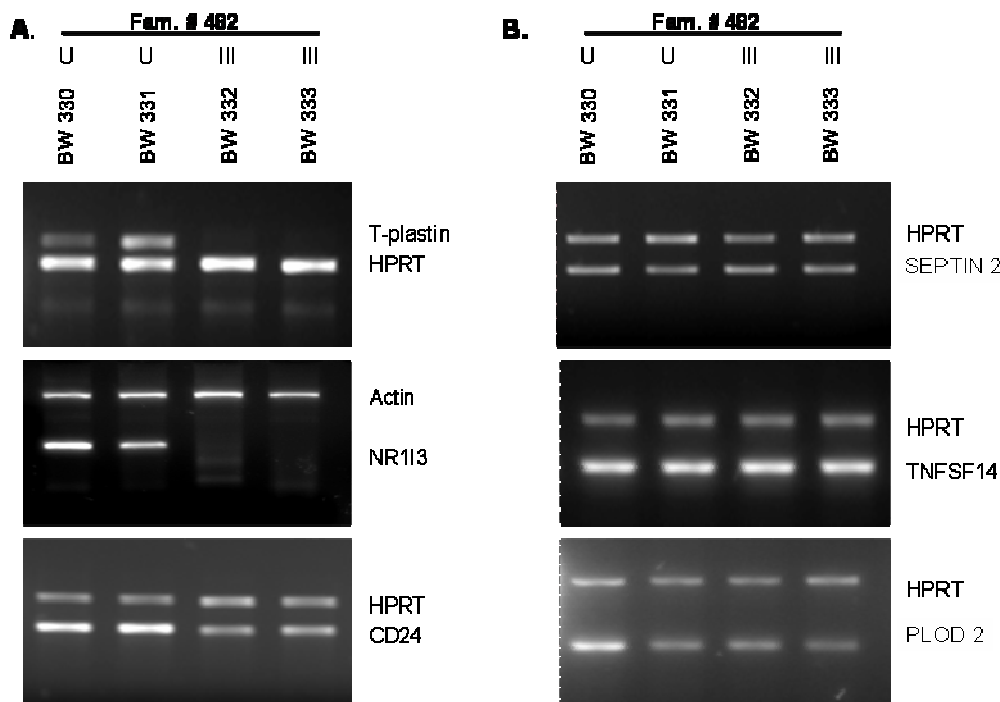


**Fig. 10** Confirmation of the microarray-based results in SMA discordant family #482.

(A) RT-PCR analysis in one SMA discordant family #482 revealed up-regulation of three candidate genes (*T-plastin*, *NR113* and *CD24*) in unaffected vs. affected sibs. (B) Transcript levels of *SEPTIN 2*, *TNFSF14* and *PLOD 2* are not up-regulated in unaffected individuals compared with the affected ones. *HPRT* and *actin* were used as internal genes to verify that equal amounts of RNA were loaded. Family number is indicated at the top. Representative results are shown from multiple separate experiments. U: unaffected sib; III: type III SMA.



For *T-plastin* the same significant difference was found between affected and unaffected siblings in three out of four SMA discordant families. In family #800, the two phenotypically different sibs showed equally *T-plastin* expression (Fig. 11 A). Additionally, *T-plastin* was found in an unaffected *SMN1*-deleted mother (Fig. 15 A) as compared to her affected son (data not shown). For the second selected transcript, *NR1I3*, an up-regulation of the candidate was found in asymptomatic vs. symptomatic sibs in two other SMA discordant families (#34 and #167) (Fig. 11 B). In the other two families (#800 and #646) no significant difference was observed. Regarding the *CD24* transcript, was differentially expressed, but no correlation between phenotype and its expression was observed (Fig. 11 C). At this step another candidate (*CD24*) was excluded as potential modifier in SMA model.

Further investigations of the possible involvement of the two remaining candidate genes (*NR1I3* and *T-plastin*) in SMA disease model were performed. The two most highly expressed genes in unaffected sibs detected by microarray method were confirmed by RT-PCR to be differentially expressed in SMA discordant sibs and therefore were analyzed by linking each gene to their chromosomal location and with the help of databases: NetAffx (*Affymetrix*), Ensembl, UCSC, NCBI.

### 5.2.5. Description of NR1I3 candidate

**Nuclear receptor subfamily 1, group I, member 3 (NR1I3); MIM: 603881; 1q23.3.** The constitutive androstane receptor (CAR; NR1I3) is a nuclear hormone receptor that is predominantly expressed in the liver (Baes et al. 1994; Wei et al. 2002). It has been implicated in the metabolism of xenobiotics and drugs (Wang et al. 2004; Wei et al. 2000; Zhang et al. 2002), carcinogens (Xie et al. 2003), steroids (Xie et al. 2003), heme (Huang et al. 2003; Huang et al. 2004; Xie et al. 2003), bile acids (Guo et al. 2003; Saini et al. 2004; Zhang et al. 2004), and thyroid hormone (Maglich et al. 2004). Furthermore, there is evidence that CAR activity impinges on cholesterol homeostasis (Kocarek and Mercer-Haines 2002; Wang et al. 2003) and signalling pathways that control food consumption (Qatanani et al. 2004). In large part, the effects that CAR exerts on these processes are dependent on the receptor's ability to modulate hepatic gene expression (Maglich et al. 2002; Ueda et al. 2002). The battery of CAR target genes include members of all three phases of xeno/endobiotic metabolism and clearance, such as certain cytochrome P450, UDP-glucuronosyltransferase, sulfotransferase, glutathione transferase, aldehyde dehydrogenase, and avidin-biotinylated enzyme complex transporter families (Maglich et al. 2002; Ueda et al. 2002). Thus far, CAR response elements have been mapped in a number of the corresponding human genes, including *CYP2B6* (Sueyoshi et al. 1999; Wang and Negishi 2003), *CYP3A4* (Goodwin et al. 2002), *CYP3A5* (Burk et al. 2004), *CYP2C8* (Ferguson et al. 2005), *CYP2C9* (Ferguson et al. 2002), *CYP2C19* (Chen et al. 2003), *UGT1A1* (Sugatani et al. 2001), *MDR1* (Burk et al. 2005), and *ALAS1* (Podvinec et al. 2004). NR1I3 is a nuclear receptor that acts as a specific, retinoid-independent activator. In the mouse, the constitutive activity of this receptor, which they called CAR-beta (constitutive androstane receptor-beta), results from a ligand-independent recruitment of transcriptional coactivators such as SRC1 (Forman et al. 1998). Zhang and colleagues identified in 2002 the xenobiotic receptor CAR as a key regulator of acetaminophen

metabolism and hepato toxicity (Zhang et al. 2002). Known CAR activators as well as high doses of acetaminophen induced expression of 3 acetaminophen-metabolizing enzymes in wildtype but not in *CAR*-null mice, and the *CAR*-null mice were resistant to acetaminophen toxicity. Inhibition of CAR activity by administration of the inverse agonist ligand androstanol 1 h after acetaminophen treatment blocked hepatotoxicity in wildtype but not in *CAR*-null mice. The same group found that administration of androstanol even 3 h after the toxic acetaminophen dose resulted in a 50 % protection in wildtype mice (Zhang et al. 2002).

Most studies of CAR regulation have focused on mouse CAR. In mouse, CAR is localized cytosolically in the absence of inducer, such as the prototypical inducer phenobarbital (Kawamoto et al. 1999; Zelko et al. 2001). Recent studies have identified a number of CAR interacting proteins that complex with the cytosolic receptor, including two heat shock proteins that may function to anchor CAR to the cytoskeleton (Kobayashi et al. 2003; Yoshinari et al. 2003). Upon exposure to an inducing agent, CAR is released from this complex by a mechanism that probably involves protein phosphatase 2A, in turn accumulating in the nucleus, where the receptor heterodimerizes with RXR and subsequently interacts with coregulators such as SRC-1 (Makinen et al. 2002) to regulate target genes. It is currently unknown whether CAR activity is governed similarly in human hepatocytes although the available evidence supports such a hypothesis (Maglich et al. 2003; Pascussi et al. 2000). It is odd that most of the inducing agents that act through the CAR signalling pathway do not interact directly with the receptor (Huang et al. 2004; Moore et al. 2000; Zhang et al. 2002).

### 5.2.6. Description of T-plastin candidate

**T-plastin (fimbrin); MIM: 300131; Xq23.** T plastin is an actin binding protein broadly expressed with role in actin filament organization. The actin cytoskeleton is involved in cell motility, cell-substrate interactions, transport processes, cytokinesis, and the establishment and maintenance of cell morphology (Schmidt and Hall 1998).

Of particular importance are the actin crosslinking proteins, which direct the formation of distinct F-actin assemblies and integrate these actin complexes into overall cellular physiology through their responsiveness to signals such as calcium fluxes and phosphorylation events (Matsudaira 1994). The largest family of actin crosslinking proteins, which includes fimbrin,  $\alpha$ -actinin and  $\beta$ -spectrin, is characterized by the conserved ~250 amino acids F-actin binding domain (ABD) (Matsudaira 1991). The fimbrins are unique among the ABD-containing crosslinking proteins, as they possess two tandem repeats of the ABD within a single polypeptide chain (Wu et al. 2001). Due to the close proximity of the ABDs, plastin directs the formation of tightly bundled F-actin assemblies that participate in dynamic processes, including cytokinesis in yeast (Wu et al. 2001) and host cell invasion by enteropathic bacteria (Adam et al. 1995; Galan and Zhou 2000; Prevost et al. 1992). T-plastin possesses an N-terminal headpiece that contains two segments with homology to calcium binding EF-hands modules. The crosslinking activities of the three human isoforms (T, L and I) are modulated by calcium, although in different manners depending on

the isoform and phosphorylation state (de Arruda et al. 1990; Namba et al. 1992). The two ABDs are composed of two tandemly arranged 125 amino acids residues calponin homology (CH) domains. The majority of the ABD-containing crosslinking proteins form non-covalent homodimers, resulting in bivalent molecules that support the crosslinking of adjacent actin filaments (Fig. 12). The specific features of the dimerization domains control the separation and relative orientation of the ABDs and thus function as a critical determinant of the mechanical behaviour of the resulting F-actin networks (Matsudaira 1991). Recently, it has been shown that ABP1 of T-plastin is not only involved in actin-bundling, but may also control actin turnover, stabilization and assembly, independently of its bundling capacity (Giganti et al. 2005). Each CH domain is composed of four  $\alpha$ -helical segments, in which three form a loose bundle of helices, with the fourth  $\alpha$ -helix perpendicular to the major bundle. These segments are connected by extended and variable loops and sometimes two additional short helices. The complete crystal structure of plastin has not yet been resolved, but the structure of the N-terminal actin-binding domain 1 (ABD1) of T-plastin and the complete crosslinking core of *Arabidopsis thaliana* plastin and of *Schizosaccharomyces pombe* plastin have been solved (Goldsmith et al. 1997; Klein et al. 2004). Additional methods, such as electron microscopy, image analysis and homology modelling, have led to a general model of the plastin structure and to a view of how this protein crosslinks actin filaments (Fig. 12).

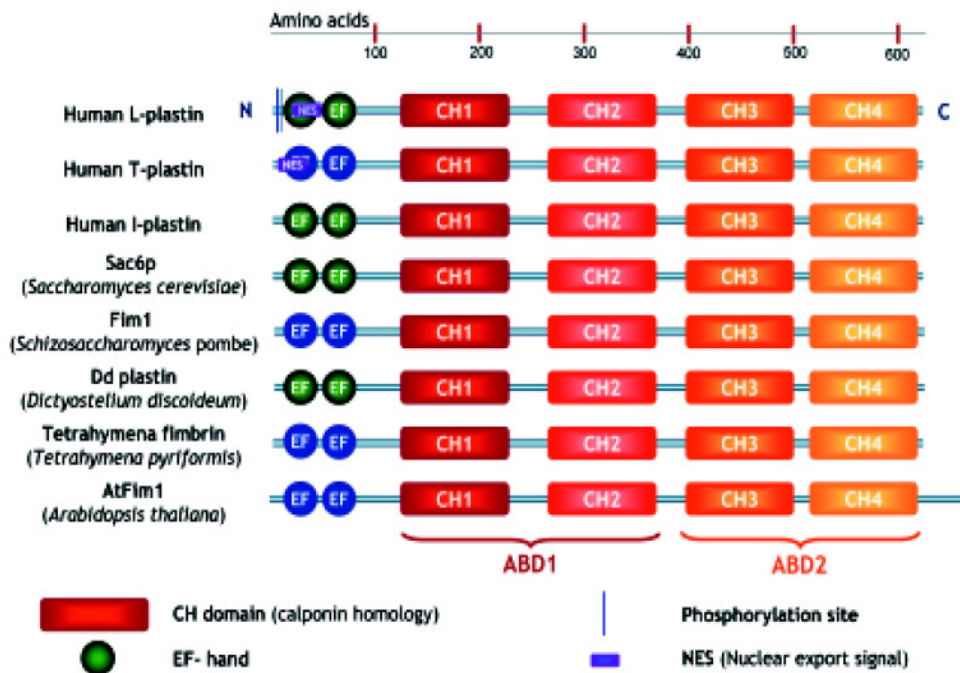


**Fig. 12 Domain organization of plastin isoforms from different species. A scale (in amino acids) is drawn on top of the figure. Domains in blue have no or less functionality. ABD=actin-binding domain. Note that each actin-binding domain consists of two CH domains. Human T- and L-plastin contain an NES, but it is unknown if plastins from other species are also endowed with a similar targeting signal (Delanote et al. 2005b).**

The actin crosslinking core of plastin has a compact architecture (Klein et al. 2004), and the ABDs pack in such a way that the CH1 domain and the CH4 domain make contact, involving conserved residues on the molecular surface of the CH1–CH4 interface. Electron density in regions connecting the CH domains is poorly defined, indicating that these segments are highly dynamic. The potential structural plasticity of ABD1 by reorganization of the CH domains is also confirmed by other crystal structures of utrophin, dystrophin, plectin and  $\alpha$ -actinin (Garcia-Alvarez et al. 2003; Keep et al. 1999; Liu et al. 2004).

Using an actin affinity matrix to identify actin-binding proteins in the budding yeast *Saccharomyces cerevisiae*, the Sac6 protein was identified, which localizes with cytoplasmic actin cables and cortical actin patches (Drubin et al. 1988). Its actin regulatory role was confirmed when the gene encoding this protein was found to suppress an actin mutation (Adams et al. 1989). Sac6p shows 43 % and 36 % identity with chicken plastin and human plastin, respectively. Mutant budding yeast cells lacking this gene display temperature sensitivity defects in growth, morphology, endocytosis and sporulation (Adams et al. 1991; Kubler and Riezman 1993). Surprisingly, overexpression of Sac6p is lethal (Sandrock et al. 1999). This could be explained by competition with an essential actin-binding protein, or by titrating out some other essential factors for growth. Next to stabilizing actin filaments, yeast plastin also has a role in the polymerization of G-actin (Cheng et al. 1999).

Adams and colleagues demonstrated a high degree of functional conservation between evolutionarily divergent plastins (Adams et al. 1995). They demonstrated that human T- and L-plastin could both substitute for yeast plastin in a *Sac6* null mutant, and restore functional defects. However, the third isoform, I-plastin, could not complement this temperature sensitive growth defect, illustrating the functional differences between human isoforms. The fission yeast *Schizosaccharomyces pombe* also contains a plastin homologue, called Fim1. It is not essential for viability but has a role in cell morphogenesis. In mitotic cells, Fim1 plays a role in formation of the actin ring during cytokinesis (Nakano et al. 2001).

*Dictyostelium discoideum* plastin shows 48 %–50 % identity with human plastins, and localizes to cortical structures associated with cell surface extensions (Prassler et al. 1997). In the ciliate *Tetrahymena*, plastin is localized in the cleavage furrow bundle during cytokinesis of dividing cells (Watanabe et al. 1998). This protein crosslinks actin filaments in a calcium-insensitive manner (Shirayama and Numata 2003; Watanabe et al. 2000). *Tetrahymena* plastin has a higher affinity for actin than the other plastin forms (Shirayama and Numata 2003). At least 3 plastin-like proteins may exist in the plant model system *Arabidopsis thaliana* (Kovar et al. 2000; McCurdy and Kim 1998). The AtFim1 isoform contains an additional 65 amino acids at its carboxy-terminal end, and is Ca<sup>2+</sup> insensitive because of less conserved Ca<sup>2+</sup>-binding domains. AtFim1 inhibits *Zea mays* profilin-induced actin depolymerization *in vitro* and *in vivo* (Kovar et al. 2000). L-plastin is often used as a myeloid lineage protein marker in zebrafish (*Danio rerio*) (Herbomel et al. 1999). Spatio-temporal expression of the L-plastin zebrafish homologue reveals a high level of conservation between zebrafish and mammals. Thus zebrafish constitutes an informative model system for the study of normal and anomalous human myelopoiesis (Bennett et al. 2001).

Generally, plastins are located in focal adhesions, ruffling membranes, lamellipodia, filopodia, or in specialized surface structures with highly ordered microfilaments bundles such as microvilli and

stereocilia. Sometimes they co-localize with stress fibers. In vertebrates, plastin contributes to the formation of specialized structures such as intestinal microvilli (Glenny et al. 1981; Mooseker 1983) and auditory stereocilia (Hofer et al. 1997). T-plastin is associated with the actin core bundle of microspikes in epithelial cells (Daudet and Lebart 2002) and was proposed to participate in the assembly of all these structures mentioned above (Arpin et al. 1994). In mesenchymal cell, T-plastin localizes to focal adhesion and the leading edge (Arpin et al. 1994), a broad lamellar membrane extension harbouring a dynamic branched actin network (Svitkina and Borisy 1999). T-plastin causes the reorganization and elongation of the actin structure by the WASP-Arp2/3 complex polymerization unit, and concomitantly increases actin-based force (Giganti et al. 2005). Several independent reports indicate that T-plastin is involved in the cellular response to DNA-damaging agents and toxins. T-plastin expression is enhanced in cisplatin-resistant human bladder, prostatic, head and neck cancer cell lines, in comparison to their cisplatin-sensitive counterparts (Hisano et al. 1996). Cisplatin is an anticancer agent that acts by binding to DNA and interfering with DNA repair. *T-plastin* mRNA was 12-fold more abundant in cisplatin-resistant cells in comparison to parental cells (Hisano et al. 1996). Furthermore, *T-plastin* was also up-regulated in UV radiation-resistant cells (Higuchi et al. 1998). Increased expression of *T-plastin* has been observed in Chinese hamster ovary (CHO) cells in which G2 arrest has been induced by X-radiation and by topoisomerase II inhibitor, etoposide (Sasaki et al. 2002). In contrast, when *T-plastin* expression was down-regulated, radiation-induced G2 arrest decreased in CHO cells, indicating a correlation between *T-plastin* expression and G2/M cell-cycle control (Sasaki et al. 2002). In an animal model of the autoimmune disease, systemic lupus erythematosus (SLE, a chronic rheumatoid disease) and in human patients, antibodies against T and L-plastin (a second plastin isoform expressed only in leukocytes) were found in serum (Mine et al. 1998). The presence of T- and L-plastin antibodies was correlated with the presence of the anti-Sm antibody, a typical SLE auto-antibody that recognizes a nuclear antigen. T-plastin was also found to be involved in invasion by at least two enteropathic bacteria: *Shigella flexneri* and *Salmonella typhimurium* (Adam et al. 1995; Prevost et al. 1992; Zhou et al. 1999). These two bacteria have different mechanisms for entering non-phagocytic cells by using specific effector proteins. In both cases, T-plastin was involved in cytoskeletal rearrangements during bacterial invasion. These rearrangements consist of distinct nucleation zones involving strong actin polymerization in close proximity to the contact site between bacterium and cell. These structures then push cellular protrusions during invasions of *Sigella flexeri* (Adam et al. 1995; Prevost et al. 1992). During *Salmonella typhimurium* invasions, T-plastin is first recruited to membrane ruffles induced by bacterium via a Cdc42-dependent signalling process that is activated by the bacterial effector protein, SopE. Then, another secreted bacterial effector protein, SipA, forms a complex with T-plastin and F-actin, which results in a marked increase in the actin-bundling activity of T-plastin. SipA also inhibits actin depolymerization. This leads to stabilization of actin filaments at the point of bacterium-host cell contact, which leads to more efficient *Salmonella* internalization (Zhou et al. 1999). Although T-plastin has a clear role in actin-bundling, there is sometimes apparently incongruent information as to their exact actin-binding properties. Actin-bundling activity by mammalian plastins has been clearly established, but there is additional evidence for actin

filament stabilization (Nakano et al. 2001) and for filament anti-depolymerization activities (Belmont and Drubin 1998; Brower et al. 1995; Giganti et al. 2005; Lebart et al. 2004). In some organisms (yeast and plants), there is even indication that plastins have actin polymerization ability (Cheng et al. 1999; Kovar et al. 2000).

The actin cytoskeleton of eukaryotic cells a dynamic meshwork that is involved in many biological phenomena such as cell motility, cell substrate adhesion, intracellular transport, endo- and exocytosis, cytokinesis and cell morphology (Delanote et al. 2005b). Cell morphology and motility depend on the remodelling of the cytoskeletal architecture and require locally restricted membrane protrusion and invagination, driven by cycles of actin polymerization and depolymerization (Carlier et al. 2003a; Carlier et al. 2003b; Pollard 2003; Pollard et al. 2000). L-plastin, was first noted as a polypeptide which appeared to be induced accompanying tumorigenesis of human fibroblasts (Goldstein et al. 1985; Leavitt et al. 1982; Leavitt and Kakunaga 1980). Constitutive expression of the L-plastin was found to be restricted to replicative hematopoietic cells while constitutive expression of T-plastin appeared to be a property of other replicative cells of solid tissues such as fibroblasts, endothelial cells and epithelial cells. However, many different types of human tumor-derived cell lines (non-hematopoietic cell types) were found to synthesize both L- and T-plastin together, suggesting that L-plastin gene was activated constitutively accompanying tumorigenesis (de Arruda et al. 1990; Lin et al. 1988). These two human cell type-specific isoforms have 80 % amino acid identity (Lin et al. 1988). I-plastin was discovered as a polypeptide that is specifically expressed in the small intestine, colon and kidney and is 86 % identical to the chicken fimbrin isoform (Lin et al. 1993a; Lin et al. 1993b; Lin et al. 1994b). The three isoforms share 70 % homology in their amino acid sequence but are encoded by three distinct genes on chromosomes 3 (I-plastin), 13 (L-plastin), and X (T-plastin) (Lin et al. 1993a; Lin et al. 1993b; Lin et al. 1994b).

Overexpression of T- or L-plastin in a fibroblast-like cell line induced cell rounding and simultaneous actin stress fiber rearrangements. In polarized epithelial cells, overexpression of T-plastin increased the length and density of microvilli (Leavitt et al. 1982; Leavitt and Kakunaga 1980; Lin et al. 1993b).

T-plastin may serve as potential target for Rho proteins by mediating their remodelling role. RhoA and Rac1 control the formation of the distinct actin-containing structures, stress fibers and membrane ruffles, respectively (Ridley and Hall 1992a, b; Ridley et al. 1992). The involvement of T-plastin in the Rho cascades provides a molecular basis for how Rho proteins regulate the formation of specialized actin-containing structures such as filopodia or stress fiber (Dutartre et al. 1996). T-plastin protein was found to be redistributed together with VASP in HtTA-1 cells overexpressing V12CDC42Hs into highly dynamic membranes regions (Dutartre et al. 1996). CDC42Hs is one of the Rho protein subgroup and represents the human homologue of the yeast *Saccharomyces cerevisiae* CDC42Sc (Shinjo et al. 1990). CDC42Sc was originally identified as a cell cycle gene essential for proper bud orientation (Adams et al. 1990; Johnson and Pringle 1990). V12CDC42Hs is a constitutively activated mutant with a glycine (position 12) to valine substitution which exhibits decreased intrinsic GTPase activity (Hart et al. 1991). In human HeLa-derived HtTA-1 cells, expression of V12CDC42Hs is driven by a tetracycline-repressible promoter and may be induced upon removal of the antibiotic from the culture medium (Gossen and Bujard 1992). VASP

(vasodilator-stimulated phosphoprotein) is a substrate for cAMP and cGMP-dependent protein kinases (Reinhard et al. 1992). The observed redistribution of T-plastin in HtTA-1 cells expressing V12CDC42Hs provides a link between the Rho protein and its regulatory function in remodelling the actin cytoskeleton. CDC42Hs might either transduce a regulatory signal to plastin, or might direct the assembly of docking sites for plastin and thereby might determine the sites where plastin will be recruited and will generate actin bundle (Dutartre et al. 1996).

T-plastin interacts also with ataxin-2 (ATX2) in mouse brain (Ralser et al. 2005b). It has been proposed that ATX2 might function in RNA metabolism (Shibata et al. 2000). In addition, ATX2 interacts with the cytoplasmic poly(A)-binding protein (PABP) (Ralser et al. 2005a) that functions in translation initiation and mRNA decay regulation and forms part of the so-called stress granules (Kedersha and Anderson 2002; Kedersha et al. 2000). The interaction of T-plastin with ATX2 links this protein to RNA metabolism pathway and/or function in translation.

Taken together, T-plastin protein was found an ideal candidate for our study. Further investigations into the cellular role of T-plastin were required to explore and elucidate its function in related pathways with SMN protein. Another reason for taking this gene differentially expressed in SMA discordant families was the hope to discover additional molecular mechanisms that might mediate or contribute to the protection of some individuals to develop SMA.

### **5.3. T-plastin, a potential gene modifier in SMA discordant families**

T-plastin gene, identified from the microarray analysis was a very interesting gene, since it is located on chromosome X. This correlates with the observation that in almost all SMA discordant families mainly the females are protected to develop SMA despite lacking *SMN1* gene (see Fig. 1 in appendix). Besides, the remaining candidate gene was chosen because of its expression pattern and potential connection with SMA (see below). T-plastin gene was found to be significantly higher expressed in asymptomatic sibs, revealing 39-fold increase in comparison with symptomatic ones (see 4.9.19.6. Basic data interpretation).

#### **5.3.1. *T-plastin* and *SMN* transcripts are expressed at high level in spinal cord and muscles**

To test T-plastin expression in different tissues, two biological samples were selected: first, one SMA fetus in order to check the T-plastin expression during development in SMA model; second, RNA isolated from one control, adult individual purchased from *ClonTech*. The RNA samples were used in RT-PCR reactions using T-plastin and SMN primers listed in table 6. As internal control, *HPRT* gene was co-amplified. In both SMA fetus and adult control, *T-plastin* was found to be expressed at high levels in spinal cord and muscles pointing out a very important involvement of *T-plastin* in these tissues (Fig. 13). As expected the *SMN* expression level in the SMA fetus was reduced in spinal cord. This data confirm the previously published results of Lefebvre et al. in 1997 and Burlet et al. in 1998. Importantly, low levels of SMN do not

induce low level of T-plastin. In the same manner, *SMN* was found to be expressed at high levels in spinal cord of control samples.

It has been previously reported that the relative amount of *SMN* transcript in normal human fetal tissues was higher in kidney and brain and similar in skeletal muscle, heart and thymus of 16-week-old fetuses.

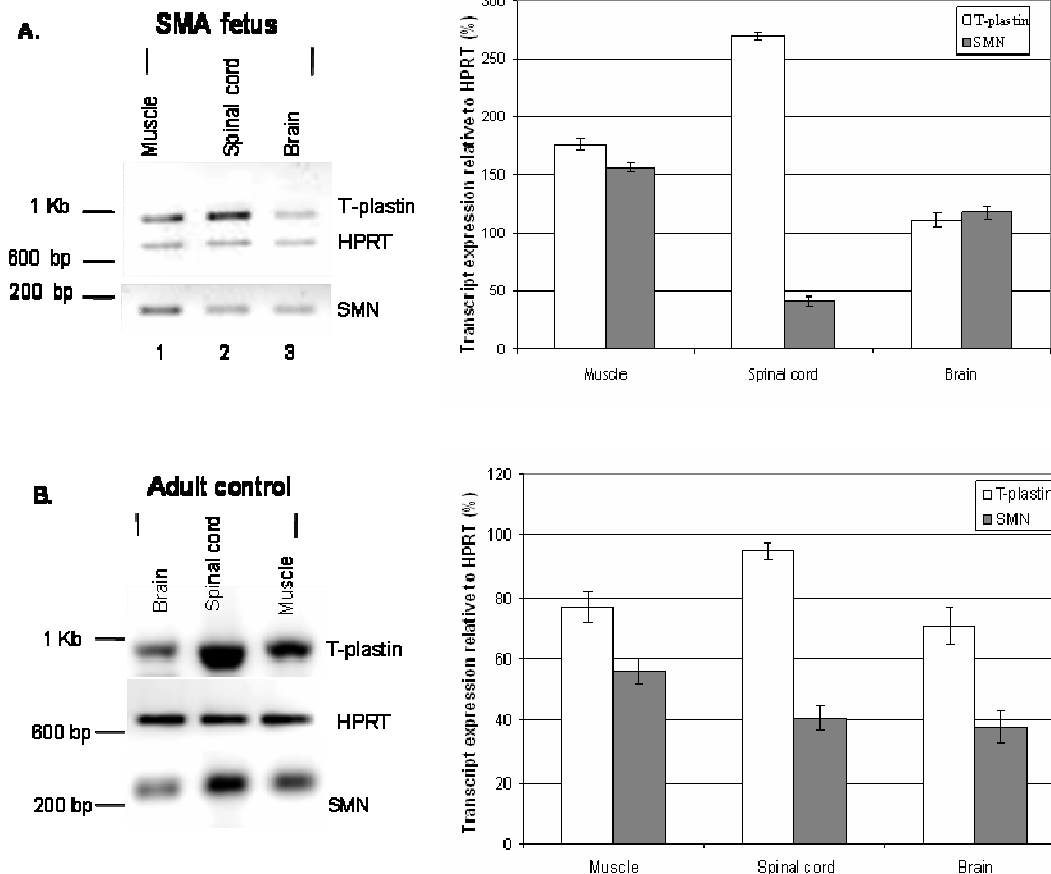


**Fig. 13 (A) Semi-quantitative RT-PCR of *T-plastin* relative to *HPRT* in muscle (lane1), spinal cord (lane 2) and brain (lane 3) from a SMA fetus. *T-plastin* is highly expressed in spinal cord as compared to *SMN* in the SMA fetus. The diagrammatic representation shows the *T-plastin* and *SMN* expression relative to *HPRT*; mean values  $\pm$  S.D. (n=3) are given. (B) *T-plastin* and *SMN* are expressed at high levels in spinal cord and muscle in adult, healthy control sample.**

The amount of SMN protein in skeletal muscle, heart, brain and kidney was higher during fetal life than in postnatal period, as compared with actin and  $\beta$ -tubulin protein levels (Burllet et al. 1998). The SMN protein level was markedly deficient in fetal muscle tissues from all three forms of SMA, being more reduced in severe than milder forms, as compared with age-matched controls (Burllet et al. 1998). Nerve impulses, which travel from the brain, along the spinal cord and onto motor neurons, control the muscle movements. The neurons affected in SMA are the lower motor neurons. These neurons are found in a specific part of the spinal cord, whereas the upper motor neurons reside in the brain. This means that the brain is not

affected. The accumulation of SMN in growth cones and NMJs during neuronal differentiation and neuromuscular maturation suggests that cytoplasmic SMN may possess a neuronal- and muscle-specific function (Fan and Simard 2002). Given the fact that *T-plastin* is highly expressed in both spinal cord and muscle in normal tissues, it points out a high implication of this gene in the structure and specific functions, very possible at NMJs level.

### 5.3.2. Characterization of T-plastin antibody

A polyclonal antibody was raised against human T-plastin by immunization of two New Zealand rabbits with a synthetic peptide ( $H_2N$ -MATTQISKDELDELKC- $CONH_2$ ) corresponding to the N-terminus of the protein (see Methods). Since human and murine T-plastin bear 100 % identical epitope sequence, this antibody is useful for recognizing both human and murine proteins. The specificity of the T-plastin antibody was demonstrated by Elisa and preabsorbion assays (*Eurogentec*) and subsequently confirmed by Western blot analysis. To detect endogenous T-plastin, 10  $\mu$ g of total protein extract from cell lysates of human HEK293, primary fibroblasts, EBV-transformed lymphoblastoid cell lines and rat PC12 cells were resolved by 12% SDS-PAGE gels and electrophoretically transferred to nitrocellulose membranes overnight.

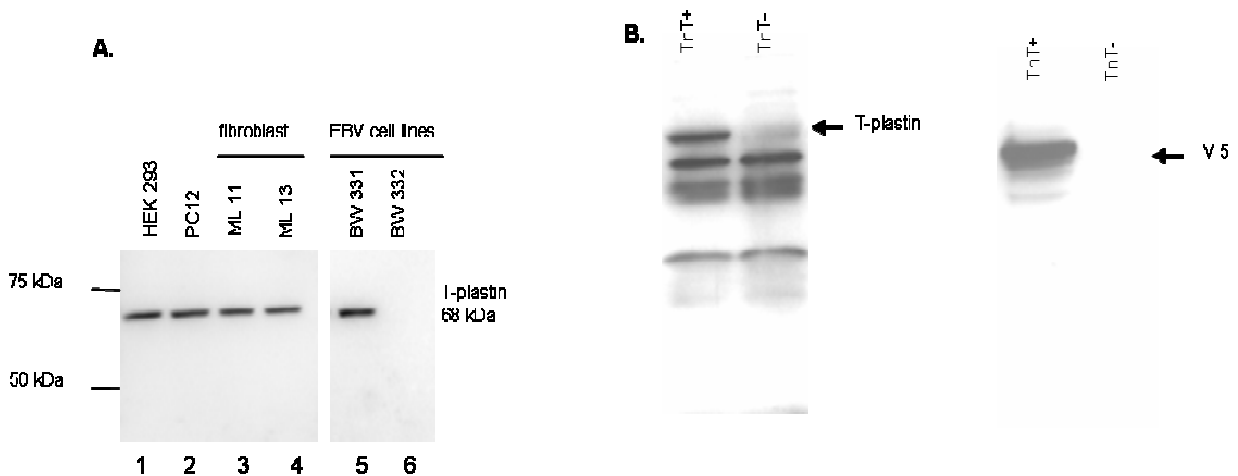


**Fig. 14** Verification of the specificity of the polyclonal antibody against T-plastin. (A) Proteins were extracted from HEK293 cells (lane 1), rat PC12 cells (lane 2), human fibroblast cell lines (lane 3 and 4) and EBV transformed lymphoblastoid cell lines (lane 5, expressing T-plastin and lane 6 not expressing T-plastin). The anti-T-plastin antibody recognized T-plastin at 68 kDa. (B) A recombinant T-plastin-V5 protein was obtained by use of the TnT system (*Promega*). The T-plastin protein was detected either by using the unpurified anti-T-plastin serum (left) or the anti-V5 tag antibody (right). As negative control a TnT negative reaction without adding plasmid DNA (TnT-) was performed in the same conditions. The unspecific bands were detected by comparison with the TnT negative reaction. The size of the protein ladder is specified on the left side of the figure. TnT+: TnT reaction with DNA plasmid added.

The optimal conditions for Western blot were determined at 1:5,000 dilution in 2 % Milk-TBS Tween solution with 3 h incubation at 4°C. On the Western blot of whole cell lysate of HEK293 cell, PC12 cells, primary fibroblasts, and EBV-transformed lymphoblastoid cells, the antibody recognized corresponding to the predicted 68 kDa T-plastin band (Fig. 14 A). Additionally, the T-plastin antibody was checked for the specificity using Western blot against recombinant T-plastin protein produced by the TnT system (*Promega*). A plasmid encoding human T-plastin V5-tagged was used for the *in vitro* transcription/translation reaction and 2 µl of TnT reaction mix resolved on 12 % SDS-PAGE gel. The blots were probed either with an anti-V5 tag antibody or with the polyclonal antibody against T-plastin. Both antibodies recognized specifically the T-plastin band around 70 kDa (Fig. 14 B).

### 5.3.3. T-plastin is expressed in both EBV-transformed lymphoblastoid cells and native blood belonging to unaffected *SMN1*-deleted sibs

Unlike the L and I isoforms, which are expressed in a limited number of cell types, T-plastin is expressed in a wide variety of tissues, including the epithelium, endothelium, fibroblasts, muscles and brain (Lin et al. 1994). In this respect, T-plastin actually resembles a housekeeping gene, except that its expression is uniquely excluded from all leukocytes (Lin et al. 1999). To prevent the *T-plastin* gene to be expressed, leukocytes are endowed with a specific suppressing factor or are devoid of a *T-plastin* gene-specific activating factor. In either case, this type of gene regulation must be unique, because no other gene has such a sharply contrasted expression pattern divided between leukocytes and non-leukocytes. Thus, a systematic analysis of the mechanisms governing *T-plastin* gene expression should provide an opportunity to identify novel regulatory gene sequences and transcription factors. To exclude that the T-plastin expression in EBV-transformed lymphoblastoid cell lines was not induced by the EBV transformation, the T-plastin expression was also analyzed in native blood. To determine and whether the difference between the unaffected and affected sibs can be demonstrated directly from unfractionated whole blood, RT-PCR and Western blot analyses were performed on the total RNA/proteins isolated from peripheral blood from one unaffected *SMN1*-deleted individual (#783) that showed T-plastin expression in the EBV-transformed lymphoblastoid cells (EBV T36/91).

The total RNA was subjected to multiplex PCR reaction using as internal control *HPRT* gene (Fig. 15 A). The total protein lysates extracted from both EBV-transformed lymphoblastoid cells and fresh blood were loaded onto a 12% SDS-PAGE gel and analyzed by Western blot with antibodies against T-plastin. As shown in Fig. 15 B, T-plastin protein can be readily detected from the whole blood.

The RNA and protein data on cells isolated from fresh blood demonstrated that T-plastin expression is not restricted to solid tissues and is expressed among the hematopoietic cell types in unaffected sibs belonging to SMA discordant families. In the same time it has been excluded any activation mechanism during the EBV transformation. The significance of T-plastin protein in hematopoietic cells in unaffected, healthy sibs remains to be determined and points out to an unique mechanism that might activate T-plastin gene in leukocytes. This mechanism behind *T-plastin* activation in fresh blood in unaffected sibs is unknown and

requires further investigations.

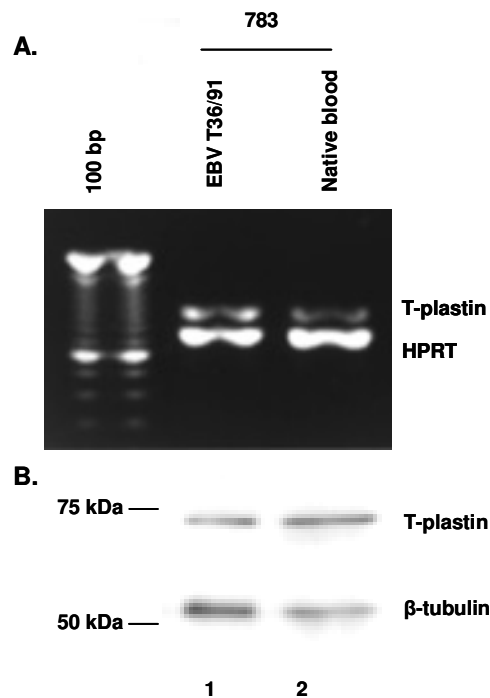


**Fig. 15 Confirmation of T-plastin expression in both lymphoblastoid cell culture and peripheral fresh blood in one asymptomatic sib homozygous deleted for *SMN1* gene. (A) RT-PCR analysis of one unaffected mother carrying a homozygous deletion of *SMN1*, who showed the same expression in EBV transformed cell lines and native blood, excluding an activation of *T-plastin* due to EBV transformation. 100bp: DNA ladder. (B) Western blot analysis revealed that T-plastin is translated in both analyzed tissues.  $\beta$ -tubulin was used as loading control. The size of the protein ladder is specified on the left side of the figure.**

#### 5.3.4. *T-plastin* is expressed in 6.5 % in the control population

T-plastin is normally absent in hematological cell types but widely distributed at various levels in other tissue types and nonhematopoietic malignancies (Lin et al. 1993b). Among all tissues/cells surveyed, T-plastin was shown to be absent from all hematopoietic cell types or whole blood studied and from malignant B-cell and T-cell lines studied (Lin et al. 1999).

Detection of T-plastin expression at both RNA and protein level in unaffected individuals that carry homozygous *SMN1* deletion revealed that T-plastin expression might be a rare event that happen in human population. This observation supports the idea that T-plastin expression is not restricted only to solid tissues. Whether the correlation of *T-plastin* expression in SMA discordant families with the phenotype is highly significant is going to be calculated. All unaffected *SMN1*-deleted sibs expressed *T-plastin* in EBV-transformed lymphoblastoid cells. To test whether the expression pattern is unique for SMA

discordant families, 46 control individuals, 67 classical type I, II and III SMA patients with either deletion or mutation of *SMN1* and 12 SMA patients with no mutation or deletion of *SMN1* gene (see table T1 in appendix) were tested for *T-plastin* expression by semi-quantitative analysis (RT-PCR). For controls RNA extracted from fresh blood was used. For the SMA population the RNA was isolated from EBV-transformed lymphoblastoid cells.

In the control population, *T-plastin* was expressed in 3/46 (6.5 %). In classical type I, II and III SMA patients, *T-plastin* was highly expressed in 5.9 % of the SMA population with *SMN1* deletion or mutation, in 7.4 % medium and 13.8 % very weak expressed (table 25 and Fig. F7 in appendix). For the SMA individuals that carry neither deletion nor mutation of *SMN1* gene, *T-plastin* was expressed in 8 % of the population.

**Table 25 T-plastin expression among SMA patients and control individuals.**

			<b>T-plastin expression</b>			
<b>Phenotype</b> ( <i>SMN1</i> Genotype)	<b>Gender</b>	<b>No. of individuals</b>	<b>-</b>	<b>+</b>	<b>++</b>	<b>+++</b>
<b>Type I SMA</b> del/del or del/mut	♀	13	10	2	1	-
	♂	12	11	-	1	-
<b>Type II SMA</b> del/del or del/mut	♀	13	7	3	1	2
	♂	12	10	2	-	-
<b>Type III SMA</b> del/del or del/mut	♀	5	4	1	-	-
	♂	12	7	1	2	2
		<b>N=67</b>	<b>N=49</b>	<b>N=9</b>	<b>N=5</b>	<b>N=4</b>
			<b>73 %</b>	<b>13.4 %</b>	<b>7.4 %</b>	<b>5.9 %</b>
<b>SMA</b> wt/wt	♀	5	5	-	-	-
	♂	7	6	-	-	1
		<b>N=12</b>	<b>N=11</b>	<b>N=0</b>	<b>N=0</b>	<b>N=1</b>
			<b>92 %</b>	<b>0 %</b>	<b>0 %</b>	<b>8 %</b>
<b>Controls</b> (wt/wt)	♀	21	18	-	2	1
	♂	25	25	-	-	-
		<b>N= 46</b>	<b>N=43</b>	<b>N=0</b>	<b>N=2</b>	<b>N=1</b>
			<b>93.5 %</b>	<b>0 %</b>	<b>4.3 %</b>	<b>2.2 %</b>

del/del: homozygous deletion of *SMN1* gene; del/mut: deletion of *SMN1* gene on one chromosome and mutation of *SMN1* gene on the other chromosome; wt/wt: *SMN1* gene is present on both chromosomes; - no *T-plastin* expression; +: very weak *T-plastin* expression; ++: mild *T-plastin* expression; +++: strong *T-plastin* expression.

This expression pattern is unexpected since no expression of this gene was observed in the lymphocyte cells so far in the control population. This study revealed for the first time the evidence that *T-plastin* expression in fresh blood is a rare event that occurs in 6.5 % of the control population. Moreover, the expression of *T-plastin* itself in leukocytes is not enough to protect the individuals to develop SMA. Additional factors that modulate *T-plastin* expression function or localization may be important.

This result explains, at least in part, the case of family #800 where both unaffected and affected sibs express T-plastin, but one is protected to develop SMA. The LN 421 individual resembles the case of the classical SMA patients that express *T-plastin* by an unidentified mechanism, but this is not the complete background to drive to a protected phenotype. Like in complex diseases, a certain genotype can protect or predispose for a certain phenotype but not exclusively. To find out whether this is the case, an analysis of the haplotype blocks in T-plastin genomic region of individuals divided in “expression” vs. “non-expression” groups was carried out (see 5.3.8.3 Haplotype analysis of the *T-plastin* genomic region reveals a *trans*-acting mechanism to regulate *T-plastin* its expression).

### **5.3.5. Validation of the significant difference of T-plastin expression between unaffected and affected sibs at protein level**

To determine whether the *T-plastin* transcripts were associated with protein expression, Western blot analysis was performed using the polyclonal antibody against T-plastin. From five SMA discordant families, proteins from EBV-transformed lymphoblastoid cells and primary fibroblasts cultures from one SMA discordant family were analyzed by Western blot analysis. All blots were first probed with anti- $\beta$ -tubulin antibody to ensure that equal amount of proteins were loaded on the SDS-PAGE gel for each family. Afterwards the same blots were reprobed and analyzed for the expression level of T-plastin.

Similar to the findings from RT-PCR, the affected sibs did not express T-plastin protein, but the protein was expressed in unaffected sibs (Fig. 16 A). In contrast, in lysates extracted from primary fibroblasts cultures, no protein expression differences could be observed (Fig. 16 B).

In 2003 it has been also demonstrated by Helmken and colleagues that the modulating effects of a modifying factor is likely to be tissues-specific, because only in protein samples derived from lymphoblastoid cell lines, but not primary fibroblasts, a difference in SMN and SMN-interacting partners levels was observed (Helmken et al. 2003). In the same way, these results support the idea that the modulating effects of T-plastin are tissue-specific.

### **5.3.7. Functional analysis of T-plastin protein**

#### **5.3.7.1. SMN and T-plastin associate together *in vivo*, but do not interact directly**

It has been described that SMN interacts with cytoskeletal protein profilin IIa *in vivo* (Sharma et al. 2005). To find the relevance of the interplay between T-plastin and SMN protein in a related pathway, it has been

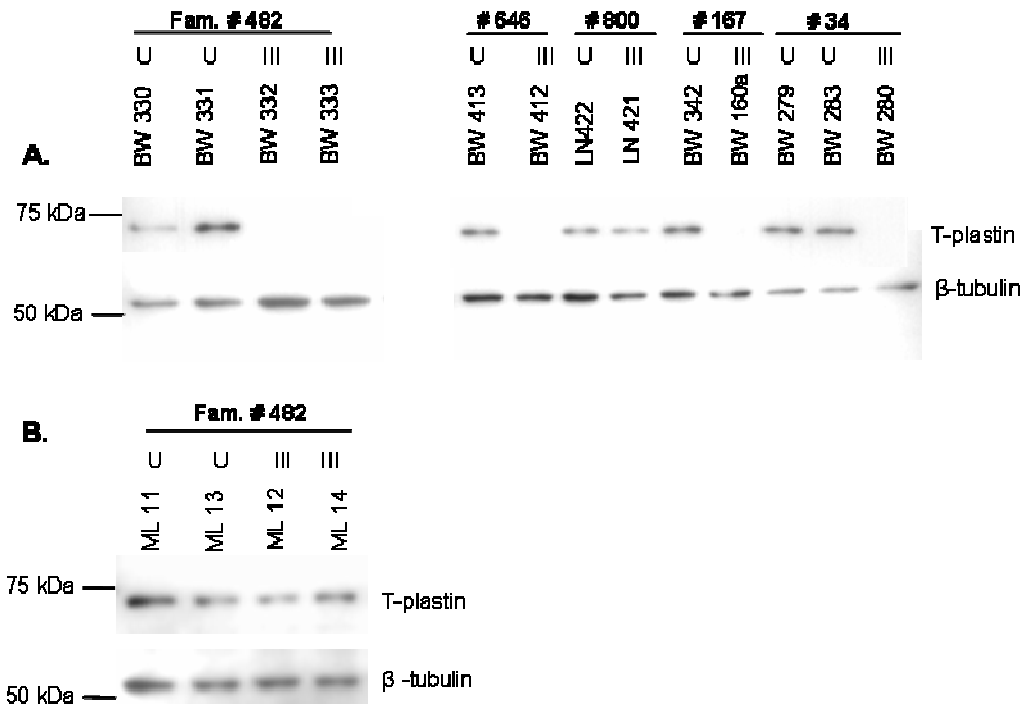


**Fig. 16** Semi-quantitative analysis of T-plastin protein in cell lines derived from SMA discordant families. (A) Western blot analysis of proteins extracted from EBV cell lines from five SMA discordant families showing that all unaffected siblings expressed T-plastin. (B) Western blot analysis of protein content in primary fibroblasts cultures revealed no down-regulation of T-plastin in affected individuals compared with the unaffected sibs.  $\beta$ -tubulin was used to verify that equal amounts of total protein lysates were loaded. U: unaffected; III: type III SMA.

explored whether any relationship may point to a direct physical interaction or cellular complex formation. In the first step we investigated whether a physical interaction between T-plastin and SMN occurs *in vivo*. Therefore, co-immunoprecipitations using total cell lysate isolated from HEK 293 cells were performed. The co-immunoprecipitation analysis revealed that these two proteins associate *in vivo*. Using HEK293 cell lysate, SMN was precipitated applying antibody directed against endogenous T-plastin indicating a complex formation (Fig. 17 A). The association between T-plastin and SMN suggests that the two proteins have an associated function. Next, *in vitro* binding experiments were performed to answer the question of whether the two proteins interact directly. A construct encoding for the full-length T-plastin fused to a V5 tag generated in pcDNA 3.1 vector was used for the *in vitro* transcription/translation system to obtain the V5-tagged protein, used as bait in GST-pull down experiments. The prey-protein, SMN-GST was purified after IPTG induction using Magne-GST Pull-Down System (*Promega*). After GST-pull down the blots were stained with an anti V5 antibody and no direct interaction between SMN and T-plastin was observed (Fig. 17 B). This experiment was repeated at least three times and similar results were observed.

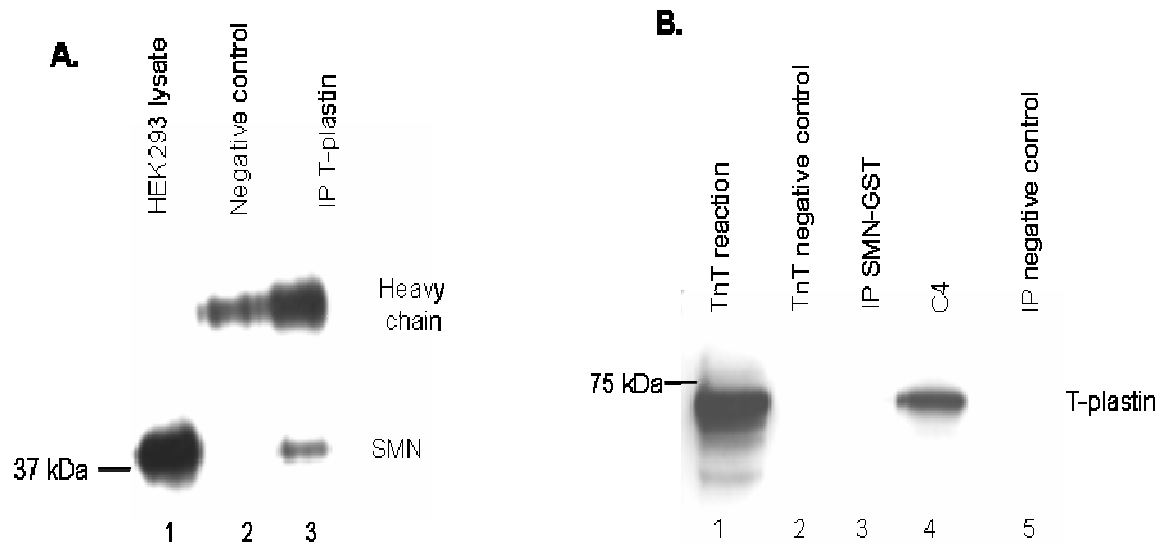


**Fig. 17 T-plastin associates with SMN. (A)** T-plastin and SMN associates *in vivo* as shown by co-immunoprecipitation. Western blot analysis of HEK2993 cell lysates incubated with polyclonal anti-T-plastin antibody bound to protein G-Sepharose for IP reaction and stained with monoclonal anti-SMN antibodies on Western blot. The T-plastin protein precipitated endogenous SMN protein (lane 3). In the negative control (lane 2) protein G-beads carrying T-plastin antibody in IP buffer were used (lane 1: total protein extract isolated from HEK2993 cells was loaded to serve as positive control for SMN protein). **(B)** SMN and T-plastin do not interact directly with each other. Full-length T-plastin-V5 protein produced by the TnT system (*Promega*) and GST-fused SMN were subjected to pull down reaction using MagneGST Pull-Down System (*Promega*). For Western blot analysis an anti-V5 antibody was used to detect the recombinant T-plastin protein. Lane 1: positive control for T-plastin-V5; lane 2: the TnT reaction with no plasmid DNA added; lane 3: the SMN-GST protein precipitated no T-plastin protein; lane 4: C4, supernatant saved after capture; lane 5: IP negative: immunoprecipitation using the TnT negative reaction.

Taken together, these observations suggest that T-plastin and SMN are part of the same complex, but another protein represents the link that brings together the two proteins. The protein content of the T-plastin-SMN complex is unknown and requires further investigations.

### 5.3.7.2. Endogenous SMN co-localizes with V5-tagged T-plastin in the perinuclear area of HEK293 cells

In mammalian COS cells, T-plastin-GFP localized preferentially to membrane ruffles, lamellopodium protrusions, and adhesion sites (Timmers et al. 2002), which broadly corresponds to the reported distribution of T-plastin in various animal cell types observed after immunostaining (Dutartre et al. 1996; Prassler et al. 1997).

Because all plastin isoforms regulate the actin cytoskeleton, they have always been considered as cytoplasmic proteins. Very recently, it has been reported that endogenous as well overexpressed T-plastin was able to shuttle between nucleus and cytoplasm in HeLa and Jurkat cells (Delanote et al. 2005a). It has been identified a strong leucine-rich nuclear export signal (NES) in T-plastin.

The SMN protein is found in the cytoplasm and nucleus (Battaglia et al. 1997; Lefebvre et al. 1997). In the nucleus of most cells, SMN is concentrated in structures termed gems, which often co-localize with coiled bodies (Liu and Dreyfuss 1996).

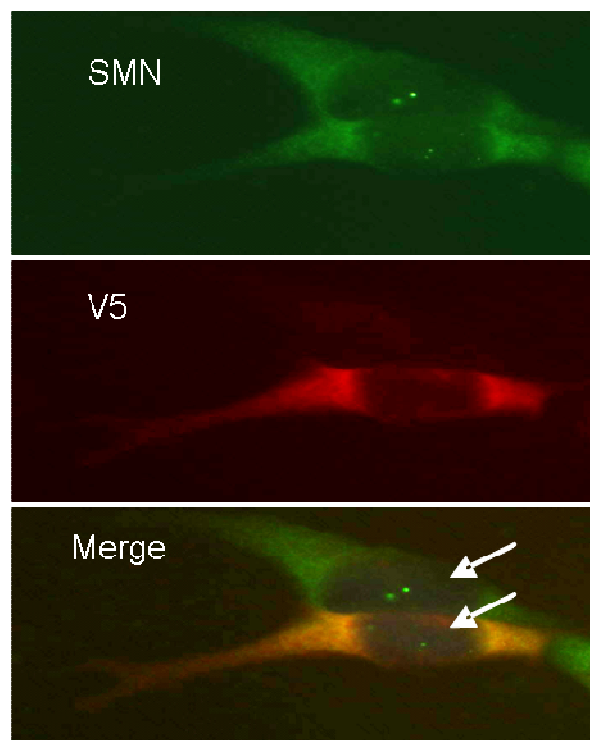


**Fig. 19** Co-localization of the endogenous SMN and T-plastin-V5 in the perinuclear area of HEK293 cells. Double staining of T-plastin-V5 with anti-V5 antibody conjugated with AlexaFluor 568 (red) and of SMN with anti-SMN-FITC antibody (green) showed co-localization of both proteins mainly in the perinuclear area of transfected cells. White arrows indicate gems.

To study the expression of T-plastin in mammalian cells, transfected HEK293 with 1  $\mu$ g of plasmid encoding for the full-length-V5 tagged T-plastin cells were analyzed for the presence of recombinant T-plastin protein and endogenous SMN by indirect immunofluorescence staining using a monoclonal antibody against SMN directly labelled with FITC and a monoclonal antibody directed against V5 tag to detect the recombinant T-plastin protein.

T-plastin was located in the cytoplasm, mainly in a perinuclear distribution, while SMN localized in both cytoplasm (in a diffused manner) (Fig. 18) and nucleus (as gems, indicated with white arrows in Fig. 18). The co-localization in the perinuclear area of the two proteins supports the idea that cytoplasmic complexes comprising SMN and T-plastin are formed in mammalian cells.

### **5.3.7.3. T-plastin and SMN levels increase under NGF stimulation in PC12 cells.**

PC12 cells were used as a model system to test the expression of T-plastin during neurite outgrowth, a hallmark of neuronal differentiation. PC12 cells are rat pheochromocytoma cells of sympathoadrenal origin and represent a useful model for the analysis of neuronal differentiation (Greene and Tischler 1976). Treatment of undifferentiated PC12 cells with nerve growth factor (NGF) drives differentiation into a sympathetic neuronal phenotype and outgrowth of neurites.

The effects of neuronal differentiation under NGF treatment in PC12 cells were analyzed for the expression of both T-plastin and SMN. PC12 cells were grown on collagen-coated culture dishes and stimulated with NGF for one, two and three days, respectively. The whole cell lysates were applied on 12 % SDS-PAGE gel and Western blots were first probed with an antibody against  $\beta$ -tubulin to ensure that equal amounts of protein were loaded. The same blots were reprobbed with an anti-SMN antibody and a polyclonal anti-T-plastin antibody. At least three independent experiments were analyzed by Western blot and subsequently densitometrically evaluated. The housekeeping gene,  $\beta$ -tubulin used as loading control did not display changes of expression levels (Fig. 19). It has been already demonstrated that NGF treatment of PC12 cells does not change the levels of  $\beta$ -actin and  $\beta$ -tubulin (Yu and Rasenick 2006).

Both, T-plastin and SMN proteins became up-regulated upon stimulation of cells with NGF for 24, 48 and 72 h, respectively, as shown in Fig. 19. An increase of SMN protein levels in PC12 cells has been reported previously as a consequence of neuronal differentiation (van Bergeijk et al. 2007). SMN was also found up-regulated during neuritogenesis in PC12-derived, dexamethasone-inducible UR16 cell line (Navascues et al. 2004). The UR16 cell line has been created by Guerrero et al. (1988) and is a stable PC12 subline that contains a mouse *N-ras* gene driven by dexamethasone-inducible promoter (Guerrero et al. 1988). Quantitative immunoblotting analysis revealed that SMN levels are up-regulated to similar extents in both the nucleus and cytoplasm (Navascues et al. 2004). Dynamic regulation of the actin network, particularly at the growth cone, is an important element of neuronal differentiation and plasticity. An up-regulation of transcripts encoding proteins in actin gelation, actin depolymerization, formation and organization of actin filaments, linkage of signaling pathways to F-actin reorganization and alteration of actin organization in dendrites and growth cone was already shown (Angelastro et al. 2000). The diversity

of the roles of these proteins underscores the complexity of the mechanisms by which NGF regulates actin function and points to several new candidates that might mediate NGF-promoted synaptic plasticity.

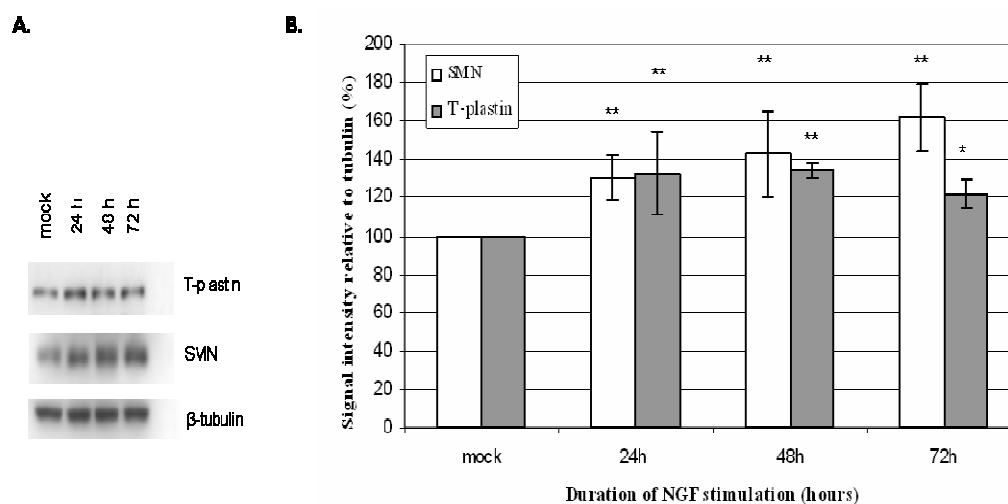


**Fig. 19** Expression of T-plastin and SMN proteins during neuronal differentiation of PC12 cells. (A) PC12 cells were grown on collagen coated dishes and treated with 100 ng/ml nerve growth factor (NGF) for 24, 48 and 72h, respectively, or non-treated (mock, lane 1) and harvested after the indicated times. Equal amounts of total cell lysates were analyzed by Western blot analysis with antibodies against  $\beta$ -tubulin (control). The Western blot analysis showed that T-plastin and SMN level increased after 24 h under NGF stimulation and remains at high level during neurite outgrowth. (B) Protein levels were quantified by densitometry, normalized against  $\beta$ -tubulin and statistically analyzed by *t*-test. Data show mean values  $\pm$  SD of three independent experiments. \* $p < 0.005$ ; \*\* $p < 0.001$ .

Tau protein is classically defined as a microtubule-associated protein that plays an important role in promotion and stabilization of axonal microtubules (Hashiguchi et al. 2000; Maas et al. 2000). Interaction between tau and actin is dependent on NGF treatment (Yu and Rasenick 2006). Endogenous tau expression is low in PC12 cells without NGF treatment, and increases after NGF stimulation (Drubin et al. 1985). In the same manner, T-plastin protein levels that associate with SMN and/or actin may increase under NGF stimulation in differentiating PC12 cells.

T-plastin was significantly up-regulated in PC12 cells during neuronal differentiation within three days of continuous NGF induction. It has been shown previously that Gemin 2 and SmB, two binding partners of SMN, did not display changes of expression levels during differentiation of PC12 cells (van Bergeijk et al. 2007). The same group showed that PRMT5 (the protein that adds methyl groups at Sm proteins arginine-rich motifs) like the other components of the SMN complex, was not altered during differentiation of PC12

cells. Interestingly, during the course of neuronal differentiation coilin levels decreased, indicating a putative concomitant change in Cajal body number and structure (van Bergeijk et al. 2007). It has been shown that SMN and Gemin, as well as SMN and Sm proteins containing particles do not co-localize in living neurons (Zhang et al. 2006).

These results demonstrate that SMN is not co-regulated with other components of the SMN complex and the methylosome during differentiation of PC12 cells, suggesting an independent role of this protein. The presence of SMN and T-plastin in one and the same complex may point toward diverse types of SMN complexes that have functions in neurons, other than its well characterized role to assemble snRNPs in all cells.

#### **5.3.7.4. The affinity of T-plastin for SMN increases during neurite outgrowth**

To further establish T-plastin-SMN association, co-immunoprecipitation experiments were carried out in NGF differentiated PC12 cells. Protein extracts of PC12 cells isolated at different NGF stimulation time points were analyzed by immunoprecipitation experiments using antibodies against T-plastin for IP and against SMN and  $\beta$ -actin for Western blot. In Fig. 20 it is shown that when PC12 cells were exposed to NGF for 36 h, the interaction of T-plastin with SMN increased up to 20 % (Fig. 20 A and B), while, the interaction of T-plastin with  $\beta$ -actin was not changed. NGF treatment did not alter the amount of  $\beta$ -actin or tubulin (as shown above).

It was also been found that the interaction between T-plastin and SMN occurred after 8 h of NGF treatment, increased under a long-term (36-72 h) NGF stimulation. The increase was significant ( $p < 0.002$ ) (Fig. 20 B) and after 72 h NGF treatment the affinity of T-plastin for SMN increased up to 50 %. These studies suggest that NGF stimulation of PC12 cells might induce the reorganization of SMN and promote T-plastin interaction with SMN during neurite differentiation.

The protein-protein-interactions in a certain complex could be permanent or transient. Transient complexes associate and disassociate *in vivo* according to the environment or to the presence of external factors and involve proteins that also exist as independent entities (Nooren and Thornton 2003a, b) In contrast a permanent interaction is usually very stable (Nooren and Thornton 2003a).

The T-plastin protein associates permanent with SMN (Fig. 17 A) but, interestingly, under NGF stimulation a transient complex occurs suggesting that during neuronal differentiation, a signal might trigger SMN to T-plastin (or T-plastin to SMN) and together contribute to a specific function during this biological process. SMN protein was shown already to be involved in more than one multiprotein complex (Gubitz et al. 2004; Monani 2005; Rossoll et al. 2003; Yong et al. 2004; Zhang et al. 2006). The formation of a complex between T-plastin and SMN might play a central role during PC12 differentiation and is important to find the reason for the high specificity of T-plastin for SMN in this biological process.

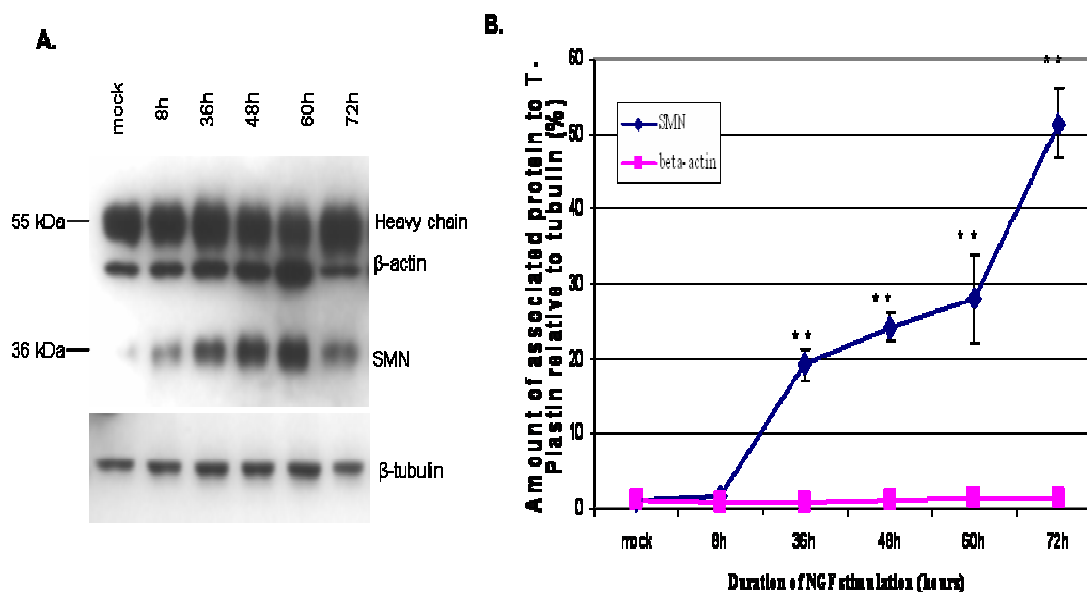


**Fig. 20** Analysis of *in vivo* interaction between T-plastin and SMN, and between T-plastin and  $\beta$ -actin during neurite differentiation. (A) PC12 cells stimulated with 100 ng/ml NGF for 8, 36, 48, 60 and 72 h were used for immunoprecipitation experiments using anti-T-plastin antibody. Western blot analyses showed that T-plastin precipitated both SMN and  $\beta$ -actin with different affinities. Equal loading was verified with anti- $\beta$ -tubulin antibody. (B) The diagrammatic representation shows the quantitative analysis of T-plastin association with SMN, and  $\beta$ -actin during neurite outgrowth. Only the affinity between T-plastin and SMN was significantly increased but not of T-plastin to  $\beta$ -actin. Data shown represent the mean  $\pm$  SD of three independent immunoprecipitates (\*\* $p < 0.002$ ).

#### 5.3.7.5. Endogenous T-plastin and SMN co-localize along neurites and at the growth cone level in PC12 cells-derived neurons

In general, the members of the plastin family have been identified in cellular regions with a high actin filament turnover. The plastin homologue fimbrin forms actin filament bundles *in vitro* and *in vivo* oriented with the same polarity (Coluccio and Bretscher 1989; Matsudaira et al. 1983). The relevance of T-plastin protein expression in unaffected sibs was further analyzed using PC12 cell-derived neurons using confocal immunofluorescence microscopy.

Differentiated PC12 cells were analyzed for the presence of T-plastin protein by indirect immunofluorescence staining using the polyclonal antibody against T-plastin. After two and three days of NGF treatment, neuronal- and glial-like cells appeared. We detected diffuse T-plastin staining within the cytoplasm and, interestingly T-plastin protein accumulated in growth cone-like structures and varicosities of neuronal-like cells during the formation of neurite processes (Fig. 21 A).

SMN accumulates in growth cone-like structures during neuronal differentiation, making SMN a new marker of growth cones (Fan and Simard 2002). Given the abundance of actin in neurites and growth cones, the distribution of T-plastin and actin was assessed by superimposing images of T-plastin conjugated with AlexaFluor 488 with AlexaFluor 568 phalloidin staining- the later binding F-actin. After 24 h NGF treatment, T-plastin co-localizes with F-actin within the cytoplasm under the membrane cortex and at growth cone levels (Fig. 21 B).

The redistribution and accumulation of cytoplasmic SMN at the periphery of the cell body and in growth cone-and filopodia like structures in both neuronal- and glial-like cells has already been shown (Fan and Simard 2002). Subcellular localization in growth cones was confirmed by demonstrating the presence of GAP43, a protein involved in neurite outgrowth (Aigner and Caroni 1995) along the neurite processes and localization of both SMN and GAP43 within growth cones.

Profilin IIa, a motor neuron-specific microfilament-associated, actin-binding protein involved in actin polymerization (Lambrechts et al. 2000b; Lambrechts et al. 1997) has been shown to interact directly with SMN (Giesemann et al. 1999). These interaction may mediate actin and SMN transport in neurite outgrowth. Two additional SMN partners (Mourelatos et al. 2001; Rossoll et al. 2002), namely the RNA-binding proteins hnRNP-R and hnRNP-Q co-localize with SMN in distal axons of embryonic motor neurons (Rossoll et al. 2002).

In plant epidermal cells and yeast cells, plastin-GFP was also found to associate with specific elements of the actin filament cytoskeleton. In plant cells, fluorescence localized to fine actin filaments within transvacuolar cytoplasmic strands and within the cell cortex. The thicker actin cables within the subcortex, visualised by rhodamine-phalloidin labelling, were not observed with plastin-GFP (Timmers et al. 2002).

In the case of yeast cells, plastin-GFP only associated with cortical actin patches (Timmers et al. 2002). T-plastin is a cytoplasmic protein broadly expressed regulating actin assembly and cellular motility. The actin skeleton plays an important role in axon initiation, growth, guidance, branching and retraction, and also in synapse formation and stability (Luo 2002). It has been observed that Smn associates with cytoskeletal elements in spinal dendrites and axons (Pagliardini et al. 2000).

Recently, cytoskeletal-based active transport of Smn-containing granules in neuronal processes and growth cones has been demonstrated in transfected cultured neurons (Zhang et al. 2003). Deficiency of Smn protein leads to alteration of  $\beta$ -actin protein and mRNA localization in axons and growth cones (Rossoll et al. 2003). The reduced level of  $\beta$ -actin suggests that functions such as growth cone movement and the release of synaptic vesicles (Bloom et al. 2003), which also require actin, might be disturbed in SMA and thus contribute to the specific pathology of SMA disease.

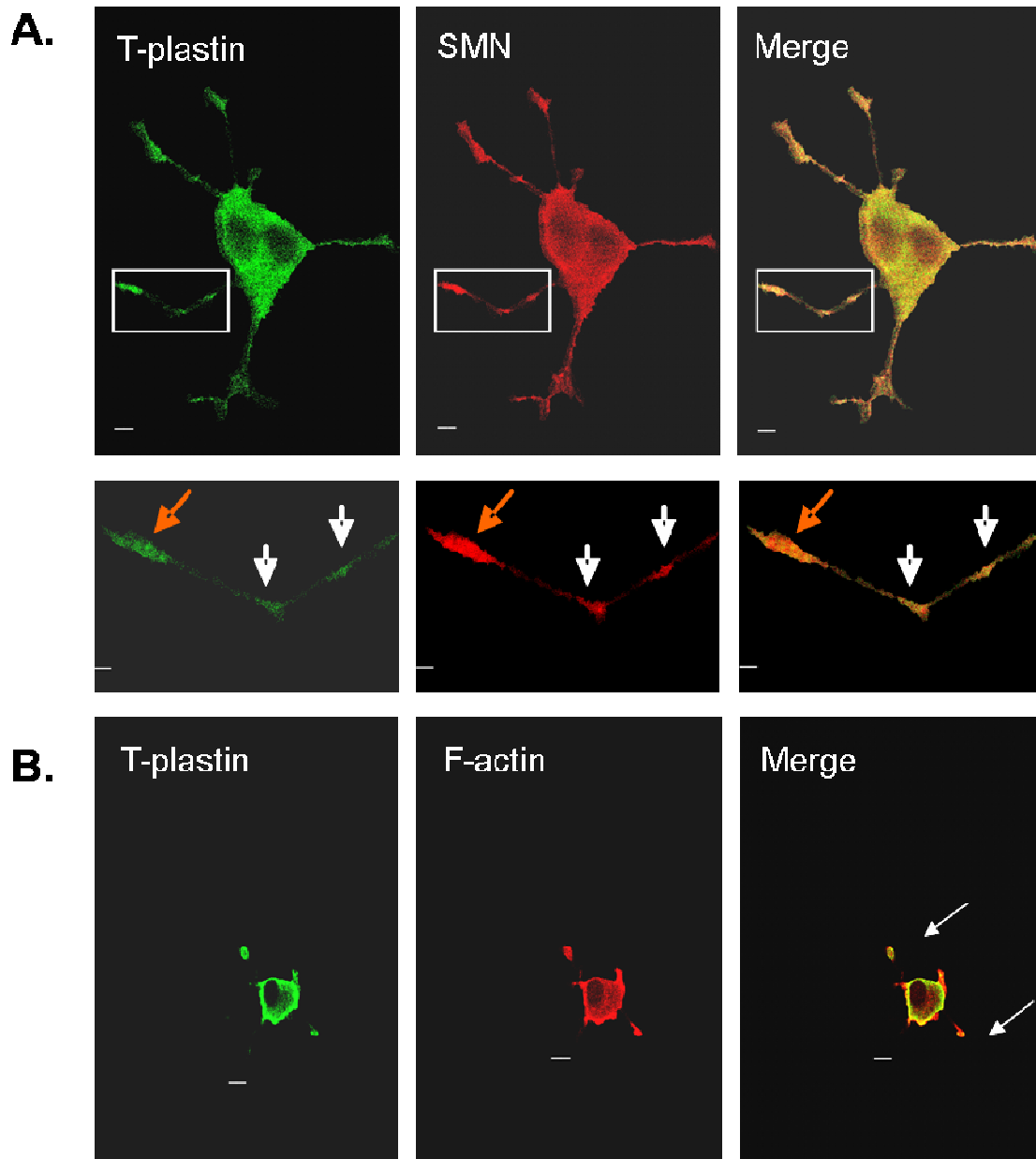


**Fig. 21** Co-localization of endogenous T-plastin with SMN and F-actin in neurites and the growth cones in PC12 derived neurons. (A) T-plastin (green) and SMN (red) were detected by double-labeled immunofluorescence using anti-T-plastin antibody directly conjugated with AlexaFluor 488 and anti-SMN antibody directly conjugated with AlexaFluor 568. Higher magnification of one region (inset from top panel is enlarged in bottom panel) shows the frequent co-localization between SMN and T-plastin within neurites (white arrows) and growth cones (orange arrow). (B) Co-localization of F-actin and T-plastin at growth cones in PC12 derived motor neurons. F-actin was stained with phalloidin conjugated with AlexaFluor 568 (red) and anti-T-plastin antibody directly conjugated to AlexaFluor 488 (green). The co-localization (indicated by arrows) at growth cones was observed. Bar: 20  $\mu$ m.

### 5.3.7.6. T-plastin-depleted PC12 cells exhibit a significant reduction in neurite length

To address the role of T-plastin in PC12 cell differentiation, PC12 cells in which endogenous T-plastin was knocked down were generated. To model this effect of T-plastin loss in cultured PC12 cells siRNA oligos directed against rat *T-plastin* and DharmaFect 4 Transfection reagent (*Dharmacon*) were used. PC12 cells were cultured in collagen type-I coated culture dishes and for immunostaining procedures differentiating PC12 cells were grown on collagen type I-coated coverslips (see Methods) to increase the attachment of PC12 cells during transfection procedures.

The efficacy of antisense T-plastin siRNA oligos was evaluated by Western blot analysis (Fig. 22 A and B) of whole cell lysates harvested from PC12 cells transfected either with control siRNA or with T-plastin siRNA oligos. The proteins were resolved on 12 % SDS-PAGE gel and transferred to a nitrocellulose membrane; blots were probed first with anti- $\beta$ -tubulin antibody and then with anti-T-plastin antibody to detect the efficiency of the knocking-down procedure.

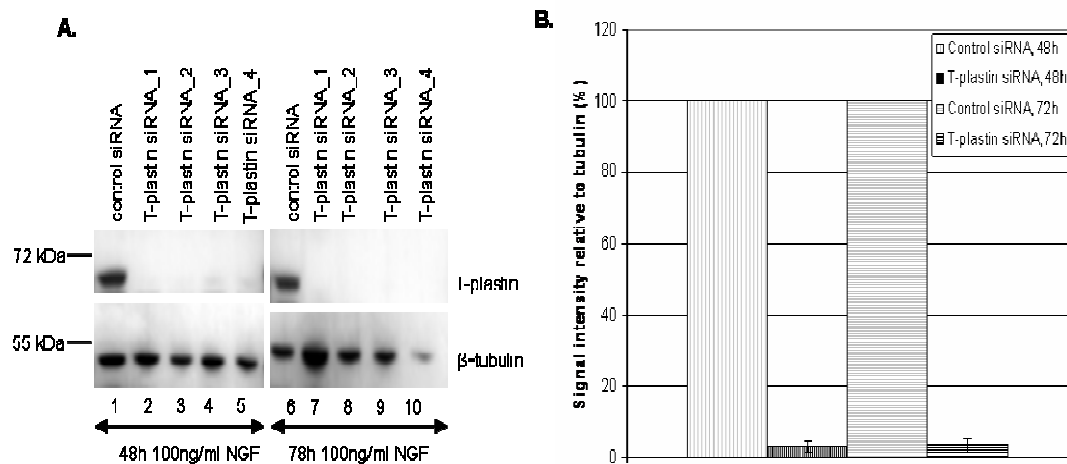


**Fig. 22** Knock-down of T-plastin in PC12 cells. (A) PC12 cells were treated either with control siRNA (lane 1 and 6) or with siRNA directed against N- terminus of rat T-plastin (lanes 2-5 and 7-10) using as transfection reagent DharmaFect 4 (*Dharmacon*). PC12 cells were double transfected (a second transfection step was performed 24 h after the first transfection). Cells were allowed to differentiate 48 h (left) or 72 h (right) under NGF (100 ng/ml) stimulation. Western blot analysis revealed a significant reduction in the amount of T-plastin in T-plastin siRNA treated PC12 cells as compared to control siRNA treated PC12 cells. (B) Knock-down of T-plastin protein level was determined relative to  $\beta$ -tubulin. Results represent the mean  $\pm$  SD from four independent experiments ( $p < 0.001$  compared with control siRNA treated cells by *t*-test).

The experiments were repeated four times and a double-step transfection protocol was approached. Therefore, after 24 h after the first transfection, a second transfection step was performed and cells were allowed to differentiate 48 or 72 h under NGF after the second transfection step. With this technique, T-plastin protein in transfected PC12 cells was nearly undetectable at two and three days *in vitro* (Fig. 22 A). Densitometric analysis of T-plastin signals showed a significant decrease of  $93 \pm 3\%$  relative to  $\beta$ -tubulin and compared to cells transfected with control siRNA on day two and three after the second transfection and neuronal differentiation (Fig. 22 B).

In cultured PC12 cells-derived neurons in which T-plastin expression was suppressed, there was much greater percentage of shorter neurons (Fig. 23 A, lane 2) when compared with PC12 cells transfected with control siRNA (Fig. 23 A, lane 1). In the same time, the complexes localized at the growth cones seem to be disturbed as long as no clear growth cone structure could be observed (Fig. 23 B).

Silencing of T-plastin by siRNA in PC12 cells-derived neurons resulted in a significant reduction in the average axon length. To study the effect of suppression on neurite outgrowth, neurite lengths were measured by morphometrical analysis of maximum neurite lengths (van Bergeijk et al. 2007).

More than 200 cells in three independent experiments were measured and the reduction was significant ( $p < 0.05$ ) as shown in Fig 24. These results indicate that T-plastin is required for normal axon outgrowth.

Because T-plastin is ubiquitously expressed in epithelial cells, it is more likely that inactivation of T-plastin may play a role in modulating the actin cytoskeleton. In transformed cells, altered cell morphology is often accompanied by decreased expression of actin-binding proteins (Janmey and Chaponnier 1995; Vandekerckhove et al. 1990). It is conceivable that down-regulation of T-plastin leads to an aberrant G2/M cell-cycle control and consequently to an increase in damage sensitivity (Sasaki et al. 2002). It has been shown that the bundling activity of T-plastin is regulated by GTPase-mediated transduction pathway (Dutartre et al. 1996; Zhou et al. 1999).

#### **5.3.7.7. T-plastin overexpression in PC12 cells leads to an increase in size of the neurites**

To answer the question whether T-plastin might modulate neurite outgrowth, PC12 cells were transiently transfected with a construct that encodes for the human full-length T-plastin protein. The efficiency of the transfection was assessed by Western blot (Fig. 25). The T-plastin-V5 tagged protein was successfully expressed after 48 and 72 h, respectively, under NGF treatment. The same blots were reprobated with an anti-T-plastin antibody to check for the increased T-plastin expression as compared to mock. PC12 cells overexpressing T-plastin were double transfected as described in methods and allowed to differentiate for 48 and 72 h and afterwards were double immunostained with either antibodies directed against V5 and SMN or against V5 and with AlexaFluor 568 phalloidin. It has been observed that upon NGF treatment, PC12 cells that overexpressed T-plastin extended more and longer neurites compared to cells that do not overexpressed T-plastin (Fig. 23 lane 3). To confirm this observation, neurite outgrowth was quantified. Cells with neurites were defined as ones that possess at least one neurite of greater than two-body length and 100 cells were assayed in each group. It has been found that cells overexpressing T-plastin

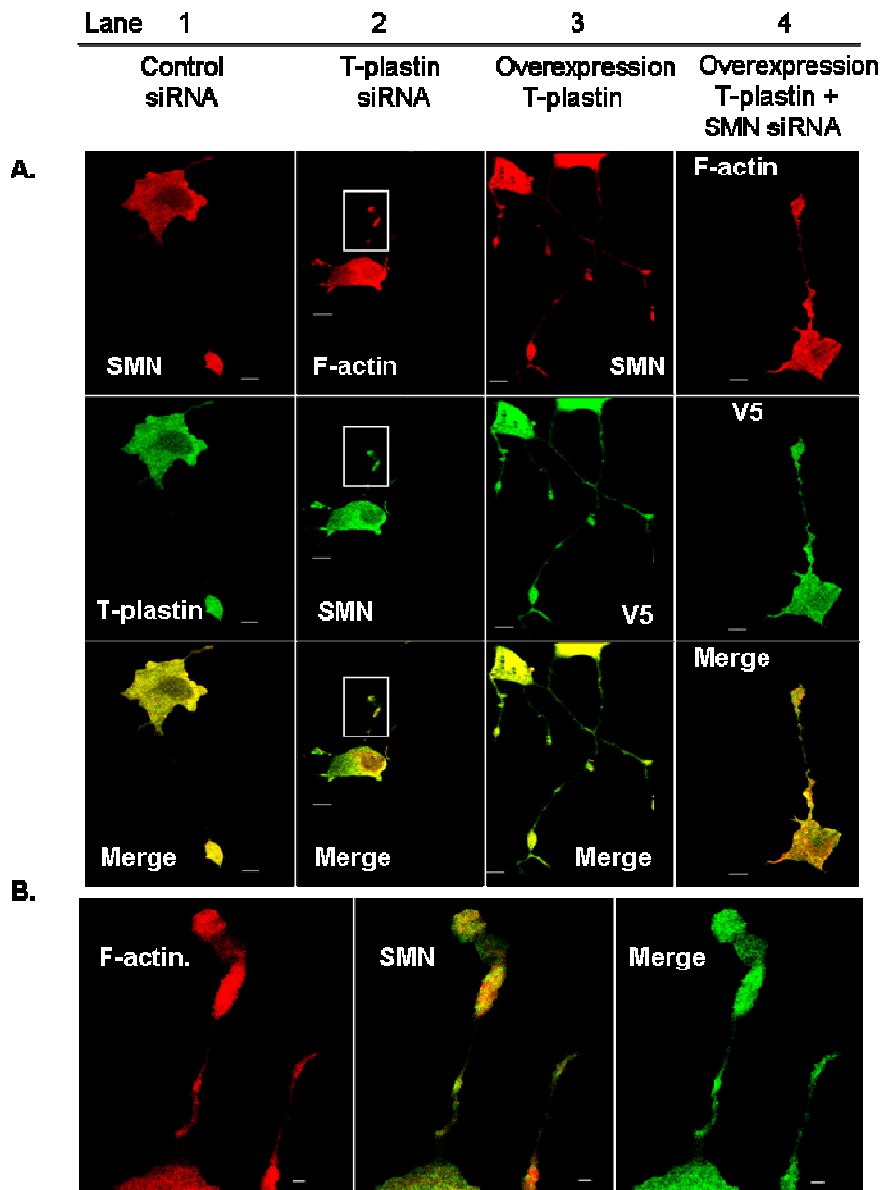


**Fig. 23 T-plastin modulates neurite outgrowth.** (A) PC12 cells were transfected either with control siRNA, T-plastin siRNA, T-plastin-V5 plasmid DNA or simultaneously with both, T-plastin-V5 plasmid DNA and T-plastin siRNA (as indicated above the figure) and allowed to differentiate for 72 h under NGF. Neuron-like processes from T-plastin-depleted PC12 cells (lane 2) exhibited a significant reduction in neurites length (relative changes of neurites length are shown in Fig. 24 B). compared with control siRNA treated cells (lane 1) In lane 3, PC12 cells overexpressing T-plastin showed longer neurites and an increase in secondary structure number. Overexpression of T-plastin in SMN-depleted PC12 cells shoed partial rescue of the neurite length (lane 4). (B) Insets from lane 2 top panel, are enlarged at higher magnification. The distribution of SMN protein at growth cone level seems to be disturbed. Bar: 20  $\mu$ m.

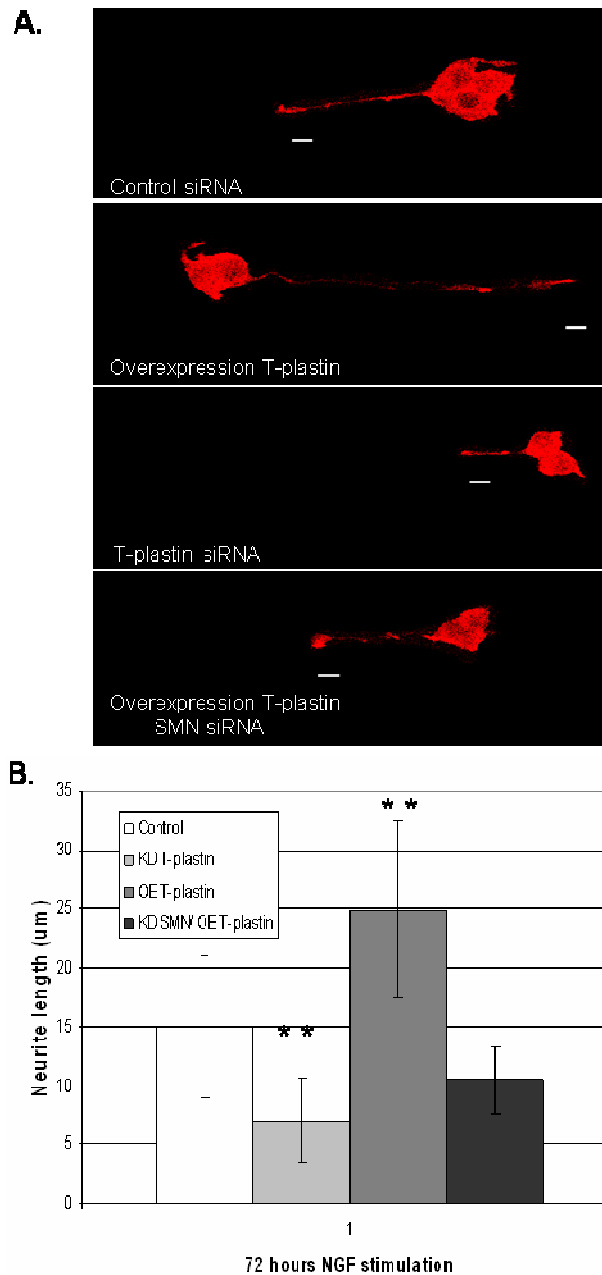


**Fig. 24** To assess neurite length, cells were plated as described in Methods and treated with 100 ng/ml NGF. (A) For quantification of the neurite length only the neurons that allowed a clear distinction between axon and dendrites were scored. After transfection and neuronal differentiation of PC12 cells, maximum lengths of neurites were determined after three days of differentiation. PC12 cells were stained with phalloidin conjugated with AlexaFluor 568. Representative images are shown. Bar: 10 µm. (B) Mean value of neurite length of each group is graphically shown as determined from total counted neuron axons (n=100 for each group)  $**p < 0.002$  when compared with control treated cells by *t*-test.

showed longer neurites with approximately 10 % (SD +/- 4.1) (Fig. 24 B). It has previously shown that in differentiating PC12 cells, overexpression of Smn as well as hnRNP-R leads to enhanced neurite outgrowth. These effects depends on the interaction of these two proteins (Rossoll et al. 2003). T-plastin protein functions in the formation of actin bundles that are required for cell locomotion and maintenance of the cellular architecture. Cultured fibroblasts that overexpressed T-plastin showed increased motility and altered cellular architecture, cells presenting more cytoplasmic pseudopods (Arpin et al. 1994). Overproduction of T-plastin in fibroblast-like CV-1 cells did not led to such striking modifications of the cortical actin cytoskeleton (Arpin et al. 1994) as was observed with villin (Friederich et al. 1989); high production level of T-plastin caused a partial loss of adherence and rounding-up of the cells. T-plastin was recruited to villin-induced F-actin spikes (Friederich et al. 1989) and the avidity of overproduced T-plastin for F-actin structures in CV-1 cells is increased in the presence of villin and depends on a specific organization of microfilaments (Arpin et al. 1994).

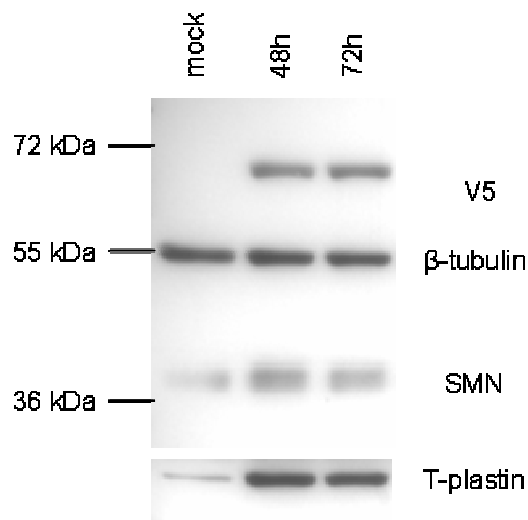


**Fig. 25 Western blot analysis of PC12 cells transfected with human T-plastin-V5 plasmid DNA. High levels of T-plastin were expressed after 48 h and 72 h as shown by staining with V5 antibodies to detect the recombinant protein. Control PC12 cells were transfected with the empty pcDNA 3.1 vector. The blots were striped and reprobbed with an antibody against T-plastin to check for the overexpressed amounts of T-plastin.**

It has been shown that IGF-1 (insulin-like growth factor-1) is a potent and specific activator and enhancer of axon outgrowth by cortical spinal motor neurons both *in vitro* and *in vivo* (Ozdinler and Macklis 2006). At the same time, 10 % of axons overexpressing T-plastin (Fig. 23 A, lane 3; Fig. 26 A) were significantly higher elongated when compared with the control siRNA treated cells. Along the neurites were observed growth-cone-like structures where T-plastin and SMN co-localize (Fig. 26 A). These results suggest that T-plastin might act in both initiation of axonal growth and in the same time in axon elongation. In epithelial

cell line LLC-PK1, the overexpressed T-plastin isoform remained associated with highly organized actin bundles of the microvilli and was able to increase the length and density of the brush border microvilli, particularly at the periphery of the cell (Arpin et al. 1994). About 30 % of transfected differentiated PC12 cells that overexpressed T-plastin showed cytoplasmic hair-like projections (Fig. 26 B). This morphological alteration obviously reflects that overexpression of T-plastin induced changes in the cytoskeletal proteins.

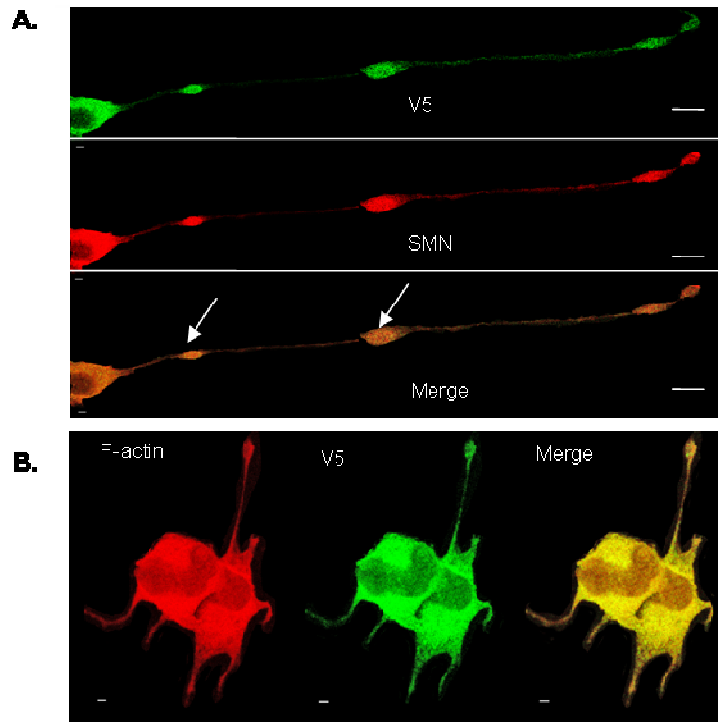


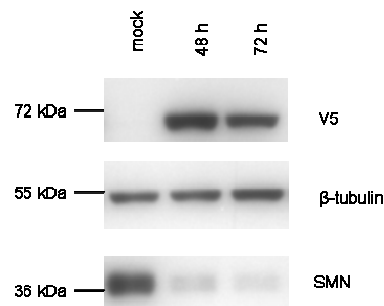
**Fig. 26** Representative images of PC12 cells transfected with T-plastin-V5 that were allowed to differentiate for 72 h with NGF. (A) After fixation, cells were double stained with SMN antibody conjugated with AlexaFluor 568 and with anti-V5 antibody conjugated with AlexaFluor 488 to detect the T-plastin localization. Along the axons T-plastin and SMN co-localize at growth cone and growth cone-like structures (indicated by arrows). (B) 30 % of PC12 cells derived neurons overexpressing T-plastin showed hair-like cytoplasmic projection. Bar: 20  $\mu$ m.

#### 5.3.7.8. T-plastin overexpression is able to rescue partially the neurite length in SMN-depleted PC12 cells

Because reduced SMN protein levels lead to reduced axonal growth (Jablonka et al. 2000), we examined whether overexpression of T-plastin in SMN-depleted PC12 cells affects neurite outgrowth in differentiating neuronal cells. For this purpose, PC12 cells were co-transfected with expression constructs for wild-type T-plastin and SMN siRNA oligos. Western blot of lysates revealed successful down-regulation of SMN as well as overexpression of the T-plastin protein (Fig. 27 A and B). Morphologically,

none obvious abnormalities were detected but the neurites were assessed for measurements (Fig. 23 lane 4, Fig. 24 A). Neurite lengths were measured after two or three days in culture with NGF. The size of the neurites was intermediate between the T-plastin-depleted cells and T-plastin overexpressing axons (Fig. 24 B). T-plastin was able at least in part to rescue the length of neurites. Taken together these experiments demonstrated that T-plastin is a potent enhancer of axon elongation. This role is highly relevant to understand the basic developmental biology of motor neurons population and to develop future treatments to promote the survival of vulnerable or diseased motor neurons involved in SMA. It is also relevant for developing strategies for regenerating injured spinal cord.

**A.**



**B.**

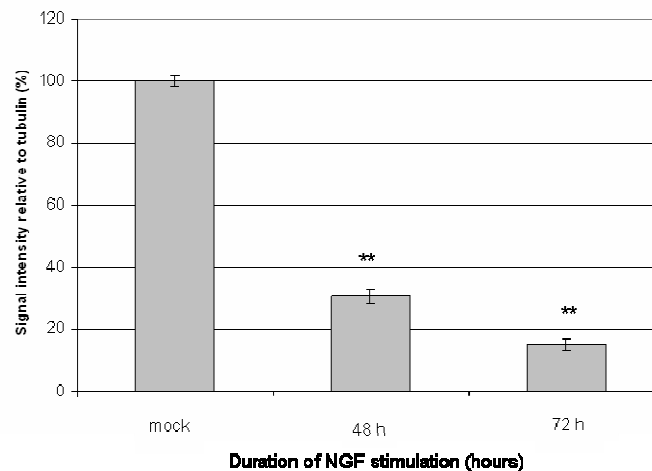


**Fig. 27 Overexpression of T-plastin and knockdown of SMN in PC12 cells. (A)** PC12 cells were co-transfected with siRNA oligos directed against rat *Smn* transcripts and with a pcDNA 3.1 plasmid that encodes for the human T-plastin using Lipofectamine 2000 reagent (*Invitrogen*). Cells were incubated overnight and a second round of transfection under the same conditions was performed. Cells were allowed to differentiate for 48 h and 72 h, respectively. Cells were harvested, and lysates were analyzed by Western blot with antibodies against  $\beta$ -tubulin, SMN and V5-tag. Endogenous SMN was successfully down-regulated whereas expression of the recombinant T-plastin was shown by staining with anti-V5 antibody. **(B)** Quantitative analysis of SMN protein in PC12 cells after knocking-down *Smn* with siRNA oligos directed against rat *Smn*. \*\*:  $p < 0.002$ .

### 5.3.7.9. Molecular analysis of the *T-plastin* coding region, promoter, 3'UTR and intron 1

The structure of L-plastin and T-plastin genes were found to be similar in that both were approximately 90 kb in length with 16 exons each (Lin et al. 1993b). The gene is located on human chromosome X and encodes for a 68 kDa polypeptide. To answer the question of whether *T-plastin* activation in asymptomatic individuals might be the cause of any mutation in the coding region, all 16 exons were screened for any nucleotide differences in 5 SMA discordant families (marked with "5" in T2 in appendix). The complete coding region from genomic fragments was sequenced using intronic flanking primers (see table 7 and Fig. F4 in appendix). Additionally, the whole 3'UTR region was sequenced and no mutation or DNA sequence variation was found. Therefore, to find the mechanism responsible for the activation of *T-plastin* gene in unaffected sibs that carry *SMN1* deletion or mutation, the regulatory elements known to regulate T-plastin expression were sequenced. It is known that *T-plastin* promoter includes 3 kb of the upstream flanking region from the start site. The basal promoter is located within 300 bp upstream of the primary transcription initiation site (Lin et al. 1999). A potential enhancer has been mapped approximately 500 bp upstream of the basal promoter (Lin et al. 1999). An unusual feature of the *T-plastin* gene sequence is the high density of CpG dinucleotides in a 1.5 kb region spanning the region from the 5' vicinity of the transcription initiation site to the beginning of the first intron (Lin et al. 1999). Thus, the *T-plastin* enhancer-promoter-first exon-first intron region was screened in all discordant individuals and again no nucleotide variation was found. Taken together, these results suggested that the intrafamilial phenotypic variability in SMA families associated with *T-plastin* expression cannot be explained by either mutation or polymorphism in the complete coding region, 3'UTR region or regulatory elements. Other molecular mechanisms must be responsible for differential *T-plastin* expression: either an epigenetic modification of the CpG island or an activation/inactivation mechanism of the *T-plastin* enhancer.

### 5.3.8. Expression analysis of the *T-plastin* gene

The only known epigenetic modification of DNA in mammals is methylation of cytosine at position C5 in CpG dinucleotide (Bird 2002). The mammalian DNA methylation machinery is composed of two components, the DNA methyltransferases (DMTs), which establish and maintain DNA methylation patterns, and the methyl-CpG-binding proteins (MBPs) which are involved in "reading" methylation marks (Hendrich and Tweedie 2003; Robertson 2002). In normal cells, DNA methylation occurs predominantly in repetitive genomic regions including satellite DNA and parasitic elements (such as long interspersed transposable elements (LINES), short interspersed transposable elements (SINES) and endogenous retroviruses) (Yoder et al. 1997). CpG islands, particularly those associated with promoters, are generally unmethylated, although an increasing number of exceptions are being identified (Bird 1986; Song et al. 2005). DNA methylation represses transcription directly, by inhibiting the binding of specific transcription factors, and indirectly, by recruiting methyl-CpG-binding proteins and their associated repressive chromatin remodelling activities (Robertson 2005). The *T-plastin* promoter-first exon-first intron region has

the characteristics of a CpG island (Lin et al. 1999). It is known that genes having the so-called CpG island can be regulated by DNA methylation at the C nucleotide of CG dinucleotides (Bird 1986; Eden and Cedar 1994). Thus, the CG-rich 1.5 kb region of the *T-plastin* gene appears to be a typical CpG island and therefore a potential target for methylation.

#### **5.3.8.1. *T-plastin* CpG island: quantitative evaluation of methylation level using pyrosequencing method**

The finding that many genes controlling normal cellular homeostasis can be silenced inappropriately by structural chromatin changes that involve DNA methylation has encouraged a search for agents that might reverse these changes and, therefore, restore principal cellular pathways. The dimethylating agent 5-azacytidine and its deoxy derivative 5'-aza-2'-deoxycytidine were first synthesized in Czechoslovakia as potential chemotherapeutic agents for cancer (Cihak 1974). The analysis of DNA methylation was revolutionized by the introduction of sodium bisulfite conversion of genomic DNA. The differential rates at which cytosine and 5-methyl cytosine are deaminated by sodium bisulfite to yield uracil and thymine, respectively showed that the usefulness of this chemical reaction in conjunction with PCR amplification and sequencing (Frommer et al. 1992).

To investigate the inactivation mechanism of *T-plastin* gene in affected *SMN1*-deleted sibs and the most of the control and SMA population, 16 samples were selected for methylation analysis by pyrosequencing. All 16 samples were males showing an SMA phenotype and were checked by RT-PCR for *T-plastin* expression (the samples are marked with "4" in table T1 in appendix and the complete raw data are shown in table T9 that is contained in the attached CD-ROM). Eight patients showed *T-plastin* expression were grouped as "T-plastin-positive population"; another eight samples were selected from the non-expressing *T-plastin* SMA patients and grouped as "T-plastin-negative population". Only male samples were included in the pyrosequencing experiment in order to avoid any "methylation noise" due to the inactivated X chromosome in female samples. This analysis was performed under the assumption that if *T-plastin* expression is regulated by DNA methylation, a higher methylation level should be expected in "T-plastin-negative" group. The methylation mean for each sample was calculated as the mean of the methylation of the complete analyzed CpG region. No difference in methylation level could be observed between the two groups (Fig. 28 A). Therefore, the positive group had similar methylation level as the negative control group. As shown already by Lin et al. in 1999, no correlation between the two groups could be detected, suggesting that methylation does not play an important role in T-plastin expression.

To investigate the possibility of the CpG island as potential target for methylation, Lin and colleagues selected three T-plastin expressing cell lines (HT-1080, HuT-12 fibrosarcoma cells and MCF-7 breast carcinoma cells) and five T-plastin-negative lines and cells (CEM, K562, Jurkat, Molt-4 leukemia cells and PBL) for comparison (Lin et al. 1999). The *T-plastin* CpG island was unmethylated in cultured cells that do not express T-plastin but was variably methylated at different locations in cultured cells that do not express T-plastin. However, because the *T-plastin* CpG island was found unmethylated in T-plastin-

negative PBL, it does not appear that DNA methylation plays a role in the inactivation of *T-plastin* gene in normal lymphocytes (Lin et al. 1999).

The possible difference in methylation profile was also checked in five SMA discordant families (marked with “4” in table T2 in appendix) using the DNA isolated from EBV-transformed lymphoblastoid cells from unaffected and affected sibs, respectively. Surprisingly, the levels of methylation for female samples were very low in the analyzed region, suggesting the possibility that *T-plastin* CpG island might be hypomethylated even on the inactivated X-chromosome (Fig. 28 B). The complete raw data of methylation analysis for both SMA discordant families and control groups are contained in the attached CD-ROM.

The methylation level was calculated and for each CpG site and again no significant difference was observed between unaffected vs. affected SMA discordant sibs (Fig. F9 in appendix), or between “T-plastin-positive population” vs. “T-plastin-negative population” (Fig. F10 in appendix).

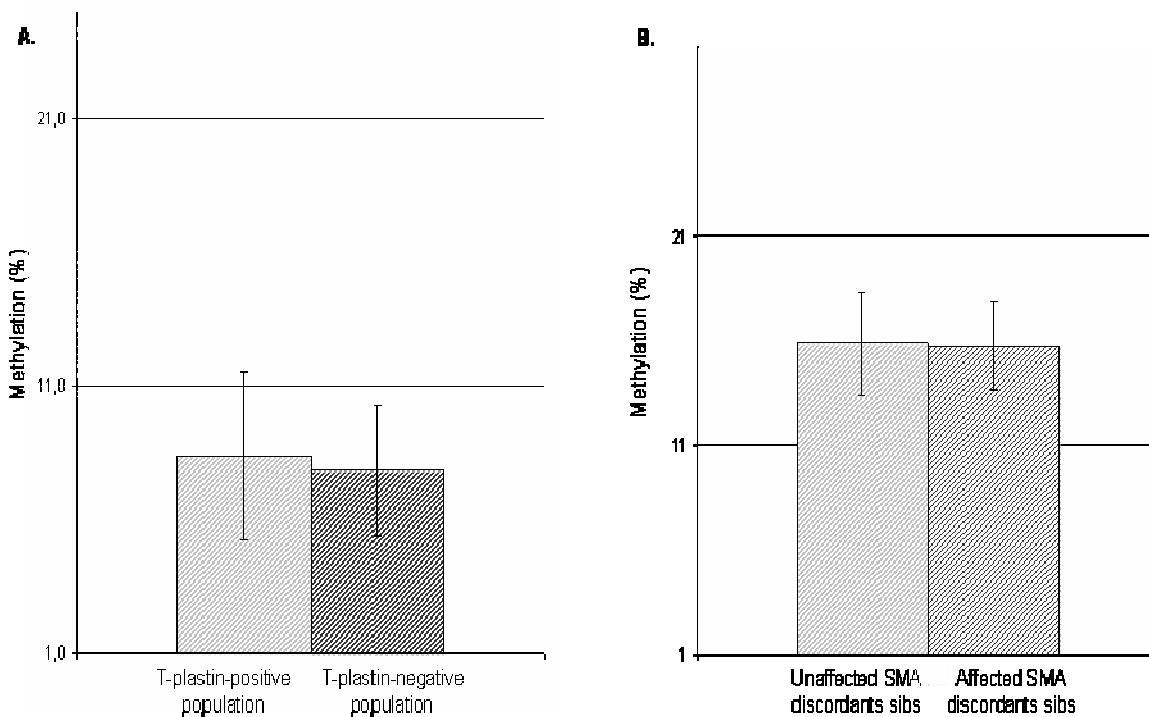


**Fig. 28 Methylation analysis of *T-plastin* CpG islands using Pyro Q-CpG Software. (A) DNA samples were isolated from EBV-transformed cell lines belonging to 8 males (“T-plastin-positive population” group) who showed T-plastin expression and 8 males that failed to show any T-plastin expression (“T-plastin-negative population” group) by RT-PCR. Both control groups showed similar ranges of methylation (~8 %). (B) CpG methylation pattern within the *T-plastin* CpG island region in five SMA discordant families. No significant difference was observed between the unaffected (n=7) vs. affected SMA discordant sibs (n=6), both groups presenting methylation levels close to 16 %. The methylation percentage was calculated as the methylation mean of all 99 CpG sites analyzed in each group. The error bars indicate SD.**

The results showed that the CpG island located in the promoter-first exon-first intron region is not methylated in both unaffected and affected *SMN1*-deleted sibs. In conclusion, the DNA methylation of the CG-rich region located within the *T-plastin* genomic area is not responsible for the activation of this gene in unaffected sibs *SMN1*-deleted in SMA discordant families. Another mechanism should be the cause for the differential expression of *T-plastin* in phenotypically discordant sibs.

#### **5.3.8.2. *In vivo* footprinting of *T-plastin* enhancer in EBV-transformed lymphoblastoid cells of SMA discordant families**

Within the eukaryotic nucleus, each gene is embedded within a chromosomal environment of other DNA sequences that have the potential to affect its expression. In some cases, regulatory elements-enhancers or silencers-associated with nearby genes could be close enough to disrupt normal expression patterns. In other cases, a transcriptionally active gene is surrounded by regions of condensed chromatin that could overflow their borders and silence the gene (Bell et al. 2001). Promoters consist of several composite elements and/or individual binding sites for transcription factors. Enhancers also consist of composite elements and/or single binding sites. They modulate the level of transcription depending on the type of tissue, developmental stage, stage of the cell cycle, induction by hormones or other molecular signals (Buratowski 1994). An enhancer can act over many kb 3' or 5' from the transcription start site, possibly from within an intron, and its activity does not depend on its orientation. Within 250 bp upstream from the first exon of *T-plastin* gene, an Sp1 motif, a CCAAT box and four AP2 motifs were identified (Lin et al. 1999). However, no sequence similar to the canonical TATA box on the transcription initiator (Smale and Baltimore 1989) was found in this region. A more stringent analysis resulted in the identification of a few AP1 motifs, a TEF1 motif and a CREB motif in the first exon (Lin et al. 1999). An enhancer was mapped to within a 20 bp fragment, approximately 500 bp upstream of the basal promoter (Lin et al. 1999). A summarized overview of *T-plastin* genomic region is represented in Fig. F4 in appendix. The *T-plastin* promoter has a weak basal activity and expression may be controlled by upstream enhancer elements and by methylation of the CpG island (Lin et al. 1999). Therefore, to answer to the important question by which mechanism *T-plastin* is activated in unaffected *SMN1*-deleted sibs, the investigation whether *T-plastin* enhancer binding site is occupied in EBV-transformed lymphoblastoid cell lines was verified by an *in vivo* footprinting approach using dimethylsulphate (DMS) treatment and ligation-mediated PCR (LM-PCR).

EBV-transformed cell lines derived from 5 SMA discordant families (marked with "4" in table T2 in appendix), two positive controls and two negative controls for *T-plastin* expression (marked with "2" in table T2 in appendix) were treated *in vivo* with DMS, which resulted in partial methylation of guanines at the N7 position. DNA was then extracted from the cells and cleaved at the methylated bases by treatment with piperidine. A representative autoradiogram from the *in vivo* footprint analysis of EBV-transformed lymphoblastoid cell lines by LM-PCR is shown in Fig. 29, on the minus strand. The portion of the gel corresponds to nucleotides -744 to -849 (84 nt) within *T-plastin* genomic region. As shown, comparison

between positive (+) vs. negative control (-), as well as unaffected (U) vs. affected (III) sibs showed partial protection of the region where the *T-plastin* enhancer has been described. The protection of the guanines in the enhancer site was not absolute, which may result from the sites in some clones not being occupied. Similar results were obtained in three independent experiments.

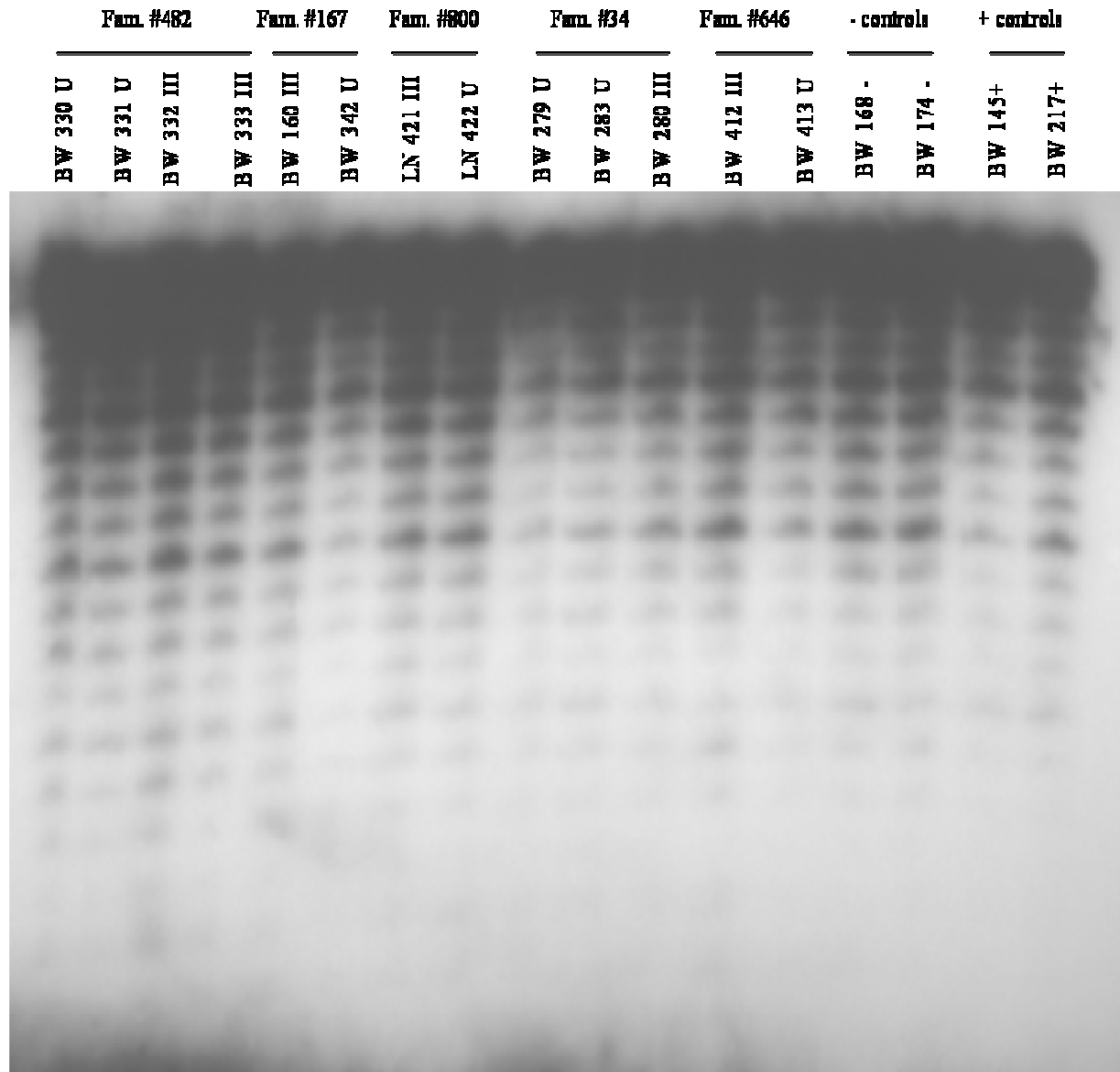


Fig. 29 *In vivo* DNA footprint of the human *T-plastin* enhancer in EBV-transformed cell lines derived from five SMA discordant families, two positive and two negative controls for T-plastin expression. U: unaffected; III: type III SMA; -: controls that do not express T-plastin; +: controls that do express T-plastin.

### 5.3.8.3. Haplotype analysis of the *T-plastin* genomic region revealed a *trans*-acting mechanism to regulate its expression

Searching for the mechanism that is responsible for the activation of *T-plastin* gene in asymptomatic *SMN1*-deleted sibs by sequencing, epigenetic analysis and DNA footprinting failed to show any difference at DNA level within the *T-plastin* genomic region. In hope to find the answer whether *T-plastin* expression is regulated at transcription level by an so far unidentified *cis*-element, a haplotype association study was carried out in 12 SMA discordant families (see table T2 in appendix; the SMA discordant families are marked with “3”), 2 control families (see table T10 in appendix), 4 SMA classical families (see table T10 in appendix) where *T-plastin* was observed to be expressed by the SMA patients (that are marked with “1” in table T1 in appendix) and 7 male SMA patients that do express *T-plastin* (see table T1 in appendix; the SMA patients are marked with “1”). Searches for correlations between human genetic variations and disease phenotypes have often been fruitful for strongly hereditary diseases, but have had limited success at finding genetic risk factors for complex diseases (Castellana et al. 2006). This failure is likely due at least in part to the challenges of distinguishing many relatively weak correlations from the noise produced by chance associations with the millions of known sites of common variation. Haplotypes are a combination of alleles at different markers along the same chromosome that are inherited as a unit (Castellana et al. 2006). Many methods are based on the haplotype block model (Daly et al. 2001), which proposed that the genome consists of discrete regions of strongly correlated variations separated by recombination hotspots, across which correlations have been eliminated by frequent historical recombination. Or they may use haplotypes to identify “haplotype tagging SNPs” (htSNPs), a subset of SNPs that contain most of the information contained in the full SNP set (Johnson et al. 2001), which can reduce the cost of genotyping and the difficulty of finding meaningful associations in the resulting data. Information about recombination is important for locating disease-causing mutation by linkage methods and has a profound effect on the extent of statistical association between the presence of two SNPs in the genome, known as linkage disequilibrium- a key property for disease association studies across the human genome (Crawford and Nickerson 2005).

The specific role of the haplotypes in a candidate gene association study depends on the hypothesis being tested. For example, haplotypes can represent a combined effect of several sites along the same chromosome (*cis*-acting loci) that cannot be detected when sites are tested one by one (Crawford and Nickerson 2005). Therefore, a haplotype-based association study was carried out in hope to answer the question why not all *T-plastin*-expressing individuals are protected to develop SMA, and whether the *T-plastin* expression is induced by a *cis*-or a *trans*-acting factor/element. For the female SMA patients, the parents were necessary in order to reconstruct the *T-plastin* haplotype blocks. For the male SMA patients, the parents were not necessary, given the fact that the *T-plastin* gene is localized on chromosome X. All individuals were directly genotyped by pyrosequencing. The pedigree or family based method relies on the fact that different loci on the same chromosome (haplotype) will be inherited as a unit unless they are separate by recombination event (Crawford and Nickerson 2005).

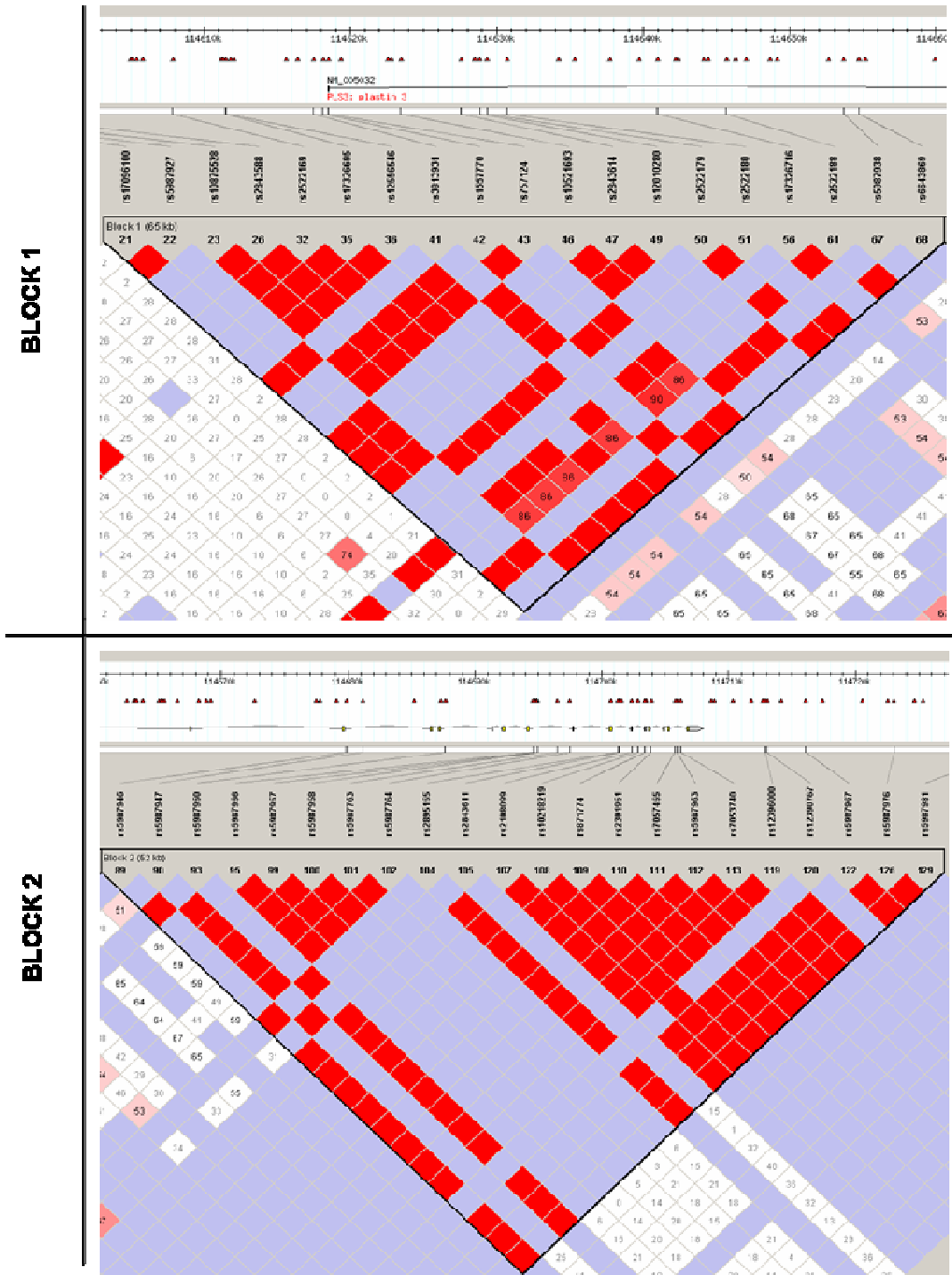
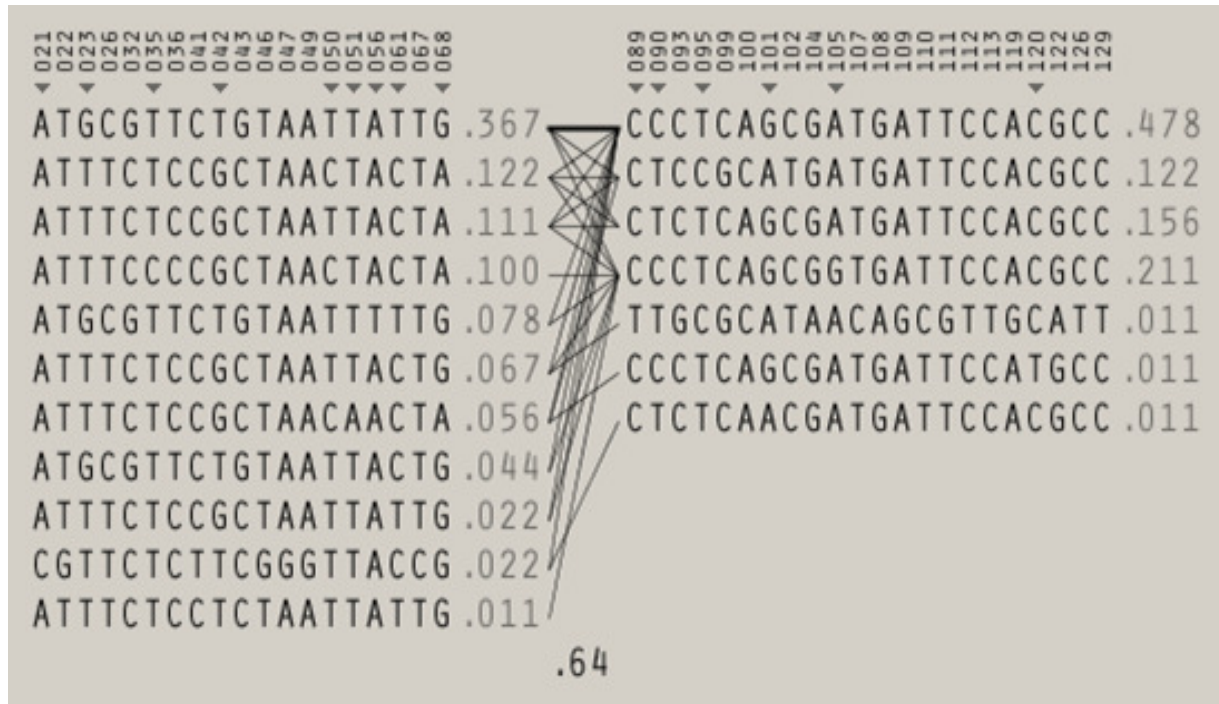


Fig. 30 Linkage disequilibrium (LD) of the SNP markers in the *T-plastin* genomic region (block one in the upper part and block two in the lower part) in the HapMap. Standard colour scheme is used to display linkage disequilibrium with red colour for very strong LD, pink red and blue for intermediate LD, and white for no LD.



**Fig. 31 Haplotype frequencies of the HapMap selected SNPs in the *T-plastin* gene. The hnSNPs are marked with up-side-down triangles. Numbers next to each haplotype block represent haplotype frequencies. In the crossing area, a value of 0.64 is shown to represent the level of recombination between the two blocks.**

The approved Human Genome Organization (HUGO) name for *T-plastin* is plastin 3 (T isoform) and its coordinates are chrX: 113,559,700-113,649,270. Within 117 kb region two blocks were selected from the HapMap data (<http://www.hapmap.org>) (Fig. 30 and Fig. 31):

1. Block 1 (65 kb) includes 9 SNPs (rs 1709610, rs 1087528, rs 1736695, rs 1557770, rs 2522179, rs 2522180, rs 17326716, rs 2522188, rs 6643869);
2. Block 2 (52 kb) includes 6 SNPs (rs 5987946, rs 5987947, rs 5987956, rs 5987763, rs 2843611, rs 12396000).

The gene encoding *T-plastin* gene spans about 90 kb and contains 16 exons, 15 introns, one 5'-UTR and one 3'-UTR region. In its 5' flanking region, consensus recognition sequences for a number of transcription factors were identified (Lin et al. 1999). No association between *T-plastin* expression and SMA protection, as well as no mutation were found in *T-plastin* genomic region. Therefore, it is important to determine whether there are LD blocks existing in the *T-plastin* gene of the SMA discordant sibs that can be used to identify a set of SNP markers that might explain why not all *T-plastin* expressing individuals *SMN1*-deleted are rescued to develop SMA. The 15 SNP markers selected for the genotyping are listed in table 26. Three were located in the 5'-upstream region, and only one in the coding region.

Most of them were located in non-coding region and just one in the 3'-downstream area. The first block spans the 5'-upstream region and the whole promoter-first exon-first intron region and is followed by the second block crossing a 52 kb region. This spans the *T-plastin* genomic region from exon 2 to 3'-downstream region (Fig. 30). The *T-plastin* htSNPs are represented for the European population in Fig. 31. Only one haplotype with a frequency of 0.367 in block 1 suggests that this is the most frequent haplotype in European population representing about 40 % of the total haplotypes identified at this locus (Fig. 31, left). For block 2, two haplotypes were found with a frequency of 0.478 and 0.221, respectively. Together, these two most frequent haplotypes represent 68 % of the total haplotypes found in this particular region (Fig. 31, right). The recombination frequency between the two blocks is 64 % (Fig. 31, crossing area).

**Table 26 Chromosomal positions and gene location of the *T-plastin* SNPs**

#	SNP ID	Chromosome position	Location in <i>T-plastin</i> gene	Variation allele *
1	rs17096100	114672875	5'-upstream	A/C
2	rs10875528	114674791	5'-upstream	G/T
3	rs17326695	114694801	5'-upstream	C/T
4	rs1557770	114701431	Exon 1	G/T
5	rs2522179	114712647	Intron 1	C/T
6	rs2522180	114714000	Intron 1	A/T
7	rs17326716	114724272	Intron 1	A/T
8	rs2522188	114728933	Intron 1	C/T
9	rs6643869	114738023	Intron 1	A/G
10	rs5987946	114763159	Intron 3	C/T
11	rs5987947	114764437	Intron 3	C/T
12	rs5987956	114777911	Intron 8	C/T
13	rs5987763	114779799	Intron 8	A/G
14	rs2843611	114784651	Intron 10	A/G
15	rs12390767	114796311	3'-downstream	C/T

\*: Variation allele sequences are based on the plus strand sequence

All the individuals taken in the study were genotyped by pyrosequencing and the raw data are represented in table T11 in appendix. No correlation between a certain haplotype and *T-plastin* expression was observed and the calculation of the significance of the association is in progress. An overview on the haplotypes blocks reconstruction is given in table T12 in appendix.

Taken together, the *T-plastin* haplotype blocks analysis strongly suggests that the *T-plastin* expression is regulated by a *trans*-acting factor and further investigations are required to identify putative factors able to regulate *T-plastin* transcription.

## 5.4. Search for modifying genes by genome-wide scan analysis

Genom-wide association studies have recently received a great deal of attention as a tool for detecting the genetic variation responsible for human common diseases. SNP markers are preferred over microsatellite markers for association studies, because of their high abundance along the human genome (SNPs with minor allele frequency  $>0.1$  occur once every  $\sim 600$  kb) (Wang et al. 1998), their low mutation rate, and the accessibility of high-throughput genotyping. Recent studies (Daly et al. 2001; Dawson et al. 2002; Gabriel et al. 2002; Johnson et al. 2001; Patil et al. 2001) have shown that the human genome can be partitioned into blocks with limited haplotype diversity, such that only a small fraction of SNPs captures most haplotypes. Haplotype blocks, together with the corresponding tag SNPs and common haplotypes determined by haplotype block-partitioning algorithms, can be used in the genome-wide association studies, as well as in the fine-scale mapping of complex disease genes.

To identify susceptibility loci for SMA modifying factors and potential activator factors able to modulate *T-plastin* expression, a genome-wide analysis was conducted in a set of 42 SMA discordant families of different origin (see table T2 in appendix) composed of 172 individuals. In 38 families, at least two siblings with different phenotypes (affected vs. asymptomatic or different types of SMA) plus parents were available. This valuable and unique collection of families allowed us to carry out a whole genome scan in order to search for the modifying gene(s). Nowadays, one of the most common methods to study associations between genetic variation in “candidate” modifier genes and clinical phenotype is the identification of single nucleotide polymorphisms (SNPs). In contrast to gene mutations occurring in less than 1 % of the individuals in a population, SNPs are present in more than 1 % of the individuals and comprise common genetic variation in normal individuals (Davies et al. 2005). Evidence of linkage between a SNP and disease phenotype indicates that the SNP is located in a modifier gene or that the SNP is in linkage with a modifier gene.

The readily available GeneChip Mapping 10K SNP array was recently shown to allow detection of homozygous deletions, amplifications, and copy number reductions of regions  $>10$  Mb in polyploid cells from tumor cell lines, using genotypes in combination with copy number information from hybridization intensities (Bignell et al. 2004). The power of any modifier gene study is determined by population size, the degree of clinical effect on the gene in question and the allele frequency (Davies et al. 2005).

### 5.4.1. Power simulation of the genome scan analysis

Initially a linkage study was simulated including 38 discordant SMA families. Under the assumption of a recessive mode of inheritance of a single modifying locus in all families a maximum LOD score of 10.03, and under the assumption of a dominant mode of inheritance a maximum LOD score of 7 could be achieved (see F8 and F9 in appendix). Under the assumption that only 75 % of the families are linked to the modifying locus a LOD score of 5.2 could be achieved for a recessive mode of inheritance and a LOD score of 3.8 could be reached for a dominant mode of inheritance. In 28/38 families (74 %) the females

are less affected or even asymptomatic as compared to their more severely affected brothers or sisters. By assuming that a gender specific modifier might act,  $\frac{3}{4}$  of the families might likely be linked to only one locus. The LOD score would fall under the statistical significance of  $z=3$  if only half of the families were linked to a certain modifier gene. A maximum LOD score of 2.5 could be achieved for a recessive and 1.8 for a dominant mode of inheritance.

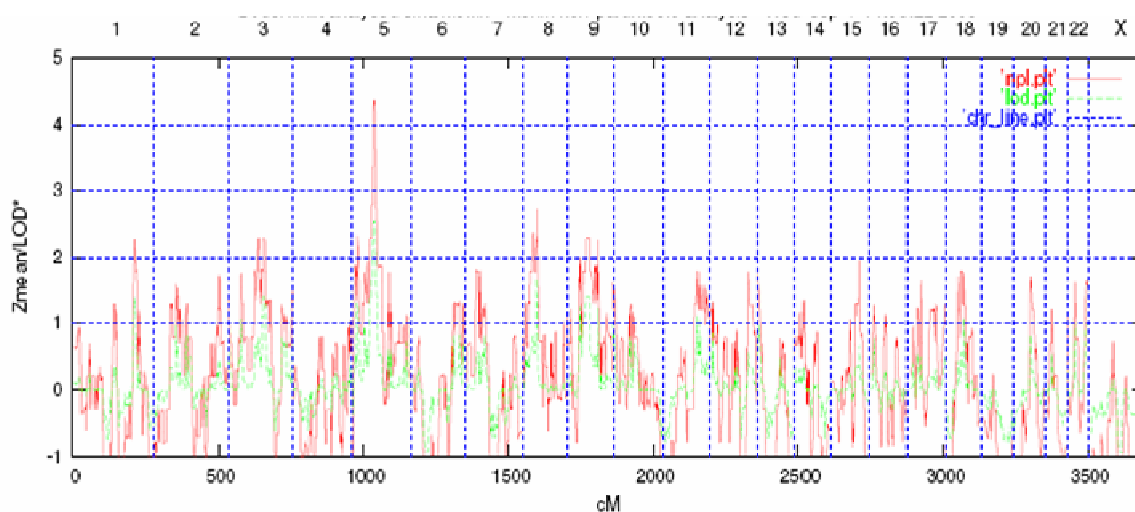


**Fig. 32 Summary of the genome-scan for SMA modifying susceptibility loci in 42 SMA discordant families. The figure shows non-parametric analysis using MERLIN software.**

#### 5.4.2. Non-parametric linkage data interpretation

The genome scan was performed by comparison of unaffected/milder affected sibs with the affected/more severe affected sibs, individually assuming each of the different modes of transmission described (recessive and dominant). Each SNP was scored as AA, BB (homozygous) or AB (heterozygous) depending on the genotype or as “no call” in the event of equivocal results. “No call” results were excluded and informative loci selected.

Non-parametric multipoint linkage analysis was performed using allele frequency with MERLIN software (Abecasis et al. 2002). The results are summarized in Fig. 32. The most significant allele sharing among affected relatives in families was detected on chromosome 5 with a LOD score above 4. The peak is located in the *SMN* gene region as a proof that all affected individuals share the same genotype (*SMN1* deletion). No other susceptibility loci reached the significant evidence for linkage. In addition, suggestive evidence of linkage was detected on chromosomes 1, 3, 8 and 9 with a LOD score above 2.

### 5.4.3. Parametric linkage data interpretation

Because the non-parametric analysis includes information only from affected individuals, its power to detect linkage is expected to be lower than the power of parametric approaches that use information from all available relatives (Lee et al. 2000). Therefore we carried out the parametric linkage analysis under the assumption of heterogeneity. Under the assumption that the modifying gene is present in the unaffected or less affected sibs and is inherited in a recessive mod three regions (on chromosome 3, 7 and 16, respectively) were found as susceptibility regions. None of the regions detected by this assumption reached a significant LOD score of 3 (Fig. 33 A).

Under the assumption that the modifier gene is inherited in a dominant mod, three loci were detected: the highest on chromosome 7, followed by a lower peak located on chromosomes 22 (Fig. 33 B). Again no significant LOD score of 3 was reached by any of the loci. By various programs Allegro, GENEHUNTER and MODscore and by varying some of the parameters the same region from chromosome 22 was obtained. A summary of parametric linkage analysis for regions detected on chromosomes 3, 7, 16 and 22 is shown in table 27. Interestingly, the same region on chromosome 7 was detected as suggestive region in both assumptions with a LOD score around 1.5. The displayed suggestive regions are summarized in table T6 that is contained in the attached CD-ROM.

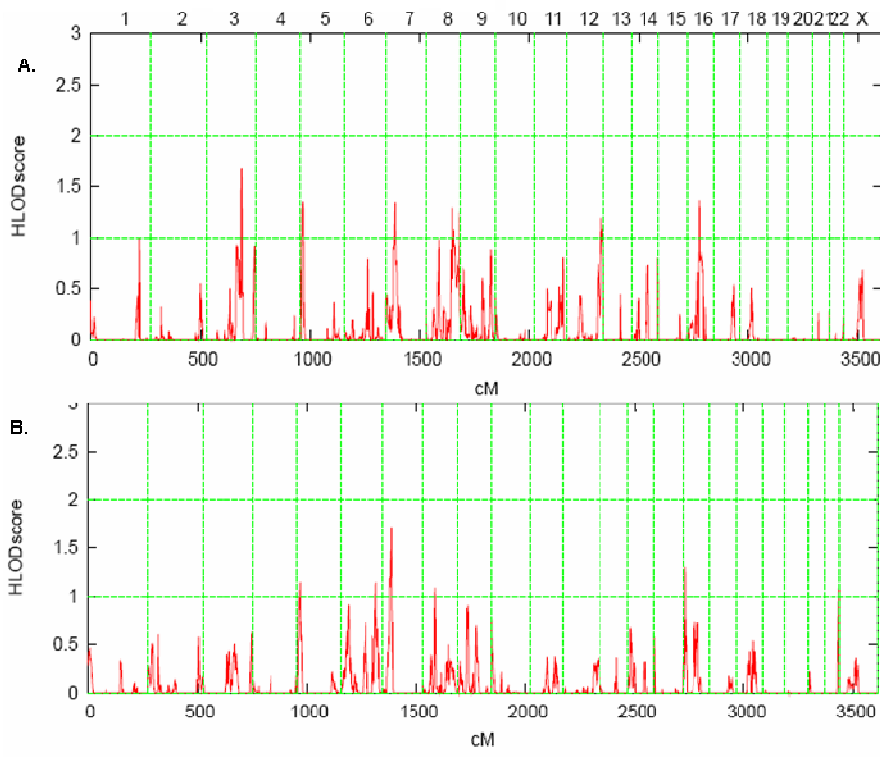


**Fig. 33 Parametric analysis under the assumption of recessive (A) or dominant (B) mod of inheritance using ALLEGRO software. The highest pick under recessive mode of inheritance was located on chromosome 3 and reached a LOD score of 1.67 (A). The highest pick under dominant mod of inheritance reached a LOD score of 1.69 on chromosome 7 (B).**

**Table 27** Susceptibility regions on chromosomes 3, 7, 16 and 22 detected by parametric linkage analysis.

Mode of inheritance	LOD score	Chromosome	% of the families that contributed to the LOD score	Region (in Mb)	Limiting SNPs (from-to)
Recessive	1.67	3q	0.7	12	rs951300-rs1874952
	1.38	16p	0.54	8	rs2077685-rs1366076
Dominant	1.69	7p	0.50	3.8	rs1316623-rs31032848
	1.09	22q	0.48	2.3	rs4437069-rs2340603

#### 5.4.4. Gene organization into categories according to their molecular function

The purpose for the genome-scan analysis was to detect loci that influence clinical features of SMA disease. A linkage to the regions that contain putative modifier genes of the SMA disorder was expected to give us one or more modifier genes.

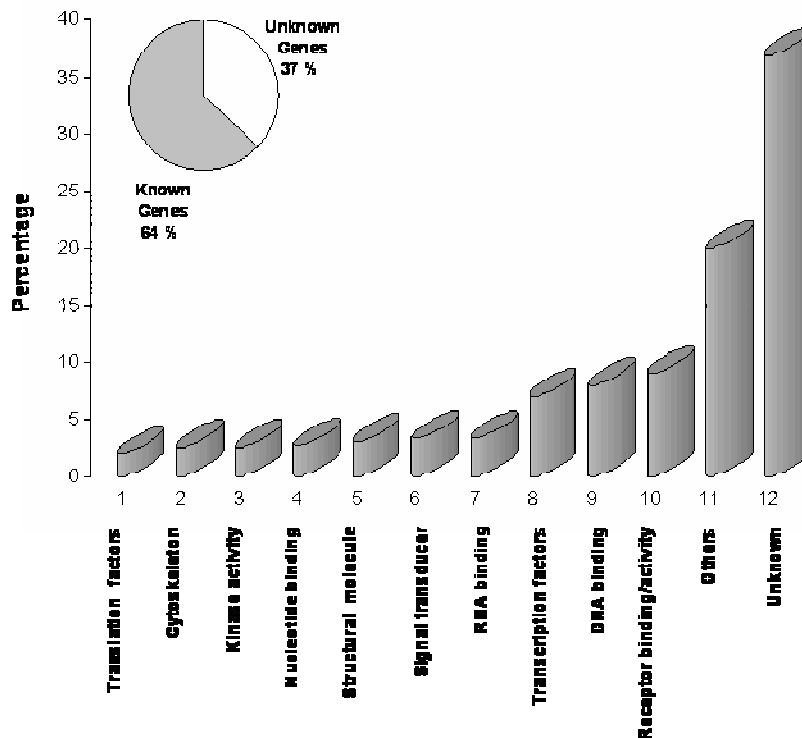


**Fig. 34** Percentage of genes grouped according to their annotation as defined by Gene Ontology (Ashburner et al. 2000). The percent of known genes is shown for each group. The insert (*pie chart*) shows that 37 % of the identified genes by genome scan analysis do not have a known molecular function.

---

The design included a distinction between unaffected/less affected phenotype and affected/more affected phenotype. As shown in table T2 in appendix, 11 families comprise discordant unaffected vs. affected sibs and 31 families comprise discordant less affected vs. more affected sibs. The genes were grouped according to their annotations as defined by Gene Ontology. Gene Ontology (Ashburner et al. 2000) represents a controlled vocabulary to describe genes and gene products attributes in an organism (<http://www.geneontology.org>). The three organizing principles of Gene Ontology are molecular function, biological process and cellular component. The genes found in all four suggestive loci were grouped according to their corresponding molecular function (Fig. 34).

Most of the genes were found to be involved in transcription regulation (7 %), DNA binding (8 %), and either to bind or to function as receptors (9 %). Twenty percent of the genes were grouped as “Others” when small group sizes or single cases were annotated. A high percentage of genes had unknown function or the product was hypothetical (37 %). These results suggest that the proteins involved in these pathways pathways that act in signalling and/or DNA regulation/transcription might be critical in SMA development and progression.

Signal transduction at the cellular level refers to the movement of signals from outside the cell to inside. The movement of signals can be simple, like that associated with receptor molecules of the acetylcholine class: receptors that constitute channels which, upon ligand interaction, allow signals to be passed in the form of small ion movement, either into or out of the cell. These ion movements result in changes in the electrical potential of the cells that, in turn, propagates the signal along the cell. More complex signal transduction involves the coupling of ligand-receptor interactions to many intracellular events. These events include phosphorylations by tyrosine kinases and/or serine/threonine kinases. Protein phosphorylations change enzyme activities and protein conformations. The eventual outcome is an alteration in cellular activity and changes in the program of genes expressed within the responding cells.

## 6. DISCUSSION

Spinal muscular atrophy (SMA) is an autosomal recessive neuromuscular disorder that results in the loss of motor neurons in the spinal cord. The genomic region containing the defective gene is located in 5q13 and is particularly unstable and prone to large-scale deletions. The presence of phenotypic discordance in SMA families provides the unique chance to identify the highly complex regulation of SMN protein and to identify additional factors able to influence the SMA phenotype, except for *SMN2* gene.

Using a combination of candidate gene approach, microarray and genome-wide scan analyses, the present study revealed for the first time the evidence that at both molecular and transcriptional levels, SMA discordant sibs present a number of genes differentially expressed/regulated that are likely to act as SMA modifier genes. Together, these three approaches were chosen in order to maximize the chance to find potential modifiers of the spinal muscular atrophy phenotype.

### 6.1. *ZNF265*, *hnRNP-R* and *HDAC6* are not responsible for the phenotypic variability of the SMA discordant sibs

The candidate gene approach was performed in hope that any SMN-interacting protein might modulate SMN transcription/translation and functions as potential modifier of the SMA discordant phenotypes. It was therefore obvious to ask whether proteins that either, interact, associate or are involved in the same pathway with SMN influence the variability of the SMA phenotype of the discordant sibs. *ZNF265*, *hnRNP-R* and *HDAC6* were checked either for mutations or expression differences in SMA discordant sibs.

*ZNF265* co-localizes with SMN in the nucleus, with the SR protein SC35, snRNP protein antigen Sm (Adams et al. 2001), YY1 and p300 (Adams et al. 2001), both of which have been shown to co-localize within active transcriptional compartments and, in the case of p300, with RNA polymerase II (Bannister and Kouzarides 1996; Ogryzko et al. 1996; von Mikecz et al. 2000; Yang et al. 1996). These co-localizations are consistent with a role of *ZNF265* in transcription and/or splicing. *In vitro* splicing reactions showed that *ZNF265* is immunoprecipitated in a complex that includes spliced mRNA (Adams et al. 2001). This result indicated that *ZNF265* binds directly or indirectly to mRNA, but much less to pre-mRNA. Overexpression of *ZNF265* resulted in exclusion of exons 2 and 3 from the Tra2- $\beta$ 1 pre-mRNA, which led to an increase in the production of the  $\beta$ 3 alternatively spliced isoform (Adams et al. 2001). Taken together, it was obvious to ask whether *ZNF265* might influence the variability of the SMA phenotype, since localizes with SMN and influences the alternative splicing of hTra2- $\beta$ 1, the splicing factor responsible for the up-regulation of full-length transcripts encoded by *SMN2* gene.

The analysis of *ZNF265* gene in 30 sibs belonging to 12 SMA discordant families by sequencing the complete coding region revealed neither a mutation nor a polymorphism within the coding region or exon-intron boundaries. It has been concluded therefore that the intrafamilial phenotypic variability in SMA discordant families is not caused by mutations/polymorphisms within *ZNF265* gene.

hnRNP-R is mainly expressed in motor axons and at much lower degree in sensory axons. Highest

expression levels of hnRNP-R during development of the spinal cord can be found during late embryogenesis around E19 (Rossoll et al. 2002). The reduction of hnRNP-R level after birth apparently is due to post-transcriptional and/or post-translational mechanisms as previously observed for Gemin 2 (Jablonka et al. 2001; Wang and Dreyfuss 2001a). hnRNP-R co-localizes with SMN in the cytoplasm of the motor neurons including the axons. Thus it is unlikely that hnRNP-R participates in specific functions of SMN complexes such as pre-mRNA splicing and regeneration of the spliceosomal complexes (Pellizzoni et al. 1999). hnRNP-R specifically binds mRNAs, being involved in mRNA processing including editing, in mRNA transport and finally acts as a regulator, which modify binding to ribosomes and RNA translation (Blanc et al. 2001; Grosset et al. 2000; Mizutani et al. 2000). Such functions appear highly important for neurons with long processes, in particular motor neurons in which specific mRNAs have to be transported over long distances. Because hnRNP-R and SMN are closely interacting proteins, part of the same cellular protein complex, the same pathway and exhibit the same cellular location in motor neurons, hnRNP-R was a good candidate as potential modifier in SMA discordant families.

In order to test whether hnRNP-R might act as modifying factor in SMA, five SMA discordant families were tested for SNPs association with SMA/unaffected phenotype. No nucleotide variance was found within the *hnRNP-R* gene coding region but two SNPs located in the intronic region were selected for association studies in all five SMA discordant families: rs2842604 (A/C) and rs911927 (C/G). The nucleotide variants were checked by sequencing and no association between a certain allele and SMA phenotype was found. Additionally, *hnRNP-R* gene was checked at transcription level to verify whether any difference between discordant sibs at RNA level could be observed and again no difference at *hnRNP-R* transcript levels and was observed. Therefore, and *hnRNP-R*, as *ZNF265*, was excluded to act as potential modifier in SMA discordant families.

*HDAC6* is expressed in several tissues including the testis, liver and brain (Grozinger et al. 1999; Verdel and Khochbin 1999). It was later shown, however, that HDAC6 enhances cell motility through the deacetylation of  $\alpha$ -tubulin, indicating that *HDAC6* is related to cell migration rather than transcriptional regulation (Haggarty et al. 2003; Hubbert et al. 2002; Palazzo et al. 2003). In addition, a recent report showed that *HDAC6* is also related to the transported of misfolded protein in the proteasome system (Kawaguchi et al. 2003). Because SMN protein was found to be involved in gene repression (Zou et al. 2004) via interaction with HDAC proteins, *HDAC6* gene (besides, located on chromosome X) was chosen as candidate gene as potential modifier in SMA model.

Therefore, two SNPs located in the coding region of *HDAC6* gene were found interesting since both of them cause an amino acid exchange at protein level. One SNP, rs146379 causes a leucine to proline exchange at position 700; the other one, rs1127346 causes a threonine to isoleucine substitution at position 994. Both SNPs were not informative since all individuals (both unaffected and affected) were carrying T allele for rs146379 and for C allele for rs1127346. Therefore *HDAC6* gene was excluded as well to function as potential factor able to modify the SMA phenotype.

Taken together, these experiments supported the idea that other molecular mechanisms must be responsible for the intrafamilial phenotypic discrepancies in SMA discordant families, mechanisms hard to

be detected by candidate gene approach. A number of proteins were already identified to interact either directly or indirectly with SMN (see table 1). A part of them have been already analyzed for a potential modifying effect on SMA discordant phenotype. Gemin 2, Gemin 3, p80 coilin, ZPR1, hnRNP-Q, FUSE binding protein, profilin 2 a/b, hnRNP-G, RHA and p53 were shown to have no influence on SMA phenotype (Helmken et al. 2003; Helmken et al. 2000). Furthermore, hTra2- $\beta$ 1, the splicing factor responsible for up-regulation of full-length *SMN2* transcript (Hofmann et al. 2000), failed as well to show any difference at both DNA and RNA level in SMA discordant families (Helmken and Wirth 2000). Therefore, a differential gene expression profiling in SMA discordant siblings was the best option. The microarray technology provides the insight into temporal changes that occur in cells, and into the molecular differences between unaffected and affected SMA discordant siblings.

## 6.2. T-plastin, a novel candidate gene detected by expression profiling analysis

cDNA microarray is a potent powerful tool to monitor global transcription profile of hundreds to tens of thousand of genes at once (Alizadeh and Staudt 2000; Golub et al. 1999). To more closely define and elucidate the mechanism(s) leading to protection against SMA phenotype *in vivo*, the gene expression profile of SMA discordant sibs was examined by Affymetrix oligonucleotide arrays. This study provides for the first time a detailed insight into a complex set of *in vivo* differences in SMA discordant phenotypes. Using cultured lymphoblastoid cell lines of unaffected vs. affected *SMN1*-deleted individuals, 286 out of 22,000 probe sets were differentially regulated in SMA discordant sibs (tables T3 and T4 that are contained in attached CD-ROM). Identification of transcriptional up- or down-regulated gene classes might facilitate the understanding of molecular mechanisms underlying SMN biological functions.

Total RNA isolated from EBV-transformed lymphoblastoid cell cultures from SMA discordant family #482, two type I and two type III SMA patients was used to hybridize HG-U133A Affymetrix chip to detect transcripts differentially expressed in asymptomatic vs. symptomatic sibs. The two types of SMA patients (type I and type III) were used under the assumption that only the transcripts differentially expressed due to the modifier gene and not due to the lack of SMN protein would be detected. The data from unaffected siblings were compared with the data from affected sibs and pools of transcripts up- and down-regulated in unaffected than affected sibs were detected. To exclude all the transcripts co-regulated by *SMN1* deletion, these transcripts pools were compared with the transcripts found to be differentially expressed in the two SMA types used as controls. Because we assumed that the modifying factor(s) should be expressed/over-expressed in asymptomatic sibs protecting them in this way to develop SMA, the up-regulated genes were the central issue of expression profiling analysis. The most highly represented genes in up-regulated transcripts group are involved in metal ion binding or acts as receptors or enzymes (Fig. 9 B). It is notable that a large number of proteins also play a role in DNA binding and nuclei acids binding (Fig. 9 B). It is important to point out that these expression differences were identified in the RNA samples isolated from EBV-transformed lymphoblastoid cell lines rather than motor neurons, the cell type

affected by the loss/lower amount of the SMN protein. Therefore, these differences in expression between SMA discordant sibs may reflect only in part the transcripts modulated by the modifier(s).

Therefore, for the confirmation analysis using RT-PCR, the six candidate genes (*T-plastin*, *SEPTIN 2*, *NR1I3*, *CD24*, *TNFSF14* and *PLOD 2*) were selected based on the fold difference in gene expression profiling. Only two candidates (*T-plastin* and *NR1I3*) (Fig. 11 and 12) confirmed the Affymetrix based results. The two candidates were found to be expressed/overexpressed in all unaffected individuals from 5 SMA discordant families. For *NR1I3*, an up-regulation in asymptomatic vs. symptomatic sibs was found only in three SMA discordant families. Because it was hard to connect this gene to SMA pathology and development (see 5.2.5. Description of *NR1I3* candidate), we focus on the remaining candidate. RT-PCR and Western blot studies showed that T-plastin is consistently up-regulated in unaffected *SMN1*-deleted sibs (Fig. 10, 11 and 16). This protein has not been previously associated with SMA. The high levels of expression for T-plastin in fresh blood (Fig. 15), and perhaps in the motor neurons of the unaffected *SMN1*-deleted sibs, suggested a possible role for this protein in maturation of motor neurons. T-plastin was found to be expressed in all unaffected individuals in SMA discordant families, except for family #800, where both unaffected and affected sibs showed its expression (see 6.3 T-plastin is expressed in all unaffected sibs that carry *SMN1* deletion/mutation and in 6.5 % of the control population).

This approach revealed for the first time the up-regulation of a cytoskeletal protein, namely T-plastin, implying that this pathway is likely to be modified in unaffected sibs *SMN1*-deleted. Another cytoskeletal protein, *SEPTIN 2*, was found also to be up-regulated 3-fold but the different expression could not be confirmed by RT-PCR (Fig. 10).

Plastins are actin-bundling proteins highly conserved from yeast to humans (Shirayama and Numata 2003; Watanabe et al. 2000; Wu et al. 2001). T-plastin contributes to protrusive force generation in two ways – by crosslink formation and by filament stabilization (Giganti et al. 2005). This is in agreement with the observation that overexpression of this protein in cultured epithelial cells can cause the elongation of microvilli (Arpin et al. 1994). In line with a role in the biogenesis of membrane protrusions, T-plastin associates with the developing actin cytoskeleton of embryonic intestinal microvilli (Chafel et al. 1995) and stereocilia of the inner ear (Daudet and Lebart 2002). T-plastin might control actin turnover and the length of the actin filaments in these structures, which is crucial for their biological function (Schneider et al. 2002). T-plastin is associated not only with the F-actin bundle of epithelial cell microvilli but also with the leading edge of migrating fibroblasts (Arpin et al. 1994), which contains a branched network of filaments (Svitkina and Borisy 1999) that this protein might stabilize. In line with this, yeast plastin is required for the stabilization of Arp2/3-dependent branched network of filaments in actin patches (Young et al. 2004). Taken together, these observations suggest that T-plastin causes the reorganization and elongation of an actin structure initiated by the WASP-Arp2/3 complex polymerization unit, and concomitantly increases actin-based force (Giganti et al. 2005). This complex has a crucial role in the formation of branched-actin-filament networks during diverse processes ranging from cell motility to endocytosis (Goley et al. 2006).

The transformation of cytoplasm from a liquid to a solid was observed to be tightly associated with the cells' ability to move, and this sol-to-gel transition is now known to be caused by changes in the state of

polymerization and organization of the actin protein (Stossel 1994). Actin is found only in eukaryotes. It comprises a highly conserved family of proteins, that fall into three broad classes:  $\alpha$ -,  $\beta$ - and  $\gamma$ -isoforms (dos Remedios et al. 2003). Actin binds a substantial number of proteins, collectively called actin binding proteins (ABPs) (Pollard and Cooper 1986). At least twelve ABPs are membrane-associated proteins, and another nine are membrane receptors or ion transporters. Thirteen ABPs crosslink actin filaments, whereas others enable filaments to interact with other elements of the cytoskeleton. Actin also binds more than thirty other ligands including drugs and toxins (dos Remedios and Thomas 2001). Classification of these ABPs can be reduced to monomer-binding proteins, filament-depolymerizing proteins, filament end-binding proteins, filament severing proteins, crosslinking proteins, stabilizing proteins and motor proteins (dos Remedios et al. 2003). The actin crosslinking proteins direct the formation of distinct F-actin assemblies and integrate the actin complexes into overall cellular physiology through their responsiveness to signals such as calcium fluxes and phosphorylation events (Matsudaira 1994).

### **6.3. T-plastin is expressed in all unaffected sibs that carry *SMN1* deletion/mutation and in 6.5 % of the control population**

T-plastin is normally absent in hematological cell types but widely distributed at low levels in other tissue types and nonhematopoietic malignancies (Lin et al. 1993b). Among all tissues/cells surveyed, T-plastin was shown to be absent from all hematopoietic cell types or whole blood studied and from malignant B-cell and T-cell lines studied (Lin et al. 1999). We determined that the difference between the unaffected and affected sibs is demonstrated directly from unfractionated whole blood. Western blot analysis on protein isolated from peripheral blood from one unaffected *SMN1*-deleted individual (#783) that showed T-plastin expression in the EBV-transformed lymphoblastoid cells (EBV T36/91) showed that T-plastin protein can be readily detected from the whole blood (Fig. 15). This observation in lymphocytes cells isolated from fresh blood demonstrated that T-plastin expression is not restricted to solid tissues and is expressed among the hematopoietic cell types in unaffected sibs belonging to SMA discordant families. In the same time it has been excluded any activation mechanism during the EBV transformation. The significance of T-plastin protein in hematopoietic cells in unaffected, healthy sibs remains to be determined and points out to a unique mechanism that might activate *T-plastin* gene in leukocytes. This mechanism behind *T-plastin* activation in fresh blood in unaffected sibs is unknown and requires further investigations. Detection of T-plastin expression at both RNA and protein level in unaffected individuals that carry homozygous *SMN1* deletion revealed that T-plastin expression might be a rare event that happen in human population. We demonstrated that this expression pattern is unique for SMA discordant families, as long as all unaffected sibs analyzed for T-plastin expression showed its expression by both RT-PCR and Western blot. In the control population, *T-plastin* was expressed in 3/46 (6.5%). In classical type I, II and III SMA patients, *T-plastin* was highly expressed in 5.9 % of the SMA population with *SMN1* deletion or mutation, and in 20.8 % medium or weak expressed. For the SMA individuals that carry neither deletion nor mutation of *SMN1* gene, T-plastin was expressed in 8 % of the population. This study revealed for the

first time the evidence that *T-plastin* expression in fresh blood is a rare event that occurs in 6.5 % of the control population. Moreover, the expression of *T-plastin* itself in leukocytes is not enough to protect the individuals to develop SMA. Additional factors that modulate *T-plastin* expression function or localization may be important. This result explains, at least in part, the case of family #800 where both unaffected and affected sibs express T-plastin, but one is protected to develop SMA. The LN 421 individual resembles the case of the classical SMA patients that express *T-plastin* by an unidentified mechanism, but this is not the complete background to drive to a protected phenotype. The factor(s) responsible for this unique gene regulation in both SMA discordant families and the control population required further investigations.

#### 6.4. *T-plastin* is activated by a *trans*-acting factor

To answer the question what might be the reason for differentially expression of *T-plastin* gene in discordant SMA sibs, the complete coding region and the *cis*-regulatory elements were checked by sequencing in the first step. Because no mutation or nucleotide variation could be found in any of the analyzed region, the activation of *T-plastin* in both lymphocytes from fresh blood and EBV-transformed lymphoblastoid cell lines in asymptomatic sibs was assessed by epigenetic changes in the CpG island region described by Lin et al. (Lin et al. 1999). DNA methylation is a well-recognized epigenetic modifier in the control of gene expression.

In this study the pyrosequencing method was used to determine the methylation profile of *T-plastin* CpG island. Initial experiments demonstrated that the pyrosequencing method gives accurate and reproducible estimates of methylated cytosine content of one to six CpGs simultaneously (Colella et al. 2003; Tost et al. 2003; Uhlmann et al. 2002). The profile of CpG island methylation was assessed in EBV-transformed lymphoblastoid cell lines belonging to five SMA discordant families, eight T-plastin expressing and eight T-plastin non-expressing controls. Comparison between the two types of controls, expressing or not T-plastin suggested no correlation between methylation and T-plastin expression (Fig. 28 A). The *T-plastin* CpG island methylation has been investigated and reported in the literature by Lin and colleagues (Lin et al. 1999) and are similar with our data. However, a comparison between SMA discordant sibs was performed in hope to explain the activation mechanism in asymptomatic siblings and again no difference in methylation level was detected (Fig. 28 B).

An enhancer was mapped to within a 20 bp fragment, approximately 500 bp upstream of the basal promoter (Lin et al. 1999). Therefore, we investigated whether *T-plastin* enhancer binding might be occupied in EBV-transformed lymphoblastoid cell lines derived from SMA discordant families by *in vivo* footprinting approach using dimethylsulphate (DMS) treatment and ligation-mediated PCR (LM-PCR).

Preliminary results indicate that the enhancer might be occupied on the active X chromosome (Fig. 29). Comparison between the SMA discordant sibs or between controls that express or not T-plastin suggest a partially protection within the enhancer region (Fig. 29). This may have resulted from the sites in some clones not being occupied in case of males, or/and from the inactivated X chromosome in the case of female individuals. These observations indicate that some proteins might be bound in the *T-plastin*

enhancer region but, nevertheless, further investigations are required.

Because not all *T-plastin*-expressing individuals are protected to develop SMA, 12 SMA discordant families, 2 control families, 4 classical SMA families together with 7 male SMA patients were used to determine the haplotypes in *T-plastin* region responsible for this discrepancy and to answer the question whether *T-plastin* expression is induced by a *cis*- or a *trans*-acting factor/element. A set of 15 htSNPs identified in the *T-plastin* genomic region was used in association studies to correlate a certain haplotype with T-plastin expression. No correlation was found, suggesting that additional factors may play a role in regulation of the *T-plastin* gene expression in both SMA discordant families and control population.

All these observations reported here support the idea that the expression of the *T-plastin* gene does not depend on any *cis*-element described in *T-plastin* genomic region, and likely a *trans*-acting element/factor might be responsible for the unexpected *T-plastin* expression in fresh blood in healthy *SMN1*-deleted sibs and in some 6.5 % of the control population. It can not be ruled out the likely possibility that there are additional regulatory regions in the *T-plastin* gene that have been so far not detected.

### 6.5. T-plastin might play an important role during NMJ formation

T-plastin is an actin crosslinking protein that causes the reorganization and elongation of the actin structures (Giganti et al. 2005). For the first time, *T-plastin* was found to be up-regulated in asymptomatic *SMN1*-deleted sibs. This study shows that T-plastin and SMN associate together (Fig. 17 A and 20 A) but do not interact directly (Fig. 17 B). Clinical studies (Crawford and Pardo 1996) coupled with the data from recently developed animal models (Cifuentes-Diaz et al. 2001; Frugier et al. 2000; Monani et al. 2000) point toward the possibility that SMA is a developmental defect in neuromuscular interaction (Greensmith and Vrbova 1997). Consequently, the expression of *T-plastin* gene was investigated in one SMA fetus and one adult control using RNA samples isolated from brain, spinal cord and muscle. Interestingly, *T-plastin* was found to be expressed at very high levels in spinal cord and high levels in muscles (Fig. 13). These observations suggest that T-plastin protein might be involved in maturation of NMJ. It has been reported that the amount of SMN varies during myogenesis *in vitro* (Burlet et al. 1998) and is down-regulated in adult compared with fetal skeletal muscle and spinal cord (Williams et al. 1999). The presence of SMN and T-plastin at high levels in spinal cord and skeletal muscle during embryogenesis may be crucial during NMJ maturation. Functional interaction between the motor neuron and its target muscle is critical in NMJ formation (Fan and Simard 2002). Taken together, these observations provide a strong evidence for T-plastin involvement during neuronal differentiation and neuromuscular maturation, suggesting that T-plastin may possess a motor neuron-specific function.

### 6.6. T-plastin and SMN form a novel axon-specific complex

SMN accumulates in growth-cone-like structures during neuronal differentiation (Fan and Simard 2002). The presence of SMN in axons and dendrites of nerve cells, at a long distance from the nucleus, indicates

some additional role for this protein for the characteristic loss of motor neurons in SMA (Sharma et al. 2005).

Rat pheochromocytoma PC12 cells differentiate in the presence of NGF into cells with long neurite extensions or neuronal processes (Tischler and Greene 1975). Although they are not motor neurons, this model is an useful *in vitro* model (Greene and Tischler 1976). SMN was found to be concentrated at the ends of neuronal processes, the growth cones and at branch points (Jablonka et al. 2001). This study shows for the first time that T-plastin co-localizes with SMN and F-actin within the cytoplasm and along the neurite-like extensions, branch points and growth cones (Fig. 21 and 23). This novel association opens a new view on the role of T-plastin-SMN complex in SMA pathogenesis. It has been reported that a complex SMN-Gemin 2 present in axons and dendrites is deficient of spliceosomal Sm proteins (Zhang et al. 2006) suggesting that additional functions except for snRNP biogenesis might be responsible for motor neuron degeneration in SMA.

Several studies have surveyed the global change of differentially expressed genes in PC12 cells, before and after NGF treatment (Angelastro et al. 2000; Brown et al. 1999; Lee et al. 2005; Mayumi et al. 1998). SMN protein level has been already reported to be up-regulated after 24 h NGF stimulation in PC12 cells (Navascues et al. 2004). Interestingly, T-plastin amount was also found to be up-regulated in differentiated PC12 cells under NGF stimulation (Fig. 19). Diverse actin binding proteins, such as thymosin  $\beta$ 4 and Arp2/3 have been shown to be induced by NGF in PC12 cells (Angelastro et al. 2000). Arp2 and Arp3 belong to a recently discovered family of proteins that are related to the sequence and structure of actin (Machesky and May 2001). These two actin-like proteins are assembled into Arp2/3 complex that is associated with dynamic cortical regions of mammalian cells that are rich in cytoskeletal actin (Cossart 2000). Nucleation of filament assembly by Arp2/3, first observed by Welch et al. (Welch et al. 1997a; Welch et al. 1997b; Welch et al. 1997c), is unlike any other ABP. Extracellular signals, such as growth factors are transmitted through G-protein-coupled receptors to Wiskott-Aldrich syndrome protein (WASP), the neuronal homolog of WASP (N-WASP), or suppressor of cAMP receptor 1 (Scar 1) (dos Remedios et al. 2003). Activated WASP has sites that bind both an actin monomer and the Arp2/3 complex (Amann and Pollard 2001). T-plastin modulates actin dynamics and generate force independent of cross-bridge formation in a WASP-Arp2/3-dependent polymerization system, a mechanism that might be applicable to other F-actin-stabilizing and/or bundling proteins (Giganti et al. 2005). Because T-plastin does not affect the polymerization kinetics of the pure actin *in vitro* (Giganti et al. 2005), it is unlikely that this protein increases the rate of actin polymerization by keeping Arp2/3-nucleated filaments uncapped or by nucleating new free barbed ends. T-plastin might act through its stabilizing effect and might influence the elongation phase of actin filaments nucleated by Arp2/3 or generated by cofilin-mediated severing (Giganti et al. 2005).

The Rho GTP-binding family proteins are important regulators of cytoskeleton organization (Hall 1998) and several reports showed a transient up-regulation of Rho mRNA under NGF treatment in PC12 cells (Lee et al. 2005; Zalcman et al. 1995). Rho GTPases activate WASP/WAVE (WASP family Verprolin-homologous; WAVE or Scar) proteins that induce actin polymerization via the Arp2/3 complex (Millard et

al. 2004). The involvement of Rho GTPases in actin cytoskeleton organization has been directly demonstrated by microinjecting serum-starved Swiss 3T3 fibroblasts with a constitutively activated mutant RhoA. This treatment led to a dramatic change in the cell shape and stimulated actin polymerization (Peterson et al. 1990). Subsequent analysis demonstrated that indeed, RhoA and Rac1 control the formation of distinct actin-containing structures, stress fiber and membrane ruffles, respectively (Ridley and Hall 1992a, b; Ridley et al. 1992). Several GTPases, including RhoA, RhoB, RhoD and Cdc42 affect specific steps of vesicle trafficking between different intracellular compartments (Bader et al. 2004; Matas et al. 2005). The filaments crosslinked by T-plastin are closely bundled because of the proximity of the two binding domains in its primary amino acid sequence. The redistribution of T-plastin in the presence of active Cdc24 protein provides a link between the Rho protein and its regulatory function in the remodelling of the actin cytoskeleton (Dutartre et al. 1996). How Cdc42 might regulate plastin activity is unknown. One possibility is that Cdc42 transduces a regulatory signal to T-plastin. Another possibility is that Cdc42 might direct the assembly of docking sites for plastin and thereby might determine the sites where plastin will be recruited and will generate actin bundles (Dutartre et al. 1996). PI3-kinase activity is required for proper localization of the Cdc42 at the tips of the growing axons (Schwamborn and Puschel 2004). Therefore, redistribution of T-plastin under Cdc42 expression/activation into highly dynamic membrane regions is consistent with the involvement of both proteins in cytoskeletal reorganization in growth cone guidance and those associated with neuronal migration and polarization of axons and dendrites.

Interestingly, under NGF stimulation, the affinity of T-plastin for SMN protein increases in differentiated PC12 cells (Fig. 20), suggesting that, the induced activation of Rho kinases by NGF treatment might increase the ability of T-plastin protein to associate stronger with SMN protein and to participate actively in the redistribution of SMN to the leading edge of the growing axons. Surprisingly, the affinity of T-plastin protein for  $\beta$ -actin was not changed during neurite differentiation (Fig. 20), suggesting that this transient interaction between T-plastin and SMN may be relevant for axonal outgrowth.

A number of ABPs have been reported to localize to the growth cone: ADF/cofilin (Endo et al. 2003; Meberg 2000), Arp2/3 (Goldberg et al. 2000), filamin (Letourneau and Shattuck 1989), GAP43 (Dent and Meiri 1992; Frey et al. 2000; He et al. 1997), profilin (Faivre-Sarrailh et al. 1993; Kim et al. 2001; Wills et al. 1999), etc. SMN co-localizes with profilin II in gems and growth cones of differentiated PC12 cells (Sharma et al. 2005). Profilin IIa is highly expressed in developing and adult neurons (Lambrechts et al. 2000a; Sharma et al. 2005) and, as a regulator of actin dynamics, it is involved in correct neurite outgrowth (Da Silva et al. 2003). SMN co-localizes also with GAP43 (a major component of motile growth cones) in growth cones (Aigner et al. 1995). Taken together, these results suggest that the role of SMN in neurite outgrowth and axon pathfinding is based on the dynamic actin cytoskeleton.

When a chemoattractant is detected on one side of the growth cone, F-actin-driven protrusion is favoured on that side of the growth cone (Bentley and O'Connor 1994; Lin et al. 1994a). This preferential protrusion can take form of filopodia, lamellipodia/ruffles, and intrapodia (Dent and Gertler 2003). Thus, actin anticapping and leaky capping proteins, such as Ena/VASP proteins and GAP43, respectively, are likely to play important roles in this initial protrusion phase because these proteins are known to enhance actin

polymerization (Bear et al. 2002; Dent and Meiri 1998; He et al. 1997; Lanier et al. 1999). These newly formed protrusions must then be stabilized against retraction. Any F-actin bundling/stabilizing proteins (such as T-plastin,  $\alpha$ -actinin, fascin, filamin) are likely to be essential for the continued protrusion of filopodia or lamellipodia. The bundled and crosslinked actin filaments must be stabilized through a mechanism that involves adhesion to substrate (Suter and Forscher 2000). In addition, severing/recycling proteins such as cofilin and profilin may be activated to keep the level of free G-actin and barbed ends high for continued polymerization (Endo et al. 2003; Meberg and Bamberg 2000). The interaction of SMN protein with GAP43 (Aigner and Caroni 1995), T-plastin (Fig. 18, 19 and 22) and profilin (Sharma et al. 2005) suggests that SMN might be involved in directed protrusion, engorgement, and consolidation in response to any attractive cue. SMN protein together with these three cytoskeletal proteins might play a key role in the actin polymerization/depolymerization balance across the growth cone over time.

### **6.7. T-plastin is involved in neurite-like extension formation in differentiated PC12 cells**

Understanding the pathway of action of the T-plastin protein in the neuron-like cells is central to define the possible involvement of this protein in modifying the SMA phenotype in asymptomatic *SMN1*-deleted sibs. The T-plastin protein has an essential housekeeping role in almost all cells, except for leukocytes (Lin et al. 1999).

SMN deficient mouse motor neurons have reduced axon outgrowth, while overexpression of SMN in PC12 cells leads to longer neurite extension (Rossoll et al. 2003). To assess the effect of T-plastin loss on SMN localization and on neurite outgrowth, knockdown experiments were performed using antisense oligos against rat *T-plastin* in differentiated PC12 cells. It was observed that the localization of SMN at the growth cone was disturbed, and the length of neurites decreased significantly (Fig. 23, lane 2 and Fig. 24). Instead, the overexpression of T-plastin protein in differentiated PC12 cells led to an increase in length of neurite-like extensions up to 10 % compared with the control treated cells (Fig. 23, lane 3; Fig. 24 and Fig. 26 A). Taken together, these results suggest that, indeed, T-plastin plays a role in neurite outgrowth during axonal differentiation. The increased length of the neurites in PC12 cells overexpressing T-plastin may figure out how this protein might protect sibs with homozygous *SMN1* deletion but overexpressing T-plastin (Fig. 15 and 16) to develop SMA. One possible scenario is that T-plastin might stabilize the whole growth cone protein complex and to convert this temporary change into a stable axon shaft. It has been shown that the growth cone undergoes a systematic maturation that is continuously repeated during elaboration of the axon (Bray and Chapman 1985). The three stages to form a new axon segment are termed protrusion, engorgement and consolidation (Goldberg and Burmeister 1986). T-plastin protein as bundling protein is probably capable to function in all these three steps depending on the internal state of the growth cone. When SMN protein is present at low/lower levels in unaffected *SMN1*-deleted sibs, it is possible that the overexpression of T-plastin might help the growth cone structure to reach its target (the muscle in case of motor neurons) by its capacity to bundle and stabilize F-actin filaments. This hypothesis

is based on the observation that in differentiated SMN-depleted PC12 cells, the overexpression of T-plastin rescued, at least partially, the neurite length (Fig. 23 lane 4; Fig. 24). The effect of T-plastin loss/overexpression in neuron-like cells suggest that the axon growth, guidance (and perhaps branching) might be susceptible to cytoskeletal perturbation due to involvement of T-plastin protein on F-actin filament formation and stabilization.

It is known that SMN has no effect by its own on actin polymerization (Sharma et al. 2005), however when T-plastin is overexpressed/expressed results in a positive effect of SMN on actin filament formation.

About 50 % of the translational machinery is associated with the cytoskeleton in eukaryotic cells (Hesketh and Pryme 1991). Ribosomes and RNA are localized in restricted peripheral F-actin-rich domains of the myelinated axon, called "Periaxoplasmic Ribosomal Plaques" (PARPs) (Koenig and Martin 1996; Koenig et al. 2000). Intracellular transport mechanisms are better known now. Specific adaptor proteins have been identified in yeasts that link molecular motors to mRNA for transporting it to its target location (Long et al. 2000).  $\beta$ -actin and  $\gamma$ -actin have distinctive distributions in embryonic cortical neurons in culture. Normally,  $\gamma$ -actin is distributed uniformly throughout the cell body and neurites, but  $\beta$ -actin alone is distributed along axons and enriched in growth cones and filopodia. Similarly,  $\gamma$ -actin mRNA is restricted to the cell body, while  $\beta$ -actin mRNA is distributed along immature axons and enriched in growth cones. Of interest is that the  $\beta$ -actin mRNA is localized in RNP-like granules that are in close proximity to microtubules along axons, while in growth cones, RNPs co-localize with actin filaments (Bassell et al. 1998). This suggests that actin may be synthesized locally in growth cones where an enrichment of actin is needed to support actin-based growth cone motility (Sotelo-Silveira et al. 2006). Local synthesis of both actin and  $\beta$ -tubulin were also identified in axonal fields severed from sympathetic neuron cell bodies (Eng et al. 1999). More than 20 proteins were identified, consisting of cytoskeletal proteins, heat shock proteins, ER proteins, metabolic enzymes, antioxidant proteins, and proteins associated with neurodegenerative diseases.

### **6.8. Genome-wide scan in SMA discordant families revealed evidence for new susceptibility loci**

Family studies strongly suggest that individual differences in the clinical features of illness are influenced by familial factors (Cardno et al. 1999a; Cardno et al. 1999b; Cardno et al. 2002; Kendler et al. 1997). Modifier genes have been most thoroughly studied in "single-gene" disorders such as cystic fibrosis. Although variation in the CFTR gene is responsible for susceptibility to the disorder, clinical manifestations have been associated with polymorphisms in other genes, as reviewed by Cutting (Cutting 2005). The presence of such modifier genes may have several implications. Most importantly, they may lead to the development of new treatments.

Another goal of the present study was to detect genomic region in which there is excess sharing by unaffected *SMN1*-deleted individuals. Several regions yielded linkage analysis, however none of these were significant. Regions on chromosomes 3q, 7p, 16p and 22q, respectively, are suggestive for linkage.

The results suggested that there is none major modifier locus but rather several loci that might contain genes with potential modifying effect on the SMA phenotype. On the other hand, these peaks may reveal the true location of genetic protecting factors for SMA; certainly, these results suggest that additional typings are needed in these areas.

Three areas, one on chromosome 16p, one on chromosome 3q and another one on chromosome 22q, respectively, are interestingly, since contain genes that were previously described to be involved either in RNA processing or in response to stress, two pathways in which both T-plastin and SMN were reported to be involved (see below).

On chromosome 16p, the best candidate as putative gene modifier for SMA is represented by A2BP1. A2BP1 (ataxin-binding protein 1) is predominantly expressed in brain and muscle and co-localizes with ataxin-2 (ATX2) in the trans-Golgi network (Shibata et al. 2000). A2BP1 has an RNP RNA-binding motif, and ATX2 also contain two RNA splicing motifs, which are shared with snRNPs (Neuwald and Koonin 1998; Shibata et al. 2000). Interestingly, snRNPs have multiple RNP motifs which are present in A2BP1. Thus, the complex of ataxin-2 and A2BP1 may be involved in RNA processing (Shibata et al. 2000). If the RNA-binding domain in both proteins are functional, one possible role of the ataxin-2-A2BP1 complex may be RNA transport in neurons (Shibata et al. 2000). Surprisingly, an interaction of ataxin-2 with T-plastin was discovered in mouse brain, linking ataxin-2 to pathways that play a role in actin filament formation and organization (Ralsler et al. 2005b). Interestingly, proteomics-based results showed that T-plastin and PABP are contained together in a large protein complexes of 216 subunits and 39 subunits mainly consisting of proteins involved in RNA processing (Blagoev et al. 2003; Ho et al. 2002). This observation is quite remarkable in the light that ataxin-2 directly interacts with the cytoplasmic PABP (poly-(A)-binding protein) (Ralsler et al. 2005a). In the nucleus, SMN appears to be directly involved in pre-mRNA splicing, transcription and metabolism of ribosomal RNA (Jones et al. 2001; Pellizzoni et al. 2001c; Pellizzoni et al. 1998). Of special interest was the observation of an activation of genes involved in RNA metabolism in *Smn* mutant mice (Olaso et al. 2006). Five percent of the genes regulated in *Smn* mutant mice were involved in pre-mRNA splicing, ribosomal RNA processing or RNA decay (Olaso et al. 2006).

On chromosome 3p another gene (eIF2A) was found by the genome-scan analysis that might be correlated to the response to stress. Stress response is a protective cellular process induced by a variety of environmental stress including chemical exposure, heat shock and UV irradiation (Hua and Zhou 2004a). Stress granules are phase dense particles that appear in the cytoplasm of plant and animal cells subjected to environmental stress (Kedersha et al. 1999; Nover et al. 1989). In mammalian cells, the assembly of stress granules is initiated by phosphorylation of eukaryotic initiation factor eIF2A (Kedersha et al. 1999). The proteins found to accumulated in stress granules include the RNA-binding proteins TIA-1 (T-cell internal antigen 1), TIAR (TIA-1 related protein), and PABP, as well as a subset of eIFs, including eIF2, eIF2B, eIF3, eIF4F and eIF4G (Kedersha and Anderson 2002; Kedersha et al. 2002; Kimball et al. 2003). eIF2A (eukaryotic initiation factor 2A), is a 65-kDa protein that catalyzes the formation of the puromycin-sensitive 80S preinitiation complex and the poly (U)-directed synthesis of polyphenylalanine at low  $Mg^{2+}$  concentration (Merrick and Anderson 1975). eIF2A might not function in the initiation of

translation of bulk mRNA but rather is involved in a small subset of mRNA initiation events (Zoll et al. 2002). These alternative initiation events could include re-initiation, internal initiation, or non-AUG initiation. The initial stress response is mediated by the RNA-dependent protein kinase (PKR)-like ER membrane-localized kinase (PERK), which is activated by homeodimerization and autophosphorylation in response to ER stress (Harding et al. 1999; Liu et al. 2000). PERK activation in turns leads to phosphorylation of the subset of eIF2A at Ser 51 resulting in transient inhibition of protein synthesis (Harding et al. 1999). This inhibition of protein synthesis is thought to be important in re-establishing cellular homeostasis by reducing the load of misfolded proteins (Park et al. 2007). Under conditions of ER stress, translational attenuation resulting from phosphorylation of eIF2A is considered critical to decrease the load on newly synthesized protein in the ER as well as to protect cells from potential noxious effects of accumulated misfolded proteins (Park et al. 2007). This may allow cells to overcome the effects of ER stress and avoid cell death. SMN co-localizes with TIA-1/R and G3BP2 in SGs (Hua and Zhou 2004a, b). Several lines of evidence indicate that SMN is important for SG assembly. To form large and smooth granules, the Tudor domain, as well as exon 6 and 7 of SMN are indispensable (Hua and Zhou 2004b). Defects of SG formation in SMA fibroblasts, which express lower levels of SMN protein, support the notion that SMN plays a role in SG formation (Hua and Zhou 2004b).

Stress granules are highly dynamic structures and resemble several nuclear RNA-containing structures (e.g., speckles, coiled bodies, gems, and nucleoli) (Kedersha et al. 2000), that are sites of active RNA metabolism (Gall et al. 1999; Mattern et al. 1999; Mintz and Spector 2000; Zeng et al. 1997). Stress granules may be sites of mRNA triage at which untranslated mRNAs accumulate during stress before being directed to sites of degradation, reinitiation or repackaging as mRNPs (Kedersha et al. 2000).

T-plastin has been shown to be involved in both pathways described above (RNA metabolism and response to stress), and might play crucial functions in bringing together proteins involved in various cellular processes in response to a particular signal. On the other hand, a combination of factors might be responsible for the higher SMN and co-regulated SMN-interacting proteins as previously shown by Helmken and co-workers (Helmken et al. 2003). Unknown proteins involved in translational processes are likely to be involved directly in the protected SMA phenotype, whereas is unclear at this juncture whether T-plastin is the cause or the result of the modified SMA phenotype. Interestingly, on chromosome 22q, two enzymes involved in signal transduction (MAPK11 or p38 $\beta$  and MAPK12 or p38 $\gamma$ ) were found good candidates as potential/additional modifiers.

The MAPK pathway is a three layer signalling cascade, in which the MAPK elements (the most downstream tier) are activated upon tyrosine and threonine phosphorylation within a conserved Thr–Xxx–Tyr motif in the activation loop of the kinase domain. This phosphorylation is catalyzed by dual-specificity kinases, MAPK kinases (MAPKK, MEK). MAPKKs are regulated by serine/threonine phosphorylation within a conserved motif, located in the kinase activation loop, catalyzed by MAPKK kinases (MAPKKK or MEKK; the most upstream tier). The latter are activated by various upstream activators, including kinases and small GTP-binding proteins (Katz et al. 2007). The p38-MAPK is another stress-activated MAPK cascade. p38-MAPK activation is mediated by phosphorylation on a conserved motif that includes a

glycine residue between the canonical threonine and tyrosine (Katz et al. 2007).

The p38 mitogen-activated protein kinases are activated in response to various extracellular signals in eukaryotic cells and play a critical role in the cellular responses to these signals. The four mammalian isoforms (p38 $\alpha$ , p38 $\beta$ , p38 $\gamma$ , and p38 $\delta$ ) are coexpressed and coactivated in the same cells. The exact role of each p38 isoform has not been entirely identified, in part due to the inability to activate each member individually. Human p38 $\alpha$  and p38 $\beta$  are ubiquitously expressed whereas p38 $\gamma$  is mainly expressed in skeletal muscle (Avitzour et al. 2007).

The candidate modifier genes might influence the severity of SMA phenotype through a variety of mechanisms. Each candidate gene should be tested simultaneously with all the other potential modifier genes. Interaction can occur between the candidate genes, for example, when they act in the same pathway.

## 6.9. Future directions

Although the absence of the *SMN1* gene is responsible for the majority of the SMA cases, the clinical phenotype in SMA discordant sibs confirms the rare occurrence of asymptomatic persons with *SMN1* homozygous deletions.

In order to identify potential phenotypic modifiers, three methods were approached in order to maximize the chance to detect them. T-plastin gene was identified in this study by microarray technology to be up-regulated in all unaffected sibs belonging to six SMA discordant families.

It is now required to determine whether the differential expression of *T-plastin* gene is directly or indirectly responsible for the modified SMA phenotype. Concomitantly, collaborations together with Christine E. Beattie from Centre for Molecular Neurobiology, the Ohio State University and with Gary Bassel from Department of Cell Biology, Atlanta are carrying out. We intend to puzzle out the T-plastin involvement *in vivo* by approaching two directions:

- I. First, we would like to define the localization of endogenous as well as overexpressed T-plastin in N2A neuroblastoma cells and primary mouse motor neurons. The effects of T-plastin levels on axon growth are planned to be checked in differentiated ES cells in motor neurons. It is also intended to measure the axon length, the growth cone size, as well as the distribution of  $\beta$ -actin in the distal part and growth cones of motor axons. Furthermore, SMN should be knocked down using antisense RNA and T-plastin overexpressed by retroviral system in primary motor neuron derived from mice.
- II. Second, we would like to answer the question of whether T-plastin overexpression results in motor axon defects in zebrafish and whether the overexpression of T-plastin rescues the axon defects associated with *Smn* knockdown in an *in vivo* model. Our study is strongly supported by the *in vivo* experiments in zebrafish. The lab of Christine Beattie showed that the motor axons defects in *smn* morphants are rescued by overexpression of human *T-plastin* mRNA. Analysis of motor axons showed a significant rescue of the aberrant axonal outgrowth in *hT-plastin* RNA

---

injected embryos ( $p > 0.0001$ ) compared to Smn MO alone (Fig. F11 in appendix) suggesting that T-plastin is also playing an important role in the SMA zebrafish model as well.

The preliminary results are very exciting and the characterization of the T-plastin-SMN complex is in progress in our lab.

Another goal of our study is to understand the activation mechanism of *T-plastin* gene in unaffected *SMN1*-deleted sibs and in 6.5 % of the control population. The finding of the factor able to govern *T-plastin* gene expression should provide an opportunity to discover novel regulatory mechanisms that may act specifically in motor neurons from asymptomatic sibs with homozygous absence of *SMN1* gene, but differently from that mechanism found in rare cases of classical SMA patients that are not protected by T-plastin expression itself.

The best candidate genes detected by the genome-wide scan analysis will be further analyzed.

Another *in vivo* approach on long term is to generate transgenic mice that overexpressed T-plastin specifically in motor neurons and to cross bred these mice with SMA mice. This model will help us to better decipher the effects of T-plastin overexpression during neuron differentiation and maturation.

Furthermore, modifier gene studies will lead to a better understanding of SMA pathophysiology and will provide the possibility of new therapeutic interventions.

## 7 SUMMARY

Spinal muscular atrophy (SMA) is a common inherited disorder characterized by neurodegeneration of  $\alpha$ -motor neurons. SMA is caused by mutation and/or deletion of the *SMN1* gene that encodes the survival of motor neuron protein (SMN). The severity of SMA is strongly influenced by the *SMN2* gene, the highly homologous copy of *SMN1*. The more *SMN2* copies a patient has, the milder is the SMA phenotype. Homozygous *SMN1* deletion in unaffected persons is a rare event suggesting that the SMA phenotype is modified by other factors.

Using a combination of candidate gene approach, expression profiling and genome-wide scan, the present study reveals for the first time the evidence that at both molecular and transcriptional levels, SMA discordant sibs present a number of genes differentially regulated/expressed that are likely to act as SMA modifier genes.

By candidate gene approach, *ZNF265*, *hnRNP-R* and *HDAC6* were excluded to be responsible for the phenotypic discrepancies between SMA discordant sibs, since no difference at both DNA and RNA level was detected in any analyzed gene.

The microarray expression analysis of the SMA discordant families revealed for the first time, a transcript that encodes for a cytoskeletal protein, namely T-plastin, to be the most up-regulated gene in asymptomatic vs. symptomatic *SMN1*-deleted sibs. Along with the up-regulation of T-plastin a number of protein kinases and transcription factors were found slightly up-regulated suggesting that the cytoskeleton together with signalling molecules might modulate the SMA phenotype. A closer look to a possible involvement of T-plastin in SMA pathophysiology revealed exciting observations.

First, T-plastin was found to be expressed at high levels in spinal cord and muscle of fetal and adult tissues by semi-quantitative PCR, an observation that provides a strong evidence for T-plastin implication in neuronal differentiation and neuromuscular maturation. Moreover, T-plastin associates with SMN as shown by Co-IP experiments, but this interaction, as demonstrated by *in vitro* binding assay, is mediated by another so far unknown protein.

Second, T-plastin and SMN were found by immunofluorescence to co-localize along the axons, at branch points and at the growth cones in neurite-like extensions in differentiated PC12 cells. Interestingly, the T-plastin protein amount was found to be up-regulated in differentiated PC12 cells under NGF stimulation, an observation that might propose a possible function for T-plastin as substrate for signalling molecules. Moreover, under NGF stimulation, the affinity of T-plastin for SMN increased up to 50% suggesting that a transient complex might occur during neuronal differentiation that contributes to a specific role during this biological process.

Third, the effect of T-plastin loss/overexpression in differentiated PC12 cells (cells presenting either shorter neurites when T-plastin was depleted or longer neurites when T-plastin was overexpressed) hints to a perturbation in the axon growth, guidance (and perhaps branching) due to the involvement of T-plastin in F-actin filament formation and stabilization. Interestingly, by *in vitro* experiments it has been observed that in differentiated PC12 cells expressing low amount of SMN protein, but overexpressing T-

plastin, the length of the neurites was rescued at least in part by higher T-plastin levels. This suggests that a higher amount of T-plastin protein might help the growth cone structures to reach their target (the muscle in case of motor neurons).

While all analyzed unaffected *SMN1*-deleted sibs expressed T-plastin in both peripheral blood and EBV-transformed lymphoblastoid cell lines, only 6.5 % of the control population expressed T-plastin. In classical SMA patients, *T-plastin* was highly expressed in 5.9 %, medium in 7.4 % and very weak in 13.4 %. Finally, 8 % patients without *SMN1* mutations expressed *T-plastin*. These data suggest that *T-plastin* expression in leukocytes happens as a rare event in humans and its expression in blood significantly correlates with an SMA protection. Nevertheless, not all blood-T-plastin-expressing *SMN1*-deleted individuals are SMA protected, which suggest a potential differential regulation in the spinal cord.

The answer to the question by which mechanism *T-plastin* is expressed in unaffected sibs with homozygous absence of *SMN1* gene or in control population and classical SMA patients, was not found. No correlation between the T-plastin expression and any mutation or DNA variation in the *T-plastin* coding region, promoter, 3'UTR or intron 1 was observed. Moreover, epigenetic analysis of the *T-plastin* regulatory region (promoter-first exon-first intron) revealed no differences in DNA modification level. These observations together with the haplotype analysis of two blocks described within the *T-plastin* genomic region in both SMA discordant families and control population, strongly suggest that likely a *trans*- rather than a *cis*-acting factor is responsible for the differential expression between SMA discordant sibs or between SMA discordant families and control population. In hope to find additional modifying genes or factors that are able to regulate T-plastin expression, a genome-wide scan analysis was performed in 42 SMA discordant families. Regions on chromosomes 3q, 7p, 16p and 22q, respectively, are suggestive for linkage and require further investigations, however, none of these reached a significant LOD score.

Taken together, the discovery of the T-plastin protein as a modulator of the SMA phenotype provides the opportunity to identify novel regulatory mechanisms that may act specifically in motor neurons from asymptomatic sibs with *SMN1* homozygous deletion.

## 8 ZUSAMMENFASSUNG

Die Spinale Muskelatrophie (SMA) ist eine der häufigsten rezessiv erblichen Erkrankungen beim Menschen, die sich durch Degeneration der  $\alpha$ -Motoneuronen im Rückenmark kennzeichnet. SMA wird durch homozygote Mutationen und/oder Deletionen des *SMN1*-Gens verursacht, welches für das *survival of motor neuron* (SMN) Protein codiert. Der Schweregrad der SMA wird im Wesentlichen durch das *SMN2*-Gen beeinflusst, eine hoch homologe Kopie des *SMN1*-Gens. Je mehr *SMN2*-Kopien ein Patient hat, desto milder ist der SMA-Phänotyp. Das Auftreten von homozygoten *SMN1*-Deletionen bei nicht betroffenen Personen ist sehr selten und weist auf eine Modifikation des SMA-Phänotyps durch andere Faktoren hin.

Im Rahmen der Arbeit wurde in phänotypisch diskordanten SMA Familien eine Kombination aus Kandidatengenstrategie, differentieller Expressionsuntersuchungen und genomweiter Kopplungsanalyse bei der Suche nach einem SMA-modifizierendem Gen angewandt. Diese Studie liefert den ersten Beweis, dass in phänotypisch diskordanten SMA Familien eine Reihe von Transkripten unterschiedlich reguliert/exprimiert werden, die als potentielle SMA-modifizierende Gene in Frage kommen.

In der differentieller Expressionuntersuchung nach Microarray-Analyse zeigte T-Plastin, ein Zytoskelettprotein, die stärkste Heraufregulation (39-fach) in allen asymptomatischen *SMN1*-deletierten Geschwistern im Vergleich zu ihren betroffenen Geschwistern. Zusätzlich war auch eine Anzahl von Proteinkinasen und Transkriptionsfaktoren verstärkt exprimiert, die gemeinsam darauf hindeuten, dass das Zytoskelett zusammen mit verschiedenen Signalmolekülen möglicherweise den SMA-Phänotyp modifizieren. Eine genauere Untersuchung einer möglichen Rolle von T-Plastin in der Pathophysiologie von SMA führte zu folgenden Ergebnissen:

Erstens, wurde eine starke Expression mittels semi-quantitativer multiplex RT-PCR von T-Plastin im fetalen und adulten Rückenmark und in Muskeln nachgewiesen, was einen starken Hinweis für eine Beteiligung bei der neuronalen Differenzierung und der neuromuskulären Reifung darstellt.

Mittels *in vitro* Co-Immünpräzipitation wurde gezeigt, dass T-Plastin mit SMN assoziieren kann, wobei es sich nicht um eine direkte Interaktion handelt, wie es *in vitro* pull-down Experimente bewiesen. Zweitens, Studien mittels Konfokaler Immunfluoreszenz-Lasermikroskopie zeigten eine Co-Lokalisation von T-Plastin und SMN entlang der Axone, an Verzweigungen und an Wachstumskegeln in neuriten-ähnlichen Ausläufern in differenzierten PC12-Zellen. Interessanterweise wurde eine erhöhte Menge an T-Plastin Protein während der neuronalen Differenzierung von PC12-Zellen unter Stimulation mit neuronalem Wachstumsfaktoren (NGF) gemessen, was nahe legt, dass T-Plastin ein mögliches Substrat für unterschiedliche Signalmoleküle darstellen könnte. Ferner nahm die Affinität von T-Plastin für SMN unter NGF-Stimulation um 50% zu. Dies läßt vermuten, dass während der neuronalen Differenzierung ein transientser Komplex auftritt, der zu einer spezifischen Rolle in diesem biologischen Prozeß beiträgt.

Drittens, deuten die Auswirkungen des Verlustes bzw. der Überexpression von T-Plastin in differenzierten PC12-Zellen (die Zellen zeigten kürzere Neuriten bei T-Plastin Depletion bzw. längere Neuriten bei T-Plastin Überexpression) auf eine Störung des Wachstums, der Wegfindung und evtl. der Verzweigung von

Axonen hin, was durch einen Einfluss von T-Plastin auf die Bildung und Stabilisierung von F-Aktin-Filamenten erklärt werden könnte. Interessanterweise konnte in *in vitro* Experimenten beobachtet werden, dass in differenzierten PC12-Zellen mit niedriger SMN-Expression aber einer Überexpression von T-Plastin die Länge der Neuriten zumindest zum Teil durch höhere T-Plastin-Konzentrationen wiederhergestellt werden konnte. Dies legt nahe, dass eine größere Menge des T-Plastin Proteins möglicherweise den Wachstumskegeln dabei helfen kann, ihr Ziel zu erreichen (den Muskel im Falle von Motoneuronen).

Während alle asymptotischen *SMN1*-deletierten Geschwister T-Plastin sowohl im nativen Blut als auch in Epstein-Barr-Virus (EBV) transformierten lymphoblastoiden Zelllinien exprimierten, zeigten nur 6,5 % der Kontrollen eine Expression im Blut. In klassischen SMA-Patienten fand sich eine starke Expression des T-Plastins in 5,9 %, eine mittlere in 7,4 % und eine sehr schwache in 13,4 %. Dies deutet darauf hin, dass die Expression von T-Plastin im Blut hochsignifikant mit einer SMA-Protektion korreliert. Da allerdings nicht alle *SMN1*-deletierten Personen einen SMA-Schutz entwickeln, könnte dies auf eine im Rückenmark unterschiedliche Regulation hinweisen. Die Antwort auf welche Mechanismen für die Expression von T-Plastin in allen asymptotischen Geschwistern, wenigen Kontrollen und SMA-Patienten verantwortlich sind, konnte nicht abschließend beantwortet werden.

Es wurde weder eine Mutation oder DNA-Variation im codierenden Bereich, noch in der 3' nicht-translatierten Region, im Promotor oder Intron 1 des Genes identifiziert. Außerdem, haben auch epigenetische Studien der CpG-reichen Promotorregion keine Unterschiede aufgedeckt.

Letztlich wurde eine umfangreiche Analyse der *tagging* SNPs (*single nucleotide polymorphisms*) der Haplotypblöcke, die das T-Plastin auf genomischer Ebene abdecken in phänotypisch-diskordanten SMA-Familien und Kontrollen durchgeführt und keine Assoziation mit der Expression des T-Plastin Gens gefunden. Insgesamt weisen diese Ergebnisse auf eine *trans*-aktivierende Regulation der Expression von T-Plastin im Blut hin.

Um diesen Faktor zu identifizieren, wurde eine genomweite Kopplungsanalyse in 42 phänotypisch diskordanten SMA-Familien durchgeführt. Mehrere Regionen auf den Chromosomen 3q, 7p, 16p und 22q zeigten eine mögliche Kopplung und müssen durch weitere Untersuchungen bestätigt werden.

Zusammenfassend stellt die Entdeckung des T-Plastin Proteins als Modulator des SMA-Phänotyps neue Wege dar, regulatorische Mechanismen zu identifizieren, die spezifisch in Motoneuronen von asymptotischen Geschwistern mit *SMN1*-Deletion auftreten und von der Erkrankung schützen.

## 9. PUBLICATIONS, LECTURES AND POSTER CONTRIBUTIONS

### 9.1. ORIGINAL PUBLICATIONS

Helmken C., Hofmann Y., Schoenen F., Oprea G., Raschke H., Rudnik-Schoneborn S., Zerres K., Wirth B. (2003) Evidence for a modifying pathway in SMA discordant families: reduced SMN level decreases the amount of its interacting partners and Htra2-beta1. *Hum Gen.*114:11-21

Oprea G. E., McWhorter M., Rossoll W., Kröber S., Debey S., Schulze J. L., Wienker T. F., Beattie C., Bassell G., and Wirth B. (2007) Plastin-3 protects individuals with homozygous *SMN1* deletions from developing spinal muscular atrophy; *Manuscript in preparation*.

### 9.2. PRINTED LECTURE CONTRIBUTIONS

Oprea G., Wirth B. (2005) Identification of Potential Gene Modifiers in SMA Discordant Families. *Medgen* 17:51 (W08 03) (The 16th Annual Meeting of the German Society of Human Genetics, Neurogenetics Session, Halle, Germany)

Helmken C., Bordeianu G., Hofmann Y., Schoenen F., Raschke H., Rudnik-Schoenenborn S., Zerres K., Wirth B. (2003) First Evidence for a Modifying Pathway in SMA Discordant Families. SMN regulates its Interacting Partners and its own Splicing Factor hTra2 $\beta$ . *Medgen.* 15:276 (W4 01) (The 14th Annual Meeting of the German Society of Human Genetics, Neurogenetics Session, Marburg, Germany)

### 9.3. PRINTED POSTER CONTRIBUTIONS

Oprea G., Wirth B. (2006) Identification of Potential Gene Modifiers in SMA Discordant Families. *Medgen.* 18:114 (P296) (The 17th Annual Meeting of the German Society of Human Genetics, Heidelberg, Germany)

## 10. REFERENCES

- Abecasis GR, Cherny SS, Cookson WO, Cardon LR (2002) Merlin--rapid analysis of dense genetic maps using sparse gene flow trees. *Nat Genet* 30: 97-101
- Abreu PC, Greenberg DA, Hodge SE (1999) Direct power comparisons between simple LOD scores and NPL scores for linkage analysis in complex diseases. *Am J Hum Genet* 65: 847-57
- Adam T, Arpin M, Prevost MC, Gounon P, Sansonetti PJ (1995) Cytoskeletal rearrangements and the functional role of T-plastin during entry of *Shigella flexneri* into HeLa cells. *J Cell Biol* 129: 367-81
- Adams AE, Botstein D, Drubin DG (1989) A yeast actin-binding protein is encoded by SAC6, a gene found by suppression of an actin mutation. *Science* 243: 231-3
- Adams AE, Botstein D, Drubin DG (1991) Requirement of yeast fimbrin for actin organization and morphogenesis in vivo. *Nature* 354: 404-8
- Adams AE, Johnson DI, Longnecker RM, Sloat BF, Pringle JR (1990) CDC42 and CDC43, two additional genes involved in budding and the establishment of cell polarity in the yeast *Saccharomyces cerevisiae*. *J Cell Biol* 111: 131-42
- Adams AE, Shen W, Lin CS, Leavitt J, Matsudaira P (1995) Isoform-specific complementation of the yeast sac6 null mutation by human fimbrin. *Mol Cell Biol* 15: 69-75
- Adams DJ, van der Weyden L, Kovacic A, Lovicu FJ, Copeland NG, Gilbert DJ, Jenkins NA, Ioannou PA, Morris BJ (2000) Chromosome localization and characterization of the mouse and human zinc finger protein 265 gene. *Cytogenet Cell Genet* 88: 68-73
- Adams DJ, van der Weyden L, Mayeda A, Stamm S, Morris BJ, Rasko JE (2001) ZNF265--a novel spliceosomal protein able to induce alternative splicing. *J Cell Biol* 154: 25-32
- Aigner L, Arber S, Kapfhammer JP, Laux T, Schneider C, Botteri F, Brenner HR, Caroni P (1995) Overexpression of the neural growth-associated protein GAP-43 induces nerve sprouting in the adult nervous system of transgenic mice. *Cell* 83: 269-78
- Aigner L, Caroni P (1995) Absence of persistent spreading, branching, and adhesion in GAP-43-depleted growth cones. *J Cell Biol* 128: 647-60
- Alizadeh AA, Staudt LM (2000) Genomic-scale gene expression profiling of normal and malignant immune cells. *Curr Opin Immunol* 12: 219-25
- Almond BA, Hadba AR, Freeman ST, Cuevas BJ, York AM, Detrisac CJ, Goldberg EP (2003) Efficacy of mitoxantrone-loaded albumin microspheres for intratumoral chemotherapy of breast cancer. *J Control Release* 91: 147-55
- Amann KJ, Pollard TD (2001) The Arp2/3 complex nucleates actin filament branches from the sides of pre-existing filaments. *Nat Cell Biol* 3: 306-10
- Anderson KN, Baban D, Oliver PL, Potter A, Davies KE (2004) Expression profiling in spinal muscular atrophy reveals an RNA binding protein deficit. *Neuromuscul Disord* 14: 711-22
- Anderson P, Kedersha N (2002) Visibly stressed: the role of eIF2, TIA-1, and stress granules in protein translation. *Cell Stress Chaperones* 7: 213-21
- Anderson P, Kedersha N (2006) RNA granules. *J Cell Biol* 172: 803-8
- Andrade LE, Chan EK, Raska I, Peebles CL, Roos G, Tan EM (1991) Human autoantibody to a novel protein of the nuclear coiled body: immunological characterization and cDNA cloning of p80-coilin. *J Exp Med* 173: 1407-19
- Andreadis A (2005) Tau gene alternative splicing: expression patterns, regulation and modulation of function in normal brain and neurodegenerative diseases. *Biochim Biophys Acta* 1739: 91-103
- Andreassi C, Angelozzi C, Tiziano FD, Vitali T, De Vincenzi E, Boninsegna A, Villanova M, Bertini E, Pini A, Neri G, Brahe C (2004) Phenylbutyrate increases SMN expression in vitro: relevance for treatment of spinal muscular atrophy. *Eur J Hum Genet* 12: 59-65
- Andreassi C, Jarecki J, Zhou J, Coover DD, Monani UR, Chen X, Whitney M, Pollok B, Zhang M, Androphy E, Burghes AH (2001) Aclarubicin treatment restores SMN levels to cells derived from type I spinal muscular atrophy patients. *Hum Mol Genet* 10: 2841-9
- Angelastro JM, Klimaschewski L, Tang S, Vitolo OV, Weissman TA, Donlin LT, Shelanski ML, Greene LA (2000) Identification of diverse nerve growth factor-regulated genes by serial analysis of gene expression (SAGE) profiling. *Proc Natl Acad Sci U S A* 97: 10424-9
- Arpin M, Friederich E, Algrain M, Vernel F, Louvard D (1994) Functional differences between L- and T-plastin isoforms. *J Cell Biol* 127: 1995-2008

- Ashburner M, Ball CA, Blake JA, Botstein D, Butler H, Cherry JM, Davis AP, Dolinski K, Dwight SS, Eppig JT, Harris MA, Hill DP, Issel-Tarver L, Kasarskis A, Lewis S, Matese JC, Richardson JE, Ringwald M, Rubin GM, Sherlock G (2000) Gene ontology: tool for the unification of biology. The Gene Ontology Consortium. *Nat Genet* 25: 25-9
- Avitzour M, Diskin R, Raboy B, Askari N, Engelberg D, Livnah O (2007) Intrinsically active variants of all human p38 isoforms. *Febs J* 274: 963-75
- Ayer DE, Lawrence QA, Eisenman RN (1995) Mad-Max transcriptional repression is mediated by ternary complex formation with mammalian homologs of yeast repressor Sin3. *Cell* 80: 767-76
- Azzouz M, Le T, Ralph GS, Walmsley L, Monani UR, Lee DC, Wilkes F, Mitrophanous KA, Kingsman SM, Burghes AH, Mazarakis ND (2004) Lentivector-mediated SMN replacement in a mouse model of spinal muscular atrophy. *J Clin Invest* 114: 1726-31
- Baccon J, Pellizzoni L, Rappsilber J, Mann M, Dreyfuss G (2002) Identification and characterization of Gemin7, a novel component of the survival of motor neuron complex. *J Biol Chem* 277: 31957-62
- Bader MF, Doussau F, Chasserot-Golaz S, Vitale N, Gasman S (2004) Coupling actin and membrane dynamics during calcium-regulated exocytosis: a role for Rho and ARF GTPases. *Biochim Biophys Acta* 1742: 37-49
- Baes M, Gulick T, Choi HS, Martinoli MG, Simha D, Moore DD (1994) A new orphan member of the nuclear hormone receptor superfamily that interacts with a subset of retinoic acid response elements. *Mol Cell Biol* 14: 1544-52
- Baez MV, Boccaccio GL (2005) Mammalian Smaug is a translational repressor that forms cytoplasmic foci similar to stress granules. *J Biol Chem* 280: 43131-40
- Baker BS (1989) Sex in flies: the splice of life. *Nature* 340: 521-4
- Bannister AJ, Kouzarides T (1996) The CBP co-activator is a histone acetyltransferase. *Nature* 384: 641-3
- Baron P, Galimberti D, Meda L, Prat E, Scarpini E, Conti G, Moggio M, Prella A, Scarlato G (2000) Synergistic effect of beta-amyloid protein and interferon gamma on nitric oxide production by C2C12 muscle cells. *Brain* 123 ( Pt 2): 374-9
- Barth S, Liss M, Voss MD, Dobner T, Fischer U, Meister G, Grasser FA (2003) Epstein-Barr virus nuclear antigen 2 binds via its methylated arginine-glycine repeat to the survival motor neuron protein. *J Virol* 77: 5008-13
- Bassell GJ, Kelic S (2004) Binding proteins for mRNA localization and local translation, and their dysfunction in genetic neurological disease. *Curr Opin Neurobiol* 14: 574-81
- Bassell GJ, Zhang H, Byrd AL, Femino AM, Singer RH, Taneja KL, Lifshitz LM, Herman IM, Kosik KS (1998) Sorting of beta-actin mRNA and protein to neurites and growth cones in culture. *J Neurosci* 18: 251-65
- Bates S, Vousden KH (1999) Mechanisms of p53-mediated apoptosis. *Cell Mol Life Sci* 55: 28-37
- Battaglia G, Princivalle A, Forti F, Lizier C, Zeviani M (1997) Expression of the SMN gene, the spinal muscular atrophy determining gene, in the mammalian central nervous system. *Hum Mol Genet* 6: 1961-71
- Battle DJ, Lau CK, Wan L, Deng H, Lotti F, Dreyfuss G (2006) The Gemin5 protein of the SMN complex identifies snRNAs. *Mol Cell* 23: 273-9
- Bear JE, Svitkina TM, Krause M, Schafer DA, Loureiro JJ, Strasser GA, Maly IV, Chaga OY, Cooper JA, Borisy GG, Gertler FB (2002) Antagonism between Ena/VASP proteins and actin filament capping regulates fibroblast motility. *Cell* 109: 509-21
- Belcher CE, Drenkow J, Kehoe B, Gingeras TR, McNamara N, Lemjabbar H, Basbaum C, Relman DA (2000) The transcriptional responses of respiratory epithelial cells to Bordetella pertussis reveal host defensive and pathogen counter-defensive strategies. *Proc Natl Acad Sci U S A* 97: 13847-52
- Bell AC, West AG, Felsenfeld G (2001) Insulators and boundaries: versatile regulatory elements in the eukaryotic. *Science* 291: 447-50
- Belmont LD, Drubin DG (1998) The yeast V159N actin mutant reveals roles for actin dynamics in vivo. *J Cell Biol* 142: 1289-99
- Bennett CM, Kanki JP, Rhodes J, Liu TX, Paw BH, Kieran MW, Langenau DM, Delahaye-Brown A, Zon LI, Fleming MD, Look AT (2001) Myelopoiesis in the zebrafish, Danio rerio. *Blood* 98: 643-51
- Bentley D, O'Connor TP (1994) Cytoskeletal events in growth cone steering. *Curr Opin Neurobiol* 4: 43-8
- Bergin A, Kim G, Price DL, Sisodia SS, Lee MK, Rabin BA (1997) Identification and characterization of a mouse homologue of the spinal muscular atrophy-determining gene, survival motor neuron. *Gene* 204: 47-53

- Bergstrom TF, Josefsson A, Erlich HA, Gyllensten U (1998) Recent origin of HLA-DRB1 alleles and implications for human evolution. *Nat Genet* 18: 237-42
- Bertrand S, Burllet P, Clermont O, Huber C, Fondrat C, Thierry-Mieg D, Munnich A, Lefebvre S (1999) The RNA-binding properties of SMN: deletion analysis of the zebrafish orthologue defines domains conserved in evolution. *Hum Mol Genet* 8: 775-82
- Biamonti G, Riva S (1994) New insights into the auxiliary domains of eukaryotic RNA binding proteins. *FEBS Lett* 340: 1-8
- Bignell GR, Huang J, Greshock J, Watt S, Butler A, West S, Grigorova M, Jones KW, Wei W, Stratton MR, Futreal PA, Weber B, Shaper MH, Wooster R (2004) High-resolution analysis of DNA copy number using oligonucleotide microarrays. *Genome Res* 14: 287-95
- Bird A (1992) The essentials of DNA methylation. *Cell* 70: 5-8
- Bird A (2002) DNA methylation patterns and epigenetic memory. *Genes Dev* 16: 6-21
- Bird AP (1986) CpG-rich islands and the function of DNA methylation. *Nature* 321: 209-13
- Bjerling P, Silverstein RA, Thon G, Caudy A, Grewal S, Ekwall K (2002) Functional divergence between histone deacetylases in fission yeast by distinct cellular localization and in vivo specificity. *Mol Cell Biol* 22: 2170-81
- Blagoev B, Kratchmarova I, Ong SE, Nielsen M, Foster LJ, Mann M (2003) A proteomics strategy to elucidate functional protein-protein interactions applied to EGF signaling. *Nat Biotechnol* 21: 315-8
- Blanc V, Navaratnam N, Henderson JO, Anant S, Kennedy S, Jarmuz A, Scott J, Davidson NO (2001) Identification of GRY-RBP as an apolipoprotein B RNA-binding protein that interacts with both apobec-1 and apobec-1 complementation factor to modulate C to U editing. *J Biol Chem* 276: 10272-83
- Bloom O, Evergren E, Tomilin N, Kjaerulf O, Low P, Brodin L, Pieribone VA, Greengard P, Shupliakov O (2003) Colocalization of synapsin and actin during synaptic vesicle recycling. *J Cell Biol* 161: 737-47
- Boda B, Mas C, Giudicelli C, Nepote V, Guimiot F, Levacher B, Zvara A, Santha M, LeGall I, Simonneau M (2004) Survival motor neuron SMN1 and SMN2 gene promoters: identical sequences and differential expression in neurons and non-neuronal cells. *Eur J Hum Genet* 12: 729-37
- Boisvert FM, Cote J, Boulanger MC, Cleroux P, Bachand F, Autexier C, Richard S (2002) Symmetrical dimethylarginine methylation is required for the localization of SMN in Cajal bodies and pre-mRNA splicing. *J Cell Biol* 159: 957-69
- Brahe C (2000) Copies of the survival motor neuron gene in spinal muscular atrophy: the more, the better. *Neuromuscul Disord* 10: 274-5
- Brahe C, Servidei S, Zappata S, Ricci E, Tonali P, Neri G (1995) Genetic homogeneity between childhood-onset and adult-onset autosomal recessive spinal muscular atrophy. *Lancet* 346: 741-2
- Brahe C, Vitali T, Tiziano FD, Angelozzi C, Pinto AM, Borgo F, Moscato U, Bertini E, Mercuri E, Neri G (2005) Phenylbutyrate increases SMN gene expression in spinal muscular atrophy patients. *Eur J Hum Genet* 13: 256-9
- Brahms H, Meheus L, de Brabandere V, Fischer U, Luhrmann R (2001) Symmetrical dimethylation of arginine residues in spliceosomal Sm protein B/B' and the Sm-like protein LSm4, and their interaction with the SMN protein. *Rna* 7: 1531-42
- Braun A, Aszodi A, Hellebrand H, Berna A, Fassler R, Brandau O (2002) Genomic organization of profilin-III and evidence for a transcript expressed exclusively in testis. *Gene* 283: 219-25
- Bray D, Chapman K (1985) Analysis of microspike movements on the neuronal growth cone. *J Neurosci* 5: 3204-13
- Brichta L, Hofmann Y, Hahnen E, Siebzehrubl FA, Raschke H, Blumcke I, Eyupoglu IY, Wirth B (2003) Valproic acid increases the SMN2 protein level: a well-known drug as a potential therapy for spinal muscular atrophy. *Hum Mol Genet* 12: 2481-9
- Broccolini A, Engel WK, Askanas V (1999) Localization of survival motor neuron protein in human apoptotic-like and regenerating muscle fibers, and neuromuscular junctions. *Neuroreport* 10: 1637-41
- Brower SM, Honts JE, Adams AE (1995) Genetic analysis of the fimbrin-actin binding interaction in *Saccharomyces cerevisiae*. *Genetics* 140: 91-101
- Brown AJ, Hutchings C, Burke JF, Mayne LV (1999) Application of a rapid method (targeted display) for the identification of differentially expressed mRNAs following NGF-induced neuronal differentiation in PC12 cells. *Mol Cell Neurosci* 13: 119-30

- Brzustowicz LM, Lehner T, Castilla LH, Penchaszadeh GK, Wilhelmsen KC, Daniels R, Davies KE, Leppert M, Ziter F, Wood D, et al. (1990) Genetic mapping of chronic childhood-onset spinal muscular atrophy to chromosome 5q11.2-13.3. *Nature* 344: 540-1
- Buhler D, Raker V, Luhrmann R, Fischer U (1999) Essential role for the tudor domain of SMN in spliceosomal U snRNP assembly: implications for spinal muscular atrophy. *Hum Mol Genet* 8: 2351-7
- Buratowski S (1994) The basics of basal transcription by RNA polymerase II. *Cell* 77: 1-3
- Burd CG, Dreyfuss G (1994) RNA binding specificity of hnRNP A1: significance of hnRNP A1 high-affinity binding sites in pre-mRNA splicing. *Embo J* 13: 1197-204
- Burge CB, Tuschl PA, Sharp PA (1999) Splicing of precursors to mRNAs by the spliceosomes, in: R.F. Gesteland, J.F. Atkins (Eds.), *The RNA World*. Cold Spring Harbour Laboratory Press, Cold Spring Harbour, New York: 525-560
- Burghes AH (1997) When is a deletion not a deletion? When it is converted. *Am J Hum Genet* 61: 9-15
- Burglen L, Lefebvre S, Clermont O, Burlet P, Viollet L, Cruaud C, Munnich A, Melki J (1996) Structure and organization of the human survival motor neurone (SMN) gene. *Genomics* 32: 479-82
- Burk O, Arnold KA, Geick A, Tegude H, Eichelbaum M (2005) A role for constitutive androstane receptor in the regulation of human intestinal MDR1 expression. *Biol Chem* 386: 503-13
- Burk O, Koch I, Raucy J, Hustert E, Eichelbaum M, Brockmoller J, Zanger UM, Wojnowski L (2004) The induction of cytochrome P450 3A5 (CYP3A5) in the human liver and intestine is mediated by the xenobiotic sensors pregnane X receptor (PXR) and constitutively activated receptor (CAR). *J Biol Chem* 279: 38379-85
- Burlet P, Burglen L, Clermont O, Lefebvre S, Viollet L, Munnich A, Melki J (1996) Large scale deletions of the 5q13 region are specific to Werdnig-Hoffmann disease. *J Med Genet* 33: 281-3
- Burlet P, Huber C, Bertrand S, Ludosky MA, Zwaenepoel I, Clermont O, Roume J, Delezoide AL, Cartaud J, Munnich A, Lefebvre S (1998) The distribution of SMN protein complex in human fetal tissues and its alteration in spinal muscular atrophy. *Hum Mol Genet* 7: 1927-33
- Byers RK, Banker BQ (1961) Infantile muscular atrophy. *Arch Neurol* 5: 140-64
- Caceres JF, Misteli T, Screaton GR, Spector DL, Krainer AR (1997) Role of the modular domains of SR proteins in subnuclear localization and alternative splicing specificity. *J Cell Biol* 138: 225-38
- Campbell L, Hunter KM, Mohaghegh P, Tinsley JM, Brasch MA, Davies KE (2000) Direct interaction of Smn with dp103, a putative RNA helicase: a role for Smn in transcription regulation? *Hum Mol Genet* 9: 1093-100
- Campbell L, Potter A, Ignatius J, Dubowitz V, Davies K (1997) Genomic variation and gene conversion in spinal muscular atrophy: implications for disease process and clinical phenotype. *Am J Hum Genet* 61: 40-50
- Cardno AG, Bowen T, Guy CA, Jones LA, McCarthy G, Williams NM, Murphy KC, Spurlock G, Gray M, Sanders RD, Craddock N, McGuffin P, Owen MJ, O'Donovan MC (1999a) CAG repeat length in the hKCa3 gene and symptom dimensions in schizophrenia. *Biol Psychiatry* 45: 1592-6
- Cardno AG, Jones LA, Murphy KC, Sanders RD, Asherson P, Owen MJ, McGuffin P (1999b) Dimensions of psychosis in affected sibling pairs. *Schizophr Bull* 25: 841-50
- Cardno AG, Sham PC, Farmer AE, Murray RM, McGuffin P (2002) Heritability of Schneider's first-rank symptoms. *Br J Psychiatry* 180: 35-8
- Carissimi C, Saieva L, Baccon J, Chiarella P, Maiolica A, Sawyer A, Rappsilber J, Pellizzoni L (2006) Gemin8 is a novel component of the survival motor neuron complex and functions in snRNP assembly. *J Biol Chem*
- Carlier MF, Le Clainche C, Wiesner S, Pantaloni D (2003a) Actin-based motility: from molecules to movement. *Bioessays* 25: 336-45
- Carlier MF, Wiesner S, Le Clainche C, Pantaloni D (2003b) Actin-based motility as a self-organized system: mechanism and reconstitution in vitro. *C R Biol* 326: 161-70
- Carnegie GK, Sleeman JE, Morrice N, Hastie CJ, Pegg MW, Philp A, Lamond AI, Cohen PT (2003) Protein phosphatase 4 interacts with the survival of motor neurons complex and enhances the temporal localisation of snRNPs. *J Cell Sci Pt*
- Cartegni L, Krainer AR (2002) Disruption of an SF2/ASF-dependent exonic splicing enhancer in SMN2 causes spinal muscular atrophy in the absence of SMN1. *Nat Genet* 30: 377-84
- Cartegni L, Krainer AR (2003) Correction of disease-associated exon skipping by synthetic exon-specific activators. *Nat Struct Biol* 10: 120-5

- Caruso JF, Signorile JF, Perry AC, Leblanc B, Williams R, Clark M, Bamman MM (1995) The effects of albuterol and isokinetic exercise on the quadriceps muscle group. *Med Sci Sports Exerc* 27: 1471-6
- Castellana N, Dhamdhare K, Sridhar S, Schwartz R (2006) Relaxing haplotype block models for association testing. *Pac Symp Biocomput*: 454-66
- Chafel MM, Shen W, Matsudaira P (1995) Sequential expression and differential localization of I-, L-, and T-fimbrin during differentiation of the mouse intestine and yolk sac. *Dev Dyn* 203: 141-51
- Chan YB, Miguel-Aliaga I, Franks C, Thomas N, Trulzsch B, Sattelle DB, Davies KE, van den Heuvel M (2003) Neuromuscular defects in a *Drosophila* survival motor neuron gene mutant. *Hum Mol Genet* 12: 1367-76
- Chang HC, Hung WC, Chuang YJ, Jong YJ (2004) Degradation of survival motor neuron (SMN) protein is mediated via the ubiquitin/proteasome pathway. *Neurochem Int* 45: 1107-12
- Chang JG, Hsieh-Li HM, Jong YJ, Wang NM, Tsai CH, Li H (2001) Treatment of spinal muscular atrophy by sodium butyrate. *Proc Natl Acad Sci U S A* 98: 9808-13
- Chang M, Bellaoui M, Boone C, Brown GW (2002) A genome-wide screen for methyl methanesulfonate-sensitive mutants reveals genes required for S phase progression in the presence of DNA damage. *Proc Natl Acad Sci U S A* 99: 16934-9
- Charroux B, Pellizzoni L, Perkinson RA, Shevchenko A, Mann M, Dreyfuss G (1999) Gemin3: A novel DEAD box protein that interacts with SMN, the spinal muscular atrophy gene product, and is a component of gems. *J Cell Biol* 147: 1181-94
- Charroux B, Pellizzoni L, Perkinson RA, Yong J, Shevchenko A, Mann M, Dreyfuss G (2000) Gemin4. A novel component of the SMN complex that is found in both gems and nucleoli. *J Cell Biol* 148: 1177-86
- Chen Y, Ferguson SS, Negishi M, Goldstein JA (2003) Identification of constitutive androstane receptor and glucocorticoid receptor binding sites in the CYP2C19 promoter. *Mol Pharmacol* 64: 316-24
- Cheng D, Marner J, Rubenstein PA (1999) Interaction in vivo and in vitro between the yeast fimbrin, SAC6P, and a polymerization-defective yeast actin (V266G and L267G). *J Biol Chem* 274: 35873-80
- Cifuentes-Diaz C, Frugier T, Tiziano FD, Lacene E, Roblot N, Joshi V, Moreau MH, Melki J (2001) Deletion of murine SMN exon 7 directed to skeletal muscle leads to severe muscular dystrophy. *J Cell Biol* 152: 1107-14
- Cifuentes-Diaz C, Nicole S, Velasco ME, Borra-Cebrian C, Panozzo C, Frugier T, Millet G, Roblot N, Joshi V, Melki J (2002) Neurofilament accumulation at the motor endplate and lack of axonal sprouting in a spinal muscular atrophy mouse model. *Hum Mol Genet* 11: 1439-47
- Cihak A (1974) Biological effects of 5-azacytidine in eukaryotes. *Oncology* 30: 405-22
- Claus P, Bruns AF, Grothe C (2004) Fibroblast growth factor-2(23) binds directly to the survival of motoneuron protein and is associated with small nuclear RNAs. *Biochem J* 384: 559-65
- Cobben JM, van der Steege G, Grootsholten P, de Visser M, Scheffer H, Buys CH (1995) Deletions of the survival motor neuron gene in unaffected siblings of patients with spinal muscular atrophy. *Am J Hum Genet* 57: 805-8
- Colella S, Shen L, Baggerly KA, Issa JP, Krahe R (2003) Sensitive and quantitative universal Pyrosequencing methylation analysis of CpG sites. *Biotechniques* 35: 146-50
- Coller HA, Grandori C, Tamayo P, Colbert T, Lander ES, Eisenman RN, Golub TR (2000) Expression analysis with oligonucleotide microarrays reveals that MYC regulates genes involved in growth, cell cycle, signaling, and adhesion. *Proc Natl Acad Sci U S A* 97: 3260-5
- Coluccio LM, Bretscher A (1989) Reassociation of microvillar core proteins: making a microvillar core in vitro. *J Cell Biol* 108: 495-502
- Covert DD, Le TT, McAndrew PE, Strasswimmer J, Crawford TO, Mendell JR, Coulson SE, Androphy EJ, Prior TW, Burghes AH (1997) The survival motor neuron protein in spinal muscular atrophy. *Hum Mol Genet* 6: 1205-14
- Corden JL, Patturajan M (1997) A CTD function linking transcription to splicing. *Trends Biochem Sci* 22: 413-6
- Cossart P (2000) Actin-based motility of pathogens: the Arp2/3 complex is a central player. *Cell Microbiol* 2: 195-205
- Crawford DC, Nickerson DA (2005) Definition and clinical importance of haplotypes. *Annu Rev Med* 56: 303-20

- Crawford TO (2004) Concerns about the design of clinical trials for spinal muscular atrophy. *Neuromuscul Disord* 14: 456-60
- Crawford TO, Pardo CA (1996) The neurobiology of childhood spinal muscular atrophy. *Neurobiol Dis* 3: 97-110
- Cusin V, Clermont O, Gerard B, Chanterreau D, Elion J (2003) Prevalence of SMN1 deletion and duplication in carrier and normal populations: implication for genetic counselling. *J Med Genet* 40: e39
- Cutting GR (2005) Modifier genetics: cystic fibrosis. *Annu Rev Genomics Hum Genet* 6: 237-60
- Da Silva JS, Medina M, Zuliani C, Di Nardo A, Witke W, Dotti CG (2003) RhoA/ROCK regulation of neuritogenesis via profilin IIa-mediated control of actin stability. *J Cell Biol* 162: 1267-79
- Daly MJ, Rioux JD, Schaffner SF, Hudson TJ, Lander ES (2001) High-resolution haplotype structure in the human genome. *Nat Genet* 29: 229-32
- Daudet N, Lebart MC (2002) Transient expression of the t-isoform of plastins/fimbrin in the stereocilia of developing auditory hair cells. *Cell Motil Cytoskeleton* 53: 326-36
- Davies J, Alton E, Griesenbach U (2005) Cystic fibrosis modifier genes. *J R Soc Med* 98 Suppl 45: 47-54
- Dawson E, Abecasis GR, Bumpstead S, Chen Y, Hunt S, Beare DM, Pabial J, Dibling T, Tinsley E, Kirby S, Carter D, Papaspyridonos M, Livingstone S, Ganske R, Lohmussaar E, Zernant J, Tonisson N, Remm M, Magi R, Puurand T, Vilo J, Kurg A, Rice K, Deloukas P, Mott R, Metspalu A, Bentley DR, Cardon LR, Dunham I (2002) A first-generation linkage disequilibrium map of human chromosome 22. *Nature* 418: 544-8
- de Arruda MV, Watson S, Lin CS, Leavitt J, Matsudaira P (1990) Fimbrin is a homologue of the cytoplasmic phosphoprotein plastin and has domains homologous with calmodulin and actin gelation proteins. *J Cell Biol* 111: 1069-79
- de Ruijter AJ, van Gennip AH, Caron HN, Kemp S, van Kuilenburg AB (2003) Histone deacetylases (HDACs): characterization of the classical HDAC family. *Biochem J* 370: 737-49
- Debey S, Schoenbeck U, Hellmich M, Gathof BS, Pillai R, Zander T, Schultze JL (2004) Comparison of different isolation techniques prior gene expression profiling of blood derived cells: impact on physiological responses, on overall expression and the role of different cell types. *Pharmacogenomics J* 4: 193-207
- Deininger PL, Batzer MA (1999) Alu repeats and human disease. *Mol Genet Metab* 67: 183-93
- Delanote V, Van Impe K, De Corte V, Bruyneel E, Vetter G, Boucherie C, Mareel M, Vandekerckhove J, Friederich E, Gettemans J (2005a) Molecular basis for dissimilar nuclear trafficking of the actin-bundling protein isoforms T- and L-plastin. *Traffic* 6: 335-45
- Delanote V, Vandekerckhove J, Gettemans J (2005b) Plastins: versatile modulators of actin organization in (patho)physiological cellular processes. *Acta Pharmacol Sin* 26: 769-79
- Dent EW, Gertler FB (2003) Cytoskeletal dynamics and transport in growth cone motility and axon guidance. *Neuron* 40: 209-27
- Dent EW, Meiri KF (1992) GAP-43 phosphorylation is dynamically regulated in individual growth cones. *J Neurobiol* 23: 1037-53
- Dent EW, Meiri KF (1998) Distribution of phosphorylated GAP-43 (neuromodulin) in growth cones directly reflects growth cone behavior. *J Neurobiol* 35: 287-99
- DiDonato CJ, Chen XN, Noya D, Korenberg JR, Nadeau JH, Simard LR (1997a) Cloning, characterization, and copy number of the murine survival motor neuron gene: homolog of the spinal muscular atrophy-determining gene. *Genome Res* 7: 339-52
- DiDonato CJ, Ingraham SE, Mendell JR, Prior TW, Lenard S, Moxley RT, 3rd, Florence J, Burghes AH (1997b) Deletion and conversion in spinal muscular atrophy patients: is there a relationship to severity? *Ann Neurol* 41: 230-7
- DiDonato CJ, Lorson CL, De Repentigny Y, Simard L, Chartrand C, Androphy EJ, Kothary R (2001) Regulation of murine survival motor neuron (Smn) protein levels by modifying Smn exon 7 splicing. *Hum Mol Genet* 10: 2727-36
- DiDonato CJ, Morgan K, Carpten JD, Fuerst P, Ingraham SE, Prescott G, McPherson JD, Wirth B, Zerres K, Hurko O, et al. (1994) Association between Ag1-CA alleles and severity of autosomal recessive proximal spinal muscular atrophy. *Am J Hum Genet* 55: 1218-29
- Diehn M, Alizadeh AA, Rando OJ, Liu CL, Stankunas K, Botstein D, Crabtree GR, Brown PO (2002) Genomic expression programs and the integration of the CD28 costimulatory signal in T cell activation. *Proc Natl Acad Sci U S A* 99: 11796-801

- dos Remedios CG, Chhabra D, Kekic M, Dedova IV, Tsubakihara M, Berry DA, Nosworthy NJ (2003) Actin binding proteins: regulation of cytoskeletal microfilaments. *Physiol Rev* 83: 433-73
- dos Remedios CG, Thomas DD (2001) An overview of actin structure and actin-binding proteins. *Results Probl Cell Differ* 32: 1-7
- Dostie J, Mourelatos Z, Yang M, Sharma A, Dreyfuss G (2003) Numerous microRNPs in neuronal cells containing novel microRNAs. *Rna* 9: 180-6
- Dreyfuss G, Matunis MJ, Pinol-Roma S, Burd CG (1993) hnRNP proteins and the biogenesis of mRNA. *Annu Rev Biochem* 62: 289-321
- Drubin DG, Feinstein SC, Shooter EM, Kirschner MW (1985) Nerve growth factor-induced neurite outgrowth in PC12 cells involves the coordinate induction of microtubule assembly and assembly-promoting factors. *J Cell Biol* 101: 1799-807
- Drubin DG, Miller KG, Botstein D (1988) Yeast actin-binding proteins: evidence for a role in morphogenesis. *J Cell Biol* 107: 2551-61
- Dubowitz V (1964) Infantile Muscular Atrophy. a Prospective Study with Particular Reference to a Slowly Progressive Variety. *Brain* 87: 707-18
- Dutartre H, Davoust J, Gorvel JP, Chavrier P (1996) Cytokinesis arrest and redistribution of actin-cytoskeleton regulatory components in cells expressing the Rho GTPase CDC42Hs. *J Cell Sci* 109 ( Pt 2): 367-77
- Eden S, Cedar H (1994) Role of DNA methylation in the regulation of transcription. *Curr Opin Genet Dev* 4: 255-9
- Endo M, Ohashi K, Sasaki Y, Goshima Y, Niwa R, Uemura T, Mizuno K (2003) Control of growth cone motility and morphology by LIM kinase and Slingshot via phosphorylation and dephosphorylation of cofilin. *J Neurosci* 23: 2527-37
- Endrizzi M, Huang S, Scharf JM, Kelter AR, Wirth B, Kunkel LM, Miller W, Dietrich WF (1999) Comparative sequence analysis of the mouse and human Lgn1/SMA interval. *Genomics* 60: 137-51
- Eng H, Lund K, Campenot RB (1999) Synthesis of beta-tubulin, actin, and other proteins in axons of sympathetic neurons in compartmented cultures. *J Neurosci* 19: 1-9
- Esper L, Eldin P, Gongora C, Bayard B, Harper F, Chelbi-Alix MK, Bertrand E, Degols G, Mechti N (2006) The exonuclease ISG20 mainly localizes in the nucleolus and the Cajal (Coiled) bodies and is associated with nuclear SMN protein-containing complexes. *J Cell Biochem*
- Faivre-Sarrahil C, Lena JY, Had L, Vignes M, Lindberg U (1993) Location of profilin at presynaptic sites in the cerebellar cortex; implication for the regulation of the actin-polymerization state during axonal elongation and synaptogenesis. *J Neurocytol* 22: 1060-72
- Fakhrai-Rad H, Pourmand N, Ronaghi M (2002) Pyrosequencing: an accurate detection platform for single nucleotide polymorphisms. *Hum Mutat* 19: 479-85
- Fambrough D, McClure K, Kazlauskas A, Lander ES (1999) Diverse signaling pathways activated by growth factor receptors induce broadly overlapping, rather than independent, sets of genes. *Cell* 97: 727-41
- Fan L, Simard LR (2002) Survival motor neuron (SMN) protein: role in neurite outgrowth and neuromuscular maturation during neuronal differentiation and development. *Hum Mol Genet* 11: 1605-14
- Farina KL, Huttelmaier S, Musunuru K, Darnell R, Singer RH (2003) Two ZBP1 KH domains facilitate beta-actin mRNA localization, granule formation, and cytoskeletal attachment. *J Cell Biol* 160: 77-87
- Feldkotter M, Schwarzer V, Wirth R, Wienker TF, Wirth B (2002) Quantitative analyses of SMN1 and SMN2 based on real-time lightCycler PCR: fast and highly reliable carrier testing and prediction of severity of spinal muscular atrophy. *Am J Hum Genet* 70: 358-68
- Feng W, Gubitza AK, Wan L, Battle DJ, Dostie J, Golembe TJ, Dreyfuss G (2005) Gemins modulate the expression and activity of the SMN complex. *Hum Mol Genet* 14: 1605-11
- Ferguson SS, Chen Y, LeCluyse EL, Negishi M, Goldstein JA (2005) Human CYP2C8 is transcriptionally regulated by the nuclear receptors constitutive androstane receptor, pregnane X receptor, glucocorticoid receptor, and hepatic nuclear factor 4alpha. *Mol Pharmacol* 68: 747-57
- Ferguson SS, LeCluyse EL, Negishi M, Goldstein JA (2002) Regulation of human CYP2C9 by the constitutive androstane receptor: discovery of a new distal binding site. *Mol Pharmacol* 62: 737-46
- Ferri A, Melki J, Kato AC (2004) Progressive and selective degeneration of motoneurons in a mouse model of SMA. *Neuroreport* 15: 275-80

- Fidzianska A (2002) Suicide muscle cell programme-apoptosis. Ultrastructural study. *Folia Neuropathol* 40: 27-32
- Fidzianska A, Rafalowska J (2002) Motoneuron death in normal and spinal muscular atrophy-affected human fetuses. *Acta Neuropathol (Berl)* 104: 363-8
- Fischer U, Liu Q, Dreyfuss G (1997) The SMN-SIP1 complex has an essential role in spliceosomal snRNP biogenesis. *Cell* 90: 1023-9
- Fischle W, Dequiedt F, Hendzel MJ, Guenther MG, Lazar MA, Voelter W, Verdin E (2002) Enzymatic activity associated with class II HDACs is dependent on a multiprotein complex containing HDAC3 and SMRT/N-CoR. *Mol Cell* 9: 45-57
- Forman BM, Tzamelis I, Choi HS, Chen J, Simha D, Seol W, Evans RM, Moore DD (1998) Androstane metabolites bind to and deactivate the nuclear receptor CAR-beta. *Nature* 395: 612-5
- Frey D, Laux T, Xu L, Schneider C, Caroni P (2000) Shared and unique roles of CAP23 and GAP43 in actin regulation, neurite outgrowth, and anatomical plasticity. *J Cell Biol* 149: 1443-54
- Friederich E, Huet C, Arpin M, Louvard D (1989) Villin induces microvilli growth and actin redistribution in transfected fibroblasts. *Cell* 59: 461-75
- Friesen WJ, Dreyfuss G (2000) Specific sequences of the Sm and Sm-like (Lsm) proteins mediate their interaction with the spinal muscular atrophy disease gene product (SMN). *J Biol Chem* 275: 26370-5
- Friesen WJ, Massenet S, Paushkin S, Wyce A, Dreyfuss G (2001a) SMN, the product of the spinal muscular atrophy gene, binds preferentially to dimethylarginine-containing protein targets. *Mol Cell* 7: 1111-7
- Friesen WJ, Paushkin S, Wyce A, Massenet S, Pesiridis GS, Van Duyne G, Rappsilber J, Mann M, Dreyfuss G (2001b) The methylosome, a 20S complex containing JBP1 and pICln, produces dimethylarginine-modified Sm proteins. *Mol Cell Biol* 21: 8289-300
- Friesen WJ, Wyce A, Paushkin S, Abel L, Rappsilber J, Mann M, Dreyfuss G (2002) A novel WD repeat protein component of the methylosome binds Sm proteins. *J Biol Chem* 277: 8243-7
- Fritsche M, Haessler C, Brandner G (1993) Induction of nuclear accumulation of the tumor-suppressor protein p53 by DNA-damaging agents. *Oncogene* 8: 307-18
- Frommer M, McDonald LE, Millar DS, Collis CM, Watt F, Grigg GW, Molloy PL, Paul CL (1992) A genomic sequencing protocol that yields a positive display of 5-methylcytosine residues in individual DNA strands. *Proc Natl Acad Sci U S A* 89: 1827-31
- Frugier T, Tiziano FD, Cifuentes-Diaz C, Miniou P, Roblot N, Dierich A, Le Meur M, Melki J (2000) Nuclear targeting defect of SMN lacking the C-terminus in a mouse model of spinal muscular atrophy. *Hum Mol Genet* 9: 849-58
- Fu XD (2004) Towards a splicing code. *Cell* 119: 736-8
- Gabanella F, Carissimi C, Usiello A, Pellizzoni L (2005) The activity of the spinal muscular atrophy protein is regulated during development and cellular differentiation. *Hum Mol Genet* 14: 3629-42
- Gabriel SB, Schaffner SF, Nguyen H, Moore JM, Roy J, Blumenstiel B, Higgins J, DeFelice M, Lochner A, Faggart M, Liu-Cordero SN, Rotimi C, Adeyemo A, Cooper R, Ward R, Lander ES, Daly MJ, Altshuler D (2002) The structure of haplotype blocks in the human genome. *Science* 296: 2225-9
- Gagneux P, Wills C, Gerloff U, Tautz D, Morin PA, Boesch C, Fruth B, Hohmann G, Ryder OA, Woodruff DS (1999) Mitochondrial sequences show diverse evolutionary histories of African hominoids. *Proc Natl Acad Sci U S A* 96: 5077-82
- Galan JE, Zhou D (2000) Striking a balance: modulation of the actin cytoskeleton by Salmonella. *Proc Natl Acad Sci U S A* 97: 8754-61
- Gall JG (2003a) The centennial of the Cajal body. *Nat Rev Mol Cell Biol* 4: 975-80
- Gall JG (2003b) [A role for Cajal bodies in assembly of the nuclear transcription machinery]. *Tsitologiya* 45: 971-5
- Gall JG, Bellini M, Wu Z, Murphy C (1999) Assembly of the nuclear transcription and processing machinery: Cajal bodies (coiled bodies) and transcriptosomes. *Mol Biol Cell* 10: 4385-402
- Gallant PE (2000) Axonal protein synthesis and transport. *J Neurocytol* 29: 779-82
- Gallouzi IE, Brennan CM, Stenberg MG, Swanson MS, Eversole A, Maizels N, Steitz JA (2000) HuR binding to cytoplasmic mRNA is perturbed by heat shock. *Proc Natl Acad Sci U S A* 97: 3073-8
- Gangwani L (2006) Deficiency of the zinc finger protein ZPR1 causes defects in transcription and cell cycle progression. *J Biol Chem* 281: 40330-40
- Gangwani L, Flavell RA, Davis RJ (2005) ZPR1 is essential for survival and is required for localization of the survival motor neurons (SMN) protein to Cajal bodies. *Mol Cell Biol* 25: 2744-56

- Gangwani L, Mikrut M, Theroux S, Sharma M, Davis RJ (2001) Spinal muscular atrophy disrupts the interaction of ZPR1 with the SMN protein. *Nat Cell Biol* 3: 376-83
- Garcia-Alvarez B, Bobkov A, Sonnenberg A, de Pereda JM (2003) Structural and functional analysis of the actin binding domain of plectin suggests alternative mechanisms for binding to F-actin and integrin beta4. *Structure* 11: 615-25
- Gavrilov DK, Shi X, Das K, Gilliam TC, Wang CH (1998) Differential SMN2 expression associated with SMA severity. *Nat Genet* 20: 230-1
- Gennarelli M, Lucarelli M, Capon F, Pizzuti A, Merlini L, Angelini C, Novelli G, Dallapiccola B (1995) Survival motor neuron gene transcript analysis in muscles from spinal muscular atrophy patients. *Biochem Biophys Res Commun* 213: 342-8
- Gertler FB, Niebuhr K, Reinhard M, Wehland J, Soriano P (1996) Mena, a relative of VASP and Drosophila Enabled, is implicated in the control of microfilament dynamics. *Cell* 87: 227-39
- Giavazzi A, Setola V, Simonati A, Battaglia G (2006) Neuronal-specific roles of the survival motor neuron protein: evidence from survival motor neuron expression patterns in the developing human central nervous system. *J Neuropathol Exp Neurol* 65: 267-77
- Giesemann T, Rathke-Hartlieb S, Rothkegel M, Bartsch JW, Buchmeier S, Jockusch BM, Jockusch H (1999) A role for polyproline motifs in the spinal muscular atrophy protein SMN. Profilins bind to and colocalize with smn in nuclear gems. *J Biol Chem* 274: 37908-14
- Giganti A, Plastino J, Janji B, Van Troys M, Lentz D, Ampe C, Sykes C, Friederich E (2005) Actin-filament cross-linking protein T-plastin increases Arp2/3-mediated actin-based movement. *J Cell Sci* 118: 1255-65
- Glenney JR, Jr., Kaulfus P, Matsudaira P, Weber K (1981) F-actin binding and bundling properties of fimbrin, a major cytoskeletal protein of microvillus core filaments. *J Biol Chem* 256: 9283-8
- Goldberg DJ, Burmeister DW (1986) Stages in axon formation: observations of growth of *Aplysia* axons in culture using video-enhanced contrast-differential interference contrast microscopy. *J Cell Biol* 103: 1921-31
- Goldberg DJ, Foley MS, Tang D, Grabham PW (2000) Recruitment of the Arp2/3 complex and mena for the stimulation of actin polymerization in growth cones by nerve growth factor. *J Neurosci Res* 60: 458-67
- Goldsmith SC, Pokala N, Shen W, Fedorov AA, Matsudaira P, Almo SC (1997) The structure of an actin-crosslinking domain from human fimbrin. *Nat Struct Biol* 4: 708-12
- Goldstein D, Djeu J, Latter G, Burbeck S, Leavitt J (1985) Abundant synthesis of the transformation-induced protein of neoplastic human fibroblasts, plastin, in normal lymphocytes. *Cancer Res* 45: 5643-7
- Goley ED, Ohkawa T, Mancuso J, Woodruff JB, D'Alessio JA, Cande WZ, Volkman LE, Welch MD (2006) Dynamic nuclear actin assembly by Arp2/3 complex and a baculovirus WASP-like protein. *Science* 314: 464-7
- Golub TR, Slonim DK, Tamayo P, Huard C, Gaasenbeek M, Mesirov JP, Coller H, Loh ML, Downing JR, Caligiuri MA, Bloomfield CD, Lander ES (1999) Molecular classification of cancer: class discovery and class prediction by gene expression monitoring. *Science* 286: 531-7
- Goodwin B, Hodgson E, D'Costa DJ, Robertson GR, Liddle C (2002) Transcriptional regulation of the human CYP3A4 gene by the constitutive androstane receptor. *Mol Pharmacol* 62: 359-65
- Gossen M, Bujard H (1992) Tight control of gene expression in mammalian cells by tetracycline-responsive promoters. *Proc Natl Acad Sci U S A* 89: 5547-51
- Graham FL, Smiley J, Russell WC, Nairn R (1977) Characteristics of a human cell line transformed by DNA from human adenovirus type 5. *J Gen Virol* 36: 59-74
- Greene LA, Burstein DE, Black MM (1982) The role of transcription-dependent priming in nerve growth factor promoted neurite outgrowth. *Dev Biol* 91: 305-16
- Greene LA, Tischler AS (1976) Establishment of a noradrenergic clonal line of rat adrenal pheochromocytoma cells which respond to nerve growth factor. *Proc Natl Acad Sci U S A* 73: 2424-8
- Greensmith L, Vrbova G (1997) Disturbances of neuromuscular interaction may contribute to muscle weakness in spinal muscular atrophy. *Neuromuscul Disord* 7: 369-72
- Grimmler M, Otter S, Peter C, Muller F, Chari A, Fischer U (2005) Unrip, a factor implicated in cap-independent translation, associates with the cytosolic SMN complex and influences its intracellular localization. *Hum Mol Genet* 14: 3099-111

- Grohmann K, Schuelke M, Diers A, Hoffmann K, Lucke B, Adams C, Bertini E, Leonhardt-Horti H, Muntoni F, Ouvrier R, Pfeufer A, Rossi R, Van Maldergem L, Wilmshurst JM, Wienker TF, Sendtner M, Rudnik-Schoneborn S, Zerres K, Hubner C (2001) Mutations in the gene encoding immunoglobulin mu-binding protein 2 cause spinal muscular atrophy with respiratory distress type 1. *Nat Genet* 29: 75-7
- Grohmann K, Wienker TF, Saar K, Rudnik-Schoneborn S, Stoltenburg-Didinger G, Rossi R, Novelli G, Nurnberg G, Pfeufer A, Wirth B, Reis A, Zerres K, Hubner C (1999) Diaphragmatic spinal muscular atrophy with respiratory distress is heterogeneous, and one form is linked to chromosome 11q13-q21. *Am J Hum Genet* 65: 1459-62
- Grosset C, Chen CY, Xu N, Sonenberg N, Jacquemin-Sablon H, Shyu AB (2000) A mechanism for translationally coupled mRNA turnover: interaction between the poly(A) tail and a c-fos RNA coding determinant via a protein complex. *Cell* 103: 29-40
- Grozinger CM, Hassig CA, Schreiber SL (1999) Three proteins define a class of human histone deacetylases related to yeast Hda1p. *Proc Natl Acad Sci U S A* 96: 4868-73
- Gubitz AK, Feng W, Dreyfuss G (2004) The SMN complex. *Exp Cell Res* 296: 51-6
- Gubitz AK, Mourelatos Z, Abel L, Rappsilber J, Mann M, Dreyfuss G (2002) Gemin5, a novel WD repeat protein component of the SMN complex that binds Sm proteins. *J Biol Chem* 277: 5631-6
- Gudbjartsson DF, Jonasson K, Frigge ML, Kong A (2000) Allegro, a new computer program for multipoint linkage analysis. *Nat Genet* 25: 12-3
- Guerrero I, Pellicer A, Burstein DE (1988) Dissociation of c-fos from ODC expression and neuronal differentiation in a PC12 subline stably transfected with an inducible N-ras oncogene. *Biochem Biophys Res Commun* 150: 1185-92
- Guillemin K, Salama NR, Tompkins LS, Falkow S (2002) Cag pathogenicity island-specific responses of gastric epithelial cells to *Helicobacter pylori* infection. *Proc Natl Acad Sci U S A* 99: 15136-41
- Guo GL, Lambert G, Negishi M, Ward JM, Brewer HB, Jr., Kliewer SA, Gonzalez FJ, Sinal CJ (2003) Complementary roles of farnesoid X receptor, pregnane X receptor, and constitutive androstane receptor in protection against bile acid toxicity. *J Biol Chem* 278: 45062-71
- Gussander E, Adams A (1984) Electron microscopic evidence for replication of circular Epstein-Barr virus genomes in latently infected Raji cells. *J Virol* 52: 549-56
- Haddad H, Cifuentes-Diaz C, Miroglio A, Roblot N, Joshi V, Melki J (2003) Riluzole attenuates spinal muscular atrophy disease progression in a mouse model. *Muscle Nerve* 28: 432-7
- Haggarty SJ, Koeller KM, Wong JC, Grozinger CM, Schreiber SL (2003) Domain-selective small-molecule inhibitor of histone deacetylase 6 (HDAC6)-mediated tubulin deacetylation. *Proc Natl Acad Sci U S A* 100: 4389-94
- Hahnen E, Eyupoglu IY, Brichta L, Haastert K, Tränkle C, Siebzehrübl FA, Riessland M, Hölker I, Claus P, Romstöck J, Buslei R, Wirth B, Blümcke I (2006) *In vitro* and *ex vivo* evaluation of second-generation histone deacetylase inhibitors for the treatment of spinal muscular atrophy. *J Neurochem*: 10.1111/j.1471-4159.2006.03868.x
- Hahnen E, Forkert R, Marke C, Rudnik-Schoneborn S, Schonling J, Zerres K, Wirth B (1995) Molecular analysis of candidate genes on chromosome 5q13 in autosomal recessive spinal muscular atrophy: evidence of homozygous deletions of the SMN gene in unaffected individuals. *Hum Mol Genet* 4: 1927-33
- Hahnen ET, Wirth B (1996) Frequent DNA variant in exon 2a of the survival motor neuron gene (SMN): a further possibility for distinguishing the two copies of the gene. *Hum Genet* 98: 122-3
- Hall A (1998) Rho GTPases and the actin cytoskeleton. *Science* 279: 509-14
- Hanamura A, Caceres JF, Mayeda A, Franza BR, Jr., Krainer AR (1998) Regulated tissue-specific expression of antagonistic pre-mRNA splicing factors. *Rna* 4: 430-44
- Harding HP, Zhang Y, Ron D (1999) Protein translation and folding are coupled by an endoplasmic-reticulum-resident kinase. *Nature* 397: 271-4
- Hart MJ, Eva A, Evans T, Aaronson SA, Cerione RA (1991) Catalysis of guanine nucleotide exchange on the CDC42Hs protein by the db1 oncogene product. *Nature* 354: 311-4
- Hashiguchi M, Sobue K, Paudel HK (2000) 14-3-3zeta is an effector of tau protein phosphorylation. *J Biol Chem* 275: 25247-54
- Hausmanowa-Petrusewicz I, Fidzińska A, Niebroj-Dobosz I, Dorobek M, Bojakowski J (2000) Dystrophinopathies in females. *Folia Neuropathol* 38: 7-12

- He Q, Dent EW, Meiri KF (1997) Modulation of actin filament behavior by GAP-43 (neuromodulin) is dependent on the phosphorylation status of serine 41, the protein kinase C site. *J Neurosci* 17: 3515-24
- Hebert MD, Shpargel KB, Ospina JK, Tucker KE, Matera AG (2002) Coilin methylation regulates nuclear body formation. *Dev Cell* 3: 329-37
- Hebert MD, Szymczyk PW, Shpargel KB, Matera AG (2001) Coilin forms the bridge between Cajal bodies and SMN, the spinal muscular atrophy protein. *Genes Dev* 15: 2720-9
- Helmken C, Hofmann Y, Schoenen F, Oprea G, Raschke H, Rudnik-Schoneborn S, Zerres K, Wirth B (2003) Evidence for a modifying pathway in SMA discordant families: reduced SMN level decreases the amount of its interacting partners and Htra2-beta1. *Hum Genet* 114: 11-21
- Helmken C, Wetter A, Rudnik-Schoneborn S, Liehr T, Zerres K, Wirth B (2000) An essential SMN interacting protein (SIP1) is not involved in the phenotypic variability of spinal muscular atrophy (SMA). *Eur J Hum Genet* 8: 493-9
- Helmken C, Wirth B (2000) Exclusion of Htra2-beta1, an up-regulator of full-length SMN2 transcript, as a modifying gene for spinal muscular atrophy. *Hum Genet* 107: 554-8
- Hendrich B, Tweedie S (2003) The methyl-CpG binding domain and the evolving role of DNA methylation in animals. *Trends Genet* 19: 269-77
- Herbomel P, Thisse B, Thisse C (1999) Ontogeny and behaviour of early macrophages in the zebrafish embryo. *Development* 126: 3735-45
- Hesketh JE, Pryme IF (1991) Interaction between mRNA, ribosomes and the cytoskeleton. *Biochem J* 277 ( Pt 1): 1-10
- Higuchi Y, Kita K, Nakanishi H, Wang XL, Sugaya S, Tanzawa H, Yamamori H, Sugita K, Yamaura A, Suzuki N (1998) Search for genes involved in UV-resistance in human cells by mRNA differential display: increased transcriptional expression of nucleophosmin and T-plastin genes in association with the resistance. *Biochem Biophys Res Commun* 248: 597-602
- Hisano T, Ono M, Nakayama M, Naito S, Kuwano M, Wada M (1996) Increased expression of T-plastin gene in cisplatin-resistant human cancer cells: identification by mRNA differential display. *FEBS Lett* 397: 101-7
- Ho Y, Gruhler A, Heilbut A, Bader GD, Moore L, Adams SL, Millar A, Taylor P, Bennett K, Boutilier K, Yang L, Wolting C, Donaldson I, Schandorff S, Shewnarane J, Vo M, Taggart J, Goudreault M, Muskat B, Alfarano C, Dewar D, Lin Z, Michalickova K, Willems AR, Sassi H, Nielsen PA, Rasmussen KJ, Andersen JR, Johansen LE, Hansen LH, Jespersen H, Podtelejnikov A, Nielsen E, Crawford J, Poulsen V, Sorensen BD, Matthiesen J, Hendrickson RC, Gleeson F, Pawson T, Moran MF, Durocher D, Mann M, Hogue CW, Figeys D, Tyers M (2002) Systematic identification of protein complexes in *Saccharomyces cerevisiae* by mass spectrometry. *Nature* 415: 180-3
- Hofer D, Ness W, Drenckhahn D (1997) Sorting of actin isoforms in chicken auditory hair cells. *J Cell Sci* 110 ( Pt 6): 765-70
- Hofmann Y, Lorson CL, Stamm S, Androphy EJ, Wirth B (2000) Htra2-beta 1 stimulates an exonic splicing enhancer and can restore full-length SMN expression to survival motor neuron 2 (SMN2). *Proc Natl Acad Sci U S A* 97: 9618-23
- Hofmann Y, Wirth B (2002) hnRNP-G promotes exon 7 inclusion of survival motor neuron (SMN) via direct interaction with Htra2-beta1. *Hum Mol Genet* 11: 2037-49
- Horai S, Hayasaka K, Kondo R, Tsugane K, Takahata N (1995) Recent African origin of modern humans revealed by complete sequences of hominoid mitochondrial DNAs. *Proc Natl Acad Sci U S A* 92: 532-6
- Horiuchi T, Aigaki T (2006) Alternative trans-splicing: a novel mode of pre-mRNA processing. *Biol Cell* 98: 135-40
- Hsieh-Li HM, Chang JG, Jong YJ, Wu MH, Wang NM, Tsai CH, Li H (2000) A mouse model for spinal muscular atrophy. *Nat Genet* 24: 66-70
- Hu XY, Ray PN, Murphy EG, Thompson MW, Worton RG (1990) Duplicational mutation at the Duchenne muscular dystrophy locus: its frequency, distribution, origin, and phenotype/genotype correlation. *Am J Hum Genet* 46: 682-95
- Hua Y, Zhou J (2004a) Rpp20 interacts with SMN and is re-distributed into SMN granules in response to stress. *Biochem Biophys Res Commun* 314: 268-76
- Hua Y, Zhou J (2004b) Survival motor neuron protein facilitates assembly of stress granules. *FEBS Lett* 572: 69-74

- Huang LC, Clarkin KC, Wahl GM (1996) Sensitivity and selectivity of the DNA damage sensor responsible for activating p53-dependent G1 arrest. *Proc Natl Acad Sci U S A* 93: 4827-32
- Huang W, Zhang J, Chua SS, Qatanani M, Han Y, Granata R, Moore DD (2003) Induction of bilirubin clearance by the constitutive androstane receptor (CAR). *Proc Natl Acad Sci U S A* 100: 4156-61
- Huang W, Zhang J, Moore DD (2004) A traditional herbal medicine enhances bilirubin clearance by activating the nuclear receptor CAR. *J Clin Invest* 113: 137-43
- Hubbert C, Guardiola A, Shao R, Kawaguchi Y, Ito A, Nixon A, Yoshida M, Wang XF, Yao TP (2002) HDAC6 is a microtubule-associated deacetylase. *Nature* 417: 455-8
- Huber J, Cronshagen U, Kadokura M, Marshallsay C, Wada T, Sekine M, Luhrmann R (1998) Snurportin1, an m3G-cap-specific nuclear import receptor with a novel domain structure. *Embo J* 17: 4114-26
- Hunt SL, Hsuan JJ, Totty N, Jackson RJ (1999) unr, a cellular cytoplasmic RNA-binding protein with five cold-shock domains, is required for internal initiation of translation of human rhinovirus RNA. *Genes Dev* 13: 437-48
- Hupp TR, Meek DW, Midgley CA, Lane DP (1992) Regulation of the specific DNA binding function of p53. *Cell* 71: 875-86
- Iwahashi H, Eguchi Y, Yasuhara N, Hanafusa T, Matsuzawa Y, Tsujimoto Y (1997) Synergistic anti-apoptotic activity between Bcl-2 and SMN implicated in spinal muscular atrophy. *Nature* 390: 413-7
- Iyer VR, Eisen MB, Ross DT, Schuler G, Moore T, Lee JC, Trent JM, Staudt LM, Hudson J, Jr., Boguski MS, Lashkari D, Shalon D, Botstein D, Brown PO (1999) The transcriptional program in the response of human fibroblasts to serum. *Science* 283: 83-7
- Jablonka S, Bandilla M, Wiese S, Buhler D, Wirth B, Sendtner M, Fischer U (2001) Co-regulation of survival of motor neuron (SMN) protein and its interactor SIP1 during development and in spinal muscular atrophy. *Hum Mol Genet* 10: 497-505
- Jablonka S, Schrank B, Kralewski M, Rossoll W, Sendtner M (2000) Reduced survival motor neuron (Smn) gene dose in mice leads to motor neuron degeneration: an animal model for spinal muscular atrophy type III. *Hum Mol Genet* 9: 341-6
- Jablonka S, Wiese S, Sendtner M (2004) Axonal defects in mouse models of motoneuron disease. *J Neurobiol* 58: 272-86
- Jady BE, Darzacq X, Tucker KE, Matera AG, Bertrand E, Kiss T (2003) Modification of Sm small nuclear RNAs occurs in the nucleoplasmic Cajal body following import from the cytoplasm. *Embo J* 22: 1878-88
- Janmey PA, Chaponnier C (1995) Medical aspects of the actin cytoskeleton. *Curr Opin Cell Biol* 7: 111-7
- Johnson DI, Pringle JR (1990) Molecular characterization of CDC42, a *Saccharomyces cerevisiae* gene involved in the development of cell polarity. *J Cell Biol* 111: 143-52
- Johnson RW, Reveille JD, McNearney T, Fischbach M, Friedman AW, Ahn C, Arnett FC, Tan FK (2001) Lack of association of a functionally relevant single nucleotide polymorphism of matrix metalloproteinase-1 promoter with systemic sclerosis (scleroderma). *Genes Immun* 2: 273-5
- Jones KW, Gorzynski K, Hales CM, Fischer U, Badbanchi F, Terns RM, Terns MP (2001) Direct interaction of the spinal muscular atrophy disease protein SMN with the small nucleolar RNA-associated protein fibrillarin. *J Biol Chem* 276: 38645-51
- Kambach C, Walke S, Nagai K (1999a) Structure and assembly of the spliceosomal small nuclear ribonucleoprotein particles. *Curr Opin Struct Biol* 9: 222-30
- Kambach C, Walke S, Young R, Avis JM, de la Fortelle E, Raker VA, Luhrmann R, Li J, Nagai K (1999b) Crystal structures of two Sm protein complexes and their implications for the assembly of the spliceosomal snRNPs. *Cell* 96: 375-87
- Karginova EA, Pentz ES, Kazakova IG, Norwood VF, Carey RM, Gomez RA (1997) Zis: a developmentally regulated gene expressed in juxtaglomerular cells. *Am J Physiol* 273: F731-8
- Kashima T, Manley JL (2003) A negative element in SMN2 exon 7 inhibits splicing in spinal muscular atrophy. *Nat Genet* 34: 460-3
- Katz M, Amit I, Yarden Y (2007) Regulation of MAPKs by growth factors and receptor tyrosine kinases. *Biochim Biophys Acta*
- Kawaguchi Y, Kovacs JJ, McLaurin A, Vance JM, Ito A, Yao TP (2003) The deacetylase HDAC6 regulates aggresome formation and cell viability in response to misfolded protein stress. *Cell* 115: 727-38

- Kawamoto T, Sueyoshi T, Zelko I, Moore R, Washburn K, Negishi M (1999) Phenobarbital-responsive nuclear translocation of the receptor CAR in induction of the CYP2B gene. *Mol Cell Biol* 19: 6318-22
- Kazazian HH, Jr. (1998) Mobile elements and disease. *Curr Opin Genet Dev* 8: 343-50
- Kedersha N, Anderson P (2002) Stress granules: sites of mRNA triage that regulate mRNA stability and translatability. *Biochem Soc Trans* 30: 963-9
- Kedersha N, Chen S, Gilks N, Li W, Miller IJ, Stahl J, Anderson P (2002) Evidence that ternary complex (eIF2-GTP-tRNA(i)(Met))-deficient preinitiation complexes are core constituents of mammalian stress granules. *Mol Biol Cell* 13: 195-210
- Kedersha N, Cho MR, Li W, Yacono PW, Chen S, Gilks N, Golan DE, Anderson P (2000) Dynamic shuttling of TIA-1 accompanies the recruitment of mRNA to mammalian stress granules. *J Cell Biol* 151: 1257-68
- Kedersha N, Stoecklin G, Ayodele M, Yacono P, Lykke-Andersen J, Fritzler MJ, Scheuner D, Kaufman RJ, Golan DE, Anderson P (2005) Stress granules and processing bodies are dynamically linked sites of mRNP remodeling. *J Cell Biol* 169: 871-84
- Kedersha NL, Gupta M, Li W, Miller I, Anderson P (1999) RNA-binding proteins TIA-1 and TIAR link the phosphorylation of eIF-2 alpha to the assembly of mammalian stress granules. *J Cell Biol* 147: 1431-42
- Keep NH, Norwood FL, Moores CA, Winder SJ, Kendrick-Jones J (1999) The 2.0 A structure of the second calponin homology domain from the actin-binding region of the dystrophin homologue utrophin. *J Mol Biol* 285: 1257-64
- Keller ET, Yao Z (2002) Applications of high-throughput methods to cancer metastases. *J Musculoskelet Neuronal Interact* 2: 575-8
- Kelter AR, Herchenbach J, Wirth B (2000) The transcription factor-like nuclear regulator (TFNR) contains a novel 55-amino-acid motif repeated nine times and maps closely to SMN1. *Genomics* 70: 315-26
- Kendler KS, Karkowski-Shuman L, O'Neill FA, Straub RE, MacLean CJ, Walsh D (1997) Resemblance of psychotic symptoms and syndromes in affected sibling pairs from the Irish Study of High-Density Schizophrenia Families: evidence for possible etiologic heterogeneity. *Am J Psychiatry* 154: 191-8
- Kerr DA, Nery JP, Traystman RJ, Chau BN, Hardwick JM (2000) Survival motor neuron protein modulates neuron-specific apoptosis. *Proc Natl Acad Sci U S A* 97: 13312-7
- Kim YS, Furman S, Sink H, VanBerkum MF (2001) Calmodulin and profilin coregulate axon outgrowth in *Drosophila*. *J Neurobiol* 47: 26-38
- Kimball SR, Horetsky RL, Ron D, Jefferson LS, Harding HP (2003) Mammalian stress granules represent sites of accumulation of stalled translation initiation complexes. *Am J Physiol Cell Physiol* 284: C273-84
- Kinali M, Mercuri E, Main M, De Biasia F, Karatza A, Higgins R, Banks LM, Manzur AY, Muntoni F (2002) Pilot trial of albuterol in spinal muscular atrophy. *Neurology* 59: 609-10
- Kislauskis EH, Zhu X, Singer RH (1994) Sequences responsible for intracellular localization of beta-actin messenger RNA also affect cell phenotype. *J Cell Biol* 127: 441-51
- Klaman LD, Thorley-Lawson DA (1995) Characterization of the CD48 gene demonstrates a positive element that is specific to Epstein-Barr virus-immortalized B-cell lines and contains an essential NF-kappa B site. *J Virol* 69: 871-81
- Klein MG, Shi W, Ramagopal U, Tseng Y, Wirtz D, Kovar DR, Staiger CJ, Almo SC (2004) Structure of the actin crosslinking core of fimbrin. *Structure* 12: 999-1013
- Kobayashi H, Baumbach L, Matise TC, Schiavi A, Greenberg F, Hoffman EP (1995) A gene for a severe lethal form of X-linked arthrogryposis (X-linked infantile spinal muscular atrophy) maps to human chromosome Xp11.3-q11.2. *Hum Mol Genet* 4: 1213-6
- Kobayashi K, Sueyoshi T, Inoue K, Moore R, Negishi M (2003) Cytoplasmic accumulation of the nuclear receptor CAR by a tetratricopeptide repeat protein in HepG2 cells. *Mol Pharmacol* 64: 1069-75
- Kocarek TA, Mercer-Haines NA (2002) Squalestatin 1-inducible expression of rat CYP2B: evidence that an endogenous isoprenoid is an activator of the constitutive androstane receptor. *Mol Pharmacol* 62: 1177-86
- Koenig E, Martin R (1996) Cortical plaque-like structures identify ribosome-containing domains in the Mauthner cell axon. *J Neurosci* 16: 1400-11
- Koenig E, Martin R, Titmus M, Sotelo-Silveira JR (2000) Cryptic peripheral ribosomal domains distributed intermittently along mammalian myelinated axons. *J Neurosci* 20: 8390-400

- Kovar DR, Staiger CJ, Weaver EA, McCurdy DW (2000) AtFim1 is an actin filament crosslinking protein from *Arabidopsis thaliana*. *Plant J* 24: 625-36
- Kramer OH, Zhu P, Ostendorff HP, Golebiewski M, Tiefenbach J, Peters MA, Brill B, Groner B, Bach I, Heinzel T, Gottlicher M (2003) The histone deacetylase inhibitor valproic acid selectively induces proteasomal degradation of HDAC2. *Embo J* 22: 3411-20
- Krauer KG, Buck M, Belzer DK, Flanagan J, Chojnowski GM, Sculley TB (2004) The Epstein-Barr virus nuclear antigen-6 protein co-localizes with EBNA-3 and survival of motor neurons protein. *Virology* 318: 280-94
- Kruglyak L, Daly MJ, Reeve-Daly MP, Lander ES (1996) Parametric and nonparametric linkage analysis: a unified multipoint approach. *Am J Hum Genet* 58: 1347-63
- Kubler E, Riezman H (1993) Actin and fimbrin are required for the internalization step of endocytosis in yeast. *Embo J* 12: 2855-62
- Kurihara N, Menaa C, Maeda H, Haile DJ, Reddy SV (2001) Osteoclast-stimulating factor interacts with the spinal muscular atrophy gene product to stimulate osteoclast formation. *J Biol Chem* 276: 41035-9
- La Bella V, Cisterni C, Salaun D, Pettmann B (1998) Survival motor neuron (SMN) protein in rat is expressed as different molecular forms and is developmentally regulated. *Eur J Neurosci* 10: 2913-23
- La Spada AR, Wilson EM, Lubahn DB, Harding AE, Fischbeck KH (1991) Androgen receptor gene mutations in X-linked spinal and bulbar muscular atrophy. *Nature* 352: 77-9
- Lambrechts A, Braun A, Jonckheere V, Aszodi A, Lanier LM, Robbens J, Van Colen I, Vandekerckhove J, Fassler R, Ampe C (2000a) Profilin II is alternatively spliced, resulting in profilin isoforms that are differentially expressed and have distinct biochemical properties. *Mol Cell Biol* 20: 8209-19
- Lambrechts A, Kwiatkowski AV, Lanier LM, Bear JE, Vandekerckhove J, Ampe C, Gertler FB (2000b) cAMP-dependent protein kinase phosphorylation of EVL, a Mena/VASP relative, regulates its interaction with actin and SH3 domains. *J Biol Chem* 275: 36143-51
- Lambrechts A, Verschelde JL, Jonckheere V, Goethals M, Vandekerckhove J, Ampe C (1997) The mammalian profilin isoforms display complementary affinities for PIP2 and proline-rich sequences. *Embo J* 16: 484-94
- Lanier LM, Gates MA, Witke W, Menzies AS, Wehman AM, Macklis JD, Kwiatkowski D, Soriano P, Gertler FB (1999) Mena is required for neurulation and commissure formation. *Neuron* 22: 313-25
- Lassing I, Lindberg U (1985) Specific interaction between phosphatidylinositol 4,5-bisphosphate and profilactin. *Nature* 314: 472-4
- Leavitt J, Goldman D, Merrill C, Kakunaga T (1982) Changes in gene expression accompanying chemically-induced malignant transformation of human fibroblasts. *Carcinogenesis* 3: 61-70
- Leavitt J, Kakunaga T (1980) Expression of a variant form of actin and additional polypeptide changes following chemical-induced in vitro neoplastic transformation of human fibroblasts. *J Biol Chem* 255: 1650-61
- Lebart MC, Hubert F, Boiteau C, Venteo S, Roustan C, Benyamin Y (2004) Biochemical characterization of the L-plastin-actin interaction shows a resemblance with that of alpha-actinin and allows a distinction to be made between the two actin-binding domains of the molecule. *Biochemistry* 43: 2428-37
- Lee KH, Ryu CJ, Hong HJ, Kim J, Lee EH (2005) CDNA microarray analysis of nerve growth factor-regulated gene expression profile in rat PC12 cells. *Neurochem Res* 30: 533-40
- Lee YA, Ruschendorf F, Windemuth C, Schmitt-Egenolf M, Stadelmann A, Nurnberg G, Stander M, Wienker TF, Reis A, Traupe H (2000) Genomewide scan in german families reveals evidence for a novel psoriasis-susceptibility locus on chromosome 19p13. *Am J Hum Genet* 67: 1020-4
- Lefebvre S, Burglen L, Reboullet S, Clermont O, Bulet P, Viollet L, Benichou B, Cruaud C, Millasseau P, Zeviani M, et al. (1995) Identification and characterization of a spinal muscular atrophy-determining gene. *Cell* 80: 155-65
- Lefebvre S, Bulet P, Liu Q, Bertrand S, Clermont O, Munnich A, Dreyfuss G, Melki J (1997) Correlation between severity and SMN protein level in spinal muscular atrophy. *Nat Genet* 16: 265-9
- Lefebvre S, Bulet P, Viollet L, Bertrand S, Huber C, Belser C, Munnich A (2002) A novel association of the SMN protein with two major non-ribosomal nucleolar proteins and its implication in spinal muscular atrophy. *Hum Mol Genet* 11: 1017-27
- Letourneau PC, Shattuck TA (1989) Distribution and possible interactions of actin-associated proteins and cell adhesion molecules of nerve growth cones. *Development* 105: 505-19

- Lim SR, Hertel KJ (2001) Modulation of survival motor neuron pre-mRNA splicing by inhibition of alternative 3' splice site pairing. *J Biol Chem* 276: 45476-83
- Lin CH, Thompson CA, Forscher P (1994a) Cytoskeletal reorganization underlying growth cone motility. *Curr Opin Neurobiol* 4: 640-7
- Lin CS, Aebersold RH, Kent SB, Varma M, Leavitt J (1988) Molecular cloning and characterization of plastin, a human leukocyte protein expressed in transformed human fibroblasts. *Mol Cell Biol* 8: 4659-68
- Lin CS, Chen ZP, Park T, Ghosh K, Leavitt J (1993a) Characterization of the human L-plastin gene promoter in normal and neoplastic cells. *J Biol Chem* 268: 2793-801
- Lin CS, Lau A, Huynh T, Lue TF (1999) Differential regulation of human T-plastin gene in leukocytes and non-leukocytes: identification of the promoter, enhancer, and CpG island. *DNA Cell Biol* 18: 27-37
- Lin CS, Park T, Chen ZP, Leavitt J (1993b) Human plastin genes. Comparative gene structure, chromosome location, and differential expression in normal and neoplastic cells. *J Biol Chem* 268: 2781-92
- Lin CS, Shen W, Chen ZP, Tu YH, Matsudaira P (1994b) Identification of I-plastin, a human fimbrin isoform expressed in intestine and kidney. *Mol Cell Biol* 14: 2457-67
- Liu CY, Schroder M, Kaufman RJ (2000) Ligand-independent dimerization activates the stress response kinases IRE1 and PERK in the lumen of the endoplasmic reticulum. *J Biol Chem* 275: 24881-5
- Liu J, Taylor DW, Taylor KA (2004) A 3-D reconstruction of smooth muscle alpha-actinin by CryoEm reveals two different conformations at the actin-binding region. *J Mol Biol* 338: 115-25
- Liu Q, Dreyfuss G (1996) A novel nuclear structure containing the survival of motor neurons protein. *Embo J* 15: 3555-65
- Liu Q, Fischer U, Wang F, Dreyfuss G (1997) The spinal muscular atrophy disease gene product, SMN, and its associated protein SIP1 are in a complex with spliceosomal snRNP proteins. *Cell* 90: 1013-21
- Long RM, Gu W, Lorimer E, Singer RH, Chartrand P (2000) She2p is a novel RNA-binding protein that recruits the Myo4p-She3p complex to ASH1 mRNA. *Embo J* 19: 6592-601
- Lorson CL, Androphy EJ (1998) The domain encoded by exon 2 of the survival motor neuron protein mediates nucleic acid binding. *Hum Mol Genet* 7: 1269-75
- Lorson CL, Androphy EJ (2000) An exonic enhancer is required for inclusion of an essential exon in the SMA-determining gene SMN. *Hum Mol Genet* 9: 259-65
- Lorson CL, Hahnen E, Androphy EJ, Wirth B (1999) A single nucleotide in the SMN gene regulates splicing and is responsible for spinal muscular atrophy. *Proc Natl Acad Sci U S A* 96: 6307-11
- Lorson CL, Strasswimmer J, Yao JM, Baleja JD, Hahnen E, Wirth B, Le T, Burghes AH, Androphy EJ (1998) SMN oligomerization defect correlates with spinal muscular atrophy severity. *Nat Genet* 19: 63-6
- Luger K, Mader AW, Richmond RK, Sargent DF, Richmond TJ (1997) Crystal structure of the nucleosome core particle at 2.8 Å resolution. *Nature* 389: 251-60
- Lunn MR, Root DE, Martino AM, Flaherty SP, Kelley BP, Coovert DD, Burghes AH, Man NT, Morris GE, Zhou J, Androphy EJ, Sumner CJ, Stockwell BR (2004) Indoprofen upregulates the survival motor neuron protein through a cyclooxygenase-independent mechanism. *Chem Biol* 11: 1489-93
- Luo L (2002) Actin cytoskeleton regulation in neuronal morphogenesis and structural plasticity. *Annu Rev Cell Dev Biol* 18: 601-35
- Lynch M, Conery JS (2000) The evolutionary fate and consequences of duplicate genes. *Science* 290: 1151-5
- Maas T, Eidenmuller J, Brandt R (2000) Interaction of tau with the neural membrane cortex is regulated by phosphorylation at sites that are modified in paired helical filaments. *J Biol Chem* 275: 15733-40
- Machesky LM, May RC (2001) Arps: actin-related proteins. *Results Probl Cell Differ* 32: 213-29
- Maestri NE, Brusilow SW, Clissold DB, Bassett SS (1996) Long-term treatment of girls with ornithine transcarbamylase deficiency. *N Engl J Med* 335: 855-9
- Maglich JM, Parks DJ, Moore LB, Collins JL, Goodwin B, Billin AN, Stoltz CA, Kliewer SA, Lambert MH, Willson TM, Moore JT (2003) Identification of a novel human constitutive androstane receptor (CAR) agonist and its use in the identification of CAR target genes. *J Biol Chem* 278: 17277-83
- Maglich JM, Stoltz CM, Goodwin B, Hawkins-Brown D, Moore JT, Kliewer SA (2002) Nuclear pregnane x receptor and constitutive androstane receptor regulate overlapping but distinct sets of genes involved in xenobiotic detoxification. *Mol Pharmacol* 62: 638-46

- Maglich JM, Watson J, McMillen PJ, Goodwin B, Willson TM, Moore JT (2004) The nuclear receptor CAR is a regulator of thyroid hormone metabolism during caloric restriction. *J Biol Chem* 279: 19832-8
- Makinen J, Frank C, Jyrkkarine J, Gynther J, Carlberg C, Honkakoski P (2002) Modulation of mouse and human phenobarbital-responsive enhancer module by nuclear receptors. *Mol Pharmacol* 62: 366-78
- Manley JL, Tacke R (1996) SR proteins and splicing control. *Genes Dev* 10: 1569-79
- Marks P, Rifkind RA, Richon VM, Breslow R, Miller T, Kelly WK (2001) Histone deacetylases and cancer: causes and therapies. *Nat Rev Cancer* 1: 194-202
- Marks PA, Richon VM, Miller T, Kelly WK (2004) Histone deacetylase inhibitors. *Adv Cancer Res* 91: 137-68
- Matas OB, Fritz S, Luna A, Egea G (2005) Membrane trafficking at the ER/Golgi interface: functional implications of RhoA and Rac1. *Eur J Cell Biol* 84: 699-707
- Matsudaira P (1991) Modular organization of actin crosslinking proteins. *Trends Biochem Sci* 16: 87-92
- Matsudaira P (1994) Actin crosslinking proteins at the leading edge. *Semin Cell Biol* 5: 165-74
- Matsudaira P, Mandelkow E, Renner W, Hesterberg LK, Weber K (1983) Role of fimbrin and villin in determining the interfilament distances of actin bundles. *Nature* 301: 209-14
- Mattern KA, van der Kraan I, Schul W, de Jong L, van Driel R (1999) Spatial organization of four hnRNP proteins in relation to sites of transcription, to nuclear speckles, and to each other in interphase nuclei and nuclear matrices of HeLa cells. *Exp Cell Res* 246: 461-70
- Matthijs G, Schollen E, Legius E, Devriendt K, Goemans N, Kayserili H, Apak MY, Cassiman JJ (1996) Unusual molecular findings in autosomal recessive spinal muscular atrophy. *J Med Genet* 33: 469-74
- Maxam AM, Gilbert W (1980) Sequencing end-labeled DNA with base-specific chemical cleavages. *Methods Enzymol* 65: 499-560
- Mayeda A, Badolato J, Kobayashi R, Zhang MQ, Gardiner EM, Krainer AR (1999) Purification and characterization of human RNPS1: a general activator of pre-mRNA splicing. *Embo J* 18: 4560-70
- Mayumi K, Yaoi T, Kawai J, Kojima S, Watanabe S, Suzuki H (1998) Improved restriction landmark cDNA scanning and its application to global analysis of genes regulated by nerve growth factor in PC12 cells. *Biochim Biophys Acta* 1399: 10-8
- Mazroui R, Huot ME, Tremblay S, Filion C, Labelle Y, Khandjian EW (2002) Trapping of messenger RNA by Fragile X Mental Retardation protein into cytoplasmic granules induces translation repression. *Hum Mol Genet* 11: 3007-17
- Mazzarella R, Schlessinger D (1998) Pathological consequences of sequence duplications in the human genome. *Genome Res* 8: 1007-21
- McAndrew PE, Parsons DW, Simard LR, Rochette C, Ray PN, Mendell JR, Prior TW, Burghes AH (1997) Identification of proximal spinal muscular atrophy carriers and patients by analysis of SMNT and SMNC gene copy number. *Am J Hum Genet* 60: 1411-22
- McCurdy DW, Kim M (1998) Molecular cloning of a novel fimbrin-like cDNA from *Arabidopsis thaliana*. *Plant Mol Biol* 36: 23-31
- McWhorter ML, Monani UR, Burghes AH, Beattie CE (2003) Knockdown of the survival motor neuron (Smn) protein in zebrafish causes defects in motor axon outgrowth and pathfinding. *J Cell Biol* 162: 919-31
- Meberg PJ (2000) Signal-regulated ADF/cofilin activity and growth cone motility. *Mol Neurobiol* 21: 97-107
- Meberg PJ, Bamberg JR (2000) Increase in neurite outgrowth mediated by overexpression of actin depolymerizing factor. *J Neurosci* 20: 2459-69
- Meister G, Buhler D, Lagerbauer B, Zobawa M, Lottspeich F, Fischer U (2000) Characterization of a nuclear 20S complex containing the survival of motor neurons (SMN) protein and a specific subset of spliceosomal Sm proteins. *Hum Mol Genet* 9: 1977-86
- Meister G, Buhler D, Pillai R, Lottspeich F, Fischer U (2001a) A multiprotein complex mediates the ATP-dependent assembly of spliceosomal U snRNPs. *Nat Cell Biol* 3: 945-9
- Meister G, Eggert C, Fischer U (2002) SMN-mediated assembly of RNPs: a complex story. *Trends Cell Biol* 12: 472-8
- Meister G, Fischer U (2002) Assisted RNP assembly: SMN and PRMT5 complexes cooperate in the formation of spliceosomal UsnRNPs. *Embo J* 21: 5853-63
- Meister G, Hannus S, Plottner O, Baars T, Hartmann E, Fakan S, Lagerbauer B, Fischer U (2001b) SMNrp is an essential pre-mRNA splicing factor required for the formation of the mature spliceosome. *Embo J* 20: 2304-14

- Melki J, Abdelhak S, Sheth P, Bachelot MF, Burlet P, Marcadet A, Aicardi J, Barois A, Carriere JP, Fardeau M, et al. (1990) Gene for chronic proximal spinal muscular atrophies maps to chromosome 5q. *Nature* 344: 767-8
- Melki J, Lefebvre S, Burglen L, Burlet P, Clermont O, Millasseau P, Reboulet S, Benichou B, Zeviani M, Le Paslier D, et al. (1994a) [Physical study of big fragments and search strategy of genes. Application to locus of infant spinal muscular atrophies]. *C R Seances Soc Biol Fil* 188: 495-8
- Melki J, Lefebvre S, Burglen L, Burlet P, Clermont O, Millasseau P, Reboulet S, Benichou B, Zeviani M, Le Paslier D, et al. (1994b) De novo and inherited deletions of the 5q13 region in spinal muscular atrophies. *Science* 264: 1474-7
- Mercuri E, Messina S, Battini R, Berardinelli A, Boffi P, Bono R, Bruno C, Carboni N, Cini C, Colitto F, D'Amico A, Minetti C, Mirabella M, Mongini T, Morandi L, Dlamini N, Orcesi S, Pelliccioni M, Pane M, Pini A, Swan AV, Villanova M, Vita G, Main M, Muntoni F, Bertini E (2006) Reliability of the Hammersmith functional motor scale for spinal muscular atrophy in a multicentric study. *Neuromuscul Disord* 16: 93-8
- Merlini L, Solari A, Vita G, Bertini E, Minetti C, Mongini T, Mazzoni E, Angelini C, Morandi L (2003) Role of gabapentin in spinal muscular atrophy: results of a multicenter, randomized Italian study. *J Child Neurol* 18: 537-41
- Merrick WC, Anderson WF (1975) Purification and characterization of homogeneous protein synthesis initiation factor M1 from rabbit reticulocytes. *J Biol Chem* 250: 1197-206
- Michaud S, Reed R (1993) A functional association between the 5' and 3' splice site is established in the earliest prespliceosome complex (E) in mammals. *Genes Dev* 7: 1008-20
- Millard TH, Sharp SJ, Machesky LM (2004) Signalling to actin assembly via the WASP (Wiskott-Aldrich syndrome protein)-family proteins and the Arp2/3 complex. *Biochem J* 380: 1-17
- Miller RG, Moore DH, Dronsky V, Bradley W, Barohn R, Bryan W, Prior TW, Gelinac DF, Iannaccone S, Kissel J, Leshner R, Mendell J, Mendoza M, Russman B, Samaha F, Smith S (2001) A placebo-controlled trial of gabapentin in spinal muscular atrophy. *J Neurol Sci* 191: 127-31
- Miller S, Dykes D, Polesky H (1988) A simple salting out procedure for extracting DNA from human nucleated cells. *Nucl. Acid. Res.*: 1216:1215
- Mine M, Koarada S, Sai T, Miyake K, Kimoto M (1998) Peptide-binding motifs of the mixed haplotype Abeta2/Aalpha3 major histocompatibility complex class II molecule: a restriction element for auto-reactive T cells in (NZBxNZW)F1 mice. *Immunology* 95: 577-84
- Mintz PJ, Spector DL (2000) Compartmentalization of RNA processing factors within nuclear speckles. *J Struct Biol* 129: 241-51
- Minucci S, Pelicci PG (2006) Histone deacetylase inhibitors and the promise of epigenetic (and more) treatments for cancer. *Nat Rev Cancer* 6: 38-51
- Mirza A, Wu Q, Wang L, McClanahan T, Bishop WR, Gheyas F, Ding W, Hutchins B, Hockenberry T, Kirschmeier P, Greene JR, Liu S (2003) Global transcriptional program of p53 target genes during the process of apoptosis and cell cycle progression. *Oncogene* 22: 3645-54
- Miyajima H, Miyaso H, Okumura M, Kurisu J, Imaizumi K (2002) Identification of a cis-acting element for the regulation of SMN exon 7 splicing. *J Biol Chem* 277: 23271-7
- Miyaso H, Okumura M, Kondo S, Higashide S, Miyajima H, Imaizumi K (2003) An intronic splicing enhancer element in survival motor neuron (SMN) pre-mRNA. *J Biol Chem* 278: 15825-31
- Mizutani A, Fukuda M, Ibata K, Shiraishi Y, Mikoshiba K (2000) SYNCRIP, a cytoplasmic counterpart of heterogeneous nuclear ribonucleoprotein R, interacts with ubiquitous synaptotagmin isoforms. *J Biol Chem* 275: 9823-31
- Mohaghegh P, Rodrigues NR, Owen N, Ponting CP, Le TT, Burghes AH, Davies KE (1999) Analysis of mutations in the tudor domain of the survival motor neuron protein SMN. *Eur J Hum Genet* 7: 519-25
- Mohr E, Richter D (2000) Axonal mRNAs: functional significance in vertebrates and invertebrates. *J Neurocytol* 29: 783-91
- Monani UR (2005) Spinal muscular atrophy: a deficiency in a ubiquitous protein; a motor neuron-specific disease. *Neuron* 48: 885-96
- Monani UR, Coovert DD, Burghes AH (2000) Animal models of spinal muscular atrophy. *Hum Mol Genet* 9: 2451-7
- Monani UR, McPherson JD, Burghes AH (1999) Promoter analysis of the human centromeric and telomeric survival motor neuron genes (SMNC and SMNT). *Biochim Biophys Acta* 1445: 330-6

- Monani UR, Pastore MT, Gavrilina TO, Jablonka S, Le TT, Andreassi C, DiCocco JM, Lorson C, Androphy EJ, Sendtner M, Podell M, Burghes AH (2003) A transgene carrying an A2G missense mutation in the SMN gene modulates phenotypic severity in mice with severe (type I) spinal muscular atrophy. *J Cell Biol* 160: 41-52
- Montpetit A, Nelis M, Laflamme P, Magi R, Ke X, Remm M, Cardon L, Hudson TJ, Metspalu A (2006) An evaluation of the performance of tag SNPs derived from HapMap in a Caucasian population. *PLoS Genet* 2: e27
- Moore LB, Parks DJ, Jones SA, Bledsoe RK, Consler TG, Stimmel JB, Goodwin B, Liddle C, Blanchard SG, Willson TM, Collins JL, Kliewer SA (2000) Orphan nuclear receptors constitutive androstane receptor and pregnane X receptor share xenobiotic and steroid ligands. *J Biol Chem* 275: 15122-7
- Mooseker MS (1983) Actin binding proteins of the brush border. *Cell* 35: 11-3
- Mouaikel J, Narayanan U, Verheggen C, Matera AG, Bertrand E, Tazi J, Bordonne R (2003) Interaction between the small-nuclear-RNA cap hypermethylase and the spinal muscular atrophy protein, survival of motor neuron. *EMBO Rep* 4: 616-22
- Mourelatos Z, Abel L, Yong J, Kataoka N, Dreyfuss G (2001) SMN interacts with a novel family of hnRNP and spliceosomal proteins. *Embo J* 20: 5443-52
- Mourelatos Z, Dostie J, Paushkin S, Sharma A, Charroux B, Abel L, Rappsilber J, Mann M, Dreyfuss G (2002) miRNPs: a novel class of ribonucleoproteins containing numerous microRNAs. *Genes Dev* 16: 720-8
- Mueller PR, Wold B (1989) In vivo footprinting of a muscle specific enhancer by ligation mediated PCR. *Science* 246: 780-6
- Munsat TL (1995) Issues in amyotrophic lateral sclerosis clinical trial design. *Adv Neurol* 68: 209-18
- Munsat TL, Davies KE (1992) International SMA consortium meeting. (26-28 June 1992, Bonn, Germany). *Neuromuscul Disord* 2: 423-8
- Nakajima T, Uchida C, Anderson SF, Parvin JD, Montminy M (1997) Analysis of a cAMP-responsive activator reveals a two-component mechanism for transcriptional induction via signal-dependent factors. *Genes Dev* 11: 738-47
- Nakano K, Satoh K, Morimatsu A, Ohnuma M, Mabuchi I (2001) Interactions among a fimbrin, a capping protein, and an actin-depolymerizing factor in organization of the fission yeast actin cytoskeleton. *Mol Biol Cell* 12: 3515-26
- Namba Y, Ito M, Zu Y, Shigesada K, Maruyama K (1992) Human T cell L-plastin bundles actin filaments in a calcium-dependent manner. *J Biochem (Tokyo)* 112: 503-7
- Narayanan U, Achsel T, Luhrmann R, Matera AG (2004) Coupled in vitro import of U snRNPs and SMN, the spinal muscular atrophy protein. *Mol Cell* 16: 223-34
- Narayanan U, Ospina JK, Frey MR, Hebert MD, Matera AG (2002) SMN, the spinal muscular atrophy protein, forms a pre-import snRNP complex with snurportin1 and importin beta. *Hum Mol Genet* 11: 1785-95
- Nasim MT, Chernova TK, Chowdhury HM, Yue BG, Eperon IC (2003) HnRNP G and Tra2beta: opposite effects on splicing matched by antagonism in RNA binding. *Hum Mol Genet* 12: 1337-48
- Navascues J, Berciano MT, Tucker KE, Lafarga M, Matera AG (2004) Targeting SMN to Cajal bodies and nuclear gems during neuritogenesis. *Chromosoma* 112: 398-409
- Nayler O, Cap C, Stamm S (1998) Human transformer-2-beta gene (SFRS10): complete nucleotide sequence, chromosomal localization, and generation of a tissue-specific isoform. *Genomics* 53: 191-202
- Nesic D, Tanackovic G, Kramer A (2004) A role for Cajal bodies in the final steps of U2 snRNP biogenesis. *J Cell Sci* 117: 4423-33
- Neuwald AF, Koonin EV (1998) Ataxin-2, global regulators of bacterial gene expression, and spliceosomal snRNP proteins share a conserved domain. *J Mol Med* 76: 3-5
- Nooren IM, Thornton JM (2003a) Diversity of protein-protein interactions. *Embo J* 22: 3486-92
- Nooren IM, Thornton JM (2003b) Structural characterisation and functional significance of transient protein-protein interactions. *J Mol Biol* 325: 991-1018
- Nover L, Scharf KD, Neumann D (1989) Cytoplasmic heat shock granules are formed from precursor particles and are associated with a specific set of mRNAs. *Mol Cell Biol* 9: 1298-308
- Obermann H, Raabe I, Balvers M, Brunswig B, Schulze W, Kirchhoff C (2005) Novel testis-expressed profilin IV associated with acrosome biogenesis and spermatid elongation. *Mol Hum Reprod* 11: 53-64
- Ogg SC, Lamond AI (2002) Cajal bodies and coilin--moving towards function. *J Cell Biol* 159: 17-21

- Ogino S, Wilson RB (2004) Spinal muscular atrophy: molecular genetics and diagnostics. *Expert Rev Mol Diagn* 4: 15-29
- Ogryzko VV, Schiltz RL, Russanova V, Howard BH, Nakatani Y (1996) The transcriptional coactivators p300 and CBP are histone acetyltransferases. *Cell* 87: 953-9
- Olaso R, Joshi V, Fernandez J, Roblot N, Courageot S, Bonnefont JP, Melki J (2006) Activation of RNA metabolism-related genes in mouse but not human tissues deficient in SMN. *Physiol Genomics* 24: 97-104
- Oleynikov Y, Singer RH (2003) Real-time visualization of ZBP1 association with beta-actin mRNA during transcription and localization. *Curr Biol* 13: 199-207
- Otter S, Grimmler M, Neuenkirchen N, Chari A, Sickmann A, Fischer U (2006) A comprehensive interaction map of the human SMN-complex. *J Biol Chem*
- Ozdinler PH, Macklis JD (2006) IGF-I specifically enhances axon outgrowth of corticospinal motor neurons. *Nat Neurosci* 9: 1371-81
- Pagliardini S, Giavazzi A, Setola V, Lizier C, Di Luca M, DeBiasi S, Battaglia G (2000) Subcellular localization and axonal transport of the survival motor neuron (SMN) protein in the developing rat spinal cord. *Hum Mol Genet* 9: 47-56
- Palazzo A, Ackerman B, Gundersen GG (2003) Cell biology: Tubulin acetylation and cell motility. *Nature* 421: 230
- Pantaloni D, Carlier MF (1993) How profilin promotes actin filament assembly in the presence of thymosin beta 4. *Cell* 75: 1007-14
- Park JW, Voss PG, Grabski S, Wang JL, Patterson RJ (2001) Association of galectin-1 and galectin-3 with Gemin4 in complexes containing the SMN protein. *Nucleic Acids Res* 29: 3595-602
- Park SH, Bolender N, Eisele F, Kostova Z, Takeuchi J, Coffino P, Wolf DH (2007) The cytoplasmic Hsp70 chaperone machinery subjects misfolded and endoplasmic reticulum import-incompetent proteins to degradation via the ubiquitin-proteasome system. *Mol Biol Cell* 18: 153-65
- Parsons DW, McAndrew PE, Iannaccone ST, Mendell JR, Burghes AH, Prior TW (1998) Intragenic telSMN mutations: frequency, distribution, evidence of a founder effect, and modification of the spinal muscular atrophy phenotype by cenSMN copy number. *Am J Hum Genet* 63: 1712-23
- Pascussi JM, Gerbal-Chaloin S, Fabre JM, Maurel P, Vilarem MJ (2000) Dexamethasone enhances constitutive androstane receptor expression in human hepatocytes: consequences on cytochrome P450 gene regulation. *Mol Pharmacol* 58: 1441-50
- Patil N, Berno AJ, Hinds DA, Barrett WA, Doshi JM, Hacker CR, Kautzer CR, Lee DH, Marjoribanks C, McDonough DP, Nguyen BT, Norris MC, Sheehan JB, Shen N, Stern D, Stokowski RP, Thomas DJ, Trulson MO, Vyas KR, Frazer KA, Fodor SP, Cox DR (2001) Blocks of limited haplotype diversity revealed by high-resolution scanning of human chromosome 21. *Science* 294: 1719-23
- Paushkin S, Gubitza AK, Massenet S, Dreyfuss G (2002) The SMN complex, an assemblysome of ribonucleoproteins. *Curr Opin Cell Biol* 14: 305-12
- Pearn J (1980) Classification of spinal muscular atrophies. *Lancet* 1: 919-22
- Pellizzoni L, Baccon J, Charroux B, Dreyfuss G (2001a) The survival of motor neurons (SMN) protein interacts with the snoRNP proteins fibrillarin and GAR1. *Curr Biol* 11: 1079-88
- Pellizzoni L, Baccon J, Rappsilber J, Mann M, Dreyfuss G (2001b) Purification of native SMN complexes and identification of Gemin6 as a novel component. *J Biol Chem*
- Pellizzoni L, Baccon J, Rappsilber J, Mann M, Dreyfuss G (2002a) Purification of native survival of motor neurons complexes and identification of Gemin6 as a novel component. *J Biol Chem* 277: 7540-5
- Pellizzoni L, Charroux B, Dreyfuss G (1999) SMN mutants of spinal muscular atrophy patients are defective in binding to snRNP proteins. *Proc Natl Acad Sci U S A* 96: 11167-72
- Pellizzoni L, Charroux B, Rappsilber J, Mann M, Dreyfuss G (2001c) A functional interaction between the survival motor neuron complex and RNA polymerase II. *J Cell Biol* 152: 75-85
- Pellizzoni L, Kataoka N, Charroux B, Dreyfuss G (1998) A novel function for SMN, the spinal muscular atrophy disease gene product, in pre-mRNA splicing. *Cell* 95: 615-24
- Pellizzoni L, Yong J, Dreyfuss G (2002b) Essential Role for the SMN Complex in the Specificity of snRNP Assembly. *Science* 298: 1775-9
- Percipalle P, Zhao J, Pope B, Weeds A, Lindberg U, Daneholt B (2001) Actin bound to the heterogeneous nuclear ribonucleoprotein hrp36 is associated with Balbiani ring mRNA from the gene to polysomes. *J Cell Biol* 153: 229-36
- Peterson CA, Gordon H, Hall ZW, Paterson BM, Blau HM (1990) Negative control of the helix-loop-helix family of myogenic regulators in the NFB mutant. *Cell* 62: 493-502

- Podvinec M, Handschin C, Looser R, Meyer UA (2004) Identification of the xenosensors regulating human 5-aminolevulinic synthase. *Proc Natl Acad Sci U S A* 101: 9127-32
- Pollard TD (2003) The cytoskeleton, cellular motility and the reductionist agenda. *Nature* 422: 741-5
- Pollard TD, Blanchoin L, Mullins RD (2000) Molecular mechanisms controlling actin filament dynamics in nonmuscle cells. *Annu Rev Biophys Biomol Struct* 29: 545-76
- Pollard TD, Cooper JA (1986) Actin and actin-binding proteins. A critical evaluation of mechanisms and functions. *Annu Rev Biochem* 55: 987-1035
- Ponting CP (1997) Tudor domains in proteins that interact with RNA. *Trends Biochem Sci* 22: 51-2
- Povey S, Lovering R, Bruford E, Wright M, Lush M, Wain H (2001) The HUGO Gene Nomenclature Committee (HGNC). *Hum Genet* 109: 678-80
- Prassler J, Stocker S, Marriott G, Heidecker M, Kellermann J, Gerisch G (1997) Interaction of a Dictyostelium member of the plastin/fimbrin family with actin filaments and actin-myosin complexes. *Mol Biol Cell* 8: 83-95
- Prevost MC, Lesourd M, Arpin M, Vernel F, Mounier J, Hellio R, Sansonetti PJ (1992) Unipolar reorganization of F-actin layer at bacterial division and bundling of actin filaments by plastin correlate with movement of *Shigella flexneri* within HeLa cells. *Infect Immun* 60: 4088-99
- Qatanani M, Wei P, Moore DD (2004) Alterations in the distribution and orexigenic effects of dexamethasone in CAR-null mice. *Pharmacol Biochem Behav* 78: 285-91
- Ralser M, Albrecht M, Nonhoff U, Lengauer T, Lehrach H, Krobitsch S (2005a) An integrative approach to gain insights into the cellular function of human ataxin-2. *J Mol Biol* 346: 203-14
- Ralser M, Nonhoff U, Albrecht M, Lengauer T, Wanker EE, Lehrach H, Krobitsch S (2005b) Ataxin-2 and huntingtin interact with endophilin-A complexes to function in plastin-associated pathways. *Hum Mol Genet* 14: 2893-909
- Reinhard M, Halbrugge M, Scheer U, Wiegand C, Jockusch BM, Walter U (1992) The 46/50 kDa phosphoprotein VASP purified from human platelets is a novel protein associated with actin filaments and focal contacts. *Embo J* 11: 2063-70
- Renvoise B, Khoobarry K, Gendron MC, Cibert C, Viollet L, Lefebvre S (2006) Distinct domains of the spinal muscular atrophy protein SMN are required for targeting to Cajal bodies in mammalian cells. *J Cell Sci* 119: 680-92
- Ridley AJ, Hall A (1992a) Distinct patterns of actin organization regulated by the small GTP-binding proteins Rac and Rho. *Cold Spring Harb Symp Quant Biol* 57: 661-71
- Ridley AJ, Hall A (1992b) The small GTP-binding protein rho regulates the assembly of focal adhesions and actin stress fibers in response to growth factors. *Cell* 70: 389-99
- Ridley AJ, Paterson HF, Johnston CL, Diekmann D, Hall A (1992) The small GTP-binding protein rac regulates growth factor-induced membrane ruffling. *Cell* 70: 401-10
- Riessland M, Brichta L, Hahnen E, Wirth B (2006) The benzamide M344, a novel histone deacetylase inhibitor, significantly increases SMN2 RNA/protein levels in spinal muscular atrophy (SMA) cells. *Medgen*: 113 (abstract P293)
- Robertson KD (2002) DNA methylation and chromatin - unraveling the tangled web. *Oncogene* 21: 5361-79
- Robertson KD (2005) DNA methylation and human disease. *Nat Rev Genet* 6: 597-610
- Rochette CF, Gilbert N, Simard LR (2001) SMN gene duplication and the emergence of the SMN2 gene occurred in distinct hominids: SMN2 is unique to *Homo sapiens*. *Hum Genet* 108: 255-66
- Rodrigues NR, Owen N, Talbot K, Ignatius J, Dubowitz V, Davies KE (1995) Deletions in the survival motor neuron gene on 5q13 in autosomal recessive spinal muscular atrophy. *Hum Mol Genet* 4: 631-4
- Rodrigues NR, Owen N, Talbot K, Patel S, Muntoni F, Ignatius J, Dubowitz V, Davies KE (1996) Gene deletions in spinal muscular atrophy. *J Med Genet* 33: 93-6
- Rohatgi R, Ma L, Miki H, Lopez M, Kirchhausen T, Takenawa T, Kirschner MW (1999) The interaction between N-WASP and the Arp2/3 complex links Cdc42-dependent signals to actin assembly. *Cell* 97: 221-31
- Ronaghi M (2001) Pyrosequencing sheds light on DNA sequencing. *Genome Res* 11: 3-11
- Ross AF, Oleynikov Y, Kislauskis EH, Taneja KL, Singer RH (1997) Characterization of a beta-actin mRNA zipcode-binding protein. *Mol Cell Biol* 17: 2158-65
- Rossoll W, Jablonka S, Andreassi C, Kroning AK, Karle K, Monani UR, Sendtner M (2003) Smn, the spinal muscular atrophy-determining gene product, modulates axon growth and localization of beta-actin mRNA in growth cones of motoneurons. *J Cell Biol* 163: 801-12

- Rossoll W, Kroning AK, Ohndorf UM, Steegborn C, Jablonka S, Sendtner M (2002) Specific interaction of Smn, the spinal muscular atrophy determining gene product, with hnRNP-R and gry-rbp/hnRNP-Q: a role for Smn in RNA processing in motor axons? *Hum Mol Genet* 11: 93-105
- Rothe F, Gueydan C, Bellefroid E, Huez G, Krusys V (2006) Identification of FUSE-binding proteins as interacting partners of TIA proteins. *Biochem Biophys Res Commun* 343: 57-68
- Roy N, McLean MD, Besner-Johnston A, Lefebvre C, Salih M, Carpten JD, Burghes AH, Yaraghi Z, Ikeda JE, Korneluk RG, et al. (1995) Refined physical map of the spinal muscular atrophy gene (SMA) region at 5q13 based on YAC and cosmid contiguous arrays. *Genomics* 26: 451-60
- Rubin CM, Schmid CW (1980) Pyrimidine-specific chemical reactions useful for DNA sequencing. *Nucleic Acids Res* 8: 4613-9
- Rudnik-Schöneborn S, Rohrig D, Morgan G, Wirth B, Zerres K (1994) Autosomal recessive proximal spinal muscular atrophy in 101 sibs out of 48 families: clinical picture, influence of gender, and genetic implications. *Am J Med Genet* 51: 70-6
- Russman BS, Iannaccone ST, Samaha FJ (2003) A phase 1 trial of riluzole in spinal muscular atrophy. *Arch Neurol* 60: 1601-3
- Saini SP, Sonoda J, Xu L, Toma D, Uppal H, Mu Y, Ren S, Moore DD, Evans RM, Xie W (2004) A novel constitutive androstane receptor-mediated and CYP3A-independent pathway of bile acid detoxification. *Mol Pharmacol* 65: 292-300
- Saji S, Kawakami M, Hayashi S, Yoshida N, Hirose M, Horiguchi S, Itoh A, Funata N, Schreiber SL, Yoshida M, Toi M (2005) Significance of HDAC6 regulation via estrogen signaling for cell motility and prognosis in estrogen receptor-positive breast cancer. *Oncogene* 24: 4531-9
- Sambuughin N, Sivakumar K, Selenge B, Lee HS, Friedlich D, Baasanjav D, Dalakas MC, Goldfarb LG (1998) Autosomal dominant distal spinal muscular atrophy type V (dSMA-V) and Charcot-Marie-Tooth disease type 2D (CMT2D) segregate within a single large kindred and map to a refined region on chromosome 7p15. *J Neurol Sci* 161: 23-8
- Sandrock TM, Brower SM, Toenjes KA, Adams AE (1999) Suppressor analysis of fimbrin (Sac6p) overexpression in yeast. *Genetics* 151: 1287-97
- Sasaki Y, Itoh F, Kobayashi T, Kikuchi T, Suzuki H, Toyota M, Imai K (2002) Increased expression of T-fimbrin gene after DNA damage in CHO cells and inactivation of T-fimbrin by CpG methylation in human colorectal cancer cells. *Int J Cancer* 97: 211-6
- Schaffert N, Hossbach M, Heintzmann R, Achsel T, Luhrmann R (2004) RNAi knockdown of hPrp31 leads to an accumulation of U4/U6 di-snRNPs in Cajal bodies. *Embo J* 23: 3000-9
- Scharf JM, Damron D, Frisella A, Bruno S, Beggs AH, Kunkel LM, Dietrich WF (1996) The mouse region syntenic for human spinal muscular atrophy lies within the Lgn1 critical interval and contains multiple copies of Naip exon 5. *Genomics* 38: 405-17
- Schmidt A, Hall MN (1998) Signaling to the actin cytoskeleton. *Annu Rev Cell Dev Biol* 14: 305-38
- Schmutz J, Martin J, Terry A, Couronne O, Grimwood J, Lowry S, Gordon LA, Scott D, Xie G, Huang W, Hellsten U, Tran-Gyamfi M, She X, Prabhakar S, Aerts A, Altherr M, Bajorek E, Black S, Branscomb E, Caoile C, Challacombe JF, Chan YM, Denys M, Detter JC, Escobar J, Flowers D, Fotopulos D, Glavina T, Gomez M, Gonzales E, Goodstein D, Grigoriev I, Groza M, Hammon N, Hawkins T, Haydu L, Israni S, Jett J, Kadner K, Kimball H, Kobayashi A, Lopez F, Lou Y, Martinez D, Medina C, Morgan J, Nandkeshwar R, Noonan JP, Pitluck S, Pollard M, Predki P, Priest J, Ramirez L, Retterer J, Rodriguez A, Rogers S, Salamov A, Salazar A, Thayer N, Tice H, Tsai M, Ustaszewska A, Vo N, Wheeler J, Wu K, Yang J, Dickson M, Cheng JF, Eichler EE, Olsen A, Pennacchio LA, Rokhsar DS, Richardson P, Lucas SM, Myers RM, Rubin EM (2004) The DNA sequence and comparative analysis of human chromosome 5. *Nature* 431: 268-74
- Schneider ME, Belyantseva IA, Azevedo RB, Kachar B (2002) Rapid renewal of auditory hair bundles. *Nature* 418: 837-8
- Schrank B, Gotz R, Gunnarsen JM, Ure JM, Toyka KV, Smith AG, Sendtner M (1997) Inactivation of the survival motor neuron gene, a candidate gene for human spinal muscular atrophy, leads to massive cell death in early mouse embryos. *Proc Natl Acad Sci U S A* 94: 9920-5
- Schwamborn JC, Puschel AW (2004) The sequential activity of the GTPases Rap1B and Cdc42 determines neuronal polarity. *Nat Neurosci* 7: 923-9
- Selenko P, Sprangers R, Stier G, Buhler D, Fischer U, Sattler M (2001) SMN tudor domain structure and its interaction with the Sm proteins. *Nat Struct Biol* 8: 27-31
- Shaffer AL, Yu X, He Y, Boldrick J, Chan EP, Staudt LM (2000) BCL-6 represses genes that function in lymphocyte differentiation, inflammation, and cell cycle control. *Immunity* 13: 199-212

- Sharma A, Lambrechts A, Hao le T, Le TT, Sewry CA, Ampe C, Burghes AH, Morris GE (2005) A role for complexes of survival of motor neurons (SMN) protein with gemins and profilin in neurite-like cytoplasmic extensions of cultured nerve cells. *Exp Cell Res* 309: 185-97
- Sherr CJ (2000) Cell cycle control and cancer. *Harvey Lect* 96: 73-92
- Sherr CJ, Weber JD (2000) The ARF/p53 pathway. *Curr Opin Genet Dev* 10: 94-9
- Shibata H, Huynh DP, Pulst SM (2000) A novel protein with RNA-binding motifs interacts with ataxin-2. *Hum Mol Genet* 9: 1303-13
- Shinjo K, Koland JG, Hart MJ, Narasimhan V, Johnson DI, Evans T, Cerione RA (1990) Molecular cloning of the gene for the human placental GTP-binding protein Gp (G25K): identification of this GTP-binding protein as the human homolog of the yeast cell-division-cycle protein CDC42. *Proc Natl Acad Sci U S A* 87: 9853-7
- Shirayama S, Numata O (2003) Tetrahymena fimbrin localized in the division furrow bundles actin filaments in a calcium-independent manner. *J Biochem (Tokyo)* 134: 591-8
- Shpargel KB, Matera AG (2005) Gemin proteins are required for efficient assembly of Sm-class ribonucleoproteins. *Proc Natl Acad Sci U S A* 102: 17372-7
- Sif S, Saurin AJ, Imbalzano AN, Kingston RE (2001) Purification and characterization of mSin3A-containing Brg1 and hBrdm chromatin remodeling complexes. *Genes Dev* 15: 603-18
- Simic G, Seso-Simic D, Lucassen PJ, Islam A, Krsnik Z, Cviko A, Jelasic D, Barisic N, Winblad B, Kostovic I, Kruslin B (2000) Ultrastructural analysis and TUNEL demonstrate motor neuron apoptosis in Werdnig-Hoffmann disease. *J Neuropathol Exp Neurol* 59: 398-407
- Singer RH, Green MR (1997) Compartmentalization of eukaryotic gene expression: causes and effects. *Cell* 91: 291-4
- Singh NN, Androphy EJ, Singh RN (2004a) An extended inhibitory context causes skipping of exon 7 of SMN2 in spinal muscular atrophy. *Biochem Biophys Res Commun* 315: 381-8
- Singh NN, Androphy EJ, Singh RN (2004b) In vivo selection reveals combinatorial controls that define a critical exon in the spinal muscular atrophy genes. *Rna* 10: 1291-305
- Skordis LA, Dunckley MG, Yue B, Eperon IC, Muntoni F (2003) Bifunctional antisense oligonucleotides provide a trans-acting splicing enhancer that stimulates SMN2 gene expression in patient fibroblasts. *Proc Natl Acad Sci U S A* 100: 4114-9
- Sleeman JE, Ajuh P, Lamond AI (2001) snRNP protein expression enhances the formation of Cajal bodies containing p80-coilin and SMN. *J Cell Sci* 114: 4407-19
- Smale ST, Baltimore D (1989) The "initiator" as a transcription control element. *Cell* 57: 103-13
- Soler-Botija C, Ferrer I, Gich I, Baiget M, Tizzano EF (2002) Neuronal death is enhanced and begins during foetal development in type I spinal muscular atrophy spinal cord. *Brain* 125: 1624-34
- Song F, Smith JF, Kimura MT, Morrow AD, Matsuyama T, Nagase H, Held WA (2005) Association of tissue-specific differentially methylated regions (TDMs) with differential gene expression. *Proc Natl Acad Sci U S A* 102: 3336-41
- Sotelo-Silveira JR, Calliari A, Kun A, Koenig E, Sotelo JR (2006) RNA trafficking in axons. *Traffic* 7: 508-15
- Stanek D, Neugebauer KM (2004) Detection of snRNP assembly intermediates in Cajal bodies by fluorescence resonance energy transfer. *J Cell Biol* 166: 1015-25
- Stoecklin G, Stubbs T, Kedersha N, Wax S, Rigby WF, Blackwell TK, Anderson P (2004) MK2-induced tristetraprolin:14-3-3 complexes prevent stress granule association and ARE-mRNA decay. *Embo J* 23: 1313-24
- Stossel TP (1994) The machinery of cell crawling. *Sci Am* 271: 54-5, 58-63
- Strasswimmer J, Lorson CL, Breiding DE, Chen JJ, Le T, Burghes AH, Androphy EJ (1999) Identification of survival motor neuron as a transcriptional activator-binding protein. *Hum Mol Genet* 8: 1219-26
- Sueyoshi T, Kawamoto T, Zelko I, Honkakoski P, Negishi M (1999) The repressed nuclear receptor CAR responds to phenobarbital in activating the human CYP2B6 gene. *J Biol Chem* 274: 6043-6
- Sugatani J, Kojima H, Ueda A, Kakizaki S, Yoshinari K, Gong QH, Owens IS, Negishi M, Sueyoshi T (2001) The phenobarbital response enhancer module in the human bilirubin UDP-glucuronosyltransferase UGT1A1 gene and regulation by the nuclear receptor CAR. *Hepatology* 33: 1232-8
- Sumner CJ, Huynh TN, Markowitz JA, Perhac JS, Hill B, Coovert DD, Schussler K, Chen X, Jarecki J, Burghes AH, Taylor JP, Fischbeck KH (2003) Valproic acid increases SMN levels in spinal muscular atrophy patient cells. *Ann Neurol* 54: 647-54

- Sun Y, Grimmler M, Schwarzer V, Schoenen F, Fischer U, Wirth B (2005) Molecular and functional analysis of intragenic SMN1 mutations in patients with spinal muscular atrophy. *Hum Mutat* 25: 64-71
- Suter DM, Forscher P (2000) Substrate-cytoskeletal coupling as a mechanism for the regulation of growth cone motility and guidance. *J Neurobiol* 44: 97-113
- Svitkina TM, Borisy GG (1999) Progress in protrusion: the tell-tale scar. *Trends Biochem Sci* 24: 432-6
- Swoboda KJ, Prior TW, Scott CB, McNaught TP, Wride MC, Reyna SP, Bromberg MB (2005) Natural history of denervation in SMA: relation to age, SMN2 copy number, and function. *Ann Neurol* 57: 704-12
- Tacke R, Tohyama M, Ogawa S, Manley JL (1998) Human Tra2 proteins are sequence-specific activators of pre-mRNA splicing. *Cell* 93: 139-48
- Tang MX, Redemann CT, Szoka FC, Jr. (1996) In vitro gene delivery by degraded polyamidoamine dendrimers. *Bioconj Chem* 7: 703-14
- Thomas MG, Martinez Tosar LJ, Loschi M, Pasquini JM, Correale J, Kindler S, Boccaccio GL (2005) Staufen recruitment into stress granules does not affect early mRNA transport in oligodendrocytes. *Mol Biol Cell* 16: 405-20
- Thomas P, Smart TG (2005) HEK293 cell line: a vehicle for the expression of recombinant proteins. *J Pharmacol Toxicol Methods* 51: 187-200
- Thompson TG, DiDonato CJ, Simard LR, Ingraham SE, Burghes AH, Crawford TO, Rochette C, Mendell JR, Wasmuth JJ (1995) A novel cDNA detects homozygous microdeletions in greater than 50% of type I spinal muscular atrophy patients. *Nat Genet* 9: 56-62
- Timmers AC, Niebel A, Balague C, Dagkesamanskaya A (2002) Differential localisation of GFP fusions to cytoskeleton-binding proteins in animal, plant, and yeast cells. *Green-fluorescent protein. Protoplasma* 220: 69-78
- Tiruchinapalli DM, Oleynikov Y, Kelic S, Shenoy SM, Hartley A, Stanton PK, Singer RH, Bassell GJ (2003) Activity-dependent trafficking and dynamic localization of zipcode binding protein 1 and beta-actin mRNA in dendrites and spines of hippocampal neurons. *J Neurosci* 23: 3251-61
- Tischler AS, Greene LA (1975) Nerve growth factor-induced process formation by cultured rat pheochromocytoma cells. *Nature* 258: 341-2
- Tizzano EF, Cabot C, Baiget M (1998) Cell-specific survival motor neuron gene expression during human development of the central nervous system: implications for the pathogenesis of spinal muscular atrophy. *Am J Pathol* 153: 355-61
- Tost J, Dunker J, Gut IG (2003) Analysis and quantification of multiple methylation variable positions in CpG islands by Pyrosequencing. *Biotechniques* 35: 152-6
- Tourriere H, Chebli K, Zekri L, Courselaud B, Blanchard JM, Bertrand E, Tazi J (2003) The RasGAP-associated endoribonuclease G3BP assembles stress granules. *J Cell Biol* 160: 823-31
- Trulzsch B, Davies K, Wood M (2004) Survival of motor neuron gene downregulation by RNAi: towards a cell culture model of spinal muscular atrophy. *Brain Res Mol Brain Res* 120: 145-50
- Ueda A, Hamadeh HK, Webb HK, Yamamoto Y, Sueyoshi T, Afshari CA, Lehmann JM, Negishi M (2002) Diverse roles of the nuclear orphan receptor CAR in regulating hepatic genes in response to phenobarbital. *Mol Pharmacol* 61: 1-6
- Uhlmann K, Brinckmann A, Toliat MR, Ritter H, Nurnberg P (2002) Evaluation of a potential epigenetic biomarker by quantitative methyl-single nucleotide polymorphism analysis. *Electrophoresis* 23: 4072-9
- van Bergeijk J, Rydel-Konecke K, Grothe C, Claus P (2007) The spinal muscular atrophy gene product regulates neurite outgrowth: importance of the C terminus. *Faseb J*
- van der Vleuten AJ, van Ravenswaaij-Arts CM, Frijns CJ, Smits AP, Hageman G, Padberg GW, Kremer H (1998) Localisation of the gene for a dominant congenital spinal muscular atrophy predominantly affecting the lower limbs to chromosome 12q23-q24. *Eur J Hum Genet* 6: 376-82
- Vandekerckhove J, Bauw G, Vancompernelle K, Honore B, Celis J (1990) Comparative two-dimensional gel analysis and microsequencing identifies gelsolin as one of the most prominent downregulated markers of transformed human fibroblast and epithelial cells. *J Cell Biol* 111: 95-102
- Velasco E, Valero C, Valero A, Moreno F, Hernandez-Chico C (1996) Molecular analysis of the SMN and NAIP genes in Spanish spinal muscular atrophy (SMA) families and correlation between number of copies of cBCD541 and SMA phenotype. *Hum Mol Genet* 5: 257-63

- Venables JP, Bourgeois CF, Dalgliesh C, Kister L, Stevenin J, Elliott DJ (2005) Up-regulation of the ubiquitous alternative splicing factor Tra2beta causes inclusion of a germ cell-specific exon. *Hum Mol Genet* 14: 2289-303
- Venables JP, Elliott DJ, Makarova OV, Makarov EM, Cooke HJ, Eperon IC (2000) RBMY, a probable human spermatogenesis factor, and other hnRNP G proteins interact with Tra2beta and affect splicing. *Hum Mol Genet* 9: 685-94
- Verdel A, Khochbin S (1999) Identification of a new family of higher eukaryotic histone deacetylases. Coordinate expression of differentiation-dependent chromatin modifiers. *J Biol Chem* 274: 2440-5
- Viollet L, Barois A, Rebeiz JG, Rifai Z, Burlet P, Zarhrate M, Vial E, Dessainte M, Estournet B, Kleinknecht B, Pearn J, Adams RD, Urtizbera JA, Cros DP, Bushby K, Munnich A, Lefebvre S (2002) Mapping of autosomal recessive chronic distal spinal muscular atrophy to chromosome 11q13. *Ann Neurol* 51: 585-92
- Viollet L, Bertrand S, Bueno Brunialti AL, Lefebvre S, Burlet P, Clermont O, Cruaud C, Guenet JL, Munnich A, Melki J (1997) cDNA isolation, expression, and chromosomal localization of the mouse survival motor neuron gene (*Smn*). *Genomics* 40: 185-8
- von Mikecz A, Zhang S, Montminy M, Tan EM, Hemmerich P (2000) CREB-binding protein (CBP)/p300 and RNA polymerase II colocalize in transcriptionally active domains in the nucleus. *J Cell Biol* 150: 265-73
- Voss MD, Hille A, Barth S, Spurr A, Henrich F, Holzer D, Mueller-Lantsch N, Kremmer E, Grasser FA (2001) Functional cooperation of Epstein-Barr virus nuclear antigen 2 and the survival motor neuron protein in transactivation of the viral LMP1 promoter. *J Virol* 75: 11781-90
- Vousden KH (2000) p53: death star. *Cell* 103: 691-4
- Vousden KH, Woude GF (2000) The ins and outs of p53. *Nat Cell Biol* 2: E178-80
- Wan L, Battle DJ, Yong J, Gubitz AK, Kolb SJ, Wang J, Dreyfuss G (2005) The survival of motor neurons protein determines the capacity for snRNP assembly: biochemical deficiency in spinal muscular atrophy. *Mol Cell Biol* 25: 5543-51
- Wang CH, Xu J, Carter TA, Ross BM, Dominski MK, Bellcross CA, Penchaszadeh GK, Munsat TL, Gilliam TC (1996) Characterization of survival motor neuron (SMNT) gene deletions in asymptomatic carriers of spinal muscular atrophy. *Hum Mol Genet* 5: 359-65
- Wang H, Faucette S, Moore R, Sueyoshi T, Negishi M, LeCluyse E (2004) Human constitutive androstane receptor mediates induction of CYP2B6 gene expression by phenytoin. *J Biol Chem* 279: 29295-301
- Wang H, Faucette S, Sueyoshi T, Moore R, Ferguson S, Negishi M, LeCluyse EL (2003) A novel distal enhancer module regulated by pregnane X receptor/constitutive androstane receptor is essential for the maximal induction of CYP2B6 gene expression. *J Biol Chem* 278: 14146-52
- Wang H, Negishi M (2003) Transcriptional regulation of cytochrome p450 2B genes by nuclear receptors. *Curr Drug Metab* 4: 515-25
- Wang J, Dreyfuss G (2001a) A cell system with targeted disruption of the SMN gene: functional conservation of the SMN protein and dependence of Gemin2 on SMN. *J Biol Chem* 276: 9599-605
- Wang J, Dreyfuss G (2001b) Characterization of functional domains of the SMN protein in vivo. *J Biol Chem* 276: 45387-93
- Wang W, Dimatteo D, Funanage VL, Scavina M (2005) Increased susceptibility of spinal muscular atrophy fibroblasts to camptothecin-induced cell death. *Mol Genet Metab* 85: 38-45
- Wang X, DeKosky ST, Wisniewski S, Aston, Kamboh MI (1998) Genetic association of two chromosome 14 genes (presenilin 1 and alpha 1-antichymotrypsin) with Alzheimer's disease. *Ann Neurol* 44: 387-90
- Watanabe A, Kurasawa Y, Watanabe Y, Numata O (1998) A new Tetrahymena actin-binding protein is localized in the division furrow. *J Biochem (Tokyo)* 123: 607-13
- Watanabe A, Yonemura I, Gonda K, Numata O (2000) Cloning and sequencing of the gene for a Tetrahymena fimbrin-like protein. *J Biochem (Tokyo)* 127: 85-94
- Watanabe N, Madaule P, Reid T, Ishizaki T, Watanabe G, Kakizuka A, Saito Y, Nakao K, Jockusch BM, Narumiya S (1997) p140mDia, a mammalian homolog of Drosophila diaphanous, is a target protein for Rho small GTPase and is a ligand for profilin. *Embo J* 16: 3044-56
- Wei P, Zhang J, Dowhan DH, Han Y, Moore DD (2002) Specific and overlapping functions of the nuclear hormone receptors CAR and PXR in xenobiotic response. *Pharmacogenomics J* 2: 117-26

- Wei P, Zhang J, Egan-Hafley M, Liang S, Moore DD (2000) The nuclear receptor CAR mediates specific xenobiotic induction of drug metabolism. *Nature* 407: 920-3
- Weighardt F, Biamonti G, Riva S (1996) The roles of heterogeneous nuclear ribonucleoproteins (hnRNP) in RNA metabolism. *Bioessays* 18: 747-56
- Welch MD, DePace AH, Verma S, Iwamatsu A, Mitchison TJ (1997a) The human Arp2/3 complex is composed of evolutionarily conserved subunits and is localized to cellular regions of dynamic actin filament assembly. *J Cell Biol* 138: 375-84
- Welch MD, Iwamatsu A, Mitchison TJ (1997b) Actin polymerization is induced by Arp2/3 protein complex at the surface of *Listeria monocytogenes*. *Nature* 385: 265-9
- Welch MD, Mallavarapu A, Rosenblatt J, Mitchison TJ (1997c) Actin dynamics in vivo. *Curr Opin Cell Biol* 9: 54-61
- Whitfield ML, Sherlock G, Saldanha AJ, Murray JI, Ball CA, Alexander KE, Matese JC, Perou CM, Hurt MM, Brown PO, Botstein D (2002) Identification of genes periodically expressed in the human cell cycle and their expression in tumors. *Mol Biol Cell* 13: 1977-2000
- Wilczynska A, Aigueperse C, Kress M, Dautry F, Weil D (2005) The translational regulator CPEB1 provides a link between dcp1 bodies and stress granules. *J Cell Sci* 118: 981-92
- Will CL, Luhrmann R (2001) Spliceosomal UsnRNP biogenesis, structure and function. *Curr Opin Cell Biol* 13: 290-301
- Williams BY, Hamilton SL, Sarkar HK (2000) The survival motor neuron protein interacts with the transactivator FUSE binding protein from human fetal brain. *FEBS Lett* 470: 207-10
- Williams BY, Vinnakota S, Sawyer CA, Waldrep JC, Hamilton SL, Sarkar HK (1999) Differential subcellular localization of the survival motor neuron protein in spinal cord and skeletal muscle. *Biochem Biophys Res Commun* 254: 10-4
- Wills Z, Marr L, Zinn K, Goodman CS, Van Vactor D (1999) Profilin and the Abl tyrosine kinase are required for motor axon outgrowth in the *Drosophila* embryo. *Neuron* 22: 291-9
- Wirth B (2000) An update of the mutation spectrum of the survival motor neuron gene (SMN1) in autosomal recessive spinal muscular atrophy (SMA). *Hum Mutat* 15: 228-37
- Wirth B (2002) Spinal muscular atrophy: state-of-the-art and therapeutic perspectives. *Amyotroph Lateral Scler Other Motor Neuron Disord* 3: 87-95
- Wirth B, Brichta L, Hahnen E (2006a) Spinal muscular atrophy and therapeutic prospects. *Prog Mol Subcell Biol* 44: 109-32
- Wirth B, Brichta L, Schrank B, Lochmuller H, Blick S, Baasner A, Heller R (2006b) Mildly affected patients with spinal muscular atrophy are partially protected by an increased SMN2 copy number. *Hum Genet* 119: 422-8
- Wirth B, Hahnen E, Morgan K, DiDonato CJ, Dadze A, Rudnik-Schoneborn S, Simard LR, Zerres K, Burghes AH (1995a) Allelic association and deletions in autosomal recessive proximal spinal muscular atrophy: association of marker genotype with disease severity and candidate cDNAs. *Hum Mol Genet* 4: 1273-84
- Wirth B, Herz M, Wetter A, Moskau S, Hahnen E, Rudnik-Schoneborn S, Wienker T, Zerres K (1999) Quantitative analysis of survival motor neuron copies: identification of subtle SMN1 mutations in patients with spinal muscular atrophy, genotype-phenotype correlation, and implications for genetic counseling. *Am J Hum Genet* 64: 1340-56
- Wirth B, Rudnik-Schoneborn S, Hahnen E, Rohrig D, Zerres K (1995b) Prenatal prediction in families with autosomal recessive proximal spinal muscular atrophy (5q11.2-q13.3): molecular genetics and clinical experience in 109 cases. *Prenat Diagn* 15: 407-17
- Wirth B, Schmidt T, Hahnen E, Rudnik-Schoneborn S, Krawczak M, Muller-Myhsok B, Schonling J, Zerres K (1997a) De novo rearrangements found in 2% of index patients with spinal muscular atrophy: mutational mechanisms, parental origin, mutation rate, and implications for genetic counseling. *Am J Hum Genet* 61: 1102-11
- Wirth B, Tessarolo D, Hahnen E, Rudnik-Schoneborn S, Raschke H, Liguori M, Giacanelli M, Zerres K (1997b) Different entities of proximal spinal muscular atrophy within one family. *Hum Genet* 100: 676-80
- Witowski J, Jorres A (2006) Peritoneal cell culture: fibroblasts. *Perit Dial Int* 26: 292-9
- Wu JQ, Bahler J, Pringle JR (2001) Roles of a fimbrin and an alpha-actinin-like protein in fission yeast cell polarization and cytokinesis. *Mol Biol Cell* 12: 1061-77
- Wu JY, Maniatis T (1993) Specific interactions between proteins implicated in splice site selection and regulated alternative splicing. *Cell* 75: 1061-70

- Wysocka J, Myers MP, Laherty CD, Eisenman RN, Herr W (2003) Human Sin3 deacetylase and trithorax-related Set1/Ash2 histone H3-K4 methyltransferase are tethered together selectively by the cell-proliferation factor HCF-1. *Genes Dev* 17: 896-911
- Xiao SH, Manley JL (1998) Phosphorylation-dephosphorylation differentially affects activities of splicing factor ASF/SF2. *Embo J* 17: 6359-67
- Xie W, Yeuh MF, Radomska-Pandya A, Saini SP, Negishi Y, Bottroff BS, Cabrera GY, Tukey RH, Evans RM (2003) Control of steroid, heme, and carcinogen metabolism by nuclear pregnane X receptor and constitutive androstane receptor. *Proc Natl Acad Sci U S A* 100: 4150-5
- Yang L, Mei Q, Zielinska-Kwiatkowska A, Matsui Y, Blackburn ML, Benedetti D, Krumm AA, Taborsky GJ, Jr., Chansky HA (2003) An ERG (ets-related gene)-associated histone methyltransferase interacts with histone deacetylases 1/2 and transcription co-repressors mSin3A/B. *Biochem J* 369: 651-7
- Yang XJ, Ogryzko VV, Nishikawa J, Howard BH, Nakatani Y (1996) A p300/CBP-associated factor that competes with the adenoviral oncoprotein E1A. *Nature* 382: 319-24
- Yoder JA, Walsh CP, Bestor TH (1997) Cytosine methylation and the ecology of intragenomic parasites. *Trends Genet* 13: 335-40
- Yong J, Golembe TJ, Battle DJ, Pellizzoni L, Dreyfuss G (2004) snRNAs contain specific SMN-binding domains that are essential for snRNP assembly. *Mol Cell Biol* 24: 2747-56
- Yong J, Pellizzoni L, Dreyfuss G (2002) Sequence-specific interaction of U1 snRNA with the SMN complex. *Embo J* 21: 1188-96
- Yoshida M, Furumai R, Nishiyama M, Komatsu Y, Nishino N, Horinouchi S (2001) Histone deacetylase as a new target for cancer chemotherapy. *Cancer Chemother Pharmacol* 48 Suppl 1: S20-6
- Yoshinari K, Kobayashi K, Moore R, Kawamoto T, Negishi M (2003) Identification of the nuclear receptor CAR:HSP90 complex in mouse liver and recruitment of protein phosphatase 2A in response to phenobarbital. *FEBS Lett* 548: 17-20
- Young ME, Cooper JA, Bridgman PC (2004) Yeast actin patches are networks of branched actin filaments. *J Cell Biol* 166: 629-35
- Young PJ, Day PM, Zhou J, Androphy EJ, Morris GE, Lorson CL (2002a) A direct interaction between the survival motor neuron protein and p53 and its relationship to spinal muscular atrophy. *J Biol Chem* 277: 2852-9
- Young PJ, DiDonato CJ, Hu D, Kothary R, Androphy EJ, Lorson CL (2002b) SRp30c-dependent stimulation of survival motor neuron (SMN) exon 7 inclusion is facilitated by a direct interaction with hTra2 beta 1. *Hum Mol Genet* 11: 577-87
- Young PJ, Francis JW, Lince D, Coon K, Androphy EJ, Lorson CL (2003) The Ewing's sarcoma protein interacts with the Tudor domain of the survival motor neuron protein. *Brain Res Mol Brain Res* 119: 37-49
- Young PJ, Jensen KT, Burger LR, Pintel DJ, Lorson CL (2002c) Minute virus of mice NS1 interacts with the SMN protein, and they colocalize in novel nuclear bodies induced by parvovirus infection. *J Virol* 76: 3892-904
- Young PJ, Jensen KT, Burger LR, Pintel DJ, Lorson CL (2002d) Minute virus of mice small nonstructural protein NS2 interacts and colocalizes with the Smn protein. *J Virol* 76: 6364-9
- Yu JZ, Rasenick MM (2006) Tau associates with actin in differentiating PC12 cells. *Faseb J* 20: 1452-61
- Zalcman G, Closson V, Linares-Cruz G, Lerebours F, Honore N, Tavitian A, Olofsson B (1995) Regulation of Ras-related RhoB protein expression during the cell cycle. *Oncogene* 10: 1935-45
- Zalewska E, Hausmanowa-Petrusewicz I (2000) Effectiveness of motor unit potentials classification using various parameters and indexes. *Clin Neurophysiol* 111: 1380-7
- Zelko I, Sueyoshi T, Kawamoto T, Moore R, Negishi M (2001) The peptide near the C terminus regulates receptor CAR nuclear translocation induced by xenochemicals in mouse liver. *Mol Cell Biol* 21: 2838-46
- Zeng C, Kim E, Warren SL, Berget SM (1997) Dynamic relocation of transcription and splicing factors dependent upon transcriptional activity. *Embo J* 16: 1401-12
- Zerres K, Rudnik-Schoneborn S (1995) Natural history in proximal spinal muscular atrophy. Clinical analysis of 445 patients and suggestions for a modification of existing classifications. *Arch Neurol* 52: 518-23
- Zhang H, Xing L, Rossoll W, Wichterle H, Singer RH, Bassell GJ (2006) Multiprotein complexes of the survival of motor neuron protein SMN with Gemins traffic to neuronal processes and growth cones of motor neurons. *J Neurosci* 26: 8622-32

- Zhang HL, Pan F, Hong D, Shenoy SM, Singer RH, Bassell GJ (2003) Active transport of the survival motor neuron protein and the role of exon-7 in cytoplasmic localization. *J Neurosci* 23: 6627-37
- Zhang J, Huang W, Chua SS, Wei P, Moore DD (2002) Modulation of acetaminophen-induced hepatotoxicity by the xenobiotic receptor CAR. *Science* 298: 422-4
- Zhang J, Huang W, Qatanani M, Evans RM, Moore DD (2004) The constitutive androstane receptor and pregnane X receptor function coordinately to prevent bile acid-induced hepatotoxicity. *J Biol Chem* 279: 49517-22
- Zhang Y, Dufau ML (2002) Silencing of transcription of the human luteinizing hormone receptor gene by histone deacetylase-mSin3A complex. *J Biol Chem* 277: 33431-8
- Zhang Y, Reinberg D (2001) Transcription regulation by histone methylation: interplay between different covalent modifications of the core histone tails. *Genes Dev* 15: 2343-60
- Zhang Z, Huang C, Li J, Leonard SS, Lanciotti R, Butterworth L, Shi X (2001) Vanadate-induced cell growth regulation and the role of reactive oxygen species. *Arch Biochem Biophys* 392: 311-20
- Zhou D, Mooseker MS, Galan JE (1999) An invasion-associated Salmonella protein modulates the actin-bundling activity of plastrin. *Proc Natl Acad Sci U S A* 96: 10176-81
- Zoll WL, Horton LE, Komar AA, Hensold JO, Merrick WC (2002) Characterization of mammalian eIF2A and identification of the yeast homolog. *J Biol Chem* 277: 37079-87
- Zou J, Barahmand-pour F, Blackburn ML, Matsui Y, Chansky HA, Yang L (2004) Survival motor neuron (SMN) protein interacts with transcription corepressor mSin3A. *J Biol Chem* 279: 14922-8

***APPENDIX***

**Figures:**

- I. *F1: Pedigrees of the SMA discordant families*
- II. *F2: pcDNA 3.1\_T-plastin\_V5 vector map*
- III. *F3: Human T-plastin transcript*
- IV. *F4: T-plastin genomic region*
- V. *F5: T-plastin promoter-1<sup>st</sup> exon-1<sup>st</sup> intron region (1 kb) after bisulfite treatment*
- VI. *F6: T-plastin expression analysis by RT-PCR in 79 SMA patients*
- VII. *F7 Simulation of the genome scan analysis under the assumption of recessive mode of inheritance*
- VIII. *F8 Simulation of the genome scan analysis under the assumption of dominant mode of inheritance*
- IX. *F9 Methylation status of T-plastin CpG sites in SMA discordant families*
- X. *F10 Methylation status of T-plastin CpG sites in two control groups*
- XI. *F11 Haplotype blocks within T-plastin genomic region*
- XII. *F12 Motor axons defects in smn morphants are rescued by overexpression of human T-plastin RNA*

APPENDIX

I. Fig. F1 Pedigrees of the SMA discordant families

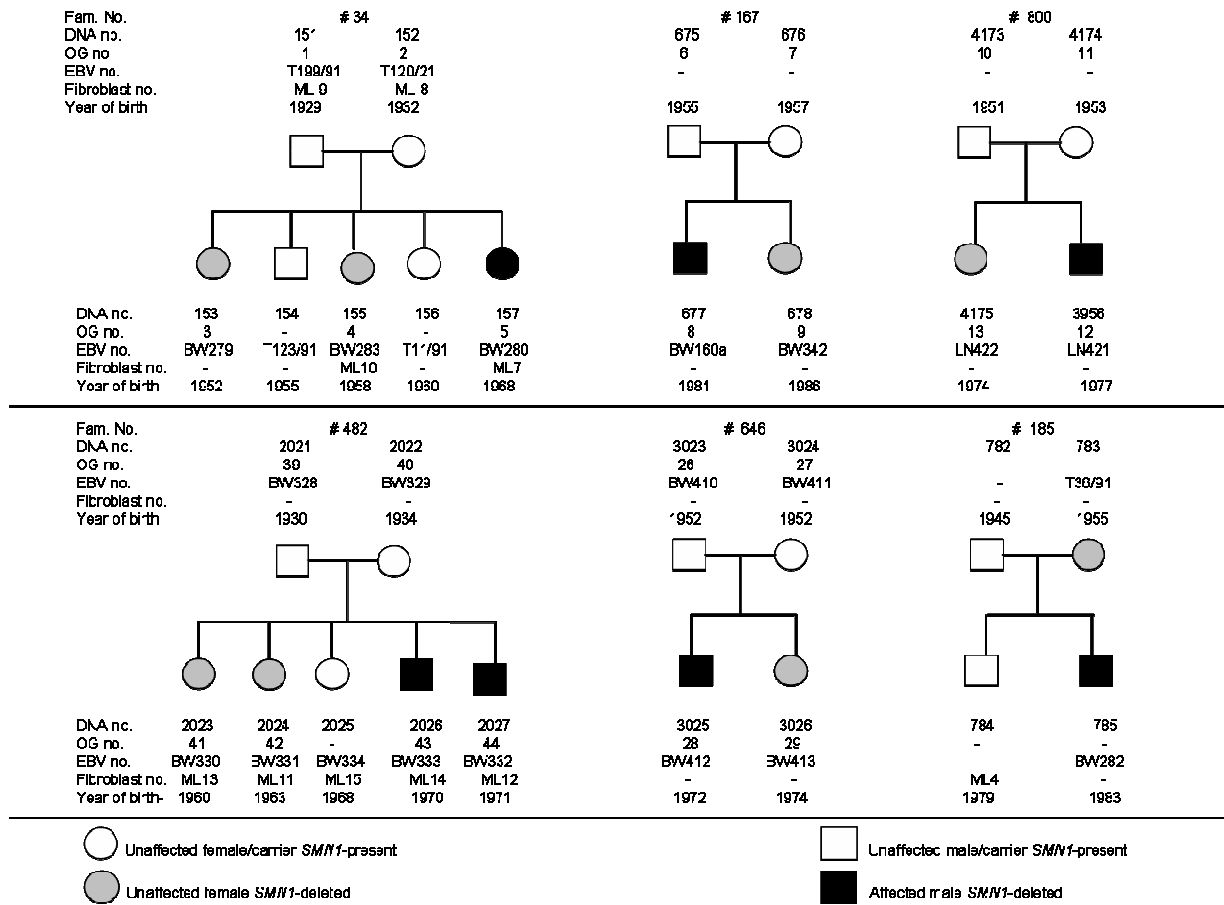
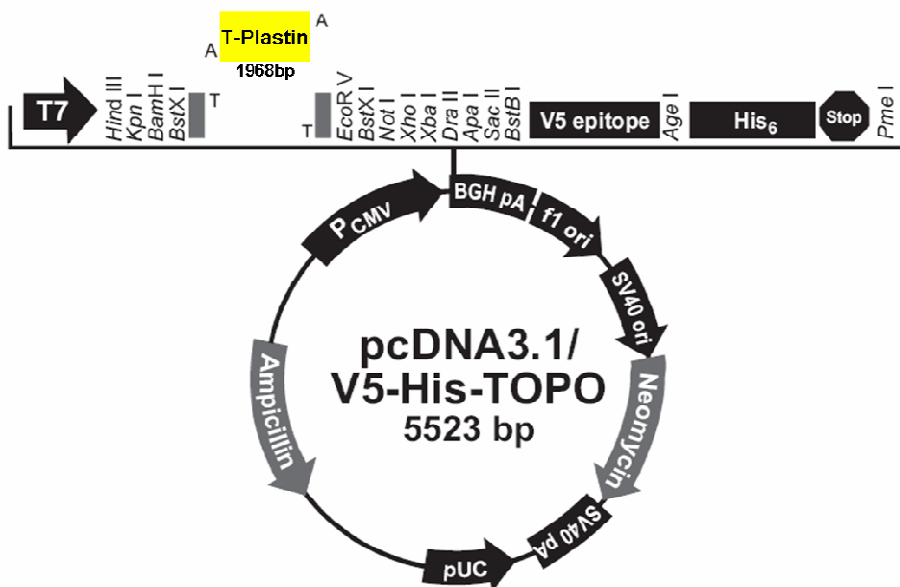


Fig. F2 pcDNA3.1\_T-plastin\_V5 vector map



APPENDIX

III. Fig. F3 Human *T-plastin* Transcript

Nucleotide and amino acid sequence of *T-plastin* transcript (NM\_013386). The 5'UTR and 3'UTR regions are highlighted on yellow background. The exon alternation is given in two different colours (black-blue). The primers used for DNA cloning (#2545 and #2586) and multiplex PCR (#2331 and #2332) are marked in red colour.

5' -UTR

1 GCGCTGGCTTTAGAGCCACAGCTGCAAAGATTCCGAGGTGCAGAAGTTGTCTGAGTGCCT  
.....Primer# 2454 (For).....

61 TGGTCGGCGGCAGTCGGGCCAGACCCAGGACTCTGCGACTTTACATCTTTTAAATGGATGA  
.....-M--D--E

121 GATGGCTACCACTCAGATTCCAAAGATGAGCTTGATGAACTCAAAGAGGCCTTTGCAAA  
3 --M--A--T--T--Q--I--S--K--D--E--L--D--E--L--K--E--A--F--A--K

181 AGTTGATCTCAACAGCAACGGATTTCATTGTGACTATGAACTTCATGAGCTCTTCAAGGA  
23 --V--D--L--N--S--N--G--F--I--C--D--Y--E--L--H--E--L--F--K--E

241 AGCTAATATGCCATTACCAGGATATAAAGTGAGAGAAATTATTCAGAAACTCATGCTGGA  
43 --A--N--M--P--L--P--G--Y--K--V--R--E--I--I--Q--K--L--M--L--D

301 TGGTGACAGGAATAAAGATGGGAAAATAAGTTTGTGACGAATTGTTTATATTTTCAAGA  
63 --G--D--R--N--K--D--G--K--I--S--F--D--E--F--V--Y--I--F--Q--E

361 GGTAAAAAGTAGTGATATTGCCAAGACCTTCCGCAAAGCAATCAACAGGAAAGAGGTAT  
83 --V--K--S--S--D--I--A--K--T--F--R--K--A--I--N--R--K--E--G--I

421 TTGTGCTCTGGGTGGAACCTCAGAGTTGTCCAGCGAAGGAACACAGCATTCTTACTCAGA  
103 --C--A--L--G--G--T--S--E--L--S--S--E--G--T--Q--H--S--Y--S--E

481 GGAAGAAAAATATGCTTTTGTAACTGGATAAACAAAGCTTTGGAAAATGATCCTGATTG  
123 --E--E--K--Y--A--F--V--N--W--I--N--K--A--L--E--N--D--P--D--C

541 TAGACATGTTATACCAATGAACCCCTAACACCGATGACCTGTTCAAAGCTGTTGGTGATGG  
143 --R--H--V--I--P--M--N--P--N--T--D--D--L--F--K--A--V--G--D--G

601 AATTGTGCTTTGTAAAATGATTAACCTTTCAGTTCCTGATACCATTGATGAAAGAGCAAT  
163 --I--V--L--C--K--M--I--N--L--S--V--P--D--T--I--D--E--R--A--I

661 CAACAAGAAGAACTTACACCCCTCATCATTGAGGAAAACCTGAACTTGGCACTGAACTC  
183 --N--K--K--K--L--T--P--F--I--I--Q--E--N--L--N--L--A--L--N--S

721 TGCTTCTGCCATTGGGTGTCATGTTGTGAACATTGGTGCAGAAGATTGAGGGCTGGGAA  
203 --A--S--A--I--G--C--H--V--V--N--I--G--A--E--D--L--R--A--G--K

781 ACCTCATCTGTTTTGGGACTGCTTTGGCAGATCATTAAAGATCGGTTTGTTCGCTGACAT  
223 --P--H--L--V--L--G--L--L--W--Q--I--I--K--I--G--L--F--A--D--I

841 TGAATTAAGCAGGAATGAAGCCCTGGCTGCTTTACTCCGAGATGGTGAGACTTTGGAGGA  
243 --E--L--S--R--N--E--A--L--A--A--L--L--R--D--G--E--T--L--E--E

901 ACTTATGAAATTTCTCCAGAAGAGCTTCTGCTTAGATGGGCAAACTTTTCATTTGGAAAA  
263 --L--M--K--L--S--P--E--E--L--L--L--R--W--A--N--F--H--L--E--N

APPENDIX

961 CTCGGGCTGGCAAAAAATTAACAACCTTTAGTGCTGACATCAAGGATTCCAAAGCCTATTT  
283 --S--G--W--Q--K--I--N--N--F--S--A--D--I--K--D--S--K--A--Y--F

1021 CCATCTTCTCAATCAAATCGACCAAAAAGGACAAAAGGAAGGTGAACCACGGATAGATAT  
303 --H--L--L--N--Q--I--A--P--K--G--Q--K--E--G--E--P--R--I--D--I

1081 TAACATGTCAGGTTTCAATGAAACAGATGATTGAAGAGAGCTGAGAGTATGCTTCAACA  
323 --N--M--S--G--F--N--E--T--D--D--L--K--R--A--E--S--M--L--Q--Q

1141 AGCAGATAAATTAGGTTGCAGACAGTTGTTACCCCTGCTGATGTTGTCAGTGGAAACCC  
343 --A--D--K--L--G--C--R--Q--F--V--T--P--A--D--V--V--S--G--N--P

1201 CAAACTCAACTT<sup>R</sup>GCTTTCGTGGCTAACCTGTTAATAAATACCCAGCACTAACTAAGCC  
363 --K--L--N--L--A--F--V--A--N--L--F--N--K--Y--P--A--L--T--K--P

1261 AGAGAACCAGGATATTGACTGGACTCTATTAGAAGGAGAACTCGTGAAGAAAGAACCTT  
383 --E--N--Q--D--I--D--W--T--L--L--E--G--E--T--R--E--E--R--T--F

1321 CCGTAACGGATGAACCTCTTGGTGCAATCT<sup>Y</sup>CACGTAACCATCTCTATGCTGACCT  
403 --R--N--W--M--N--S--L--G--V--N--P--H--V--N--H--L--Y--A--D--L

1381 GCAAGATGCCCTGGTAATCTTACAG<sup>Y</sup>TATATGAACGAATTAAAGTTCCTGTTGACTGGAG  
423 --Q--D--A--L--V--I--L--Q--L--Y--E--R--I--K--V--P--V--D--W--S

1441 TAAGGTTAATAAACCTCCATACCCGAAACTGGGAGCCAACATGAAAAGCTAGAAAACCTG  
443 --K--V--N--K--P--P--Y--P--K--L--G--A--N--M--K--K--L--E--N--C

1501 CAACTATGCTGTTGAATTAGGAAGCATCCTGCTAAATTCCTCCCTGGTTGGCATTGGAGG  
463 --N--Y--A--V--E--L--G--K--H--P--A--K--F--S--L--V--G--I--G--G

1561 GCAAGACCTGAATGATGGGAACCAAAC<sup>S</sup>CTGACTTTAGCTTTAGTCTGGCAGCTGATGAG  
483 --Q--D--L--N--D--G--N--Q--T--L--T--L--A--L--V--W--Q--L--M--R

1621 AAGATATAC<sup>M</sup>CTCAATGCTCTGGAAGATCTTGGAGATGGTCAGAAAAGCCAATGACGACAT  
503 --R--Y--T--L--N--V--L--E--D--L--G--D--G--Q--K--A--N--D--D--I

1681 CATTGTGAACTGGGTGAACAGAACGTTGAGTGAAGCTGGAAAATCAACTTCCATTGAGG  
523 --I--V--N--W--V--N--R--T--L--S--E--A--G--K--S--T--S--I--Q--S

1741 TTTTAAGGACAAGACGATCAGCTCCAGTTTGGCAGTTGTGGATTTAATTGATGCCATCCA  
543 --F--K--D--K--T--I--S--S--S--L--A--V--V--D--L--I--D--A--I--Q

1801 GCCAGGCTGTATAAACTATGACCTTGTGAAGAGTGGCAATCTAACAGAAGATGACAAGCA  
563 --P--G--C--I--N--Y--D--L--V--K--S--G--N--L--T--E--D--D--K--H

1861 CAATAATGCCAAGTATGCAGTGTCAATGGCTAGAAGAATCGGAGCCAGAGTGTATGCTCT  
583 --N--N--A--K--Y--A--V--S--M--A--R--R--I--G--A--R--V--Y--A--L

1921 CCCTGAAGACCTTGTGGAAGTAAAGCCCAAGATGGTCATGACTGTGTTGTCATGTTTGGAT  
603 --P--E--D--L--V--E--V--K--P--K--M--V--M--T--V--F--A--C--L--M

Primer# 2586 (Rev)  
1981 GGCAGGGGAATGAGAGAGTGTAAATAACCAATCTGAATAAAACAGCCATGCTCCCAG  
623 --G--R--G--M--K--R--V--\*.....

## APPENDIX

---

2041 GGCATGATTCGCAGGTCAGCTATTTCCAGGTGAAGTGCTTATGGCTTAAGGAACCTTG  
.....

2101 GCCATTCAAAGGACTTTTCATTTTGATTAACAGGACTAGCTTATCATGAGAGCCCTCAGG  
.....

2161 GGAAAGGGTTAAGAAAAACAACCTCCTCTTTCCCATAGTCAGAGTTGAATTTGTCAGGCA  
.....

2221 CGCCTGAAATGTGCTCATAGCCAAAACATTTTACTCTCTCCTCCTAGAATGCTGCCCTTG  
.....

2281 ACATTTCCATTGCTGTATGTTATTTCTTGCTCTGTTATCTTTTGCCCTCTTAGAATGTC  
.....

2341 CCTCTCTGGGACTTGCTTAGATGATGGGATATGAATATTATTAGACAGTAATTTTGCTT  
.....

2401 TCCATCCAGTATGCTAGTTCTTATTCGAGAACTATGGTCAGAGCGTATTTGGATATGAGT  
.....

2461 ATCCTTTGCTTATCTTTGTAGTACTGAAAATTGCCGAAGTAACTGGCTGTCAGAATGT  
.....

2521 AATAGAAGCTTTTCTTATTCTTTTATTCTTAAGATCAGTATCTTTTACAGTATTCTTTC  
.....

2581 TACATGATCCTTTTTTGTACATTTAAGAATATTTTGATTATATTAACAAGACTGCTGAT  
.....

2641 TTTGCTACT<sup>Y</sup>TTTTTTAAGGGGTCTTCAAGTAAGTAAACATACATCGTAGCTAGAAGAA  
.....

2701 AATGTACCTTAAATTTGCATCTTCCCTCTCATACCCAAGCTGTAAACAATTGAAATATT  
.....

2761 TGTCTTAAATCACTTGGTTCAATACATGCTTATTTGTTTTAAACCTGTATCATCAAAC  
.....

2821 CTCTCTCTAAATTTAAAATGCTGTTGAATATGATACTTTTGAGGAGAGAGTGTGCTCAGA  
.....

2881 ACTTAGACGGGATTTGGTAGCCAAGTATGCTAAGTGTACAATATATTTTTTAATTTTAC  
.....

2941 ACCTGAAACAAAGAAATGTGGTCACTAAAAATAAAAGTATATATGTAGGAATTAATGTAC  
.....

3001 TCTTGCTTTGTCAAGCTGTTTGCTATAGTTTCCAAGGTATTATGTTACTCTAACTCTGAA  
.....

3061 AAGTGATGTAATCTGGTAGCAATGTAGTAGTTCAAATAAAGGCATTAC

3'-UTR

---

APPENDIX

---

**IV. Fig. F4 *T-plastin* genomic region (human)**

#: primer number used for PCR and/or sequencing; →: forward orientation; ←: reverse orientation; +1: transcription initiation start site.  
NOTE: WHEN TWO PRIMERS WITH DIFFERENT ORIENTATION OVERLAP, ONE IS UNDERLINED, THE OTHER IS *ITALICIZED*.

→#2572

-3211 GGTGGCAGGT GCCTATAATA CCAGCTACTT GGGAGGCTGA GGCAGGAGAA

-3161 TCGCTTGAAC CCGGGAGGCA GAGGTTGCAA TGAGCTGAGA CTGTGCCGTT

-3111 GCACTACAGC TGAGGTGACA ACAGTGAAAC TCTGTCTCAA GGAAAAAAAA

-3061 AAAAGTTCAA ACCAGCAATG ACATGTTAAG AATAAAGAAT TAAAAATGGA

-3011 TAGAAGAGGA AACTGACAAC TTACTCTAGG AAAATTCAG GGAAAATTTT

-2961 AGACTATGTA CACATAATAC ATTGTGAGCT AGACTGGGA GAGTGTGGG

-2911 CAGAACAATA GGAAAAGAG CAAGAAAAG GGGGATGTGC GTATCAAAAG

-2861 GAGGAAAGAA AAGTAGTTG GACAGACAAA AAACCTAAGA GAGATATTGG

-2811 CGCCTTCTTA TGATATCAGC GGAGGACAGG AAGAATAAAT GGTTTTCAA

-2761 ATTTTGTGAT ATTGACTTTA AGTGATTTAT TACAAAGGCA TTAGGATCGA

-2711 AAATTGGAAA TGGAAGGAAA GGTA AAAACT CTTAGGTTAC →#2572  
TGATTCACAA

#2573←

-2671 GGTCTGTGAG AATCCTATAT ATATTAATAG CTTTTGTGTT CTGTGTGTTA

-2611 ACAAGAATAG ACATAAAATA ACCATTGGTT CAGCAAACAT TTACTGAACT

-2561 CCTATGTGTC AGGCACTATG CAAGTCACTG TCAAATAAAA TTAAAGCCTA

-2511 TAAGCAGGTG GAGGGAACCC TGACAAACAT CTGTGCAGGC TTTTGTGATC

-2461 AGATAAGAAA ACAATCAACT TTGGGTTACT TCGTGAATGA TCCTCTATGA

-2411 GGTAAATTGA TGGCATGAAA AATTATAAAG AAATGCTGTT TAAGAGCTTT

-2361 GAGCCTGAGG ATCCTTTCTT CCAGCAAAAT GCTAAATTTG AAAAGATCCT

-2311 TTAGATTCTG GGCAACACAA AGGTAGCTTA GTTACATCAA ACTGGCTGGG

-2261 TATCTTAATA GTATTCATTA AAATGGAGTT CTACCTGGAT →#2576  
TATATAGTGG

#2757←

-2211 AGCTTGTTAA ACAGGAATCT CAGCTAGCAT CCAAATAGGT GCTTCTGTGT

-2161 TTAGGGTGTG TTTTATCTGT TGGAAAGTTA CTGAGGCAAT GAGAACTAAT

-2111 GCCATCAGCT AGGTACTACTG CAGCTTTGAA ACTATGGACT ATTGCATTC

-2061 AATTAAAATG ACATTTCTTG ACTGAATTCT GACATCCTCA GIGATAGTGG

-2011 TGAATGAAGA CTTTATCAA AGTATAGATT CTATTAAGCT TTTAAAAAAT

-1961 TTTATTAATT TTTTGTAG AGATGAGGTC TTGCTATGTT GTCCAGGCTG

-1911 GTCTTGAACCT CCTGGCCTCA TGCAATCCTC CCACTGCACA GCCTCCCAA

→#2587

-1861 GTGCTGGATT ACAGGCGTGA GCTACCCTAC TCGGACCAAT GTAAGCTTTT

#2577←

-1811 TTGAATTA AACAGGAACT GTAAATAGCA TATACGTAGG ATTCTTAATA

-1761 TTTTACTTT AAATCTAGA ATTTGAAAA TAACTAAAA TTGAATACAA

-1711 CGTAATTGAG ACAAATATAT CTGCACTGGA AAATTTAGCT TACAGAGTCC

-1661 CTTCAATGCTA TTGCTCAGTC TGTAATTTA AGTTAAGAG CAGGTGGAAG



## APPENDIX

---

190 CAGGAACGTG CGGCGCACCG TGGGGCGGGG ~~#2521-~~ GTTGGGGGAG AGGGAGGTCG  
240 GAGAAATTC AGTTGGAGCC CTCGGGCGCC CGGGCGATCG GTCGCAACCG  
290 AAATGGGTGT GAGTGACGGG GAGTTTCCTT ACTAGCATCC GCCGCAGACA  
340 CGTTTTCTGC ACTTCACTGT ATTAAGTGGT GTTTTCTTAC TAGTTGCTCT  
390 TAACTTGTTG CCAGTCTTGG GCTGGAGTCC TAGACGCCAG CCCTTGCCCT  
440 GATTCCCCTC CGCGGCTGCG GCCCCGAAGT GGAAAGGGAG CGCACAACTT  
490 CCCTCTGTGC TCCTTCTCCA GCTACTGCCA TCCCCTCTTC CCTCCC GCCC  
540 GGA~~CT~~CAGGA AATCCCGGAG CCAGCAGCCT GCTACTCCTC CAGCCCCCAC  
590 ACGCCC GCCT CGGGTGACCT GGCTGGCTTA AGCCGACCCT GGGGCTCTGG  
640 AGAGGGGGGG CCGTGGCCGA GGAAGGCAC GAGGTTTGGG TTGCCTGCCT  
690 TCTGCCTGCT ~~#2781~~ TCCCTCCCTT GICCTTAGCG AGGGCGTCGC GAACGCACCT  
740 AGTCTCCCTA TGAGTAAGCA CTTTTTTTCC TTTCAGTAGG ~~#2780-~~ AGAACATCTC  
790 TGGGCTAGTA GGACAGTACC TTCCGTTCT CCCCTGGCCC CACACCCCTT  
840 GTCCTTTTTT CAGCTCCTTT GACTTTGCGG CCCCGGGCGC GCGGTCGGGG  
890 CGGCGGCAGT CCCGGACCTC TCCCGACTCT TGGAGAGAGA GAGGCAAAGG  
940 GCGCAGCGGA GGGAGGTAAT AGTCTACCCC CCCGCCCTT CCCC GCACAG  
990 CTGCACTTGC CTGTGTTTAC TTTTCTCCAC CCGCAGTACT TAAGCGCTGT  
1040 AATGAGAGGC CCGGGGACGC CGACCACCCC CGCCCTGGCT TCTCGCCAGT  
1090 CCCAAAGTTG CTGCCGCCGT CGCTGCTCCA GTGTGCTGGC GGTTCGACC  
1140 GCCGGGCTCC GGGACGTAAG ATGATCCCAG CCCGGGAGGT GGAGTGGGGG  
1190 TTAATGGCAT CTGACTCTAG CTTATGCGA TGCTCCTTGC CTCTCACCTG  
1240 AGCTGCACGA TATCCCAGT GGTGCAGAAG GTTGA~~ACT~~TTT TGCAGAAGGT  
1290 TGAGCTTGGA GCTAAGTGGG TTGGAGAGCC TCGCCATTTA GCGTCAGACA  
1340 GACGGGATGC TGGGGGCGCC CGGCTGTTA AGAGGGATTG GGAGGAGGGA  
1390 AGGGAGCCTG GCTAACAGTA GGTAGAAAAT GTAGGGAAAA ~~#2783~~ GTAAAAACCA  
1440 TGAGGGGCA AGCACTTACT CCACTTTGCT GGATGTCACA ATGGACTGGG  
  
1490 GAGCCTAAAC ~~#2782-~~ TTGATCCTCG AGATGCAGTT CATGGTGAAT TCCA~~ACT~~TAAG  
1527 TGGCTGGAGC CCC  
1553 ACACATACCA GTTGAATCA CGTGCCCCAA GTCTCTGATG GTCACATGAC  
1603 GTCTTTTTAC TTTAAAGCTG GAATGTAATG GTTGAGGCC ATATTCCAAA  
1653 AACCACCTCT ACGTTTAAAA AAAAAAAGGT GGGGAGGAGT GTGAACTAGC  
1703 TTCTAATCAA GGAAGTCTAC TAGGATTTTG GATGAGGGGA CCAGAAAGGG  
1753 AATTTGGTGC TCAGCTTTTA TCCAAAACAA AAACAGGAGC TGTTTTTAAA  
1803 ATAAGGGATT GAAATATATG TGAGCTGGGA CATGTATCTC CTCTCTTCTT  
1853 CAATCTCATG GTTTTCTTAA ATTTAAAAA CATCTACTA ATTATTTCTT  
1903 AGGGAAGTCA TCCTATTACT CATGCCTCAT TTTGTCCCTG AATACTAGAT

## APPENDIX

---

```

1953 TTGAAGCTAA ATCCCACAAG ATAGTGTTAA AAAGTAAGGC TCTGTTCATC
2003 TTCCTGGTC TGGCCTATAT TCTAATGAA CTGTTCCCTA TTTTAGGCAA
2053 CTACTIONAAG GTAGTAAATA ACCTCTGAC TAAAATTAAC CACCAGTTAT
2103 TTGTGGTTTT CAATTAACCTG GATTAGAAAT CATGCACAAA AACAGTGGAT
      -#2785
2153 AGTAAATTTG ATACATCGAG TTGGTTGGGT TTTTGCCGTG CAGTGGTTG
      #2784←
2203 GTAGAATAAT GAGAGGACAC TGAACAACCT TTCCCATATT GACCTATAAC
2253 CGCCCAAGTG GCCCAAGTTA AGGTTGCTTC TGGGAAAACG TGGCAATTTG
2303 GCTATTCAGA TTATATATTA CAGAGTATAG AAGAGAGGCA GAGGAGCCTC
2353 TGAGGTCAGG AGTTTAAAAG CTTTGCTTAT CTGAAAAAAA AAGAAAAAAC
2403 GGACCTGGTT GATGCATATT CAGTCTTGAA AACAACTAGG GCAGAAGATA
2453 TTTAAGAGAT TCTGACTTTG TATTCTTTTG CCAAAAACCC TTTGTCTCCT
2503 GCAGCAGCCT CTGAATGACC GGAGCACTCC AGTTTCTTGC TGTTCATCCG
2553 TTTCTGAGCC TGAAAACCTAG AACAACTTA AAGCACATTG TTCTGACCCC
2603 AAGGCTAGCC TTGTGGCACA GATGAGCTGG AAATGGATTT AAGGTGCACC
2653 TGAGTTACTA GAGTTAACTA CACTGGTAGA TAGACCCCTC TAGTGGAAAGT
2703 GAGGTGATAA TATAATTTTA GATCGAAATA ATAAATGTTT AACCTCAAAA
2753 AAAGGAAGTT ATTACCACTC AACTAGGTTA CAGTGGTAGG GGGATAAGTT
2803 CTTTTTTAAG TATTGTGAAA TCATGTCTAA ACAGAATCAT CGCTAGGCTC
2853 TAGTCCACAG CTTTTCATTG TCTTGGGATG CCTACTCATT GAACACCACC
      -#2949
2903 CCAATATTG CTGACTTTTT TTGGTGGTAT GATCTAATGA GCCCAAATTT
2953 TTATTGAAAT TAGGGGGCTG GGAGTCAAAT TCTTGATTTT TACTGTTAGA
      .....

48703 TCATTGGTCA CATAATATTG ACCTTTAGCT TTGGCTCATA TAACCAAGAA
      -#2477
48775 TTTCTATTAT GTAGCTTTTT CCTGTCACCTG CTGGGTACTT TGGCCCTTCC
48803 TTAAACTTTT TGAATGTAAT TTAAGATTTT GTCCTTAGAA GGAAAATTCA
48853 GAAATATTTT TTCTCAATAA ATTTTGGTAA GTGATGACTT CTCATTGTG
48903 TTCTTTATTA AAGCTGTATG TAGAGACATG GTAACCTATT CAGATTGTTT
49953 TGATAGTTG AAATTCGTG TAAATTATCC CTAAGATGAG AACTTAGCAA
49003 GAGTGCTTAT ATTTATCACA ATTTTTTAAA GTCTGAAACG TTTTGGTTT
      5' UTR
49053 TTCTTTAGAT CTTTAAATGG ATGAGATGGC TACCACTCAG ATTTCCAAAG exon 2
49103 ATGAGCTTGA TGAACCTCAA GAGGCCTTTG CAAAAGTTGG TGAGTATTTT
49153 TTGTAGTAAA ACTATAGGGA AGCAATATTT ATTTGGTCTC AAAGTTATTT intron 2
49203 CTCTATAAAT ATCACATGAA TGGTTAATCA AAAACATTAG GGCAAGATAG
49253 TTAATAAGTA TGGGATAAAG TTTTGAAGC TATACTTAAA ATTTGTTTAT
      #2478←
49303 TTCTTTTTTT TTTTTTGGT CGAGTGGTAG CTGATATTAT TTCCAATTTT
49353 ATGTAGTATT TAATATGGTC AAATTTTTTA GACCACAGTT CCAATCCTTA
      .....

```

## APPENDIX

```

...60853 ACACATTGCT TAAATCACAG GATACATGAT GTAAAACCTT GCTTTTTCCA
      -#2479
60903 TTTAAATGTC CATTTCCTT TCAAACAAC TATGTGCC CACAATAAGA
60953 AAATATTTA TGTAAGTGAG CTTATGAAC GAACCTCAA TGAAGGGAAA
61003 TACTCTAAT TCTGTCTTTC AATTTTTTTT CCTTTTTTGC TTGCTCTCCT
61053 TTTTACAAA GATCTCAACA GCAACGGATT CATTGTGAC TATGAACTTC exon 3
61103 ATGAGCTCTT CAAGGAAGCT AATATGCCAT TACCAGGATA TAAAGTGAGA
61153 GAAATTATTC AGAACTCAT GCTGGATGGT GACAGGAATA AAGATGGGAA
61203 AATAAGTTT GACGAATTT TTTATGTAAG TATGTGAAA TTCACAATTA
61253 TTAGAAGTAG TAGATGTTCC CTCGTCTAGT GGGATGTTAT AGTATTAAGT intron 3
61303 ACTGTTATGT TAAGTTCTTA AATATATCAT ATTAGTACTG TTATAACAT
      #2480-
61353 TCTGTCAATCC TGCCCACTAA ATGTAATTCT TTTAGCTGCT GGAATATCTT
61403 AACAAACGAA TTGAGAAAAA GAGCACTGCA GAAACAAAGA TATAACATGA
.....
...67803 CAAGTGTGTG CAATTGACAT TCTGGTGCTT CATTTCAGA AGGGGTATTG
      -#2481
67853 TAGTACTTGT TTAGCATTTC AAAAACICAA GCCCAGTTTT TTGTATCTTT
67903 TAACATCAGC TATGGAAAAA ATGTAAGTGA TCAAGATATA AAAGAATATA
68953 AATATGCTTA TTGTGCATAG TTTGAAATTA ATTGTGAATC AACAAAATTA
68003 CTTAATTAA TAGATTTTTC AAGAGGTAAA AAGTAGTGAT ATTGCCAAGA exon 4
68053 CCTTCCGCAA AGCAATCAAC AGGAAAGAAG GTATTTGTGC TCTGGGTGGA
68103 ACTTCAGAGT TGTCCAGCGA AGGAACACAG CATTCTTACT CAGGTAATCA
68153 TTTTATATGC AATAGGTAA CACAATGTGC TAAGTGGGAT GGTTGCTGTA intron 4
      #2482-
68203 ATGTCAAGGA CGGGCTCTAG AAAAACATTA CCTTCTAATT AAGAATACAG
68253 TAGAAGTCCT TTGTGACATG TATTTAGGCT TGAGACTAAT ACTTGTCATA
68303 AAGGCATTAT AAGTGTATAT TGTATGGCTT TGTTAGCTTG CAAGAGACAG
68353 GATACAATCC ATGTAATGAC AGGCTTTATT ACAGTGCATT ATACAGTAAT
68403 ATAAATATA TTTTAAGGA ATTTTGTAA TTTTCTGAGG ACTGGTTAAC
68453 GTGTTCTATT CTTTTCTTA ATTTTGTAA TCCTAATAAC CACTGTGTTG
      -#2483
68503 CATCCAAGTG TCTGGGTTT CACACAGAAT AACCACATGT TTCTGACACA
68553 TTAACTTCA GCACTACTGC ACACTATTT TAGGCTTTGG AGTCAAATAT
68603 TTAATAAGTT AGAGTATGAA CTAATGICTT GTATTTAAC ATAATTTAG
68653 AGGAAGAAAA ATATGCTTTT GTTAACTGGA TAAACAAAGC TTTGGAAAAAT exon 5
68703 GATCCTGATT GTAGACATGT TATACCAATG AACCTAACA CCGATGACCT
68753 GTTCAAAGCT GTTGGTGATG GAATTGTGCT TTGGTAAGAT GTTAGCTTGT
68803 TTTATATCCA GATATCCAAA AATAGCCTTC CATATAATTG ATATATTTGT intron 5
      #2484-
68853 TTCTGCATGC TTGACAGGTT CACCTCAAGA AATAACTAGA ATGGAAAAT
68903 ATCCAGGTTT TGCCTTTTTT ATTTAATCTC TAGGTCTGTC CATGAATCTA
.....
...72653 TTTATTATGA TCAACATGAT AAAAGTCATC TAGCTGCATT TTTTAGAGTA

```

APPENDIX

→#2485  
 72703 CATGAAAGAG ATGTTATAGT AAGCTTTAAA ATATTTGTAA ATATTTACAG  
 72753 CCACTTTATA AAAGGAAATC AGCTCTTTT TTTTACATCA GCCTTTTTT  
 72803 AAATTTTGT TTCAGTAAAA TGATTAACCT TTCAGTCCCT GATACCATTG exon 6  
 72853 ATGAAAGAGC AATCAACAAG AAGAACTTA CACCCTTCAT CATTCAGGTA  
 72903 TGCATTGTT TCCCCTCCCT TTAACATGAA ATTACTGTTT GAGGACCTGT intron 6  
 #2484←  
 73953 TCTGCAGACT TCAGCCTCTG CACTCTGTAG GCTCCCAATC AATCCTTGTA  
 73003 AAAACTGTTG AGTGTGGGAT TGTATCCAG ATTATACAGA CAGAACTGGG  
 .....  
 ...73553 AATTTGTTT TTGTGACACA TATATGGATG AAATTAATAC AGGGTATTAA  
 →#2487  
 73603 TTTCCTCATT GAATGTTATT TTCAGTGAAG GGAGAAAGTA GACTGCTAAA  
 73653 AAATGGAAAG GTCAAGAAGC AAGTGTGTAA TTGGCTGTC TTGCAGGAAA exon 7  
 73703 ACTTGAACCT GGCACCTGAC TCTGCTTCTG CCATTGGGTG TCATGTTGTG  
 73773 AACATTGGTG CAGAAGATTT GAGGGCTGGG AAACCTCATC TGGTTTGGG  
 73803 ACTGCTTTGG CAGATCATT AAGATCGGTT GTTCGCTGAC ATTGAATTAA  
 73853 GCAGGAATGA AGGTAATGGA ACACAGTCAT TCTGGCAGTT GTTTATTGGT intron 7  
 #2488←  
 73903 TATTTTTTTC TAGTCATGCA GACTTTCGTG CICTCACTTA ATGGAGGTGA  
 73953 TTAAATGGTG GTAACATAGAA TGAACATAAG GTAATGCTAT AGAGTTATTC  
 74003 AGGAAAATAG CCTAATTACA TGACTCTCTT CTTACTAGT AATTCACATT  
 .....  
 ...75503 TTTAGTAGAT TATGAGTATC TTGAAACTAG GAACTATGTC ATAGTAGTTT  
 →#2489  
 75553 TTGCACCTCT ATTACTTAAC AGTGTCAAAA GACTGAATGA ACTTGGCATG  
 75603 ACCATTATTG TGTCATATAA TAACTGTGGG ATTTTTTTTT TTTTCTTCTA  
 75653 GCCTTGGCTG CTTTACTCCG AGATGGTGAG ACTTTGGAGG AACTTATGAA exon 8  
 75703 ATTGTCTCCA GAAGAGCTTC TGCTTAGATG GGCAAACCTT CATTTGGA  
 75753 ACTCGGGCTG GCAAAAAATT AACAACTTTA GTGCTGACAT CAAGGTAAC  
 75803 GTTGAAGAA TCACAACATT TTGGGGGGAT ATAATAGCTG GAAGATTCA intron 8  
 75853 TCCCAGCTTA ACAGAGAGAA AATCCTAACA CTGTATCACC AAGCCTTGT  
 #2490←  
 75903 GICTCTTGGC CCTGAAGGTA GATTTTAGAA GAGTAATAGA GCCAGATAAG  
 76953 GTACATTAGC ACCTATGTTT TATTTGTGG GAAAAGGTAA AAATATTATG  
 .....  
 ...79053 TATAAGGCAG ATAGATGGAC TTTTCTGGGG AAAACACCTG TAAATTA  
 →#2491  
 79103 AGGCAGAGAT TTGTGCCATT TATTCTCAA AAATCCAATG CAAATAGCCT  
 79153 TCCAACATG GGACAATAGG ATACATTCAT TCCTTGTAAC TGTGATCTCA  
 79203 CTGACATTTT CAATCTTTG TAGGATTCCA AAGCCTATTT CCATCTTCTC exon 9  
 79253 AATCAAATCG CACCAAAAGG ACAAAGGAA GGTGAACCAC GGATAGATAT  
 79303 TAACATGTCA GGTTCATG TAAGTATAAG TGCTCTTTG AATTCTACAA intron 9  
 79353 TCTTGCAAAA TTATTGTCAA TTTCTTATA GTACAATAAT TTTTATAATC  
 #2492←  
 79403 GTATGAAGTA GAGTGGCAA TTTTAAGCAT TATTTTAAAA TGTATTACTG

## APPENDIX

```

79453 TACATGTAAT TCAGAGGCCA GAAACTAGC TTTGATTAT TTTGATTGT
.....
...82003 AATTTTATAA TAAGTACCAT ATGTTAGCTA AAAGAAAGTA GAACTGTATA
      -#2493
82053 CCCAGACTAT GACAGTGGGG AAATTTTCTA TATTTTLAGT GTGGCCTTTG
82103 ACAAAGTCTT CCGATTTTGT TTCAACAGGA AACAGATGAT TTGAAGAGAG exon 10
82153 CTGAGAGTAT GCTTCAACAA GCAGATAAAT TAGGTTGCAG ACAGTTTGTT
82203 ACCCCTGCTG ATGTTGTCAG TGGAAACCCC AAAGTCAACT TAGCTTTCGT
82253 GGCTAACCTG TTTAATAAAT ACCCAGCACT AACTAAGCCA GAGAACCAGG
82303 ATATTGACTG GACTCTATTA GAAGGTAAGT AAAAACCTCA ATTTCGAATG intron 10
      #2494-
82353 TGTGGGACTA TAGAGTAGAA ATACATAGGC CACAATGATT TTACAATCTA
82403 GACTTAATAA GTTTTTTTAT ATCTACAAGA AGTAGATGGC AGATGCTGAG
.....
...83653 ATAAATCAA ATTTTAAAAA TAAGCCTGTA CCTAGAGAGA ATGTATGTAC
      -#2495
83703 TTAGAAGAAAT GCTTGGAAAC TCGTATTATC GAAAAATTCT AGATCTGAAT
83753 AGAGAGATAA AATAATCTAA TATGTGTATT GGCCTATAT GCACATACAT
83803 AAAGTGTITA ATGAATCAGT AAATTTTGTG AATATTCTTA ACAGGAGAAA exon 11
83853 CTCGTGAAGA AAGAACCTTC CGTAACTGGA TGAAGTCTCT TGGTGTCAAT
83903 CCTCACGTAA ACCATCTCTA TCGTAAGCC TTCCTACTGC TATTGTAAAC intron 11
      #2496-
83953 AGTTACGAAT GTCATGAATG GATGTTAAAT AATGACAGCT CTAAGATTT
84003 TCTAGATATT AATTTGTAGC TATTATTTAT ATTGAAAAAT GTCAGTGGT
.....
...84753 TCAGCACAGA TTGATAGAAA ATATGAGTCT TGGGTATTAT TTATGGTTTT
      -#2497
84803 ATATATCTTG TTTGACAATG TAGTGTTACT GTTTTAAAGG AAAGTCAAGT
84853 CCCAGCTTCC TGAAAACACT GATTACATTA TTTTAAATC ATTAGTGACC exon 12
84903 TGCAAGATGC CCTGGTAATC TTACAGTTAT ATGAACGAAT TAAAGTTCCT
84953 GTTGACTGGA GTAAGGTAA TAAACCTCCA TACCCGAAAC TGGGAGCCAA
85003 CATGAAAAAG GTAGATAAAT AAGTTGCTGT ATATATTTGT TAGAGATTTT
      #2498-
85053 TTATTCTCGA TTAATTTCTT TTGTTTCTAA AACTCTTGAC GCTGAGCTTC intron 12
85103 TTGAGGACAA AACTGTGTCT TATTGTTTT TGTGTGCTGA TACCTAGCAT
      -#2522
85153 TATACAAGAC ACACACACAC GTATGCAGAT TAAACAAATG GAAGTCTTTA
85203 ACCATTTACT CTTGIGCCTT TGCAGCTAGA AAAGTCAAC TATGCTGTTG exon 13
85253 AATTAGGGAA GCATCCTGCT AAATCTCTCC TGGTTGGCAT TGGAGGGCAA
85303 GACCTGAATG ATGGGAACCA AACCTGACT TTAGCTTAG TCTGGCAGTT
85353 GATGAGAAGG TATAGTACAC AATTTAGCT GTTAGTCTT TACTATCATA intron 13
85403 CAGGTCTGTG ATTTAGTCTT TACTGTGTTT AATAAGTGGA TATGTCGATA
85453 ACTACACTTT TGAAATATGT TATATTTACA CTCCGAAATG AGTTTAATTA
      #2500-
85503 ATGAATATAT GTTGGATGTT AAGTGGGAGA TGCTTCCTTG CAAGTTAGGC

```

## APPENDIX

85553 AGCAGAACTA TGGTTAGTCC CTTTTTTAAA AAATAGGAAG CCTGACACAC

85603 AGATTTTCGGC CTCGTTTAGT GTCAGTGAAT TAAAAAATTG TCAGAACAAA

85653 ATTATGAACA TCTTCATGCT CATTGAAAA TAAAGATCTC TCTCTGTAAT

85703 GCTGATGAAG ATCACTATAA TGCTGAAAAG CATTTCATTAT GACTGGGCAC

85753 CAGCCAAAGC ACAGCTTATT TTATGCCATT ACCGCTATTG GAATAGTACA

85803 AAATGTGCCT ACAGTGGGCT GTTGGACCTG CTCATTAAAG CACTGTCAAT

85853 CTGCTCCTCT CTCACCACTA CAAAGAGTAG ATCAGTAGCA AGCCACTACT

86903 GCTTAAAATA TTTTTTTCAC ATAGTGTGAA TCTCTTTCCA TGAAATCTTT

86953 AGTCCTTGAA ATTTAAGGAA TATAGGGGCC AGGAGTGGTG GCTCACGCCT

86003 GTAATACCAG CACTTTGGGA GGCCAAGGAG GGTGGATCAC GAGGTCAGGA

86053 GATCAAGACC ATCCTGGCTA CACGGTGAAA CCCTGTCCCT ACTAAAAATA

86103 TAAAAAATTA GCTGGGCGTG GTGGTGGGCA CCTGTAGTCC CAGCTACTCA

86153 GGAAGCTGAG GCAGGAGAAT GGTGTGAACC CGGGAGGCGG AGCTTGCACT

86203 AGCAGGAGA TTGCGCCACT GCACTCCAGC CTGGGCGACA GAGCGAGACT

86253 CCGTCTCAAA AAAAAGAAGA AAAATTTAAG AAATATAAAA AGTGAAGAT  
 →#2501

86303 AAAGCATCTT TCTGATGTTT GCATTTTTCC TCATAAAGTA GATGGTGACC

86353 TTTTCTTCTG CTGCCTCTCT TAGATATACC CTCAATGTCC TGGAAGATCT exon 14

86403 TGGAGATGGT CAGAAAGCCA ATGACGACAT CATTGTGAAC TGGGTGAACA

86453 GAACGTTGAG TGAAGCTGGA AAATCAACTT CCATTCAGAG TTTTAAGTTC

86503 AGAATCCATA TTTGACTATT AAATATTATG TTTGCTGGAT AACATCTATC

86553 ATTTGGGAAG GCAACTTTTG GCTTCTTTGT GAGTGAAGAT TAGTGTGGG intron 14  
 #2502- →#2523

86603 CTAATGGCAC AATTCTTTAC GAATTCACCTG GGCTTTGTTT TTGGCACTTG

86653 ATATAAGTAA GCACATGTTA ATTTGTATGT ATCAAAATTC TCAGATTTGT

86703 TCTCCTTTCA CACTAGGACA AGACGATCAG CTCCAGTTTG GCAGTTGTGG exon 15

86753 ATTTAATTGA TGCCATCCAG CCAGGCTGTA TAAACTATGA CCTTGTGAAG

86803 AGTGGCAATC TAACAGAAGA TGACAAGCAC AATAATGCCA AGTAAGGGAG  
 #2524-

86853 ACTGCTAATA GTATGAAAAG AACGCAGCTT TGTAGCTGGA CAGATCTGAA intron 15

87903 TTCTAATCA GTTTCTGCCA TTTAAGAGTG GTGTCACCTT GGGAGAAACC

.....

...88053 GAGCTTAAAA ACCTACTGTA ACTTCAAAGT GAAATCAAAA CCCAAATCAA

88103 AAGAAAACAA AAAGCAAAC TGTCTAATT GGAACATCA ATATGGAATT

88153 TTGTCATCCC AGCATAATAA TTATATATGA GGAAATAGAT GTCTTACGTG  
 →#2525

88203 GTGTCCTTAA CTGACAAGAA TTTCATCCCTG ATTTTGTTC CCCCTAAAAT

88253 AGGTATGCAG TGTCAATGGC TAGAAGAATC GGAGCCAGAG TGTATGCTCT exon 16

88303 CCCTGAAGAC CTTGTGGAAG TAAAGCCCAA GATGGTCATG ACTGTGTTTG  
 →#2657

88353 CATGTTTGAT GGGCAGGGGA ATGAAGAGAG TGTAAATAA CCAATCTGAA  
 #2526-

88403 TAAAACAGCC ATGCTCCCAG GTGCATGATT CGCAGGTCAG CTATTTCCAG 3' UTR

## APPENDIX

---

88453 GTGAAGTGCT TATGGCTTAA GGAACCTCTG GCCATTCAA GGACTTTTCA  
88503 TTTTGATTAA CAGGACTAGC TTATCATGAG AGCCCTCAGG GGAAAGGGTT  
88535 TAAGAAAAAC AACTCCTCTT TCCCATAGTC AGAGTTGAAT TTGTCAGGCA  
88603 CGCCTGAAAT GTGCTCATAG CAAAACATT TTACTCTCTC CTCCTAGAAT  
→#2659  
88653 GCTGCCCTTG ACATTTCCTA TTGCTGTATG TTATTCTTG CTCTGTTATC  
#2658←  
88703 TTTTGCCCTC TTAGAATGTC CCTCTCTTGG GACTTGCTTA GATGATGGGA  
88753 TATGAATATT ATTAGACAGT AATTTTGCTT TCCATCCAGT ATGCTAGTTC  
88803 TTATTCGAGA ACTATGGTCA GAGCGTATT GGATATGAGT ATCCTTTGCT  
88853 TATCTTTGTA GTACTGAAAA TTTGCCGAAG TAACTGGCTG TGCAGAATGT  
88903 AATAGAAGCT TTTCTTATT TTTTATTCTT AAGATCAGTA TCTTTTACA  
89953 GTATTCTTTC TACATGATCC TTTTGTGAC ATTTAAGAAT ATTTTGATTA  
89003 TATTAACAA GACTGCTGAT TTTGCTACTT TTTTAAGGG GTCTTCAAGT  
→#2661  
89053 AAGTAAAAA TACATCGTAG CTAGAAGAAA AATGTACCTT AAATTTGCAT  
#2660←  
89103 CTTCCCTCTC ATACCCAAGC TGTAACAAT TGAAATATT TGTCTTAAAT  
89153 CACTTGGTTC AATACATGCT TATTTGTTTT AAAACCTGTA TCATCAAAT  
89203 CTCTCTCTAA ATTTAAAATG CTGTTGAATA TGATACTTTT GAGGAGAGAG  
89253 TGTGCTCAGA ACTTAGACGG GATTTGGTAG GCCAAGTATG CTAAGTGATC  
89303 AATATATTTT TTAATTTTAC ACCTGAAACA AAGAAATGTG GTCCTAAAA  
#2662←  
89353 ATAAAAGTAT ATATGTAGGA ATTAATGTAC TCTTGCTTGG TCAAGCTGTT  
89403 TGCTATAGTT TCCAAGGTAT TATGTTACTC TAACTCTGAA AAGTGATGTA  
89453 ATCTGGTAGC AATGTAGTAG TTCAAATAAA GGCATTTACA TAATAATTAG  
89503 TCTGTTCTTC ATGCTTTTGT C

APPENDIX

V. Fig. F5 *T-plastin* promoter-1<sup>st</sup> exon- 1<sup>st</sup> intron (1 kb) region after bisulfite treatment

t: original T nucleotide; T: original C nucleotide (C converts to T after bisulfite treatment); **CG**: potential CpG sites for DNA methylation. Each CpG is numbered with the nucleotide position in the *T-plastin* genomic region; #: primer number used in pyrosequencing (all primers are underlined); →: forward orientation; ←: reverse orientation, +1: transcription initiation start site

→ #2820

-321 tTTTaTaaga ttgtgtgaat gtgtaTt**TCG** agTTaggTaT gttggATttT

→ #2899/#2765

-271 taaTttTTtT ttagTTTaag taggaagggg agaTtTaggT gTtggggaTT

-221 attTtTTtTt TTTtgTagTa gagttgTagt TTTtatTTTt TTtgggtgTT

-155

-161 TatTTT**CG**tg TTtattttTT tggatTTTTa TTTagttgat gtgaTaggTt

-111 -80 -63

-111 **CG**tggTTTaa tTTTTttTTt ggttTTTtagg **TCG**AtgTta gTaTTaTT**CG**

-52 -49 -45 -37 → #2767

-61 agTTaatgg**C** **GgCGgTCG**ag ggg**CG**gaggg ggTtggTagg aggggagggg

-10 +1 +23 → #2967/#2822

-11 g**CG**TtggTtt **taga**gTTaTa gTtgTaaaga tt**TCG**aggtg Tagaagttgt

#2766/#2900 ← +47 +54 +57 +64 → #2824 #2821 ← +85

+40 Ttgagt**CG**t tggt**CGgCGg** Tagt**CGggTT** agaTTTagga TtTtg**CG**Att

+93 +110 +113 +116 +131

+90 tta**CG**taagt gTtttgtagg **CGTCGgCGgg** TaTtagggga g**CG**ggtttTT

+144 → #2902/#2769 +163 +177

+140 tggg**CG**tggg Taggagtggg tTT**CG**gggag agTatTt**CGg** ttaagTtTag

+196 +200+203 +208 +215 #2769/#2901 ← +238

+190 Taggaa**CG**tg **CGgCGTaTCG** tgggg**CG**ggg gttgggggag agggaggt**CG**

→ #2826 #2823 ← +262 +266 +270 +274 +278 +282 +288

+240 gagaaatTTt agttggagTT Tt**CGggCGTT** **CGggCGatCG** gt**CG**Taa**TCG**

+306 → #2903/#2771 +329 +332

+290 aaatgggtgt gagtga**CGgg** gagtttTTTt aTtagTat**TC** **GTCG**TagaTa

+340 #2770/#2968 ←

+340 **CG**ttttTtgT aTttTaTtgt attaagtggg gttttTttaT tagttgTtTt



APPENDIX

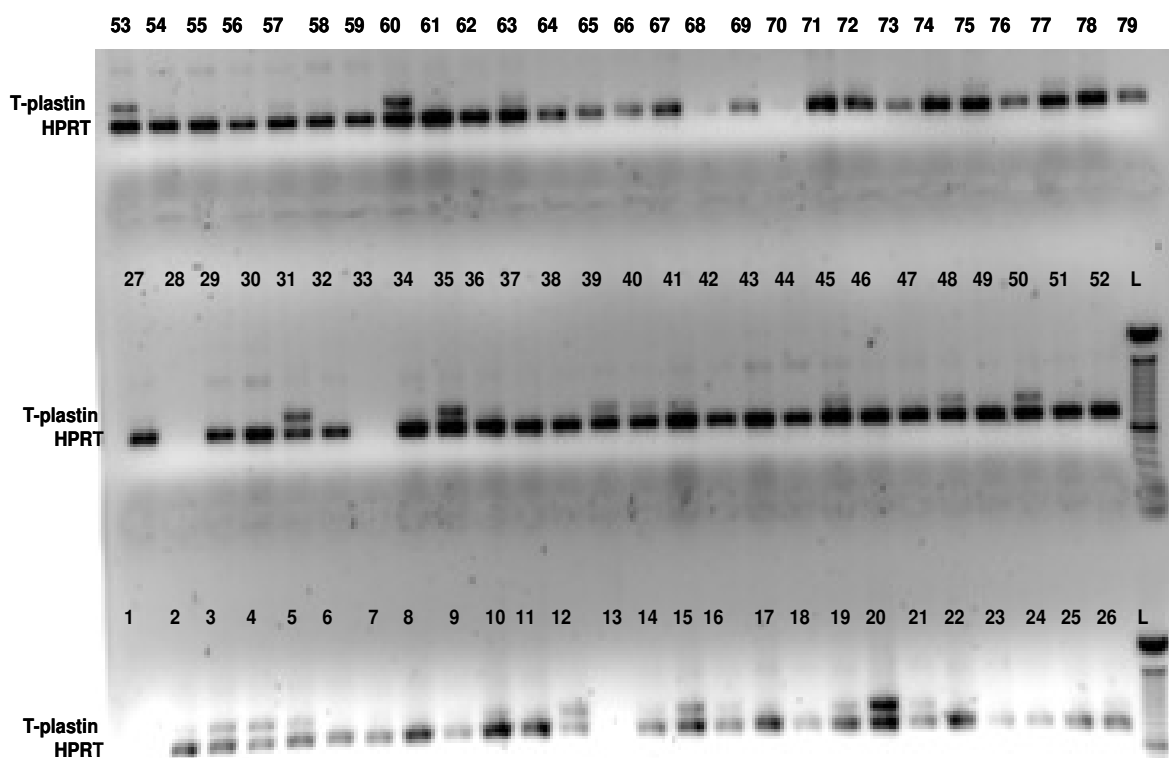
+1207

+1190 ttaatggTat TtgaTtTtag TTttatgCGa tgTtTTttgT TtTtTaTTtg

+1247 #3122/#3124 ← 3120 ←

+1240 agTtgTaCGa tatTTTTagt ggtgTagaag gttgaTttt tgTagaaggt

VI. Fig. 6 *T-plastin* expression analysis by RT-PCR in 79 SMA patients



The current number (1 from 79) corresponds to the EBV cell culture shown in Table T1 from appendix. *HPRT* gene was used as internal control. The samples where no *HPRT* transcript was amplified (1, 13, 28, 33, 68 and 70) were repeated independently. L: 100 bp DNA ladder

APPENDIX

**VII. Fig. F7 Simulation of the genome scan analysis under the assumption of recessive mode of inheritance in 30 SMA discordant families**

[FAST]SLINK

Date: 24.10.2005

```

Pedfile      : gmc_roz_nou.pro
Datafile    : datafile_roz.dat
Trak - locus
locus type  :
allele frequencies : 0.9999 0.0001
no. of lab. classes : 1
penetrance vector(s) : 0.0000 0.0000 1.0000
Marker - locus
availability :
no. of alleles : 10
allele frequencies : uniform
heterozygosity value : 0.90
Simulation
No. of pedigrees : 38
No. of persons / affecteds : 174 / 47
No. of persons available / affecteds : 168 / 47
No. of replicates : 1000
theta (trak-marker) : 0.00
alpha (prop. not linked) : 0.00, 0.25, 0.50
    
```

Marker		theta trak-marker	alpha not linked	expected max. lod	Power, $\hat{\tau}$ beta [%]		
alleles	HET-value				z > 1.0	z > 2.0	z > 3.0
1C x 0.1	0.90	0.00	0.00	10.0386	100.0	100.0	100.0
1C x 0.1	0.90	0.00	0.25	5.2626	99.7	96.9	99.0
1C x 0.1	0.90	0.00	0.50	2.5112	85.8	57.9	32.6

APPENDIX

**VIII. Fig. F8 Simulation of the genome scan analysis under the assumption of dominant mode of inheritance in 30 SMA discordant families**

[FAST]SLINK

Date: 24.10.2005

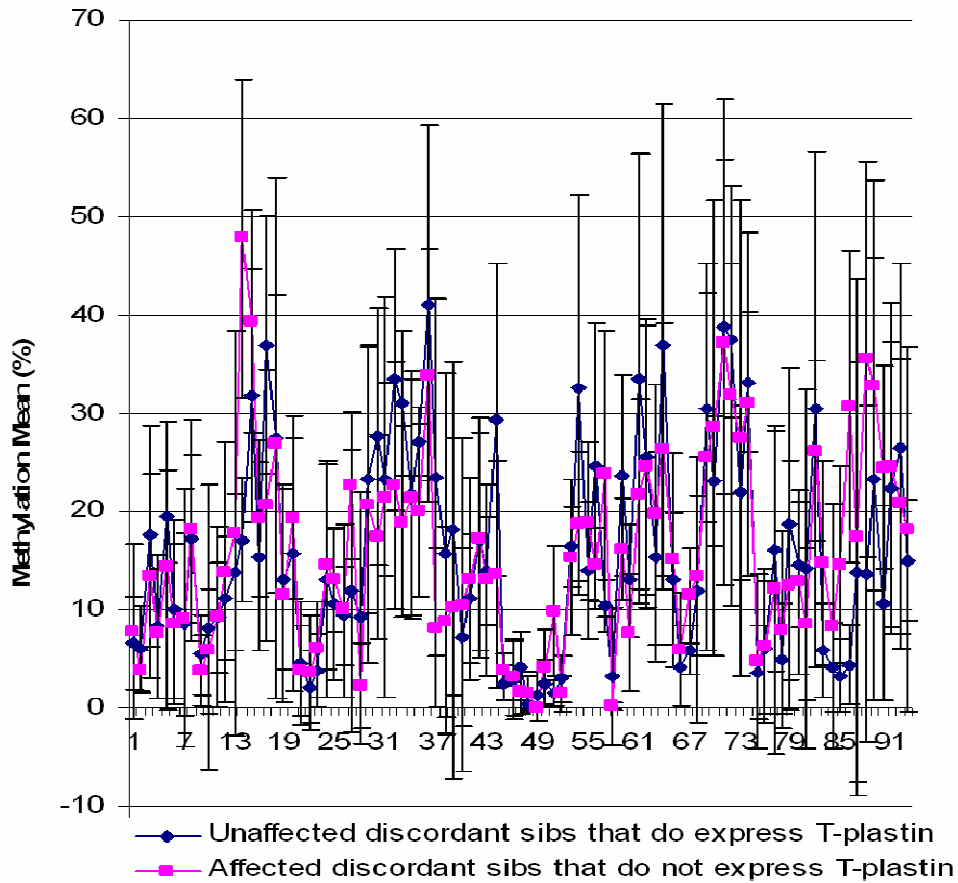
```

Pedfile      : sma_com_nou.pro
Datafile    : datafile_dom.dat
Trait - locus :
locus type  :
allele frequencies : 0.9999 0.0001
no. of lab. classes : 1
penetrance vector(s) : 0.0000 1.0000 1.0000
Marker - locus :
availability :
no. of alleles : 10
allele frequencies : uniform
heterozygosity value : 0.90
Simulation :
No. of pedigrees : 38
No. of persons / affecteds : 174 / 47
No. of persons available / affecteds : 168 / 47
No. of replicates : 1000
theta (trait-marker) : 0.00
alpha (prop. not linked) : 0.00, 0.25, 0.50
    
```

Marker		theta trait-marker	alpha not linked	expected max. lod	Power, f' beta [%]		
alleles	HET-value				z ≥ 1.0	z ≥ 2.0	z ≥ 3.0
10 x 0.1	0.90	0.00	0.30	7.1120	100.0	100.0	99.9
10 x 0.1	0.90	0.00	0.25	3.6048	98.4	98.6	67.7
10 x 0.1	0.90	0.00	0.50	1.8134	74.5	39.4	15.3

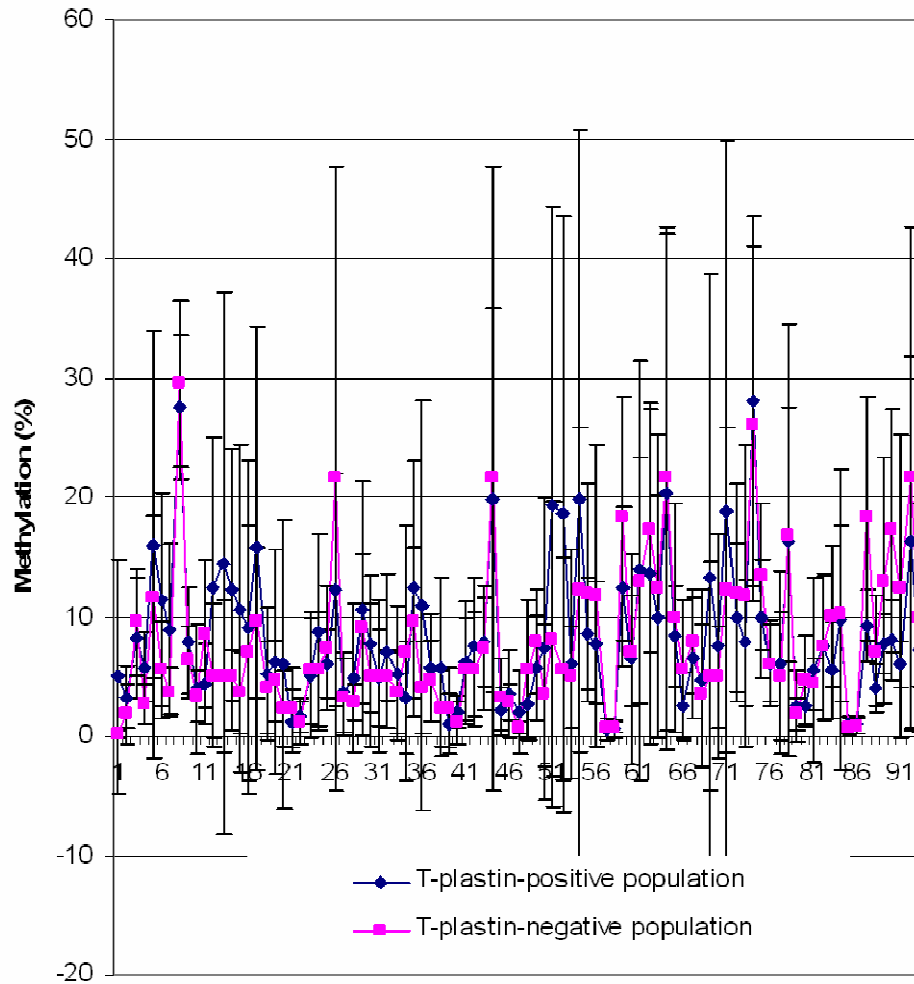
**IX. Fig.9 Methylation status of T-plastin CpG sites in SMA discordant sibs**

Methylation analysis and quantification of the 99 CpG sites in the promoter-1st exon- 1st intron region of T-plastin gene by pyrosequencing. The intensity ratio (y-axis) represents signal intensities of the methylation mean at each CpG site in both „unaffected“ vs. „affected“ groups. The error bars indicate SD.



**X. Fig. F10 Methylation status of T-plastin CpG sites in two control groups.**

The methylation level was quantified for each CpG site in the promoter-1st exon-1st intron region of T-plastin gene by pyrosequencing. The intensity ratio (y-axis) represents signal intensities of the methylation mean at each CpG site in both „T-plastin-positive population“ and „T-plastin-negative population“. The error bars indicate SD.



APPENDIX

XI. F11 Haplotype blocks within T-plastin genomic region

- A.** Block 1 (left) contains 9 haplotypes and block 2 (right) 6 haplotypes. For each haplotype, the frequency is indicated on the left side of the figure. Each haplotype was coded using one-letter symbols (capital letters for block 1 and small letters for block 2). The corresponding SNPs are indicated at the top.
- B.** Haplotype reconstruction of 7 male SMA patients (indicated on the left side); 2 female control (DNA no. 5 F and 16 F, respectively) and 4 females SMA patients. All these individuals expressed T-plastin. No correlation between a certain haplotype block and T-plastin expression was observed.

**A.**

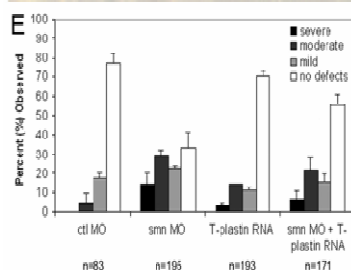
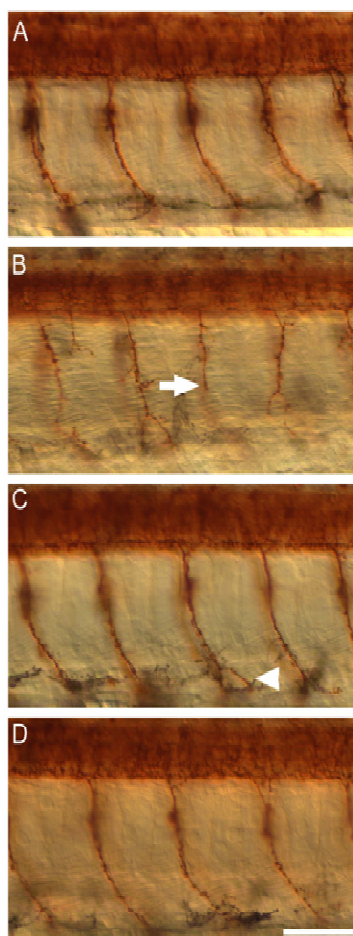
BLOCK 1										BLOCK 2								
Frequency	Haplotype	rs17096100	rs10875528	rs17326695	rs11557770	rs2522179	rs2522180	rs17326716	rs2522188	rs6643869	Frequency	Haplotype	rs5987946	rs5987947	rs5987956	rs5987763	rs2943611	rs12390767
0,367	A	A	G	T	T	T	T	A	T	G	0,478	a	C	C	T	C	A	C
0,122	B	A	T	T	G	C	T	A	C	A	0,122	b	C	T	C	A	A	C
0,111	C	A	T	T	G	T	T	A	C	A	0,156	c	C	T	T	G	A	C
0,100	D	A	T	C	G	C	T	A	C	A	0,211	d	C	C	T	G	G	C
0,078	E	A	G	T	T	T	T	T	T	G	0,011	e	T	T	C	A	A	C
0,067	F	A	T	T	G	T	T	A	C	G	0,011	f	C	C	T	G	A	T
0,056	G	A	I	I	G	C	A	A	C	A	0,011	g	C	T	T	A	A	C
0,044	H	A	G	T	T	T	T	A	C	G								
0,022	I	A	T	T	G	T	T	A	T	G								
0,022	J	C	T	T	T	T	T	A	C	G								
0,011	K	A	T	T	T	T	T	A	T	G								

**B.**

	DNA no.	Origin chr. X	BLOCK 1									BLOCK 2					
			rs17096100	rs10875528	rs17326695	rs11557770	rs2522179	rs2522180	rs17326716	rs2522188	rs6643869	rs5987946	rs5987947	rs5987956	rs5987763	rs2943611	rs12390767
MALES	4201	maternal	A	G	T	T	T	T	A	T	G	C	C	T	G	A	C
	97	maternal	A	G	T	T	T	T	A	T	G	C	C	T	G	A	C
	1927	maternal	A	G	T	T	T	T	A	T	G	C	C	T	G	A	C
	326	maternal	A	G	T	T	T	T	A	T	G	C	C	T	G	G	C
	994	maternal	A	G	T	T	T	T	A	T	G	C	T	T	G	A	C
	530	maternal	A	G	T	G	C	T	A	C	A	C	T	C	A	A	C
	935	maternal	A	T	T	G	C	T	A	C	A	C	T	C	A	A	C
	708	paternal	A	G	T	T	T	T	A	T	G	C	C	T	G	G	C
	708	maternal	A	G	T	G	T	T	A	T	G	C	C	T	G	G	C
	119	maternal	A	T	T	G	T	T	A	C	A	C	T	T	G	A	C
FEMALES	119	paternal	A	G	T	T	T	T	A	C	G	C	C	T	G	A	C
	43	maternal	A	G	T	T	T	T	A	T	G	C	C	T	G	A	C
	43	paternal	A	T	T	G	T	T	A	C	G	T	T	C	G	A	T
	16F	paternal	A	G	T	T	T	T	A	T	G	C	C	T	G	A	C
	16F	maternal	A	T	T	G	C	T	A	C	A	C	T	C	A	A	C
	256	paternal	A	G	C	G	C	T	A	C	A	C	C	T	G	G	C
	256	maternal	A	T	T	T	T	T	A	T	G	C	C	T	G	A	C
	5F	paternal	A	T	T	G	C	T	A	C	A	C	T	T	G	A	C
	5F	maternal	A	T	T	G	T	T	A	C	G	C	C	T	G	G	C

**XII. Fig. F12 Motor axons defects in *smn* morphants are rescued by overexpression of human *T-plastin* RNA.**

Lateral views of (A) control MO, (B) *smn* MO, (C) h*T-plastin* RNA, and (D) *smn* MO + h*T-plastin* embryos znp1 antibody-labeled for motor axons at 36 hpf. (E) Embryos were classified as severe, moderate, mild, or no defects, and percent of the total observed is shown. Error bars represent standard deviation. Arrow indicates a severely truncated motor axon in a *smn* morphant (B). Arrowhead indicates a mild ventral branch in a h*T-plastin* injected embryo (C). All MOs were injected at 9 ng dose, and h*T-plastin* RNA was injected at 200 pg dose. Compared to *smn* MO alone,  $p > 0.0001$  for *smn* MO + h*T-plastin* RNA; while compared to control MO,  $p = 0.147$  for h*T-plastin* overexpression embryos; Scale bar, 50  $\mu$ m



**Tables:**

- I. *T1 Classical SMA patients checked for T-plastin expression*
- II. *T2 Phenotypic and genotypic description of SMA discordant families used for genome-wide scan*
- III. *\*T3 Up-regulated transcripts detected by microarray analysis in SMA discordant families*
- IV. *\*T4 Down-regulated transcripts detected by microarray analysis in SMA discordant families*
- V. *\*T5 Up-regulated transcripts detected by microarray analysis in classical SMA patients*
- VI. *\*T6 Down-regulated transcripts detected by microarray analysis in classical SMA patients*
- VII. *\*T7 Susceptibility regions detected by the genome-wide scan analysis in SMA discordant families*
- VIII. *\*T8 Raw data for each chromosomal region detected by the genome-wide scan analysis*
- IX. *\*T9 Raw data for methylation analysis of T-plastin CpG island in two control populations*
- X. *\*T10 Raw data for methylation analysis of T-plastin CpG island in SMA discordant families*
- XI. *\*T11 Raw data for T-plastin haplotype blocks analysis*

*\*: The tables are contained in the attached CD-ROM*

APPENDIX

Table T1 Classical SMA patients checked for *T-plastin* expression

Cr. No.	EBV no.	DNA no.	Gender	SMA type	Plastin (Multiplex-PCR) Expression	Genotype	SMN1 copy No	SMN2 copy no.
17	BW 84	353	f	I	-	del/del	0	n.d.
1	T 21/91	55	f	I	-	del/del	0	2
26	BW 187	969	f	I	-	del/del	0	2
28	BW 191	997	f	I	-	del/del	0	2
32	BW 226 <sup>3</sup>	1125	f	I	-	del/del	0	2
36	BW 246	1271	f	I	-	del/del	0	3
5	BW 1	177	f	I	+	del/del	0	2
40	BW 258	1722	f	I	+	del/del	0	2
12	BW 38a	256 <sup>1</sup>	f	I	++	del/del	0	2
10	BW 27	219	f	II	-	del/del	0	3
24	BW 176	756	f	II	-	del/del	0	3
25	BW 178	851	f	II	-	del/del	0	n.d.
29	BW 208	1075	f	II	-	del/del	0	n.d.
19	BW 126a <sup>4</sup>	484	f	II	-	del/del	0	n.d.
39	BW 251	1312	f	II	+	del/del	0	2
2	T 40/91	72	f	II	+	del/del	0	3
48	BW 325	2481	f	II	+	del/del	0	n.d.
4	T 84/91	119 <sup>1</sup>	f	II	++	del/del	0	2
31	BW 217 <sup>2</sup>	1097 <sup>1</sup>	f	II	+++	del/del	0	n.d.
42	BW 299	2321	f	III	-	del/del	0	4
21	BW 164	708 <sup>1</sup>	f	IIIa	+	del/del	0	2
8	BW 21	202	f	IIIb	-	del/del	0	4
59	BW 402	3984	f	IIIb	-	del/del	0	4
37	BW 248 <sup>4</sup>	1275	m	I	-	del/del	0	2
22	BW 168 <sup>2</sup>	699	m	I	-	del/del	0	2
14	BW 61 <sup>4</sup>	306	m	I	-	del/del	0	2
18	BW 85 <sup>4</sup>	357	m	I	-	del/del	0	3
11	BW 29 <sup>4</sup>	227	m	I	-	del/del	0	3
13	BW 52	292	m	I	-	del/del	0	2
34	BW 238a <sup>4</sup>	1196	m	I	-	del/del	0	n.d.
3	T67/91 <sup>4</sup>	97	m	I	++	del/del	0	3
9	BW 26 <sup>4</sup>	215	m	II	-	del/del	0	3
16	BW 73	331	m	II	-	del/del	0	3
44	BW 315 <sup>4</sup>	2418	m	II	-	del/del	0	n.d.
47	BW 321 <sup>4</sup>	2439	m	II	-	del/del	0	3
69	LN 472	5392	m	II	-	del/del	0	3

APPENDIX

71	LN 480 <sup>4</sup>	5815	m	II	-	del/del	0	3
6	BW 2	174	m	II	-	del/del	0	3
30	BW 210	1079	m	II	-	del/del	0	3
41	BW 274 <sup>4</sup>	866	m	II	+	del/del	0	3
27	BW 190 <sup>4</sup>	994 <sup>1</sup>	m	II	+	del/del	0	3
45	BW 317 <sup>4</sup>	2429	m	III	+	del/del	0	n.d.
23	BW 174 <sup>2,4</sup>	798	m	IIIa	-	del/del	0	4
65	LN 443	4691	m	IIIa	-	del/del	0	3
43	BW 302 <sup>4</sup>	2345	m	IIIa	-	del/del	0	3
33	BW 232	1141	m	IIIb	-	del/del	0	4
15	BW 70 <sup>4</sup>	326 <sup>1</sup>	m	IIIb	++	del/del	0	3
20	BW 145 <sup>2,4</sup>	530 <sup>1</sup>	m	IIIb	+++	del/del	0	4
3	BW 250	1307	f	I	-	del/M	1	2
61	BW 420	3952	f	I	-	del/M	1	2
70	LN 476	5762	f	I	-	del/M	1	2
79	LN 525a	6536	f	I	-	del/M	1	2
63	LN 434	2833	f	II	-	del/M	1	2
78	LN 507	2648	f	II	-	del/M	1	2
77	LN 497	6124	f	IIIb	-	del/M	1	3
35	BW 243	43 <sup>1</sup>	f	II	+++	del/M	1	2
72	LN 481	4548	m	I	-	del/M	1	3
67	LN 462	4983	m	I	-	del/M	1	2
59	BW 405	3919	m	I	-	del/M	1	3
77	LN 499	6279	m	I	-	del/M	1	2
7	BW 20a	201	m	II	-	del/M	1	2
62	LN 429	4133	m	II	-	del/M	1	3
74	LN 495	5975	m	III	-	del/M	1	1
75	LN 496	6047	m	III	-	del/M	1	3
73	LN 489	5914	m	IIIb	-	del/M	1	1
50	BW 339 <sup>4</sup>	1927	m	IIIa	++	del/M	1	3
53	BW 376a	935 <sup>1</sup>	m	IIIb	+++	del/M	1	1
68	LN 470	4346	f	III	-	W/W	2	2
54	BW 377	3612	m	I	-	W/W	2	0
52	BW 361 <sup>4</sup>	2272	m	III	-	W/W	2	1
57	BW 394	3488	m	III	-	W/W	2	2
46	BW 319 <sup>4</sup>	2436	m	IIIa	-	W/W	2	1
49	BW 336 <sup>4</sup>	2245	m	IIIb	-	W/W	2	1
60	BW 409 <sup>3</sup>	4201 <sup>1</sup>	m	I	+++	W/W	2	2

---

APPENDIX

---

55	BW 380	3083	f	II	-	present	n.d.	n.d.
56	BW 392	3492	f	III	-	present	n.d.	n.d.
51	BW 346	2646	f	IIIb	-	present		n.d.
66	LN 449	3680	m	III	-	present		n.d.
64	LN 437	2128	f	III	-	del/?	1	0

- <sup>1</sup>: DNA samples used for haplotype analysis
- <sup>2</sup>: EBV-transformed lymphoblastoid cell lines used for *in vivo* footprinting experiment
- <sup>3</sup>: EBV-transformed lymphoblastoid cell lines used for microarray analysis. Additional two cell lines (BW 12 and BW 390) belonging to type III SMA patients were analyzed by this method.
- <sup>4</sup>: EBV-transformed lymphoblastoid cell lines used for T-plastin CpG island methylation analysis
- The amount of *T-plastin* transcript was scored relative to the HPRT intensity band with “-” for no expression; “+” for a very weak expression, “++” for middle expression and “+++” for a strong expression.

APPENDIX

II. Table T2 Phenotypic and genotypic description of SMA discordant families used for genome-wide scan analysis

A: age of onset; C: country; DR degree of relationship; G: genotype; MM: motor milestones; P: phenotype; S: sex.

Fam no.	DNA-No (old)	DNA no. new	S	DR	P	A	MM	G	C
1	92-808	ET1	M	father	unaffected	-	-	-	Spain
	92-809	ET2	F	mother	unaffected	-	-	-	Spain
	92-810	ET3	M	child 1	SMA IIIa	2y	Wheelch.17y	del/del	Spain
	92-812	ET4	F	child 2	SMA III b	-	Only cramps since adolescence	del/del	Spain
2	95-331	ET5	M	child 1	SMA	-	58y still walking	del/del	Spain
	95-599	ET6	M	child 2	SMA	-	Wheelch.12y	del/del	Spain
3	96-850	ET7	F	mother	unaffected	-	-	-	Spain
	96-852	ET8	F	child 1	SMA IIIb	18y	32y still walking	-	Spain
	96-853	ET9	M	child 2	SMA IIIa	2y	Wheelch.12y-	del/del	Spain
4	99-1847	ET10	M	father	unaffected	-	-	-	Spain
	99-1848	ET11	F	mother	unaffected	-	-	-	Spain
	96-1244	ET12	F	child 1	SMA IIIa	1y	type II-never walked	del/del	Spain
	99-1849	ET13	M	child 2	SMA IIIb	12y	wheelch.20y	del/del	Spain
5	91-375	ET14	M	father	unaffected	-	-	-	Spain
	91-374	ET15	F	mother	unaffected	-	-	-	Spain
	91-369	ET16	F	child 1	SMA IIIb	30y	min manif 40y still walking	SM	Spain
	91-376	ET17	F	child 2	SMA IIIa	2y	Wheelch 8y	SM	Spain
	91-370	ET18	F	child 3	SMA IIIa	1.5y	Wheelch 14y	SM	Spain
	91-372	ET19	F	child 4	SMA IIIa	1.5y	Wheelch 8y	SM	Spain
6 <sup>3</sup>	98-224	ET20	M	child 1	SMA IIIb	30y	still walking at 65l	SM/del	Spain
	00-1821	ET21	F	child 2	SMA IIIa	1.5y	Wheelch 14y	SM/del	Spain
	00-1854	ET22	F	child 3	unaffected	-	-	SM/del	Spain
7	193	JM1	M	father	unaffected	-	-	-	France
	194	JM2	F	mother	unaffected	-	-	-	France
	144	JM3	F	child 1	SMA III	-	walk unaided until ~ 6 y of age	-	France
8	192	JM4	M	child 2	SMA II	-	never walk	-	France
	197	JM5	M	father	unaffected	-	-	-	France
	198	JM6	F	mother	unaffected	-	-	-	France
	196	JM7	M	child 1	SMA II	-	never walk	-	France
	199	JM8	F	child 2	SMA III	-	walk unaided until ~ 10 y	-	France
9	67695	JM9	M	father	unaffected	-	-	-	France
	67694	JM10	F	mother	unaffected	-	-	-	France
	67690	JM11	M	child 1	SMA II	-	never walk	-	France
	67691	JM12	F	child 2	SMA III	-	walk at 16 months until 5 y	-	France

APPENDIX

	67693	JM13	F	child 3	SMA III	-	walk at 18 months (with aid) until 4 y	-	France
10	49830	KS1	M	father	unaffected	-	-	-	USA
	49831	KS2	F	mother	unaffected	-	-	-	USA
	49832	KS3	F	child 1	SMA III	-	-	-	USA
	49833	KS4	F	child 2	SMA II	-	-	-	USA
11	65088	KS5	M	father	unaffected	-	-	-	USA
	65092	KS6	F	mother	unaffected	-	-	-	USA
	65089	KS7	F	child 1	SMA III	-	-	-	USA
	65090	KS8	M	child 2	SMA II	-	-	-	USA
12	50485	KS9	M	father	unaffected	-	-	-	USA
	50486	KS10	F	mother	unaffected	-	-	-	USA
	50487	KS11	F	child 1	SMA III	-	-	-	USA
	50488	KS12	M	child 2	SMA II	-	-	-	USA
13	52828	KS13	F	mother	unaffected	-	-	-	USA
	41306	KS14	F	child 1	SMA IIIb	-	-	-	USA
	41307	KS15	M	child 2	SMA IIIa	-	-	-	USA
14	CB1F	CB1	M	father	unaffected	-	-	-	Italy
	CB1M	CB2	F	mother	unaffected	-	-	-	Italy
	CB1C1	CB3	F	child 1	SMA III	-	-	-	Italy
	CB2C2	CB4	M	child 2	SMA III	-	-	-	Italy
15	CB2M	CB5	F	mother	unaffected	-	-	-	Italy
	CB2C1	CB6	F	child 1	SMA III, more severe	-	-	-	Italy
	CB2C2	CB7	M	child 2	SMA III	-	-	-	Italy
16	CB3F	CB8	M	father	unaffected	-	-	-	Italy
	CB3M	CB9	F	mother	unaffected	-	-	-	Italy
	CB3C1	CB10	F	child 1	SMA III	-	-	-	Italy
	CB3C2	CB11	F	child 2	SMA II	-	-	-	Italy
17	CB4F	CB12	M	father	unaffected	-	-	-	Italy
	CB4M	CB13	F	mother	unaffected	-	-	-	Italy
	CB4C1	CB14	M	child 1	SMA II	-	at 10 he was wheel-chair bounded	-	Italy
18	CB4C2	CB15	F	child 2	SMA III	7 y	-	-	Italy
	CB5F	CB16	M	father	unaffected	-	-	-	Italy
	CB5M	CB17	F	mother	unaffected	-	-	-	Italy
	CB5C1	CB18	M	child 1	SMA III	-	-	-	Italy
	CB5C2	CB19	M	child 2	SMA IV	-	is almost asymptomatic at the age of 18	-	Italy
19	CB6F	CB20	M	father	unaffected	-	-	-	Italy
	CB6M	CB21	F	mother	unaffected	-	-	-	Italy
	CB6C1	CB22	M	child 1	SMA II	-	-	-	Italy
	CB6C2	CB23	F	child 2	SMA III	-	-	-	Italy
20 <sup>3</sup>	217-2	LH1	F	child 1	unaffected	-	-	del/del	Netherland
	217-7	LH2	F	child 2	unaffected	-	-	del/del	Netherland
	217-8	LH3	M	child 3	SMA IIIb	8 y	-	del/del	Netherland
	217-9	LH4	M	child 4	unaffected	-	-	del/del	Netherland
21 <sup>3</sup>	217-11	LH5	M	child 5	SMA IIIb	12 y	-	del/del	Netherland
	25-2.	LH6	M	child 1	unaffected	-	-	del/del	Netherland
	25-4.	LH7	M	child 2	SMA IIIa	1 y	-	del/del	Netherland
	25-6.	LH8	F	child 3	unaffected	-	-	-	Netherland

APPENDIX

	25-7.	LH9	F	child 4	SMA IIIa	1 y	-	del/del	Netherland
	25-8.	LH10	M	child 5	unaffected	-	-	-	Netherland
22	48	AB1	M	father	unaffected	-	-	-	USA
	47	AB2	F	mother	unaffected	-	-	-	USA
	50	AB3	F	child 1	SMA II	1 y	wheelchair	del/del	USA
	51	AB4	M	child 2	SMA IV	~20 y	walker	del/del	USA
23	110	AB5	M	father	unaffected	-	-	-	USA
	111	AB6	F	mother	unaffected	-	-	-	USA
	112	AB7	F	child 1	SMA II	17mo	wheelchiar	del/del	USA
	113	AB8	F	child 2	SMA IV	13 y	walker	del/del	USA
24	120	AB9	M	father	unaffected	-	-	-	USA
	121	AB10	F	mother	unaffected	-	-	-	USA
	123	AB11	F	child1	type IV	19y	-	-	USA
	124	AB12	F	child2	type III	-	-	-	USA
25 <sup>1,2,3,4,5</sup>	151	OG1	M	father	unaffected	-	-	-	Germany
	152	OG2	F	mother	unaffected	-	-	-	Germany
	153	OG3	F	child 1	unaffected	-	normal	del/del	Germany
	155	OG4	F	child 2	unaffected	-	normal	del/del	Germany
26 <sup>1,2,3,4,5</sup>	157	OG5	F	child 3	SMA IIIa	2y	-	del/del	Germany
	675	OG6	M	father	unaffected	-	-	-	Germany
	676	OG7	F	mother	unaffected	-	-	-	Germany
	677	OG8	M	child 1	SMA IIIa	2.5 y	2.5y climb stairs + rise = walking	del/del	Germany
	678	OG9	F	child 2	unaffected	-	-	del/del	Germany
27 <sup>1,2,3,5</sup>	4173	OG10	M	father	unaffected	-	-	-	Germany
	4175	OG11	F	mother	unaffected	-	-	-	Germany
	3956	OG12	M	child 1	SMA III	-	-	del/del	Germany
28 <sup>1,2,3,4,5</sup>	4174	OG13	F	child 2	unaffected	-	-	del/del	Germany
	1219	OG14	M	father	unaffected	-	-	-	Germany
	1220	OG15	F	mother	unaffected	-	-	-	Germany
	1221	OG16	M	child 1	unaffected	-	-	del/del	Germany
	1222	OG17	M	child 2	SMA IIIa	6 mos	-	del/del	Germany
29 <sup>1,2,5</sup>	3129	OG18	M	father	unaffected	-	-	-	Germany
	3130	OG19	F	mother	unaffected	-	-	-	Germany
	2549	OG20	M	child 1	SMA IIIb	3.5 y	wheelchair (16 y)	del/del	Germany
	2593	OG21	M	child 2	SMA IIIa	16 mos	wheelchair (5 y)	del/del	Germany
30 <sup>1,5</sup>	7125	OG22	M	father	unaffected	-	-	-	Germany
	7126	OG23	F	mother	unaffected	-	-	het. tel SMN	Germany
	7131	OG24	F	child 1	SMA IIIb	17-18 y	-	del/del	Germany
31 <sup>1,3,4,5</sup>	7133	OG25	M	child 2	SMA IIIa	2.5 y	-	del/del	Germany
	3023	OG26	M	father	unaffected	-	-	-	Germany
	3024	OG27	F	mother	unaffected	-	-	-	Germany
	3025	OG28	M	child 1	SMA III	-	-	del/del	Germany
32 <sup>1,3,5</sup>	3026	OG29	F	child 2	unaffected	-	-	del/del	Germany
	2400	OG30	F	mother	unaffected	-	-	-	Germany
	2401	OG31	F	child 1	SMA II	1 y	never walk	del/del	Germany
	2402	OG32	M	child 2	SMA II	1 y	never walk	del/del	Germany
	2404	OG33	F	child 3	unaffected	-	-	del/del	Germany
33 <sup>1,5</sup>	1027	OG34	M	father	unaffected	-	-	-	Germany
	1028	OG35	F	mother	unaffected	-	-	-	Germany
	1019	OG36	M	child 1	SMA IIIb	16 y	still walking	del/del	Germany
	1029	OG37	M	child 2	SMA IIIa	2.5 y	wheelchair (26y)	del/del	Germany

APPENDIX

34 <sup>1,2,3,4,5</sup>	1030	OG38	M	child 3	SMA IIIb	5 y	still walking	del/del	Germany
	2021	OG39	M	father	unaffected	-	-	-	Germany
	2022	OG40	F	mother	unaffected	-	-	-	Germany
	2023	OG41	F	child 1	unaffected	-	normal	del/del	Germany
	2024	OG42	F	child 2	unaffected	-	normal	del/del	Germany
	2026	OG43	M	child 3	SMA IIIb	18 y	still walking	del/del	Germany
35 <sup>1,5</sup>	2027	OG44	M	child 4	SMA IIIb	13 y	still walking	del/del	Germany
	4312	OG45	M	father	unaffected	-	-	-	Germany
	4313	OG46	F	mother	unaffected	-	-	-	Germany
	4321	OG47	F	child 1	SMA IIIa	12 mos	walk with 12 mo	del/del	Germany
36 <sup>1,5</sup>	4322	OG48	M	child 2	SMA II	7 mos	sit 6 mo, never walk	del/del	Germany
	195	OG49	M	father	unaffected	-	-	-	Germany
	196	OG50	F	mother	unaffected	-	-	-	Germany
	197	OG51	M	child 1	SMA IIIa	15 mos	wheelchair (7y)	del/del	Germany
	198	OG52	F	child 2	SMA II	13 mos	33y, sit no longer	del/del	Germany
	200	OG53	M	child 3	SMA IIIa	17 mos	wheelchair (18y)	del/del	Germany
37	2	PM1	M	father	unaffected	-	-	-	Poland
	1	PM2	F	mother	unaffected	-	-	-	Poland
	3	PM3	M	child 1	SMA II	1 y	wheelchair	del/del	Poland
38	4	PM4	M	child 2	SMA IIIa	3y	wheelchair	del/del	Poland
	5	PM5	F	mother	unaffected	-	-	-	Poland
	6	PM6	F	child 1	SMA IIIa	10 mo	wheelchair	del/del	Poland
39	7	PM7	F	child 2	SMA IIIb	9 y	walker	del/del	Poland
	8	PM8	F	child 1	SMA IV	34 y	walker	del/del	Poland
	9	PM9	F	child 2	SMA IIIb	6 y	walker	del/del	Poland
40	10	PM10	F	child 1	SMA IIIb	6 y	walker	del/del	Poland
	11	PM11	M	child 2	SMA IIIa	10 mo	wheelchair	del/del	Poland
41 <sup>3</sup>	13	PM12	M	father	unaffected	-	-	-	Poland
	12	PM13	F	mother	unaffected	-	-	-	Poland
	14	PM14	M	child 1	SMA IIIa	18 mo	wheelchair	del/del	Poland
	15	PM15	M	child 2	SMA IIIb	5 y	walker	del/del	Poland
	16	PM16	F	child 3	unaffected	-	normal	del/del	Poland

- Del: deletion of *SMN1* gene, SM: Spanish mutation (430del4)
- <sup>1</sup>: DNA samples analyzed for *ZNF265* gene
- <sup>2</sup>: DNA samples tested for *HDAC6* and *hnRNP-R* SNPs association
- <sup>3</sup>: DNA samples analyzed for *T-plastin* haplotype blocks
- <sup>4</sup>: DNA samples used for *in vivo* footprinting analysis of *T-plastin* enhancer and methylation analysis
- <sup>5</sup>: DNA samples screened for mutations/polymorphism within *T-plastin* genomic region

## ERKLÄRUNG

Ich versichere, dass ich die von mir vorgelegte Dissertation selbständig, die benutzten Quellen und Hilfsmittel vollständig angegeben und die Stellen der Arbeit – einschließlich Tabellen, Karten und Abbildungen-, die anderen Werken im Wortlaut oder dem Sinn nach entnommen sind, in jedem Einzelfall als Entlehnung kenntlich gemacht habe; dass diese Dissertation noch keiner anderen Fakultät oder Universität zur Prüfung vorgelegen hat; dass sie – abgesehen von unten angegebenen Teilpublikationen – noch nicht veröffentlicht worden ist sowie, dass ich eine solche Veröffentlichung vor Abschluss des Promotionsverfahrens nicht vornehmen werde. Die Bestimmungen der Promotionsordnung sind mir bekannt. Die von mir vorgelegte Dissertation ist von Frau Professor Brunhilde Wirth betreut worden.

Nachfolgend gennante Teilpublikationen liegen vor:

Helmken C., Hofmann Y., Schoenen F., Oprea G., Raschke H., Rudnik-Schoneborn S., Zerres K., Wirth B. (2003) „Evidence for a modifying pathway in SMA discordant families: reduced SMN level decreases the amount of its interacting partners and Htra2-beta1“. Hum Gen.114:11-21

Köln, 15. März 2007

Gabriela-Elena Oprea

## CURRICULUM VITAE

**NAME** Oprea geb. Bordeianu  
**VORNAME** Gabriela-Elena  
**GEBURTSDATUM** 7. Oktober 1977  
**GEBURTSORT** Bukarest, Rumänien  
**NATIONALITÄT** rumänisch  
**FAMILIENSTAND** verheiratet

### FACHAUSBILDUNG

2000-2002 Master in Genetik, Universität in Bukarest, Rumänien  
Masterarbeit "*Human Chronic Leukemias- Genetic Study*"  
2002 Abschluss: Magisterdiplom, Prädikat „sehr gut“ (10)

1996-2000 Studium in Biologie, Biologiefakultät, Universität Bukarest, Rumänien  
Spezialität: Zellbiologie und Genetik  
Diplomarbeit: "*Investigation of Human Genome in Chronic Leukemias*"  
2000 Abschluss: Diplom-Biologie, Prädikat „sehr gut“ (10)

### BERUFSERFAHRUNG

1. Januar 2004 – März 2007, Wissenschaftliche Angestellte (BAT IIa/ halbe) und Doktorandin am Institut für Humangenetik, Universitätsklinikum zu Köln (Prof. Dr. Brunhilde Wirth)  
Anfertigung einer Dissertation mit dem tema: „Identification of T-plastin as potential modifier gene in SMA discordant families“

1. September 2002 - 31. Dezember 2003, Wissenschaftliche Angestellte (BAT IIa/ halbe) und Doktorandin am Institut für Humangenetik, Universität Bonn (Prof. Dr. Brunhilde Wirth)

1. Mai 2001 - 30. August 2002 Wissenschaftliche Mitarbeiterin, Institut für Genetik, Bukarest, Rumänien (Prof. Dr. Lucian Gavrila)  
Molekularbiologische Arbeiten an „Cytogenetic and molecular studies of human genome in chronic leukemias before and after radio- and chemotherapy“ und „Molecular diagnosis of the rheumatoid arthritis“.